Vol. 62 July, 1958 No. 7

THE JOURNAL OF PHYSICAL CHEMISTRY

(Registered in U. S. Patent Office)

CONTENTS

THE JOURNAL OF PHYSICAL CHEMISTRY

(Registered in U. S. Patent Office)

Published monthly by the American Chemical Society at 20th and Northampton Sts., Easton, Pa.

Second-class mail privileges authorized at Easton, Pa.

The *Journal of Physical Chemistry* is devoted to the publication of selected symposia in the broad field of physical chemistry and to other contributed papers.

Manuscripts originating in the British Isles, Europe and Africa should be sent to F. C. Tompkins, The Faraday Society, 6 Gray s Inn Square, London W. C. 1, England.

Manuscripts originating elsewhere should be sent to W. Albert Noyes, Jr., Department of Chemistry, University of Rochester, Rochester 20, N. Y.

Correspondence regarding accepted copy, proofs and reprints should be directed to Assistant Editor, Allen D. Bliss, Department of Chemistry, Simmons College, 300 The Fenway, Boston 15, Mass.

Business Office: Alden H. Emery, Executive Secretary, American Chemical Society, 1155 Sixteenth St., N. W., Washington 6, D. C.

Advertising Office: Reinhold Publishing Corporation, 430 Park Avenue, New York 22, N. Y.

Articles must be submitted in duplicate, typed and double spaced. They should have at the beginning a brief Abstract, in no case exceeding 300 words. Original drawings should accompany the manuscript. Lettering at the sides of graphs (black on white or blue) may be pencilled in and will be typeset. Figures and tables should be held to a minimum consistent with adequate presentation of information. Photographs will not be printed on glossy paper except by special arrangement. All footnotes and references to the literature should be numbered consecutively and placed in the manuscript at the proper places. Initials of authors referred to in citations should be given. Nomenclature should conform to that used in *Chemical Abstracts*, mathematical characters marked for italic, Greek letters carefully made or annotated, and subscripts and superscripts clearly shown. Articles should be written as briefly as possible consistent with clarity and should avoid historical background unnecessary for specialists.

Notes describe fragmentary or incomplete studies but do not otherwise differ fundamentally from articles and are subjected to the same editorial appraisals as are articles. In their preparation particular attention should be paid to brevity and conciseness. Material included in Notes must be definitive and may not be republished subsequently.

Communications to the Editor are designed to afford prompt preliminary publication of observations or discoveries whose value to science is so great that immediate publication is imperative. The appearance of related work from other laboratories is in itself not considered sufficient justification for the publication of a Communication, which must in addition meet special requirements of timeliness and significance. Their total length may in no case exceed 500 words or their equivalent. They differ from Articles and Notes in that their subject matter may be republished.

Symposium papers should be sent in all cases to Secretaries of Divisions sponsoring the symposium, who will be responsible for their transmittal to the Editor. The Secretary of the Division by agreement with the Editor will specify a time after which symposium papers cannot be accepted. The Editor reserves the right to refuse to publish symposium articles, for valid scientific reasons. Each symposium paper may not exceed four printed pages (about sixteen double spaced typewritten pages) in length except by prior arrangement with the Editor.

Remittances and orders for subscriptions and for single copies, notices of changes of address and new professional connections, and claims for missing numbers should be sent to the American Chemical Society, 1155 Sixteenth St., N. W., Washington 6, D. C. Changes of address for the *Journal of Physical Chemistry* must be received on or before the 30th of the preceding month.

Claims for missing numbers will not be allowed (1) if received more than sixty days from date of issue (because of delivery hazards, no claims can be honored from subscribers in Central Europe, Asia, or Pacific Islands other than Hawaii), (2) if loss was due to failure of notice of change of address to be received before the date specified in the preceding paragraph, or (3) if the reason for the claim is "missing from files."

Subscription Rates (1958): members of American Chemical Society, $8.00 for 1 year; to non-members, $16.00 for 1 year. Postage free to countries in the Pan American Union; Canada, $0.40; all other countries, $1.20. Single copies, current volume, $1.35; foreign postage, $0.15; Canadian postage $0.05. Back volumes (Vol. 56-59), $15.00 per volume; (starting with Vol. 60) $18.00 per volume; foreign postage $1.20, Canadian, $0.40; $1.75 per issue, foreign postage $0.15, Canadian postage $0.05.

The American Chemical Society and the Editors of the *Journal of Physical Chemistry* assume no responsibility for the statements and opinions advanced by contributors to This Journal.

The American Chemical Society also publishes *Journal of the American Chemical Society*, *Chemical Abstracts*, *Industrial and Engineering Chemistry*, *Chemical and Engineering News*, *Analytical Chemistry*, *Journal of Agricultural and Food Chemistry* and *Journal of Organic Chemistry*. Rates on request.

THE JOURNAL OF PHYSICAL CHEMISTRY

(Registered in U. S. Patent Office) (© Copyright, 1958, by the American Chemical Society)

VOLUME 62 JULY 30, 1958 NUMBER 7

THE VAPORIZATION OF MOLYBDENUM AND TUNGSTEN OXIDES[1]

BY PAUL E. BLACKBURN, MICHAEL HOCH[2] AND HERRICK L. JOHNSTON

Contribution from the Department of Chemistry, Ohio State University, Columbus, Ohio

Received July 17, 1957

The vapor pressures above MoO_3, Mo_4O_{11}, MoO_2, WO_3 and WO_2 have been measured by the Knudsen effusion method. $MoO_3(s)$ vaporizes to $(MoO_3)_3(g)$ while $Mo_4O_{11}(s)$ disproportionates to $(MoO_3)_3(g)$ and $MoO_2(s)$, the heats of vaporization of $MoO_3(s)$ and of decomposition of $Mo_4O_{11}(s)$ being $\Delta H_{900} = 79.7$ kcal./mole of $(MoO_3)_3$ and $\Delta H_{900} = 68.7$ kcal./mole of $(MoO_3)_3$, respectively. Some $MoO_2(s)$ vaporizes to $MoO_2(g)$ with $\Delta H_0^0 = 129.8$ kcal./mole, but most of the $MoO_2(s)$ disproportionates to $MoO_3(g)$ and $Mo(s)$ with $\Delta H_0^0 = 133.6$ kcal./mole of MoO_3. $WO_3(s)$ vaporizes to $(WO_3)_3(g)$ with $\Delta H_{1500} = 108.0$ kcal./mole of $(WO_3)_3$ and $WO_2(s)$ disproportionates to $(WO_3)_3(g)$ and $W(s)$ with $\Delta H_{1500} = 90.2$ kcal./mole of $(WO_3)_3$. The calculated heat of dissociation for $MoO_2(g)$ is $D_0^0 = 284.6$ kcal./mole and for $MoO_3(g)$ is $D_0^0 = 410.3$ kcal./mole. The heat of decomposition of $(MoO_3)_3(g)$ to the monomer $MoO_3(g)$ is $\Delta H = 220.9$ kcal./mole of the trimer.

This research is concerned with the investigation of the vapor or dissociation pressures of MoO_3, MoO_2, WO_3, WO_2, and the stability of the intermediate compounds. There has been substantial disagreement among molybdenum trioxide vapor pressure data obtained by the Knudsen effusion method,[3] by transpiration measurements,[4] and by the rate of evaporation method.[5] WO_3 vapor pressures have been investigated by Ueno.[3] Calculations using Kelley's[6] and Brewer's[7] data show that MoO_2 and WO_2 should decompose to the metal and the trioxide. No measurements are available on the lower oxides of either metal.

Apparatus and Experimental Procedure

The heating was done entirely by induction, using a General Electric or a Westinghouse 20 kilowatt electronic heater.

Three furnaces were used for the research. A furnace for temperatures below the optical range was used for vapor pressure measurements on molybdenum trioxide and molybdenum dioxide–molybdenum trioxide mixtures. The remaining measurements were made in either the high temperature Pyrex glass furnace or the metal furnace previously described.[8] The only change made on the high temperature glass furnace was that the optical window was joined to the vacuum system by a dry "O" ring.

A Furnace for Temperatures below 800°.—This furnace consists of a water cooled Pyrex glass cell connected to the vacuum system by means of a flat ground glass joint sealed with a dry "O" ring. The vacuum was of the order of 1×10^{-6} mm. of mercury or less, as measured with a cold cathode ionization vacuum gauge.

Temperatures were measured with a platinum to platinum–10% rhodium thermocouple, brought into the system by means of Stupakoff seals. The thermocouple wires extending from the hot junction were insulated with porcelain protection tubes encased in an Invar tube mounted vertically from a brass base resting on the bottom of the furnace. The tip of the thermocouple was wrapped with a small piece of platinum to increase the thermal contact with the Knudsen cell. A platinum cylinder the same size as the Knudsen cell was placed just below the position occupied by the cell in order to curtail heat loss through the Invar tube.

The thermocouple leads were shielded between the hot junction and the potentiometer. To eliminate radiofrequency currents, a filter consisting of three 0.02 microfarad condensers was connected across the leads and from each lead to ground.

The thermocouple was calibrated against a like couple which had been standardized with National Bureau of Standards melting point samples.

The accuracy of the thermocouple *in situ* was checked by melting aluminum chips (National Bureau of Standards sample) in a tantalum bucket containing a platinum lined thermocouple well. The temperature was increased slowly while the chips were observed. The first indication of melting occurred at 660.0° as computed from the calibration curve described above, and the whole sample was molten at 661.2°. This compared very well with the melting point of 659.7° quoted by the National Bureau of Standards. Calibration by observing the freezing point on a cooling curve was not possible because of the rapid heat loss of such a small sample.

Knudsen Cells.—All the Knudsen cells were drawn from 0.010 inch thick sheet. Molybdenum cells were used when

(1) This work was supported in part by the Office of Naval Research under contract with the Ohio State University Research Foundation.

(2) Department of Metallurgical Engineering, University of Cincinnati, Cincinnati 21, Ohio.

(3) K. Ueno, *J. Chem. Soc. Japan*, **62**, 990 (1941).

(4) S. M. Ariya, S. A. Shchukarev and V. B. Glushkova, *Zhur. Obshchei Khim.*, **23**, 2063 (1953).

(5) J. Feiser, *Metall. Erz.*, **28**, 297 (1931).

(6) K. K. Kelley, "Thermodynamic Properties of Molybdenum Compounds," Bull. Cdb-2 Climax Molybdenum Co.

(7) L. Brewer, *Chem. Revs.*, **52**, 1 (1953).

(8) J. W. Edwards, H. L. Johnston and P. E. Blackburn, *J. Am. Chem. Soc.*, **74**, 1539 (1952).

MoO_2 was investigated, platinum cells in all other cases. The cell for the low temperature glass furnace had a thermocouple well sunk in the bottom. Cells employed in the other furnace were made with blackbody wells in the top.

All the Knudsen cells were made with the effusion orifice in the side. The orifice was not beveled to a knife edge as is the practice of some investigators. It was found that beveling the hole produced a ragged edge which introduced an uncertainty into the measurement of the area of the hole. The dimensions of the holes were measured with a traveling microscope.

Samples.—The molybdenum trioxide was obtained from the J. T. Baker Chemical Company. An analysis furnished by the company gave the purity as 99.9%, with the principal impurities being chloride, 0.002%; nitrate, 0.003%; phosphate, 0.005%; sulfate, 0.02%; ammonium, 0.001%; and heavy metals, 0.005%.

Tungsten trioxide was made by dehydrating tungstic acid at 900° to constant weight. The acid lost 0.918 mole of water for each mole of tungsten trioxide. According to the Coleman S. Bell Company, suppliers of the tungstic acid, it contained these impurities: alkalies (as sulfates), 0.30%; arsenic, 0.001%; lead, 0.005%; molybdenum, 0.005%; and iron, 0.005%.

Tungsten powder and molybdenum powder were obtained from the Callite Tungsten Corporation. The tungsten was stated to be 99.9% pure. No analysis was available for the molybdenum powder.

Molybdenum dioxide was prepared by heating a mixture of 0.138 mole of molybdenum trioxide and 0.065 mole of molybdenum powder in a nitrogen atmosphere at 750° for several hours. The excess molybdenum trioxide was removed by sublimation *in vacuo*. In order to analyze for molybdenum dioxide, the purple-brown powder was oxidized to constant weight. It was found to contain 97.8 mole % molybdenum dioxide. An X-ray powder pattern gave the characteristic molybdenum dioxide lines.[9]

Tungsten dioxide was prepared in a similar fashion by heating 0.056 mole of tungsten powder and 0.134 mole of tungsten trioxide at 1000° for seven hours. The X-ray pattern for the chocolate brown powder showed tungsten dioxide[9] and weak tungsten trioxide lines. The excess trioxide was vaporized during the first few measurements.

Experimental Results

Pressures were calculated from the measured rates of evaporation by the equation $P = m\cdot\sqrt{2\pi RT/M}$, where P is the pressure in atmospheres, R is the molar gas constant, T is the absolute temperature, M is the molecular weight of the vapor, and m is the rate of evaporation in g. cm.$^{-2}$ sec.$^{-1}$.

Sample weight losses were corrected for the weight loss of the platinum container. The curve obtained by experimentally determining the rate of evaporation of the empty container was extrapolated to the temperature of the run. Maximum correction was 15% of the total weight loss. Computation of the effective time was made by the averaging method,[8] while the effective area of the effusion orifice was obtained by multiplying the area at room temperature by the Clausing factor K',[10] and the thermal expansion factor.[11]

To obtain the heats of reaction when polymeric gaseous molecules $(MoO_3)_3$ and $(WO_3)_3$ were involved, the Clausius–Clapeyron equation was used. In all other cases free energy functions were employed to interpret the data. The functions for the condensed phases were calculated from the following data: for MoO_3(s) (1), Cosgrove and Snyder's heat capacity measurements[12]; for S_{298} of MoO_3, Seltz, *et al.*,[13a] and Smith, *et al.*[13b]; and for S_{298} of WO_3, Smith, *et al.*[13b] Estimated heat capacities used by Kelley[6] and Coughlin[14a] were made available by the former.[14b]

Using the heat capacity and entropies from the above data the free energy functions for the condensed phases were calculated. The values for Mo(s) and W(s) were calculated from Kelley's tables.[15] Free energy functions for the gas phases, MoO_3(g) and MoO_2(g) were estimated using the formulas for S_{298} and C_p given by Kubaschewski and Evans.[16] This information is contained in Table I.

TABLE I

FREE ENERGY FUNCTIONS

$-\left(\frac{F - H_0^\circ}{T}\right)$ cal./degree/mole

Substance	T, °K. 1000	1500	2000
Mo(s)	8.9	11.2	13.1
MoO_2(s)	22.4	28.1	32.4
MoO_3(s)(1)	26.3	38.1	
MoO_2(g)	74.8	80.5	84.5
MoO_3(g)	78.7	86.1	91.2
W(s)	9.9	12.3	14.0
WO_2(s)	19.5	25.0	
WO_3(s)	27.4	35.3	

MoO_3.—Table II contains the measured pressures. The amorphous yellow condensate, which turned blue after standing, was crystallized by annealing *in vacuo* at 500°. An X-ray diffraction pattern showed only MoO_3 lines.[9] According to Berkowitz, Inghram and Chupka[17] the trimer, $(MoO_3)_3$, is the main gaseous species. The Clausius–Clapeyron equation gives

$$4.576 \log P(MoO_3)_3 = -\frac{79741}{T} + 67.81 \pm 0.83$$

where P is in atmospheres.

To check for possible dissociation, 2 g. of MoO_3 was vaporized at 1000°. No residue was found within the experimental weighing error of 0.2 mg. Dissociation at higher temperatures was investigated by heating samples of MoO_3 rapidly (in 30 sec.) to 1400° in the Knudsen cell. It was found that a sample of MoO_3 weighing 2.300 g. lost 150 mg. before it reached 1000°, while 2.145 g. vaporized between 1000-1400°. The residue of 5.4 mg. did not vaporize even on prolonged heating at 1400°. Thus, above 1000° MoO_3 will dissociate to a small extent into MoO_2(s) and O_2(g).[18]

Mo_4O_{11}.—A mixture of 7.64×10^{-3} mole of MoO_3

(9) The American Society for Testing Materials: X-Ray Diffraction Data Cards. Philadelphia, 1950.

(10) S. Dushman, "Scientific Foundations of Vacuum Technique," John Wiley and Sons, New York, N. Y., 1949, p. 96.

(11) J. W. Edwards, R. Speiser and H. L. Johnston, *J. Applied Phys.*, **22**, 425 (1951).

(12) L. A. Cosgrove and P. E. Snyder, *J. Am. Chem. Soc.*, **75**, 1227 (1953).

(13) (a) Seltz, Dunkerley and DeWitt, *J. Am. Chem. Soc.*, **65**, 600 (1943); (b) Smith, Brown, Dworkin, Sasmor and Van Artsdalen, *ibid.*, **78**, 1533 (1956).

(14) (a) J. P. Coughlin, Bureau of Mines Bulletin No. 542, 1954; (b) K. K. Kelley, private communication, January 13, 1955.

(15) K. K. Kelley, Bureau of Mines Bulletin No. 476, 1950.

(16) O. Kubaschewski and E. Ll. Evans, "Metallurgical Thermochemistry," second edition, Pergamon Press Ltd., London, 1956, pp. 182–195.

(17) J. Berkowitz, M. G. Inghram and W. Chupka, *J. Chem. Phys.*, **26**, 842 (1957).

(18) If any Mo_4O_{11} was formed, it would have disproportionated to MoO_2(s) and $(MoO_3)_3$(g).

TABLE II

VAPOR PRESSURE OF MOLYBDENUM TRIOXIDE

Temp., °K.	Effective time, sec.	Wt. loss, g.	Effective area, cm.^{2} × 10^3	$(MoO_3)_3$ press., atm. × 10^7
808	6242	0.00231	53.00	1.946
836	4284	.00814	53.03	11.24
850	9134	.00168	3.834	15.18
869	2014	.01919	53.07	57.43
880	7229	.01374	3.836	159.8
890	8725	.01529	3.837	147.9
898	1399	.00242	3.837	146.6
904	1009	.04799	53.11	292.3
928	1998	.02678	3.840	1155
930	1779	.02725	3.840	1320
940	1327	.03095	3.841	2021
946	2163	.06033	3.841	2424
954	1358	.05758	3.842	3700
958	1187	.07817	3.842	5759
958	1051	.04865	3.842	4045

and 2.31×10^{-3} mole of MoO_2 was placed in a Knudsen cell, and the pressure as a function of composition was measured at 607°. Between the compositions $MoO_{2.753}$ and $MoO_{2.740}$ the $(MoO_3)_3$ partial pressure dropped by a factor of 2, indicating that Mo_4O_{11} is a stable solid at 607°.

The measured $(MoO_3)_3$ pressures above Mo_4O_{11} and MoO_2 are given in Table III. Least square treatment of our data gives for the reaction

$$Mo_4O_{11}(s) \longrightarrow (MoO_3)_3(g) + MoO_2(s) \qquad (1)$$

$$4.576 \log P(MoO_3)_3 = -\frac{68677}{T} + 53.32 \pm 0.57$$

where P is in atmospheres.

TABLE III

VAPOR PRESSURE ABOVE $Mo_4O_{11} + MoO_2$

Temp., °K.	Effective time, sec.	Wt. loss, g.	Effective area, cm.^{2} × 10^3	$(MoO_3)_3$ press., atm. × 10^7
846	29484	0.00257	3.835	7.18
869	16575	.00462	3.835	23.26
871	2790	.00080	3.835	23.95
876	8954	.00340	3.835	31.81
885	9484	.00623	3.836	55.29
912	3094	.00781	3.839	215.6
938	2072	.00949	3.841	396.6
938	2554	.01243	3.841	421.3
959	1103	.01114	3.842	883.3

MoO_2.—MoO_2 may vaporize according to the two reactions

$$MoO_2(s) \longrightarrow MoO_3(g) \qquad (2)$$

and

$$3/2MoO_2(s) \longrightarrow MoO_3(g) + {}^1/_2Mo(s) \qquad (3)$$

To determine which reaction was occurring, vaporization experiments were carried out using a platinum crucible, and X-ray diffraction patterns were taken of the condensate and residue. The condensate showed only the MoO_2 structure.[19] The residue, after vaporizing 116 mg. from 763 mg. of $MoO_2(s)$, showed the MoO_2 pattern and weak Mo lines. Both reactions 2 and 3 therefore occur side by side. The ratio of MoO_2 to MoO_3 in the gas phase was determined quantitatively by introducing a measured amount of MoO_2 into a molybdenum crucible. The crucible was heated *in vacuo* at 1650° until there was no further weight loss; 203 mg. of pure MoO_2, corrected for the 2.2% Mo content, gave a residue of 35.4 mg., and 778 mg. of MoO_2 yielded 161 mg. The composition of the vapor by weight is 29% $MoO_2(g)$ and 71% $MoO_3(g)$, assuming the residue to be Mo(s).

The experimental data on the vaporization of MoO_2 are given in Table IV. The total weight loss was divided according to the above ratio and the partial pressures of $MoO_2(g)$ and $MoO_3(g)$ were calculated. Using the free energy functions given in Table I, ΔH_0^0 for reactions 2 and 3 were calculated.

Of the possible gaseous molecules formed in reaction 3, the monomer $MoO_3(g)$ is the main species. The dimer $(MoO_3)_2$ and trimer $(MoO_3)_3$ are negligible. From our vapor pressure data on pure $MoO_3(s)$ and the heat of fusion[12,13] we calculate a $(MoO_3)_3(g)$ pressure of $10^{2.3}$ atm. at 1900°K., or 1627°. The activity of MoO_3 in MoO_2 is $10^{-3.55}$ at 1627°, calculated from the heats of formation[18] and the free energy functions. According to Berkowitz, *et al.*,[17] the concentration of monomer and dimer above pure $MoO_3(s)$ are each less than 1% of the trimer. Using the upper limit of 1%, we find that at 1627° the maximum possible partial pressures of $(MoO_3)_3(g)$, $(MoO_3)_2(g)$ and $MoO_3(g)$ in equilibrium with $MoO_2(s)$ and Mo are $10^{-8.35}$, $10^{-6.80}$ and $10^{-3.25}$ atm., respectively. Our experimental data in Table IV give an $(MoO_3)_x$ partial pressure of $10^{-3.2}$ atm. Only the monomer $MoO_3(g)$ can have a partial pressure of this order, the maximum partial pressures of the dimer and trimer are lower by orders of magnitude, showing that they are negligible.

WO_3.—Table V contains the measured pressures. X-Ray diffraction patterns of the condensate showed only WO_3 lines. According to Berkowitz, Chupka and Inghram[20] the vapor consists of 84.9% trimer and 15.1% monomer at 1120°. Over our temperature range of 267° this ratio changes considerably. Inasmuch as the trimer predominates, negligible error is introduced by considering the gas as composed only of $(WO_3)_3$. The Clausius–Clapeyron equation gives

$$4.576 \log P(WO_3)_3 = -\frac{107,950}{T} + 54.13 \pm 0.50$$

where P is in atmospheres.

WO_2.—The partial pressures of $(WO_3)_3$ above WO_2–W are given in Table VI. X-Ray diffraction patterns of the condensate showed only WO_2 lines, identifying the gas phase as $(WO_3)_x$. A platinum crucible containing 255.8 mg. of pure WO_2 was heated *in vacuo* at 1327° to constant weight, producing 73.7 mg. of residue. A yield of 72.6 mg. is calculated for the reaction

$$3/2WO_2(s) \longrightarrow \frac{1}{x}(WO_3)_x(g) + 1/2W(s) \qquad (4)$$

indicating that $WO_2(s)$ disproportionates completely.

(19) The presence of $MoO_2(s)$ in the condensate cannot be excluded since the condensate from the vapor over $MoO_2(s)$ was amorphous.

(20) J. Berkowitz, W. A. Chupka and M. G. Inghram, *J. Chem. Phys.*, **27**, 85 (1957).

TABLE IV

VAPOR PRESSURE ABOVE MoO_2 + Mo

Temp., °K.	Effective[a] time, sec.	Wt. loss, g.	MoO_2 pressure, atm. × 10^4	ΔH_0^0,[b] kcal.	MoO_3 pressure, atm. × 10^4	ΔH_0^0,[c] kcal.
1818	2221	0.0254	1.01	128.2	2.33	131.6
1835	1314	.0167	1.13	128.8	2.59	130.6
1861	830	.0176	1.89	128.8	4.36	132.4
1905	767	.0229	2.75	128.5	6.35	134.0
1949	7797	.3585	4.19	131.5	9.69	135.6
1984	275	.0306	10.5	130.5	23.7	135.2
2028	615	.0992	15.0	132.0	34.7	136.0
				Av. 129.8 ± 1.4		Av. 133.6 ± 1.8

[a] Effective area = 2.80×10^{-3} cm.^{2} [b] ΔH_0^0 for reaction $MoO_2(s) \rightarrow MoO_2(g)$. [c] ΔH_0^0 for reaction $3/2\ MoO_2(s) \rightarrow MoO_3(g) + 1/2$ Mo(s).

TABLE V

VAPOR PRESSURE OF TUNGSTEN TRIOXIDE

Temp., °K.	Effective time, sec.	Wt. loss, g.	Effective area, cm.^{2} × 10^3	$(WO_3)_3$ press., atm. × 10^6
1314	17636	0.00146	2.654	0.9670
1340	17794	.00168	2.656	1.113
1388	3136	.00279	2.659	10.65
1464	755	.00253	2.664	41.15
1503	940	.00676	2.667	89.43
1535	1000	.02136	2.669	268.2
1560	398	.02405	2.670	764.4
1569	650	.03423	2.671	668.0
1581	594	.03865	2.672	827.9

TABLE VI

VAPORIZATION DATA FOR WO_2 + W

Temp., °K.	Effective time, sec.	Wt. loss, g.	Effective area, cm.^{2} × 10^3	$(WO_3)_3$ press., atm. × 10^6
1324	17314	0.00111	2.686	0.7430
1375	15115	.00513	2.689	4.002
1507	1910	.01603	2.698	103.3
1593	1179	.01866	2.704	199.8
1595	745	.01377	2.704	233.8
1603	902	.02436	2.705	341.9
1658	715	.07169	2.709	1289.0

For the reaction

$$3/2WO_2(s) \longrightarrow WO_3(s) + \frac{1}{2}W(s)$$

we calculate $\Delta F_{1500} = -1.8 \pm 3.4$ kcal. on the basis of the heats of formation of $WO_2(s)$[16,21] and $WO_3(s)$[16,21] and the free energy functions in Table I. Since ΔF is close to zero, the activity of WO_3 in $WO_2(s)$ is close to unity. We have shown that the only volatile compound above WO_2 + W has the composition $(WO_3)_x$. Therefore, with the activity of WO_3 close to unity and with only compounds of the composition $(WO_3)_x$ present in the gas phase, the gas constitution above WO_2 + W is the same as the composition above $WO_3(s)$, that is, $(WO_3)_3$. The Clausius–Clapeyron equation gives

$$4.576 \log P(WO_3)_3 = -\frac{90{,}156}{T} + 40.52 \pm 0.59$$

where P is in atmospheres. From this equation and from that for the vapor pressure above $WO_3(s)$, we calculate ΔF_{1500} for reaction (4) to be $\Delta F_{1500} = 2.6 \pm 1.2$ kcal. This is in good agreement with the value calculated from the heats of formation.

(21) Selected Values of Chemical Thermodynamic Properties, National Bureau of Standards Circ. 500.

Discussion of the Data

The results of various investigations for the heat and entropy of vaporization of MoO_3 together with the calculated free energy change at 900°K. are given in Table VII. The agreement between the last 3 authors is very good, if one takes into account that Ariya's data extend only over a 40° temperature range, and therefore the determination of ΔH_T and ΔS_T may be subject to a large error.

TABLE VII

HEAT AND ENTROPY OF VAPORIZATION OF MoO_3

Author	Temp., °K.	ΔH_T, kcal./mole of $(MoO_3)_3$	ΔS_T, e.u.	ΔF_{900}, kcal./mole of $(MoO_3)_3$
Ueno[3], [a]	928	63.7	46.5	22.9
Ariya[4], [a]	964	68.1	56.9	18.8
Berkowitz[17]	850	80.0	65.6	21.0
This research	900	79.7	67.8	18.7

[a] The values for ΔF_{900} from Ariya[4] and Ueno's[3] data are corrected to $(MoO_3)_3(g)$.

In the absence of heat capacity data for $(MoO_3)_3$(g) we will assume that ΔH_T and ΔS_T are temperature independent. The heat of formation of $MoO_3(s)$,[22] which is $\Delta Hf_{298} = -178.0 \pm 0.1$ kcal./mole; that of $MoO_2(s)$,[18] which is $\Delta Hf_{298} = -140.9 \pm 0.1$; and our data combine to produce a heat of formation for $1/4Mo_4O_{11}$ of $\Delta Hf_{298} = -166.0 \pm 1.6$. This value is in good agreement with that of $\Delta Hf_{298} = -167.7 \pm 5$ kcal./mole which is estimated by Brewer.[7]

The entropy S_{298} of Mo_4O_{11} can be calculated using S_{298} for MoO_3[6] and MoO_2.[6] A value of $S_{298} = 88.9 \pm 1.4$ e.u. is obtained, a figure much larger than the 74.4 e.u. arrived at by adding $3MoO_3$ and MoO_2. The greater stability of Mo_4O_{11} is due to a large entropy effect.

TABLE VIII

HEAT AND ENTROPY OF VAPORIZATION OF WO_3

Author	Temp., °K.	ΔH_T kcal./mole of $(WO_3)_3$	ΔS_T, e.u.	ΔF_{1368} kcal./mole of $(WO_3)_3$
Ueno[1], [a]	1368	112.6	57.3	34.2
Berkowitz[20]	1368	130	69.5	34.9
This research	1500	108.0	54.1	33.9

[a] Ueno's[1] data are corrected to $(WO_3)_3(g)$.

The results of various investigations for the heat

(22) B. A. Staskiewicz, J. R. Tucker, and P. E. Snyder, *J. Am. Chem. Soc.*, **77**, 2987 (1955).

and entropy of vaporization of WO_3, together with the calculated free energy change at 1368°K., are given in Table VIII. The agreement among the three authors is good on ΔF_{1368}, whereas a discrepancy exists between Berkowitz's[20] values on the one hand and Ueno's[2] and ours on the other for ΔH_T and ΔS_T.

Combining our data with the heats of vaporization of Mo[6] and the dissociation energy of O_2,[23] we can calculate the dissociation energies given in Table IX.

(23) P. Brix and G. Herzberg, *Can. J. Phys.*, **32**, 110 (1954).

TABLE IX

HEATS OF DISSOCIATION

Reaction	ΔH^0_0, kcal./mole
$MoO_2(g) \longrightarrow Mo(g) + 2O$	284.6 ± 1.7
$MoO_3(g) \longrightarrow Mo(g) + 3O$	410.3 ± 2.4
$(MoO_3)_3(g) \longrightarrow 3MoO_3(g)$	220.9 ± 7.5

THE DIELECTRIC RELAXATION TIMES OF SOME AMINES, DIMETHYLTHIANTHRENE, DIBENZOTHIOPHENE, TRIPHENYLPHOSPHINE AND TRIPHENYLARSINE

BY A. H. PRICE[1]

The Edward Davies Chemistry Laboratories, University College of Wales, Aberystwyth, Wales

Received August 18, 1957

The effective dielectric relaxation time of a polar solute will vary markedly from the value for an equivalent rigid structure if the molecule contains internal relaxation mechanisms arising from rotating groups, inversion phenomena (as in ammonia), or flapping (as in thianthrene), provided the associated frequencies are not too different from those used in the measurements. Studies of a number of different model structures have been made in this way from 3×10^4 to 10^8 c./s. With the exception of tribenzylamine the molecules studied appear to be essentially rigid. The influence of the viscosity of the medium upon the relaxation times and the adequacy of the Hill treatment of this factor is also considered.

The frequency dependence of the dielectric properties of materials was first studied by Debye. He related the macroscopic dielectric properties with the molecular structure, assuming a rigid spherical molecule having a single relaxation time proportional to the macroscopic viscosity of the medium and the molecular volume. Further extensions of the theory have been made to include non-spherical molecules, distributions of relaxation times and the correct form of the viscosity factor.[2] The work described here is a survey of the dielectric absorptions of a series of molecules in the pure state and in solution, with the particular aim of assessing whether they behave as rigid structures or not. The influence of non-rigidity is very apparent for many polar solutes recently studied.[3]

Experimental

The dielectric properties of the materials were studied in the frequency range 3×10^4 to 10^8 c./sec. using a Hartshorn-Ward apparatus.[4] The general characteristics and limits of accuracy found for this apparatus have been discussed by Aihara and Davies.[3] Briefly, the loss tangent ($\tan \delta$) could be measured to an accuracy of $\pm 3\%$ or $\pm 0.06 \times 10^{-3}$ (whichever was the greater) and the permittivity to $\pm 1\%$.

The systems studied were either pure liquids or solutions in Nujol, xylene or tetrachloroethylene. For solutions the loss tangent was taken as the difference between the solution and solvent loss tangent, but a correction had to be applied to the solvent loss with Nujol as the solution viscosity was different from the viscosity of the pure solvent. Thus, Nujol (viscosity approximately 200 c.p.) had a loss tangent of 0.93×10^{-3} at 70 Mc./sec., while a solution of Nujol in tetrachloroethylene (which showed no measurable loss tangent) of viscosity 29 c.p., had a loss tangent of 0.60×10^{-3} at the same frequency. Initially, this change in solvent loss tangent was not fully appreciated and led us erroneously to postulate a resonance absorption for triethylamine.[5] The other solvents behaved normally. The xylene properties have been described elsewhere,[3] while tetrachloroethylene showed no loss tangent in the range of the apparatus.

The relaxation time (τ) is calculated for the pure media and for the concentrated solutions from the Debye equation 1

$$\tan \delta = \frac{(\epsilon_s - n^2)}{\epsilon'} \frac{\omega\tau}{1 + \omega^2\tau^2} \qquad (1)$$

where ϵ_s is the static dielectric constant, n^2 the square of the refractive index and ϵ' the permittivity at frequency f (where $\omega = 2\pi f$). For dilute solutions where $(\epsilon_s - n^2)$ is very small equation 2 is used

$$\tan \delta = \frac{(\epsilon_s + 2)^2}{\epsilon'} \frac{\pi N_0 c \mu^2}{6750kT} \frac{\omega\tau}{1 + \omega^2\tau^2} \qquad (2)$$

where c, N_0, T, k and μ are the molar concentration, Avogadro's number, the absolute temperature, Boltzmann's constant and the dipole moment, respectively.

Both equations 1 and 2 may be expressed in the form

$$\frac{\omega}{\tan \delta} = \frac{\tau}{B} \omega^2 + \frac{1}{B\tau} \qquad (3)$$

Thus a plot of $\omega/\tan \delta$ against ω^2 should be linear with slope τ/B and intercept $1/\tau B$. However, if $\omega^2\tau^2 << 1$ then equation 3 reduces to

$$\frac{\tan \delta}{\omega} = B\tau = \text{const.} \qquad (4)$$

Generally, it would seem that the apparent relaxation times are accurate to about $\pm 5\%$ if derived using equation 1, but are only accurate to about $\pm 10\%$ if equation 2 is used, due to the uncertainty in determining the value of the dipole moment.

Most of the measurements were made at room temperatures but some were made on triisoamylamine at $-13°$ using an auxiliary capacitor. This capacitor measured loss tangents to an accuracy of about $\pm 10\%$ and permit-

(1) Atomic Weapons Research Establishment, Aldermaston, Berks, England.

(2) (a) C. J. F. Bottcher, "Theory of Electric Polarization," Elsevier Publishing Co., Amsterdam, 1953; (b) M. Davies, *Quart. Revs. London*, **8**, 250 (1954).

(3) A. Aihara and M. Davies, *J. Coll. Sci.*, **11**, 671 (1956).

(4) L. Hartshorn and W. H. Ward, *J.I.E.E.*, **79**, 597 (1936).

(5) M. Davies and A. H. Price, *J. phys. rad.*, **15**, 307 (1954).

TABLE I

Solute	Solvent	Molar concn. c	t, °C.	η, c.p.	$\tau \times 10^{12}$, sec.	ϵ	n_D	Observations
Diethyl-aniline	Pure		20	2.16	70 ± 2	5.22	1.543	
	C_2Cl_4	4.98	20	1.64	61 ± 2	4.55	1.535	
	C_2Cl_4	3.63	20	1.29	52 ± 2	3.92	1.528	
	C_2Cl_4	2.47	20	1.13	46 ± 3	3.40	1.521	
	C_2Cl_4	1.80	20	1.06	42 ± 2	3.14	1.517	
	C_2Cl_4	0.92	20	0.97	37 ± 2	2.69	1.512	
	C_2Cl_4	.50	20	.94	34 ± 2	2.50	1.509	
	Nujol	.33	18		330 ± 30	2.35		$\mu = 1.91$ D[8]
Tri-isoamyl-amine	Pure		21	2.61	120 ± 3	2.29	1.433	
	Pure		13		1100 ± 100	2.38	1.435	τ from eq. 3
	Pure		−19		3000 ± 1000	2.3		τ from eq. 3
	C_2Cl_4	2.53	21	1.86	83 ± 4	2.31	1.448	
	C_2Cl_4	1.79	21	1.28	63 ± 4	2.32	1.469	
	C_2Cl_4	0.90	21	1.05	51 ± 2	2.32	1.487	
	C_2Cl_4	.44	21	0.99	40 ± 3	2.32	1.495	
	Xyl.	.66	22	0.81	54 ± 4	2.33		$\mu = 0.79$ D
	Xyl.	1.64	22	1.30	54 ± 7	2.32		calcd. from Onsager's eq.[9]
Tribenzyl-amine	Nujol	0.17	20		4240 ± 90	2.20		Absorption peak obsd.
N-Methyl-dioctyl-amine	Xyl.	0.80	21		60 ± 20	2.38		$\mu = 0.7$ D (value estd. from that of other aliphatic amines)
N-Methyl-carbazole	Xyl.	1.26	18		31 ± 3	2.83	1.527	
	Xyl.	0.63	18		22 ± 1	2.59	1.511	
Tri-*n*-propyl-amine	Pure		22	0.66	24 ± 1	2.29	1.418	
	Nujol	1.49	21	25	76 ± 3	2.21		$\mu = 0.68$ D[8]
Triphenyl-arsine	Xyl.	1.48	20		90 ± 6	2.68		$\mu = 1.07$ D[10]
	Xyl.	0.63	20		90 ± 2	2.53		
Triphenyl-phosphine	Xyl.	1.48	18		79 ± 3	2.84		$\mu = 1.39$ D[11]
	Xyl.	0.48	18		63 ± 4	2.55		
Dimethylthi-anthrene	Pure		20	2210	28300 ± 300	4.58	1.675	Absorption peak obsd.
	C_2Cl_4	4.32	20	70	2200 ± 80	4.27	1.055	
	C_2Cl_4	2.38	20	2.95	174 ± 11	3.34	1.585	
	C_2Cl_4	0.72	20	1.28	76 ± 12	2.68	1.536	
	Xyl.	2.15	16.5		82 ± 3	3.06	1.552	
	Xyl.	1.02	16.5		54 ± 3	2.74	1.528	
Dibenzothio-phene	C_2Cl_4	0.85	20	1.24	30 ± 3	2.43		$\mu = 0.85$ D[12]

tivities to about ±5%. It had an effective upper frequency limit of about 20 Mc./sec. at −18°.

Viscosities were measured at 20.00 ± 0.05° using Ostwald viscometers. A low viscosity instrument was calibrated using benzene and another using a solution of tetrachloroethylene in Nujol whose viscosity was known: the viscosities were accurate to at least ±1%. Densities of solutions and liquids were determined to a (sufficient) similar accuracy at 20°. Refractive index (n_D) values were obtained on an Abbe refractometer.

Materials.—All chemicals, unless of "Analar" grade, were purified before use, and their physical properties checked against the literature values. Xylene was prepared as described by Aihara and Davies.[3] Nujol (*i.e.*, medicinal paraffin) was used without further purification. Tetrachloroethylene was dried and fractionated. Most other liquid solutes were dried over "Analar" potassium hydroxide and fractionally distilled *in vacuo*. Commercial 2,6-dimethylthianthrene and N-methyldioctylamine were so distilled a few times. The solid solutes were recrystallized from absolute alcohol and dried. N-Methylcarbazole was prepared from carbazole and dimethyl sulfate by the method of Stevens and Tucker.[6] The product was recrystallized from absolute alcohol, m.p. 87° (lit.[7] 87°).

Results

The experimental results are summarized in Table I. Where no refractive index measurements were made the relaxation time is calculated using equation 2 and the literature value for the dipole moment (quoted in the last column). Otherwise the relaxation time is calculated from equation 1.

The viscosity is given in centipoise units (c.p.); n_D represents the refractive index; "absorption peak observed" indicates the relaxation time is obtained by direct observation of the frequency at which maximum absorption occurs.

(6) T. S. Stevens and S. H. Tucker, *J. Chem. Soc.*, **123**, 2145 (1929).

(7) Beilstein, "Handbuch der Organische Chemie," Vol. 20, Springer, Berlin, p. 436.

(8) E. G. Cowley, *J. Chem. Soc.*, 3557 (1952).

(9) L. Onsager, *J. Am. Chem. Soc.*, **58**, 1486 (1936).

(10) E. Bergmann and W. Schutz, *Z. physik. Chem.*, **B19**, 401 (1932).

(11) G. M. Phillips, J. S. Hunter and L. E. Sutton, *J. Chem. Soc.*, 146 (1945).

(12) R. G. Charles and H. Freiser, *J. Am. Chem. Soc.*, **72**, 2233 (1950).

Discussion

Diethylaniline.—The simple Debye theory predicts that

$$\tau = \frac{3V\eta}{kT} \qquad (5)$$

(where V = molecular volume) and suggests that for a particular solute τ/η will be constant. For diethylaniline in tetrachloroethylene this factor varies between 32 and 40. Comparison of the molecular volume calculated from the mean value of τ/η, with that found from the density of the pure liquid (assumed to be a system of close-packed spheres) shows that the former is 0.26 times the latter. This factor is thus a plausible estimate of the ratio of microscopic to macroscopic viscosity in this solute–solvent case.

For pure liquids Miss Hill[13] has deduced

$$\tau = \frac{3(3 - \sqrt{2})\kappa^2\eta\sigma}{2kT} \qquad (6)$$

where κ^2 is a function of the molecular moment of inertia, η and σ the liquid viscosity and the molecular radii, respectively. For solutions

$$\tau = \frac{1}{2kT}(f_A 6\kappa^2_{AB}\sigma_{AB}\eta_{AB}) + f_B\tau_B \qquad (7)$$

where τ is the observed relaxation time, τ_B that of the pure solute; the subscripts A and B refer to the solvent and solute, respectively, and AB to the mutual solute–solvent effect; f denotes the molar fraction. The mutual viscosity factor (η_{AB}) may be calculated from the variation of the solution viscosity with concentration, and κ^2_{AB} from the masses and moments of inertia of the solute and solvent. Equation 7 shows that the relaxation time should be a linear function of the solute molar fraction. This is found to be so for tetrachloroethylene solutions of diethylaniline, and a moment of inertia of 790×10^{-40} g. cm.^{2} is deduced for diethylaniline. From models an estimated mean value for the planar structure of diethylaniline, taking into account the possible extreme positions of the ethyl groups is 700×10^{-40} g. cm.^{2}. To this degree of agreement, which is probably well within the uncertainty of measuring the moment of inertia the Hill relations are satisfied on the basis of a completely rigid diethylaniline molecule.

Diethylaniline in Nujol has a relaxation time of 330×10^{-12} sec. Comparison with benzophenone in Nujol[14] ($\tau = 295 \times 10^{-12}$ sec.) suggests that diethylaniline again behaves as a rigid structure. The ratio of the apparent microscopic to macroscopic viscosities in Nujol solutions of diethylaniline appears to be 0.02. The corresponding ratio for benzophenone is 0.01.

Solutions of diethylaniline in tetrachloroethylene show no associative effects, as is established by the linear dependence of the solution dielectric constant, refractive index and dielectric absorption (at one particular frequency) on concentration.

Triisoamylamine.—Using the relation

$$\tau = \frac{h}{kT}e^{\Delta G_\epsilon/RT} \qquad (8)$$

where ΔG_ϵ is the molar free energy of activation, the data for pure triisoamylamine gave $\Delta G_\epsilon = 4$ kcal./mole, and the related $\Delta H_\epsilon = 7$ kcal./mole, $\Delta S_\epsilon = 10$ cal./°K./mole. From viscosity data[15] the activation energy for viscous flow (ΔG_η) is 4.6 kcal./mole. This suggests a close similarity between the mechanism underlying both processes and, hence, that the dielectric relaxation in the pure liquid arises from the rotation of the whole molecule effectively as a rigid structure.

As in diethylaniline, the ratio of the relaxation time of triisoamylamine in tetrachloroethylene to solution viscosity is not constant. However, from the mean value it is deduced that the ratio of the apparent microscopic to macroscopic viscosity is 0.17. The relaxation time is a linear function of the molar fraction and, hence, the system follows Hill's equations. A value of 650×10^{-40} g. cm.^{2} is found for the moment of inertia of triisoamylamine. By representing the fully extended isoamyl groups as single masses acting at their center of mass, the moment of inertia of the triisoamylamine molecule is estimated as 990×10^{-40} g. cm.^{2}. Consideration of the assumptions involved in estimating this moment of inertia and of the alternative configurations possible for the molecule, suggest that this degree of agreement is sufficiently close to imply that the dielectric relaxation process observed here is due to the rotation of the whole molecule.

Comparison of the relaxation time of triisoamylamine in xylene and in tetrachloroethylene suggest that the same mechanism underlies the dielectric relaxation process in both solvents. In xylene the ratio of the microscopic to macroscopic viscosity is 0.21.

For tri-isoamylamine in tetrachloroethylene the dielectric constant, refractive index and the dielectric absorption (at one particular frequency) vary linearly with the solute molar fraction. This shows that associative effects are absent from this system.

Tri-*n*-propylamine.—From the Debye equations the ratio of the microscopic to macroscopic viscosity is found to be 0.21 for the pure liquid. Comparison of the relaxation time for pure tri-*n*-propylamine and pure triisoamylamine shows that the former behaves as a rigid molecule. This is confirmed by the result in the Nujol solution (*cf.* diethylaniline in Nujol).

Tribenzylamine.—The variation of loss tangent with frequency for a 0.17 M solution of tribenzylamine in Nujol shows a maximum at a frequency of (37.6 ± 0.8) Mc./sec., corresponding to a relaxation time of 4240×10^{-12} sec. The absorption curve follows the Fuoss–Kirkwood[16] equation

$$\frac{\epsilon''(2 + (1/\epsilon')^2)}{\epsilon_m''(2 \times (1/\epsilon_m')^2)} = \operatorname{sech}\left[\beta \ln\left(\frac{f_m}{f}\right)\right] \qquad (9)$$

where β is the distribution parameter, ϵ'', ϵ' the loss factor and permittivity at frequency f. The subscript m refers to the properties at maximum absorption. This distribution factor (β) is found

(13) N. E. Hill, *Proc. Phys. Soc.*, **67B**, 149 (1954).

(14) W. Jackson and J. G. Powles, *Disc. Faraday Soc.*, **42A**, 101 (1946).

(15) E. C. Bingham and L. W. Spooner, *J. Rheol.*, **3**, 221 (1932).

(16) R. M. Fuoss and J. G. Kirkwood, *J. Am. Chem. Soc.*, **63**, 385 (1941).

to be 0.95. This value is higher than that found for benzophenone in Nujol ($\beta = 0.68$).[14]

Comparison between the relaxation time of tribenzylamine in Nujol with that of benzophenone in the same solvent ($\tau = 295 \times 10^{-12}$ sec.)[14] suggests a value of approximately 440×10^{-12} sec. for the relaxation time of a rigid tribenzylamine molecule. Hence, there must be a contribution to the relaxation process either from internal rotation about a C–N bond or from "inversion" at the nitrogen atom. However, Costain and Sutherland[17] and Weston[18] suggest that the frequency of "inversion" will be in a far lower frequency range, and will not contribute to the absorption in the frequency range studied here. As only one absorption peak was observed in the limited frequency range examined, it was not found possible to determine whether another absorption exists with a relaxation time of about 440×10^{-12} sec.

Taking the solution viscosity as that of Nujol (approx. 200 c.p.) we deduce that the microscopic viscosity is 0.08 times the macroscopic viscosity. The molecules in Nujol show a greater disparity between their microscopic and macroscopic viscosities than they do in xylene, where the foregoing ratio is maintained at approximately 0.2. The ratio of the microscopic to macroscopic viscosity in tribenzylamine is much larger than the value found for benzophenone (0.01) in the same solvent,[14] thus again suggesting a difference in the dielectric relaxation process.

N-Methyldioctylamine.—The dipole moment was estimated as 0.7 *D* by comparison with other long chain aliphatic amines. This gave a relaxation time of 60×10^{-12} sec. for this molecule in xylene. Comparison with *n*-octyl chloride in benzene[19] (which behaves as an effectively rigid molecule) suggests that N-methyldioctylamine also behaves as a rigid molecule.

N-Methylcarbazole.—Comparison with the relaxation time of α-chloronaphthalene in benzene[20] suggests that N-methylcarbazole in xylene behaves as a rigid molecule. This confirms the results of the ultraviolet spectrum of carbazole[21] which shows that the molecule is planar and the nitrogen atom trigonally hybridized.

General Discussion on the Amines.—No evidence was found of a possible "inversion" process in the frequency range studied. All the amines, except tribenzylamine, behaved effectively as rigid structures. The relaxation times for the pure liquids tri-*n*-propylamine, diethylaniline and triisoamylamine increased with molecular size. The same general relationship holds for the substituted amines studied here—whether in tetrachloroethylene, xylene or Nujol solutions. The ratio of the microscopic to macroscopic viscosities for diethylaniline and triisoamylamine in tetrachloroethylene and xylene is approximately 0.2. It might have been expected that the ratio in xylene would be closer to the value of 0.36 found for various solutes in benzene.[22]

Triphenylarsine and Triphenylphosphine.—Comparison of the molecular volumes of these two solutes (assuming a close packing of spherical molecules) suggests that they should have an approximately similar relaxation time. It is found that the relaxation time of triphenylarsine is greater than that of the triphenylphosphine. Comparison of these relaxation times with that of benzophenone in benzene[14] does not provide any conclusive evidence for the non-rigidity of the pyramidal molecules, so that, as for the amines, there is no suggestion of an "inversion" process near the frequency range used in these studies.

Dimethylthianthrene.—The dielectric absorption–frequency curve for dimethylthianthrene shows a maximum at 5.26 ± 0.06 Mc./s., corresponding to a relaxation time of 28.3×10^{-9} sec. A Fuoss–Kirkwood[16] distribution of relaxation times is observed with $\beta = 0.89$. When the Cole–Cole plot[23] for the variation of the loss factor (ϵ'') and permittivity (ϵ') at a particular frequency (see Table II) is studied a distribution factor of $h = 0.072$ is obtained. These two distribution factors agree with each other when interconverted using Poley's equation[24]

TABLE II

THE VARIATION OF THE LOSS FACTOR (ϵ'') AND PERMITTIVITY (ϵ') OF DIMETHYLTHIANTHRENE WITH FREQUENCY (f) AT 20°

Mc./sec.	ϵ''	ϵ'
0.113	0.037	4.58
.194	.063	4.58
.351	.123	4.57
.650	.201	4.52
1.37	.400	4.45
3.18	.669	3.75
7.25	.655	3.62
15.1	.483	3.28
32.3	.305	3.08

Solutions in tetrachloroethylene do not follow the Debye equation 3. The mean value of τ/η gives η microscopic/η macroscopic = 0.22. Neither do these solutions follow the Hill equations.[13] The Hill treatment assumes spherical molecules, which is far from the case for the plate-like dimethylthianthrene. Deviations from the Hill theory were found for chlorobenzene in Nujol solutions[13] which may indicate the role of bulky nonspherical molecules in the solvent.

Comparison of the relaxation times of dimethylthianthrene in tetrachloroethylene and in xylene with the structurally somewhat similar *o,o'*-dimethyldiphenyl in carbon tetrachloride[25] suggests that dimethylthianthrene behaves as a rigid molecule in both these solvents. The solutions in xylene have a smaller relaxation time than those in tetrachloroethylene of a similar viscosity. This is perhaps due to the greater solute–solvent component dipole interactions found in the latter sol-

(17) C. C. Costain and G. B. B. M. Sutherland, THIS JOURNAL, **56**, 321 (1952).
(18) R. E. Weston, *J. Am. Chem. Soc.*, **76**, 2645 (1954).
(19) E. Fischer, *Z. Naturforsch.*, **4a**, 707 (1949).
(20) A. Spernol and K. Wirtz, *ibid.*, **8a**, 522 (1953).
(21) E. Kernel and C. Wiegand, *ibid.*, **3b**, 93 (1948).
(22) E. Fischer, *Physik. Z.*, **40**, 645 (1939).
(23) R. H. Cole and K. S. Cole, *J. Chem. Phys.*, **9**, 341 (1941).
(24) J. Poley, see ref. 2a, p. 371, ref. 37.
(25) H. Hase, *Z. Naturforsch.*, **8a**, 695 (1953).

vent. Similar effects have been found in the comparison of cyclohexane and carbon tetrachloride as solvents.[26]

For dimethylthianthrene η microscopic/η macroscopic appears to be about 0.07, while the mean value for the solutions in tetrachloroethylene is 0.22. From the values of this ratio obtained from the amines and for dimethylthianthrene it appears that the greater the solution viscosity the smaller is this ratio.

(26) D. H. Whiffen, *Trans. Faraday Soc.*, **46**, 130 (1950).

Dibenzothiophene.—Comparison with the earlier results for N-methylcarbazole shows that this molecule behaves as a rigid structure and this confirms the deductions from ultraviolet spectra.[21]

Acknowledgments.—The author wishes to thank Dr. Mansel Davies for his guidance and help during this work; also the British Cotton Industry Research Association for the award of a Shirley Research Fellowship.

URANIUM EXTRACTION BY DI-*n*-DECYLAMINE SULFATE

BY W. J. McDOWELL AND C. F. BAES, JR.

Oak Ridge National Laboratory,[1] *Oak Ridge, Tennessee*

Received August 26, 1957

The extraction of uranium from sulfuric acid–sodium sulfate solutions by di-*n*-decylamine sulfate in benzene is examined as a function of uranium, amine, acid and sulfate ion concentration. The stoichiometry of the principal organic complex is uranium:sulfate:amine = 1:4:6. The dependence of uranium extraction on total uranium concentration and on extractant concentration is discussed in terms of the extensive association of di-*n*-decylamine sulfate in the organic phase. Data for variation of sulfate ion concentration are shown to be consistent with formation quotients of aqueous UO_2SO_4 and $UO_2(SO_4)_2^{=}$ to be found in the literature. No evidence was found for the formation of a $UO_2(SO_4)_3^{=4}$ complex.

I. Introduction

It has been known for some time that high molecular weight amines in organic diluents would extract acids and a variety of metal ions from aqueous solutions.[2,3] The use of these amines to extract uranium from sulfuric acid leach liquors has been of special interest[2] during the last few years; hence, it has become pertinent to investigate some of the fundamental chemistry of such systems. In this field of investigation Allen has published studies of the equilibria of tri-*n*-octylamine and di-*n*-decylamine with sulfuric acid[4]; Baes has published a study of the extraction of iron(III) with di-*n*-decylamine.[5]

It has been noted[2-5] that certain of these extraction measurements indicate the sulfate salts of long chain amines to be highly associated in organic diluents. More recently, light scattering measurements by Allen[6] have confirmed that this often is true. In the case of di-*n*-decylamine sulfate–benzene solutions, his measurements indicate the presence of aggregates with a molecular weight of *ca.* 30,000.

The work described here consists of a detailed examination of the extraction of uranium from acidic sulfate solutions by benzene solutions of di-*n*-decylamine under carefully controlled conditions. This amine was chosen because it was an available representative of a large class of useful amine extractants. In addition, the aqueous solubility of this amine and its sulfate salts was immeasurably small (*e.g.*, $< 1 \times 10^{-5}$ *N* amine sulfate) in the systems studied.

For the sake of brevity, in this paper DDA will be understood to be di-*n*-decylamine and DDAS to be di-*n*-decylamine sulfate with various accompanying amounts of di-*n*-decylamine bisulfate. Concentrations of DDAS will be given as normality, *N*, *i.e.*, the total number of equivalents of amine per liter, whether present as the normal sulfate or as a sulfate–bisulfate mixture. Other solute concentrations will be given, as usual, in terms of molarity, *M*. Brackets will be used to indicate concentration in equivalents or moles per liter, whichever is appropriate from the definitions above.

II. Experimental

Reagents.—Allen[4b] has outlined the method by which the authors prepared the DDA used in this and most other fundamental research in this Laboratory. It is of value to point out in addition to the information given by Allen that the deammonation of pure *n*-decylamine by rapid heating to 140° without reflux was the only one of several methods tried which gave a good yield of di-*n*-decylamine (60% as compared to 10 or 20% by other methods). Low temperature reaction with Raney nickel in a low boiling solvent under reflux and reactions of *n*-decylamine with *n*-bromodecane among others produced largely tri-*n*-decylamine.

The final product material (pure white paraffin-like crystals) had a boiling range of 195-196° at 5 ± 0.1 mm. pressure. This material was analyzed (see below) and found to have a tertiary amine content of 3 ± 1%, a primary amine content of less than 0.5%, and an apparent molecular weight of 298.6 (theoretical for di-*n*-decylamine, 297.6). Since Allen[4b] has shown that di-*n*-decyl and tri-*n*-octylamines behave very similarly in the range of aqueous acid activity in which amine bisulfate is present and it is believed that they are also similar in their uranium extraction behavior, the presence of 3% tri-*n*-decylamine should not appreciably affect the results presented here. Standard solutions of DDA in benzene were made by weight from the solid amine.

(1) Operated for the United States Atomic Energy Commission by Union Carbide Nuclear Company.

(2) E. L. Smith and J. E. Page, *J. Soc. Chem. Ind.*, **67**, 48 (Feb. 1948); J. Y. Ellenburg, G. W. Leddicotte and F. L. Moore, *Anal. Chem.*, **26**, 1045 (1954); H. A. Mahlman, G. W. Leddicotte and F. L. Moore, *ibid.*, **26**, 1939 (1954); D. J. Crouse and J. O. Denis, ORNL-1859, Oak Ridge National Laboratory, 1955; D. J. Crouse and K. B. Brown, ORNL-1959, Oak Ridge National Laboratory, 1955; Narrative Status Report, ORNL-2002, Oak Ridge National Laboratory, 1955; D. J. Crouse, K. B. Brown, W. D. Arnold, J. G. Moore, R. S. Lowrie, ORNL-2099, Oak Ridge National Laboratory, 1956.

(3) K. B. Brown, C. F. Coleman, D. J. Crouse, J. O. Denis and J. G. Moore, ORNL-1734, Oak Ridge National Laboratory, 1954.

(4) (a) K. A. Allen, THIS JOURNAL, **60**, 239 (1956); (b) **60**, 943 (1956).

(5) C. F. Baes, ORNL-1930, Oak Ridge National Laboratory, 1956.

(6) K. A. Allen, THIS JOURNAL, to be published.

The sulfate usually was prepared by contact with aqueous solutions of H_2SO_4 before dilution to final volume. Stock solutions of DDA and DDAS were stored in a 25° water-bath under an argon atmosphere.

The uranyl sulfate used in this research was prepared at this installation and was found to contain 0.032% total impurities with a SO_4^{--}/U mole ratio = 0.998. The benzene was reagent grade, thiophene free. All other reagents were standard "reagent grade."

Method of Equilibration.—All equilibrations were done in separatory funnels unless otherwise noted. These were shaken with a mechanical shaking device in a constant temperature bath at 25 ± 0.05°. Equilibration rate studies have shown that under the conditions of these experiments complete equilibrium was attained in less than 1 minute; however, equilibration times were 30 minutes or more for all experiments. Pre-equilibration of each of the solvents with that of the other phase reduced volume changes due to the small solubility of one solvent in the other.

In all equilibrations (except those at high *p*H involving hydrolysis of the uranium) DDAS in benzene was pre-equilibrated with an aqueous phase identical with that from which uranium distribution was to be studied but containing no uranium. Successive samples of aqueous phase were contacted with a given sample of organic phase until there was no change in aqueous acid concentration. Usually three to five such equilibrations were required. In most cases samples of pre-equilibrated organic phase were reserved for analysis. The phase ratio in all equilibrations was 1:1.

In most of the uranium extractions individual equilibrations with aqueous and organic phases of known composition were made; however, the special case of organic phase dilution at constant amine to uranium ratio was done differently. A 0.250 *N* benzene solution of DDAS was pre-equilibrated with an aqueous phase 1.00 *M* in total sulfate at the required *p*H. Following this, sufficient uranyl sulfate was introduced to the system to give an amine:uranium ratio of 50:1 in the organic phase. Samples of the organic phase were then diluted by various amounts and re-equilibrated with samples of the original aqueous phase. Each of the resulting aqueous phases was analyzed for uranium.

Analytical Methods.—Uranium analyses were obtained by volumetric, colorimetric and fluorimetric methods. Volumetric analyses were by the dichromate method of Kolthoff and Lingane.[7] Colorimetric analyses were done by the ferrocyanide method[8] because of its compatibility with large amounts of sulfate. The usefulness of the method was extended to lower uranium levels (1×10^{-6} *M*) by the use of 10 cm. absorption cells. Fluorimetric analyses[9] ($<1 \times 10^{-5}$ *M*) were done by the carbonate flux method regularly used in this Laboratory. In general, samples of concentrations greater than 0.005 *M* were analyzed with an accuracy of ±0.5% or better, those between 5×10^{-3} and 5×10^{-5} with an accuracy of ±2 to 5% and those from 5×10^{-5} to 4×10^{-7} with an accuracy of ±5 to 10%.[10]

Analysis of both aqueous and organic phases for acid was necessary. Aqueous phases were titrated with sodium hydroxide using phenolphthalein.[11] Organic phase acid was titrated with standard sodium ethoxide in a 75% benzene–25% ethyl alcohol mixture using bromthymol blue as the indicator. The sodium ethoxide was standardized against Bureau of Standards benzoic acid. Accuracy of all acid titrations was ±0.5% or better.

Organic amine concentrations were determined by potentiometric titration with standard perchloric acid in dioxane.[12] If the amine was in the form of the sulfate salt it was converted to the free amine previous to titration by the use of excess base in the presence of an aqueous phase. Concentrations of all amine solutions were known to ±1% or better.

III. Results and Discussion

(a) Sulfuric Acid–Amine Sulfate–Amine Bisulfate Equilibria.—In preparation for uranium extraction studies in 1.00 *M* sulfate medium, equilibrations of sulfuric acid of various concentrations in 1.00 *M* total sulfate with benzene solutions of 0.1 *N* di-*n*-decylamine were made. The resulting ratios of amine bisulfate to amine sulfate *vs.* aqueous sulfuric acid activity[13] are shown in Fig. 1. The dashed curve represents the results of Allen[4b] for 0.05 and 0.1 *N* DDAS in equilibrium with aqueous solutions containing sulfuric acid alone (as given by his equation 9 with $K_2 = 2600$). The dotted line represents the results of Baes[5] for 0.5 *M* sulfate solutions. Comparison of the three sets of measurements suggests a trend toward lower amine bisulfate contents as the aqueous sulfate level is increased; however, the scatter within each set of measurements is comparable to the differences between them so that this trend may not be real.

Di-*n*-decylamine bisulfate was found to precipitate at an aqueous acid activity of *ca.* 1.4×10^{-4} *M*[3] in satisfactory agreement with Allen's reported value of 1.6×10^{-4} *M*[3]. The area of bisulfate precipitation is indicated in Figs. 1 and 4. The accuracy of the points within the precipitation area are, of course, in question.

(b) Uranium and DDAS Concentration Variation.—Variation in the extraction of uranium into 0.100 *N* DDAS in benzene as a function of uranium concentration has been studied under two sets of aqueous phase conditions. These are: 0.75 *M* Na_2SO_4–0.25 *M* H_2SO_4 (1.00 *M* ΣSO_4 at *p*H 1.00) and 0.958 *M* Na_2SO_4–0.042 *M* H_2SO_4 (1.00 *M* ΣSO_4 at *p*H 2.00). The resulting extraction isotherms (*i.e.*, $[U]_{org}$ *vs.* $[U]_{aq}$, lower curves, Fig. 2), up to 0.004 *M* equilibrium aqueous uranium, appear to be normal, leveling off at a point indicating an amine/uranium ratio of 6. Since lower amine/uranium ratios are found at higher aqueous uranium concentrations, it is apparent that this is not a unique limiting stoichiometry. No additional inflections were found at higher aqueous uranium concentrations, however, and it appears that a ratio of six equivalents of amine per mole of uranium is characteristic of the most important complex species. Additional evidence consistent with this stoichiometry will be presented in Section IIIc.

Below an organic uranium concentration of 0.0167 *M* in 0.1 *N* DDAS (amine/uranium = 6), the extraction coefficient, $E_a^\circ = [U]_{org}/[U]_{aq}$ appears to approach a constant limiting value at each *p*H as the uranium level is decreased (Fig. 2, upper curves). The change in E_a° with change in uranium

(7) I. M. Kolthoff and J. J. Lingane, *J. Am. Chem. Soc.*, **55**, 1871 (1933).

(8) C. B. Rodden, "Analytical Chemistry of the Manhattan Project," McGraw-Hill Book Co., New York, N. Y., 1950, pp. 99–104.

(9) Ref. 8, p. 122.

(10) Concentration by extraction or evaporation usually was employed to obtain analyses in these lower ranges.

(11) In most cases where uranium was present the quantity was not sufficient to affect the accuracy of the titration. If there was sufficient uranium to disturb the end-point, titration was made with a *p*H meter to the *p*H of the existing concentration of stoichiometric uranyl sulfate.

(12) C. D. Wagner, R. H. Brown and E. D. Peters, *J. Am. Chem. Soc.*, **69**, 2609 (1948); **69**, 2611 (1947); C. E. Pifer, E. G. Wollish and M. Schmall, *Anal. Chem.*, **25**, 310 (1953).

(13) The sulfuric acid activity, $a_{H_2SO_4}$ in such solutions is given by the practical activity coefficient $(\gamma\pm)_{H_2SO_4}$, the total molarity of sulfuric acid M_1 and the total molarity of sulfate M_2 as follows: $a_{H_2SO_4} = (\gamma\mp)_{H_2SO_4}(2M_1)^2M_2$. Values of $(\gamma\pm)_{H_2SO_4}$ based on available e.m.f. measurements in sulfuric acid–sodium sulfate solutions are given by one of the authors in another publication.[14] The values used in the present case were obtained from these using available density data to convert from the molality to the molarity scale. It is assumed that the small amount of benzene present in the aqueous solutions will not alter $(\gamma\pm)_{H_2SO_4}$ appreciably.

(14) C. F. Baes, Jr., *J. Am. Chem. Soc.*, **79**, 5611 (1957).

level conforms to

$$E_a^\circ \propto \Sigma[\text{DDAS}] - 6[\text{U}]_{org} \qquad (1)$$

closely at *p*H 1 and fairly close at *p*H 2 (the agreement is indicated in Fig. 3 by the unit slope of curve 1, *p*H 1 and the near unit slope of curve 1, *p*H 2). Thus, if six equivalents of DDAS are associated with each mole of extracted uranium then the above relation indicates a first power dependence of E_a° with $\Sigma[\text{DDAS}] - 6[\text{U}]_{org}$ when the latter is varied directly by changing the amount of diluent instead of indirectly by the extraction of increasing amounts of uranium into the organic phase. In these measurements the ratio $\Sigma[\text{DDAS}]/[\text{U}]_{org}$ was held constant at 50, so that the quantity $(\Sigma[\text{DDAS}] - 6[\text{U}]_{org})$ which is plotted in Fig. 3 is only 6% less than ΣDDAS, and so these curves are not very sensitive to any possible error in the amine:uranium ratio used in the calculation. While the results at *p*H 1 show a region of unit slope (indicating again a proportionality between E_a° and $\Sigma[\text{DDAS}] - 6[\text{U}]_{org}$), there is a region of fractional power dependence at the higher DDAS concentrations at *p*H 1 and throughout the range at *p*H 2, indicating clearly that the simple proportionality in equation 1 does not hold generally if the total extractant concentration is varied.

Since DDAS is present in the organic phase as large aggregates, the most satisfactory interpretation of these data is that the uranium–DDAS complex is incorporated into the aggregates. Obvious alternative interpretations can be ruled out, such as the formation of a single low molecular weight uranium species (E_a° would be virtually constant as the DDAS concentration is changed) or a single polynuclear uranium species (E_a° would increase a $[\text{U}]_{aq}$ is increased at low uranium levels). If it is correct that the uranium–DDAS complex is present in the DDAS aggregates, it is further reasonable to expect that the uranium activity is determined primarily by the composition of the aggregates, *i.e.*, by the ratio $[\text{U}]_{org}/\Sigma[\text{DDAS}]$. Since this ratio is held constant in the case of curves 2, then $[\text{U}]_{aq}$ should be constant at each *p*H, resulting in a direct proportionality between E_a° and $\Sigma[\text{DDAS}]$. This is true only over a limited range at *p*H 1; hence, elsewhere additional factors must influence the organic uranium activity. One possibility is a change of aggregate size with concentration. Until more is known concerning possible changes in aggregate size, a detailed interpretation of these data is not justified.

(c) Stoichiometry of the Uranium(VI)–Amine Sulfate Complex.—Table I summarizes the results of a series of extractions from which it has been possible to obtain an amine–uranium coördination number over a wide range of aqueous acid conditions. In these measurements acid analyses were obtained for a series of uranium free H_2SO_4–Na_2SO_4 solutions and the 0.1036 *N* DDAS in benzene with which they were equilibrated. A portion of each DDAS sample then was used to extract 0.0100 *M* uranium(VI) from an aqueous sample otherwise identical with that with which it had been equilibrated and analysis of the resulting aqueous phase for acid and uranium was made (Table I).[15]

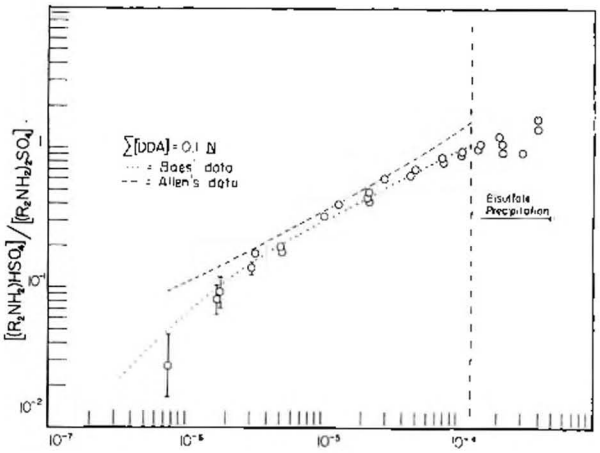

Fig. 1.—Di-*n*-decylamine sulfate–bisulfate ratio in benzene *vs.* sulfuric acid activity in 1.00 *M* total aqueous sulfate.

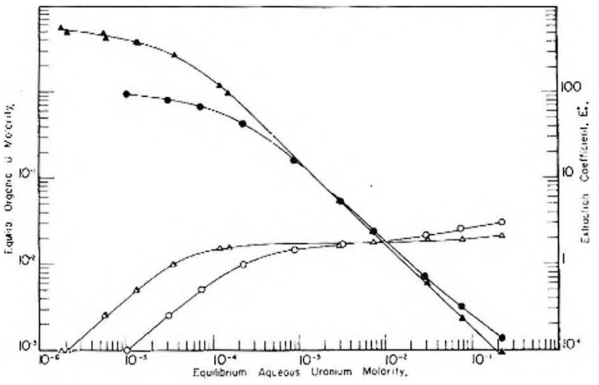

Fig. 2.—Extraction of uranium from sulfate solutions by DDAS in benzene: from aqueous 0.75 *M* in Na_2SO_4; 0.25 *M* in H_2SO_4: -○-, equilibration curve; -●-, E_a°; from aqueous 0.95 *M* in Na_2SO_4; 0.042 *M* in H_2SO_4: -△-, equilibration curve; -▲-, E_a°.

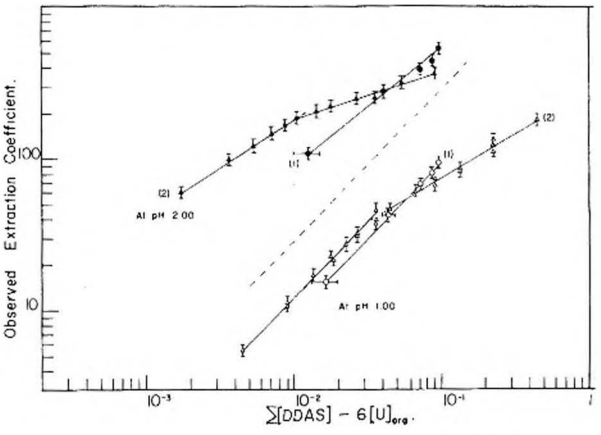

Fig. 3.—The extraction of uranium by DDAS in benzene free amine sulfate variation by (1) loading and (2) direct dilution.

From the change (on extraction of 0.0100 *M* U) in the acid molarity of the aqueous phase and the assumptions (1) that uranium(VI) is extracted to form an amine sulfate–uranyl sulfate complex free

(15) The amount of uranium remaining in the aqueous phase was so small in all cases as to have no effect on the acid determination.

Table I

Amine–Uranium Coördination Number[a]

Initial H_2SO_4, M	Equilibrium H_2SO_4, M	x, fraction of amine as bisulfate	Total organic SO_4, N	Equilibrium aq. U M	n
0.0294	0.0311	0.0676	0.1242	2.4×10^{-5}	9.3
.0394	.0419	.0868	.1252	3.4×10^{-5}	8.4
.0496	.0523	.1047	.1274	4.4×10^{-5}	6.6
.0712	.0754	.1416	.1297	5.0×10^{-5}	6.0
.0995	.1052	.1840	.1310	6.4×10^{-5}	6.2
.1388	.1462	.245	.1340	1.1×10^{-4}	6.1
.1740	.1824	.291	.1365	1.3×10^{-4}	5.9
.1978	.2073	.320	.1375	1.7×10^{-4}	6.0
.2239	.2339	.345	.1380	1.6×10^{-4}	6.1

[a] Total initial aqueous sulfate in all cases 1.00 M. Total initial uranium 0.010 M. Total amine 0.1035 N.

of amine bisulfate,[16] and (2) that the sulfate/bisulfate ratio of the uncomplexed amine is the same as that expected in the absence of uranium, it was possible to calculate an amine–uranium coördination number, n. Other values used in this calculation were: x, the fraction of the uncomplexed amine present as the bisulfate in the uranium bearing organic phase; $\Sigma[\mathrm{DDA}]$ the total equivalents of amine present; $[\mathrm{U}]_{org}$ the organic uranium molarity; and $\Sigma[\mathrm{SO_4}]_{org}$, the total sulfate molarity of the final uranium bearing organic phase. This latter quantity may then be summed as

$$\Sigma[\mathrm{SO_4}]_{org} = x(\Sigma[\mathrm{DDA}] - n[\mathrm{U}]_{org}) + \frac{(\Sigma[\mathrm{DDA}] - n[\mathrm{U}]_{org})(1 - x)}{2} + (n/2 + 1)[\mathrm{U}]_{org} \quad (2)$$

This may be solved for n to yield

$$n = \frac{(x + 1)\Sigma[\mathrm{DDA}] + 2[\mathrm{U}]_{org} - 2\Sigma[\mathrm{SO_4}]_{org}}{x[\mathrm{U}]_{org}} \quad (3)$$

The x values listed in Table I were obtained from the known relationship in the absence of uranium shown in Fig. 1, using the final equilibrium aqueous sulfuric acid activities calculated from the molarities shown in Table I.[17] The agreement of the calculated values of n (last column of Table I) with the previously suggested value of 6 is good through most of the range. The deviations in the low acid region are within experimental error, which became relatively large at the lowest acidities. The consistency of these results gives support to the validity of the assumptions listed above, which are in effect equivalent to the assumption that the extracted uranium exists in a complex with a definite (average) number of amine sulfate and no amine bisulfate. The stoichiometry of the uranium–amine sulfate complex is thus indicated to be $UO_2SO_4 \cdot 3(R_2NH_2)_2SO_4$.

In addition to the above the following supporting evidence was found for the existence of a definite amine–uranium compound with the stoichiometry indicated above. A quantity of uranium-amine sulfate complex prepared according to this ratio was freed of benzene by vacuum evaporation and the 1:4:6 (uranium:sulfate:amine) ratio was confirmed by analysis. In addition, the material was found to contain 6 molecules of water per uranium. It was possible to recrystallize this material from 1,4-dioxane. The recrystallized material was found to contain the same uranium:sulfate:amine ratio, thus indicating a definite chemical compound. The amount of water in the recrystallized material was found to be less, suggesting that water was displaced in the formation of a crystalline compound or possibly replaced by dioxane.

Equilibrations of decreasing concentrations of DDAS in benzene, chloroform and carbon tetrachloride with an aqueous solution 1.00 M in total sulfate at pH 1.00 and originally 0.002 M in uranium also have shown a limiting amine/uranium ratio of 6. All these data suggest that in benzene, chloroform and carbon tetrachloride 6 amine groups (three amine sulfates) are associated with uranium if the extraction is from an acidic sulfate solution.

Under conditions of pH higher than 3 (insufficient acid added to convert all the amine to amine sulfate) it has been found possible to obtain amine:uranium ratios of 4 and lower at much lower equilibrium uranium concentration. The resulting aqueous phases all contained hydrolyzed uranium, and the organic phases exhibited absorption spectra similar to that of hydrolyzed uranium. These lower amine/uranium ratios are consistent with reactions such as

$$2UO_2SO_{4aq} + H_2O + 2R_2NH_{org} \longrightarrow (R_2NH_2)_2SO_{4org} + U_2O_5SO_{4aq}$$

$$(R_2NH_2)_2SO_{4org} + U_2O_5SO_{4aq} \longrightarrow (R_2NH_2)_2U_2O_5(SO_4)_{2org}$$

Further, when uranium was extracted from an aqueous solution of $U_2O_5SO_4$ by a solution of free amine in benzene, UO_3 was precipitated from the aqueous phase. The quantity of UO_3 was just sufficient to liberate enough sulfuric acid to neutralize the amine.

$$U_2O_5SO_{4aq} + H_2O + R_2NH_{org} \longrightarrow 2UO_3 + (R_2NH)_2SO_{4org}$$

The resulting amine sulfate then extracted $U_2O_5SO_4$ from the aqueous solution, as above.

(d) **Acid and Sulfate Concentration Variation.**—The effect on the extraction of uranium with 0.1 N DDAS in benzene by varying sulfuric acid activity in 1.00 M total sulfate has been studied at several total uranium levels. The resulting data may be seen plotted as E_a° *vs.* $a_{H_2SO_4}$ in Fig. 4. Sulfuric acid activities from the amine sulfate neutrality point to beyond amine bisulfate precipitation have been used. The displacement of the curves from one another is, in each case, that expected from the difference in concentration of free, uncomplexed DDAS remaining in the organic phase at equilibrium (equation 1).

In the region of amine bisulfate precipitation the sharp drop in E_a° is suspected to be due mainly to the rapid removal of amine (as bisulfate) from the extractant phase. Before bisulfate precipitation occurs two effects are probably responsible for the variation of E_a° with acidity: (1) As the amine sulfate–bisulfate ratio in the organic phase changes the extraction power of the reagent may change; (2) as the aqueous acidity is decreased at a constant total sulfate concentration the dissociation of bisulfate ion will produce a change in the relative

(16) It is interesting to note in this connection that di-*n*-decylamine bisulfate precipitated from a uranium-containing organic phase contains no uranium. This, along with the reported lack of complexing between uranyl and bisulfate ions in aqueous solution, while not proving the validity of this assumption is consistent with it.

(17) The influence of the low equilibrium uranium concentration on sulfuric acid activity of the aqueous phase was considered negligible.

TABLE II

SULFATE VARIATION DATA

Total SO_4, M	% H_2SO_4	Equilib. organic SO_4, N[a]	$[SO_4^=]$, M	Ionic strength, I	K_1[b]	K_2[b]	$E^\circ_{UO_2(SO_4)_3^=}$	$(E^\circ_{UO_2(SO_4)_2^=})'$
				At *p*H 1.00				
0.097	100.0	0.1319	0.028	0.152	124	860	5805	2136
.150	75.0	.1325	.055	.259	95	645	2541	1032
.200	62.5	.1341	.079	.357	81	560	1572	734
.400	42.6	.1375	.196	.791	55	387	528	322
.800	28.5	.1390	.490	1.78	39	280	177	157
1.00	25.0	(.1400)	.660	2.32	35	250	125	125
1.50	20.0	.1413	1.08	2.66	31	212	56	71
				At *p*H 2.00				
0.005	100.0	0.1019	0.0032	0.0122	368	2700	223,000	169,000
.010	65.0	.1029	.0068	.0231	295	2080	84,000	67,000
.025	38.0	.1048	.0180	.0608	191	1350	26,500	22,400
.050	25.0	.1063	.0340	.127	138	940	12,300	10,700
.097	16.9	.1075	.078	.255	96	660	6,200	5,690
.150	13.0	.1086	.122	.399	76	525	4,130	3,870
.200	11.0	.1086	.167	.543	65	455	2,610	2,480
.400	7.2	.1090	.35	1.12	47	336	1,610	1,590
.800	5.1	.1101	.73	2.29	36	252	750	750
1.00	4.2	.1099	.93	2.88	33	231	565	565
1.50	3.2	.1115	1.42	4.43	29	200	301	338
2.00	2.7	.1145	1.91	6.00	26	180	107	128

[a] Organic amine concentration 0.1019 *N*. [b] Adjusted to ionic strength given. Aqueous uranium concentration prior to equilibration 0.002 *M*.

abundance of the various uranyl sulfate complexes which Arhland[18] reports to be formed in aqueous sulfate solution.

In order to extend the investigation of this latter effect the variation of E_a° with sulfate concentration at constant *p*H was measured. Table II gives the various sulfate levels which were used at *p*H 1.00 and 2.00. Samples of DDAS in benzene pre-equilibrated with uranium barren solutions were equilibrated with identical solutions containing 0.002 *M* uranium. The observed extraction coefficients, E_a°, may be seen plotted against total aqueous sulfate concentration in Fig. 6.

From this plot it may be noted that E_a° decreases with increasing total aqueous sulfate concentration. Thus it appears that of the several valid reactions[19] which could be written for the extraction of uranium(VI) by DDAS perhaps the following lends itself most readily to interpretation of the data

$$UO_2(SO_4)_2^{=}{}_{aq} + 3(R_2NH_2)_2(SO_4)_{org} \rightleftharpoons (R_2NH_2)_6UO(SO_4)_{4org} + SO_4^{=}{}_{aq}$$

The corresponding equilibrium constants may be written

$$K = \frac{a_{SO_4aq}}{a_{UO_2(SO_4)_2^{=}aq}} \times \frac{a_{Uorg}}{a^3_{(R_2NH_2)_2SO_4org}} \quad (4)$$

for the present purpose this is rearranged to

$$K = E^\circ_{UO_2(SO_4)_2^=}[SO_4^=]_{aq}G \quad (5)$$

in which

$$E^\circ_{UO_2(SO_4)_2^=} = [U]_{org}/[UO_2(SO_4)_2^=]_{aq} \quad (6)$$

$$G = \gamma_{Uorg}/a^3_{(R_2NH_2)_2SO_4org} \quad (7)$$

The ratio $(\gamma_{SO_4^=}/\gamma_{UO_2(SO_4)_2^=})_{aq}$ is taken to be unity since the two activity coefficients refer to similarly charged ions.

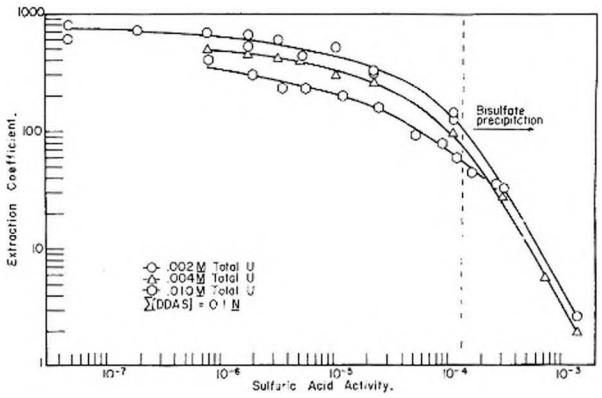

Fig. 4.—Extraction of uranium by DDAS in benzene as a function of sulfuric acid activity in 1.00 *M* total sulfate.

Since this discussion of the effects of sulfate and acid concentration on uranium extraction is restricted to measurements in which the DDAS concentration is constant at 0.1 *N* and the organic uranium concentration is nearly constant at 0.002 *M*, variation in the organic phase composition is due almost entirely to changes in the amine sulfate–bisulfate ratio. Accordingly, the terms contained in *G* are expected to vary primarily as a result of this change. Therefore, in each constant *p*H series of sulfate dependent measurements (Table II), wherein the variation of the sulfate–bisulfate ratio was relatively low, it seemed reasonable to assume as a first approximation that *G* was constant. Then by equation 5

$$E^\circ_{UO_2(SO_4)_2^=} \propto 1/[SO_4^=] \quad (8)$$

In order to test the above relationship it was nec-

(18) S. Ahrland, *Acta Chem. Scand.*, **5**, 1151 (1931).

(19) Equivalent reactions involving UO_2^{++}, UO_2SO_4 or $UO_2(SO_4)_3^{=4}$ could be used and would give an equally useful correlation with U–SO_4 complex formation quotients.

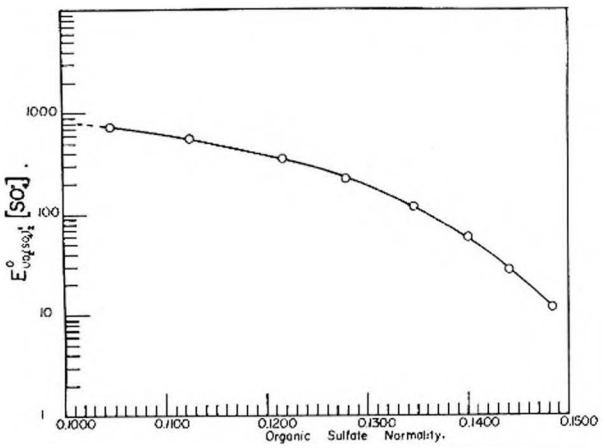

Fig. 5.—Dependence of the product, $E^0_{UO_2(SO_4)_2^{=}}$ $[SO_4^{=}]$, on organic sulfate content in benzene DDAS system; total $[SO_4]_{aq} = 1.00\ M$, varying $[H_2SO_4]_{aq}$.

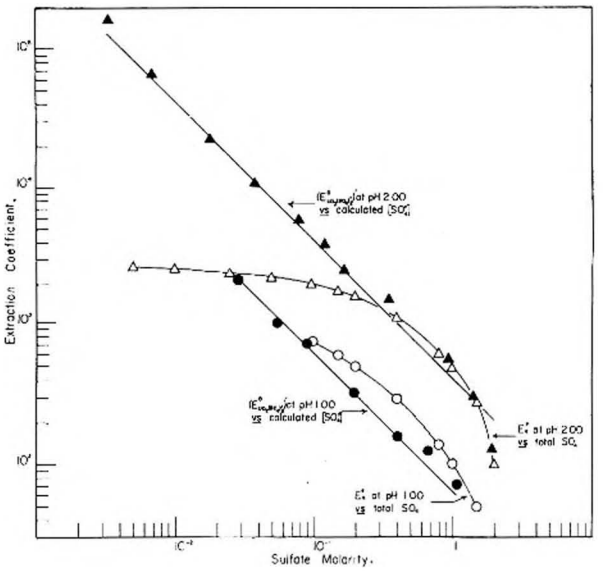

Fig. 6.—Extraction of uranium by DDAS in benzene variation of aqueous sulfate molarity: ●, $(E^0_{UO_2(SO_4)_2^{=}})'$ at pH 1.00 *vs.* calcd. $[SO_4^{=}]$; ○, E^0_a at pH 1.00 *vs.* total $SO_4^{=}$; ▲, $(E^0_{UO_2(SO_4)_3^{-4}})'$ at pH 2.00 *vs.* calcd. $[SO_4^{=}]$; △, E^0_a at pH 2.00 *vs.* total $SO_4^{=}$.

essary to calculate both $[UO_2(SO_4)_2^{=}]$ and $[SO_4^{=}]$. From studies of the complexity of uranyl sulfate Ahrland[18] gives these reactions and equilibrium quotients in 1 M ClO_4^- at 20°

(1) $UO_2^{++} + SO_4^{=} \rightleftharpoons UO_2SO_4$

(2) $UO_2^{++} + 2SO_4^{=} \rightleftharpoons UO_2(SO_4)_2^{=}$

(3) $UO_2^{++} + 3SO_4^{=} \rightleftharpoons UO_2(SO_4)_3^{-4}$

	Potentiometric	Spectrophotometric
K_1	$= 50 \pm 10$	56 ± 6
K_2	$= 350 \pm 150$	450 ± 150
K_3	$= 2500 \pm 1000$	not detd., $\ll 2500$

From the expressions for K_1, K_2 and K_3 and the summation expression for aqueous uranium

$$[U]_{aq} = [UO_2^{++}] + [UO_2SO_4] + [UO_2(SO_4)_2^{-2}] + [UO_2(SO_4)_3^{-4}] \quad (9)$$

it is possible to obtain the expression for the concentration of any one of the uranium species. Thus eq. (10) may be written

$$[UO_2(SO_4)_2^{=}] = \frac{[U]_{aq} K_2[SO_4^{=}]^2}{1 + K_1[SO_4^{=}] + K_2[SO_4^{=}]^2 + K_3[SO_4^{=}]^3} \quad (10)$$

The sulfate ion concentrations were calculated according to a method (see ref. in footnote 13) based on the assumption that the ion activity coefficient product $\gamma^2_{H^+}\gamma_{SO_4^{=}}$ for a given sulfuric acid–sodium sulfate solution is equal to $(\gamma\pm)^3_{Na_2SO_4}$ for a pure sodium sulfate solution of the same ionic strength.

In addition, for purposes of calculating $[UO_2(SO_4)^+]$, the formation quotients K_1 and K_2 given by Ahrland for ionic strength, $I = 1$ were assumed to vary with ionic strength according to this modified Debye–Hückel equation

$$\log K_a = \log K_m - 0.509(\Delta Z_i^2)\frac{I^{1/2}}{1 + 0.328\mathring{a}I^{1/2}} \quad (11)$$

In this equation K_a is the constant at infinite dilution and K_m is the concentration quotient at a given molarity, $\Delta(Z_i^2)$ is defined as Σ(ionic charge^2)$_{products}$ − Σ(ionic charge)$_{reactants}$ and $\mathring{a}$ is the minimum average distance of approach between ions in the solution, in Å. A value of 7 was used for $\mathring{a}$ here since this appeared to be a good average of values used successfully elsewhere for 2-2 electrolytes. Adjusted values for K_1 and K_2 are listed in Table II. K_3 was taken to be independent of ionic strength since (ΔZ_I^2) for the corresponding reaction is zero. It is also of interest to note that the ratio K_2/K_1 is formally independent of ionic strength.

Using these ionic strength adjusted K values and the calculated values of $[SO_4^{=}]$ for each solution, it was found that the inverse proportionality between $E_{UO_2(SO_4)_2^{=}}$ and $[SO_4^{=}]$ predicted by equation 8 (taking G as constant) was most nearly approached when K_3 was taken to be zero.[20] The resulting values of $E^o_{UO_2(SO_4)_2^{=}}$ are listed in Table II.

As was pointed out earlier, the assumption that G is constant in each series of measurements is only an approximation, since the amine bisulfate content of the organic phase varied slightly (*cf.* column 3, Table II) as a result of variation in aqueous acid activity. Accordingly, the variation of G with amine bisulfate constant was estimated from the acid variation results (Fig. 4). First, $E^o_{UO_2(SO_4)_2^{=}}$ was calculated from these results as was done above and then a plot of the product $E^o_{UO_2(SO_4)_2^{=}}$-$[SO_4^{=}]$ *vs.* the total organic sulfate concentration was constructed (Fig. 5). Since, by equation 5, the product $E^o_{UO_2(SO_4)_2^{=}}$-$[SO_4^{=}]$ is proportional to $1/G$, this curve indicates the variation of $1/G$ with the amine bisulfate content of the extractant.

Using this curve, the variation in G caused by the change in organic sulfate concentration in each series of the sulfate variation measurements was estimated and the $E^o_{UO_2(SO_4)_2^{=}}$ values were adjusted to values corresponding to a constant G (*i.e.*, that corresponding to the 1 M sulfate solution in each case). The adjusted values $(E^o_{UO_2(SO_4)^-})'$ are listed in the last column of Table II. Log-log plots of the

(20) While the uranyl trisulfate complex appears to be an important resin-phase species in the absorption of uranium from aqueous sulfate solutions by anion exchange resins (*cf.* J. Dasher, A. M. Gaudin and R. D. Macdonald, *J. Metals*, **9**, 185 (1957), this does not require the existence of important concentrations in the aqueous solutions.

adjusted values *vs.* $[SO_4^{=}]$, Fig. 6, show satisfactory fit to the slope of -1 required by equation 7 when G is constant.

The maximum uncertainty of the points on the final curve is about $\pm 15\%$ due to definable inaccuracies in measurements. Keeping either K_2 or K_1 constant at Ahrland's value, significant changes (with due allowance for the experimental scatter) in the slope of the calculated line in Fig. 6 resulted from variations in the ratio K_2/K_1 of greater than unity (*i.e.*, $K_2/K_1 = 7 \pm 1$). Keeping $K_2/K_1 = 7$, significant changes in slope resulted from variations of $\pm 50\%$ in the absolute values of K_2 and K_1. The maximum value of K_3 consistent with the unit slope of Fig. 6 was found to be *ca.* 100. Thus, in general, this treatment of these data is in agreement with Ahrland's constants for the formation of UO_2SO_4 and $UO_2(SO_4)_2^{=}$, but not for formation of $UO_2(SO_4)^{-4}$.

Acknowledgment.—The authors wish to express their appreciation to K. A. Allen for his participation in many valuable discussions concerned with this investigation and C. F. Coleman for his critical and comprehensive reading of the manuscript.

ELECTRON SPIN RESONANCE STUDIES OF RADIATION DAMAGE TO PEPTIDES[1]

BY GENE MCCORMICK AND WALTER GORDY

Department of Physics, Duke University, Durham, North Carolina

Received December 17, 1957

Effects of X-irradiation on numerous dipeptides and tripeptides have been investigated through observation of the electron spin resonance patterns of the free radicals produced by the irradiation. Most of the resonances have hyperfine structure arising from interaction of the free electron spin with the spins of hydrogen nuclei. The patterns were generally found to be different for different peptides and also different in most instances from those obtained by X-irradiation of their constituent amino acids. With few exceptions the patterns are also different from those obtained from X-irradiation of proteins. Tentative identifications of some of the free radicals produced are made from their proton hyperfine structure. For some of the peptides oxygen was found to kill the resonance and for others to alter its structure. The results indicate that certain groups containing sulfur or the tyrosine ring, when a constituent of a polypeptide or protein, can act as protective agents to prevent radiation damage to other parts of the protein or polypeptide.

Other measurements[2] in this Laboratory have shown that the amino acids are generally dissociated to form simple, often identifiable, free radicals when they are subjected to ionizing irradiation. The radicals formed from the different amino acids are generally different. From any one of the amino acids only one or two different detectable radicals are formed. The effects of irradiation on the proteins are different from those on the individual amino acids. Only a few distinct resonances are obtained for a variety of proteins. Of the numerous resonance patterns found for the different amino acids, only those characteristic of cystine or cysteine showed up in most proteins investigated. The peptides and polypeptides are intermediate structures between the proteins and their basic building blocks, the amino acids. Hence, it is of interest to examine the electron spin resonances of these intermediate structures to see whether when they are subjected to ionizing irradiations they behave more nearly like the amino acids or like the proteins. From the comparison we expect to learn more about the nature of radiation damage to proteins.

A preliminary report on peptides and polypeptides was given at a meeting of the American Physical Society.[3] The present paper gives further results on this study. We shall not discuss here either theory or experimental methods but shall confine ourselves to the results. A description of the theory of paramagnetic resonance is given elsewhere,[4] and commercial instruments are now available for observation of the resonance.[5]

The accompanying figures show the resonance curves for a number of peptides or polypeptides in the solid state after they were irradiated with 50 kv. X-rays. The curves here represent second derivatives of the resonance contours rather than the actual shape or the first derivative presentation. All curves shown are for 9000 Mc./sec. although some of the results were checked at 23,000 Mc./sec. In all cases the g-factor for the resonance was found to be very close to that of the free electron spin, 2.0023.

The resonance pattern for X-irradiated glycylglycine was observed in the earlier work[2] to be a simple doublet, unlike that of glycine, which was found to be a triplet. Thus the formation of a single peptide bond to make glycylglycine changes entirely the radical produced by the irradiation. The formation of a second peptide bond to make glycylglycylglycine, or a third to make glycylglycylglycylglycine, does not further alter the pattern from the simple doublet. See Fig. 1. This suggests that a still longer $(glycyl)_n$-glycine chain

(1) This research was supported by the Office of Ordnance Research, Department of the Army and by the United States Air Force through the Air Force Office of Scientific Research of the Air Research and Development Command. Reproduction in whole or in part is permitted for any purpose of the United States Government.

(2) W. Gordy, W. B. Ard and H. Shields, *Proc. Natl. Acad. Sci.*, **41**, 983 (1955). See also the accompanying paper, H. Shields and W. Gordy, THIS JOURNAL, **62**, 789 (1958) and related paper on proteins by W. Gordy and H. Shields in Rad. Res. 1958.

(3) G. McCormick and W. Gordy, *Bull. Am. Phys. Soc.*, **1**, 200 (1956).

(4) B. Bleaney and K. W. H. Stevens, *Rep. Progr. Phys.*, **16**, 109 (1953); K. D. Bowers and J. Owen, *ibid.* **18**, 304 (1955).

(5) Varian Associates, Palo Alto, California.

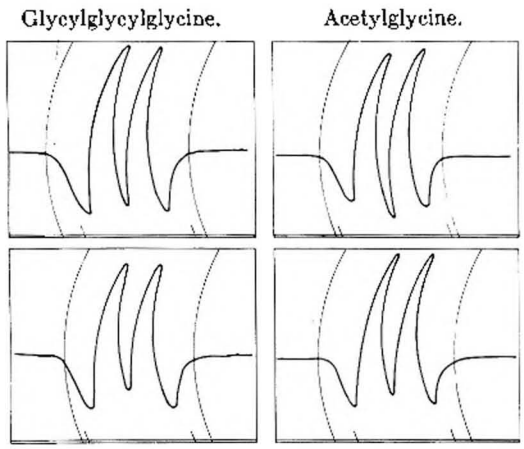

Fig. 1.—Electron spin resonance curves of some X-irradiated peptides of glycine. The samples in the powdered or polycrystalline form were observed at room temperature in air at a frequency of 9000 Mc./sec. The g-factor for the center of the resonance pattern is 2.00. The scale markers at the base of the figure are 68 gauss apart. The curves represent second derivatives of the actual absorption curves and were obtained by small amplitude magnetic modulation of the resonance frequency with a phase-sensitive, lock-in amplifier tuned to the second harmonic of the modulation frequency. They were recorded on curved coordinate paper with an Esterline–angus recorder. Except for specified variations these conditions apply also to Figs. 2–8.

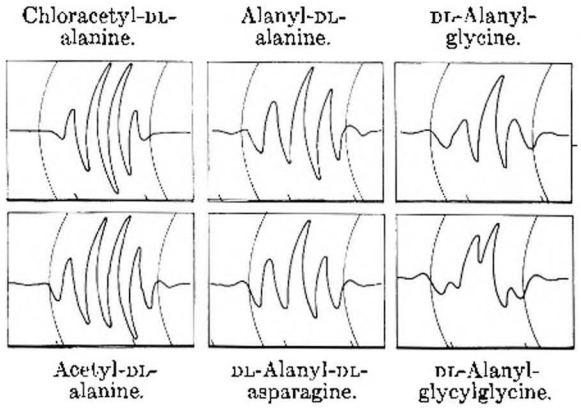

Fig. 2.—Electron spin resonance curves of some X-irradiated peptides of alanine. For further description see caption for Fig. 1.

would give the same doublet pattern. Doublets similar to that for glycylglycine are obtained for irradiated acetylglycine and acetylglycylglycine, chloroacetylglycylglycine and DL-leucylglycylglycine (at room temperature), whereas the patterns for DL-alanylglycine and DL-alanylglycylglycine are different. The doublet separation in all these substances is about 20 gauss. Most of these patterns undergo marked changes as the temperature is lowered to that of liquid nitrogen, but the doublet for glycylglycine (glycyl)$_2$-glycine or (glycyl)$_3$-glycine remains unchanged.

The doublet of irradiated glycylglycine or polyglycine is similar to that found in silk and many other proteins. Its specific origin is not yet definitely known, although we do know that the doubling originates from the interaction of the odd electron with the spin of a single hydrogen. A reasonable possibility seems to be that a proton on the carbon adjacent to the carbonyl group would be lost, to leave a radical stabilized by the resonance of I and II

where X and X′ represent the end groups. From comparison with the coupling of the protons in the free methyl radical one would expect the coupling of the CH proton in structure I to be about 25 gauss. The weight of this form would therefore be of the order of 80%. Difficulties have been encountered, however, in reconciling this model with the specific orientation-dependence found in silk. Studies on silk[6] show that the doublet in this substance has an orientation-dependence in the magnetic field. Through substitution and measurements on single crystals now in progress we hope to learn which specific radical gives rise to the doublet.

If the polypeptide chain is short, the effects of the terminal groups are often important in determining the type of radical formed. This is demonstrated in the present study, where certain dipeptides and tripeptides give patterns not formed in any of the proteins so far studied. For example, alanylglycine does not give the silk doublet but apparently two superimposed patterns, a quintet like that of alanine and a triplet like that of glycine, whereas alanylglycylglycine appears to give a mixture of the alanyl quintet and the glycylglycine doublet. See Fig. 2.

A general formula for the dipeptides formed from α-amino acids is

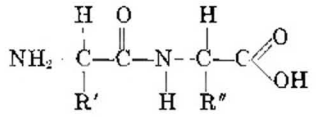

In glycylglycine, already discussed, R′ = R″ = H. We can study the effects of substitution of various other groups for H in one of the R positions by comparison of the results on the various dipeptides.

In glycylvaline, R′ = H and R″ = $(CH_3)_2(HC)$. For this compound a complex multiplet is observed, possibly with a secondary resonance superimposed in the central region. See Fig. 3. Superficially, the multiplet at room temperature has the appearance of a sextet of doublets arising from a set of five equivalent hydrogens and an additional one having a different coupling. Although this combination gives the best agreement of any we could find, it is not readily clear how such a radical could be formed by irradiation of glycylvaline nor indeed what its specific form would be. Perhaps a more complete resolution of the resonance might reveal a different pattern. At liquid air temperature the pattern has a different appearance from what it has at room temperature, but this difference possibly results from a change in couplings rather than a change in the form of the radical.

Glycylnorvaline, R′ = H, R″ = $CH_3CH_2CH_2$–, forms an entirely different pattern from that of

(6) H. Shields and W. Gordy, to be published in Rad. Res. (1958).

glycylvaline. The pattern is incompletely resolved but appears to be a triplet of doublets arising from three protons, two equivalent, each with 27 gauss splitting and a third with 18 gauss splitting. The pattern for glycyl norleucine is like that of glycyl norvaline. To form glycylleucine from glycylglycine one has simply to replace the H by the group $(CH_3)_2(CH)H_2C-$. For this compound no resonance was obtained when the sample was irradiated in air. When it was irradiated *in vacuo*, however, a septet with component spacing of 18 gauss was observed at room temperature. Glycylnorleucine, R″ = $CH_3CH_2CH_2CH_2-$, gives a pattern like that of glycylnorvaline and one entirely different from that of glycylvaline.

In the various alanyl peptides the R′ group in the above formula becomes CH_3. The alanyl peptides generally give quintet patterns with component spacings of 24 to 26 gauss. Alanylalanine and alanylasparagine, like alanine itself, give well defined quintet patterns. Alanylnorvaline, like glycylnorvaline, is different. It yields only an asymmetric doublet, whereas alanylvaline gives what may be another resonance with apparently the alanine quintet over it. That for alanylglycine appears to have the glycine triplet superimposed and that for alanylglycylglycine to have the glycylglycine doublet superimposed. The pattern for irradiated glycylalanine, R′ = H and R″ = CH_3, is a quintet with the same spacing, within experimental error, as that of alanine itself.

The radical which gives the quintet in the alanyl peptides may result from the loss of NH_2^+ after ionization to form the radical C_2H_4COX, where X represents the remainder of the molecule. Nevertheless, equal coupling of the four protons in such a radical is surprising. Hydrogen exchange, if it occurs between the carbons at a sufficiently rapid rate, could cause equalization of the observed couplings in C_2H_4-. The alanyl radicals would be represented as a mixture of

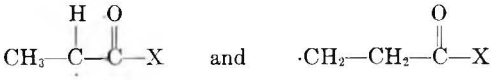

A further discussion of this mechanism for equalization of the couplings is given in the accompanying paper on amino acids.

It is entirely possible that the couplings of the protons are accidentally equal, or approximately so, without either static or dynamic symmetry of the radical. For example, if the ground state of the radical C_2H_4COX could be represented as an admixture of 91% from I and 4.5% for each of the equivalent forms of II

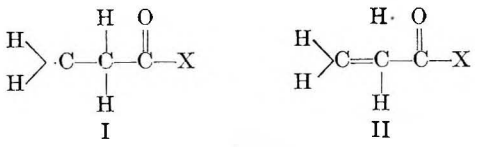

I II

one would expect the coupling of all four protons to be very nearly equal for the following reasons. The two end protons in form I should have a coupling about the same as that of the protons in the free methyl radical,[2,7] for which the component spacing is 25 gauss. For 91% contribution from form I, the coupling of the end protons should be 23 gauss. Each of the two equivalent forms of II should have the coupling of atomic hydrogen, 504 gauss, and hence for the assumed contribution of 4.5% should have a coupling of 23 gauss. This accidental admixture should give equivalent coupling of the four protons and a quintet of 92 gauss spread, close to that usually observed. One might likewise have accidental equalization of the coupling of four hydrogens with forms III and IV

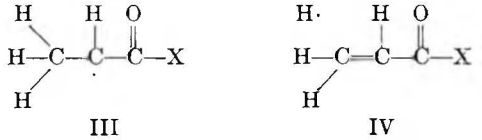

III IV

About 4.5% contribution of each of the three equivalent forms of IV would give the three end protons an isotropic coupling of 23 gauss, while the coupling of the central H should be near that of the hydrogens in the free methyl radical.

A similar explanation can be given for the equivalent or approximately equivalent coupling of the five protons in the free ethyl radical. The three equivalent forms of II must each have a contribution of 4.5% to give the CH_3 hydrogens a coupling of 23 gauss, and this would leave only 86.5% for form I, or a coupling of 22 gauss for the end protons. This model should give a sextet pattern of total spread 115 gauss, approximately that of the 130 gauss sextet found earlier[7] in X-irradiated mercury diethyl.

I II

The above explanation for the equalization of the couplings in hydrocarbon radicals which give quintet and sextet patterns would at the same time account for the rather strange fact that the coupling

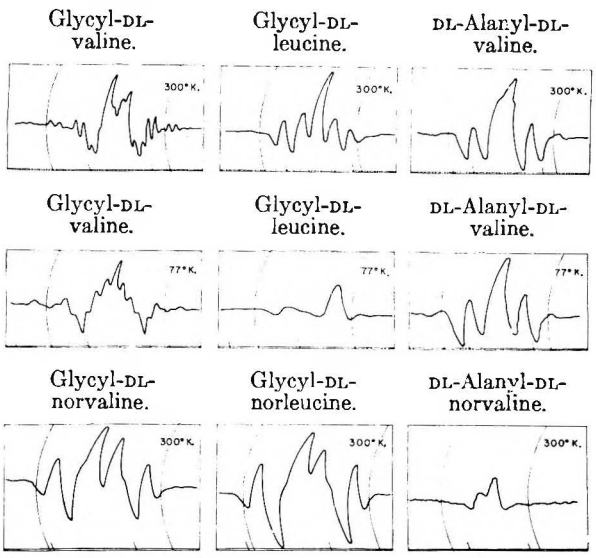

Fig. 3.—Electron spin resonance curves of X-irradiated peptides of valine and leucine.

(7) C. G. McCormick and W. Gordy, *J. Am. Chem. Soc.*, **78**, 3243 (1956).

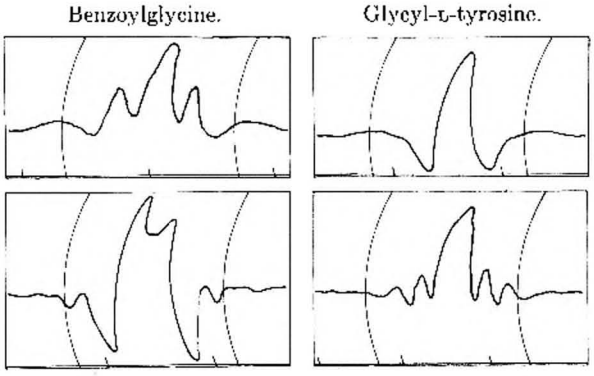

Fig. 4.—Electron spin resonance curves of some X-irradiated peptides having ringed groups.

for proton remains about the same, 23 to 26 gauss, for radicals having three, four or five coupling protons. A similar interpretation (see later discussion) accounts for the similar coupling observed in still larger radicals such as that obtained from acetylglycine.

Thus, accidental equalization of H couplings, if it occurs, provides uniform and reasonably consistent interpretations for the quintet and sextet patterns observed in the X-irradiated peptides and other organic substances without the requirement for geometrically symmetric radicals or rapid hydrogen exchange motions. Even if hydrogen exchange occurs, hyperconjugated structures such as II or IV above are needed to explain the observed increase in total coupling with the number of hyperfine components. Both hyperconjugation and hydrogen exchange may occur in some radicals.

One might expect the unsaturated tyrosine group in a polypeptide or protein to act as a pro-

tective agent to prevent radiation damage of other parts of the molecule, provided that an electron hole produced elsewhere in the molecule could migrate to this ring. Upon ionization it should lose H^+ from the hydrazyl group to form a radical stabilized by migration of the electron hole around the ring as described by resonance of the structures

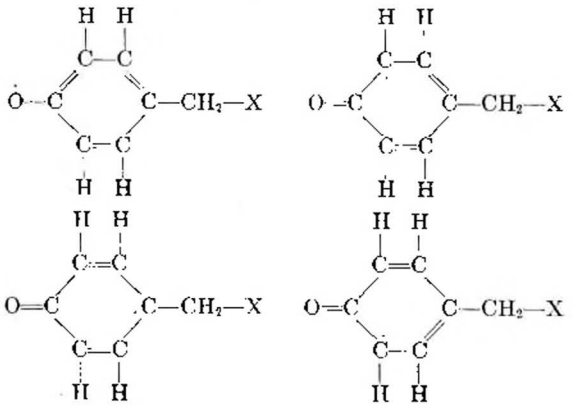

Here again X represents the remainder of the molecule exclusive of the group shown. This radical could remain attached to the peptide and give a single resonance about 25 gauss in width. The

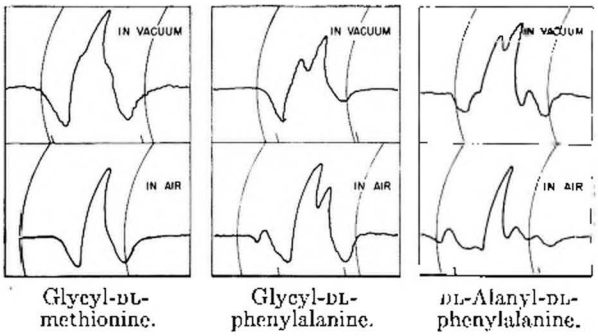

Fig. 5.—Electron spin resonance curves showing effects of air on radicals produced by X-irradiation of glycylmethionine and glycyl- and alanylphenylalanine.

coupling of the aromatic protons about the ring should give a hyperfine structure spread over about 25 gauss,[8] but this would not likely be resolvable in the solid state. The observed resonance of glycyltyrosine, Fig. 4, seems to agree with this model. The resonance of this peptide is a singlet like that of tyrosine itself (see accompanying paper.)

Glycylphenylalanine is similar to glycyltyrosine but has a very different resonance when X-irradiated. The only difference in the two peptides is that the OH on the ring in glycyltyrosine is replaced by H in glycylphenylalanine to make the R group  . A radical of the type proposed for glycyl tyrosine is therefore not possible for the phenylalanine peptides. If the interpretation given for glycyltyrosine is correct, one would expect glycyl-, acetyl- or alanylphenylalanine to have qualitatively different resonance patterns from that obtained for glycyltyrosine. Such a difference is observed. Compare Figs. 4 and 5. We shall not attempt to identify the radicals produced from the phenylalanine compounds. Since the resonance obtained for each of the three appears to have different structure, it does not seem likely that the radical in any one case is produced wholly from the phenylalanine ring. Probably the tyrosine R group would be the better protective agent in the protein chain not only because its hydroxyl proton is perhaps readily given up but also because it can possibly be restored without other damaging chemical reactions taking place, as for example, the oxygen addition described below.

Alanylphenylalanine provides an interesting example of the effects of oxygen on certain peptides and presumably on proteins with phenylalanine as a constituent. The upper patterns of Fig. 5 were obtained with the samples irradiated and observed *in vacuo* and the lower patterns with the same samples irradiated and observed in air. The strong central doublet of alanylphenylalanine is changed when the samples are irradiated in air. This change could be brought about by oxygen becoming attached to the radical R to form R—O—O, similar to that observed in our laboratory for bone[2] and a number of biological materials. Oxygen evidently does not attack the radicals

(8) G. E. Pake, S. I. Weissman and J. Townsend, *Disc. Faraday Soc.*, **19**, 147 (1955); S. I. Weissman, T. R. Tuttle, Jr., and E. de Boer, THIS JOURNAL, **61**, 28 (1957).

which produce the secondary patterns in the phenylalanine peptides, for these secondary patterns become more evident when the stronger central absorption is reduced to the sharp singlet. Interestingly, this oxygen effect is not observed in glycyltyrosine, and it might not be expected since O_2 would not likely become attached to the electronegative O in the glycyltyrosine radical.

Benzoylglycine

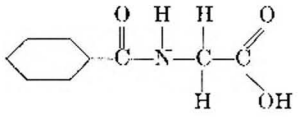

when X-irradiated gives a triplet like that of glycine itself with broad shoulders on either side (Fig. 4). If the glycine triplet arises from the radical H_2C–COOH, the formation of the same radical might be produced from benzoylglycine by ionization since the remainder, $(C_6H_5CONH)^+$, would be stabilized by resonance of the CO and CN links.

X-Irradiated phenylglycine

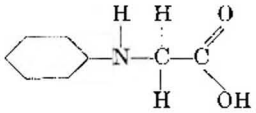

yields what appears to be a sextet with total spread of only 65 gauss with a central component which destroys the apparent symmetry of the pattern. The sextet has a closer spacing than any of the aliphatic radicals we have observed with as many components. Interestingly, phenylglycine melts on prolonged X-irradiation, and the resulting viscous liquid gives a single resonance of about 12 gauss in width.

The acetyl group combines with the amino acids to form the peptide bond although the resulting compound is unlike the regular peptides because it does not contain the amino group. The general formula for the acetyl peptide compounds is

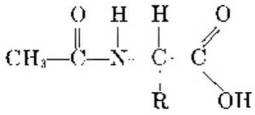

where R is a group which depends upon the particular amino acid combined with the acetyl group.

It is difficult to make an intelligent guess as to how the acetyl peptides break up under ionizing radiation. However, from the number of cases we have examined we can say that the acetyl group influences significantly the way the peptide or polypeptide breaks up under ionizing radiations. See Figs. 2, 6-8. Even the radicals formed from tripeptides containing the -SH group are altered by the terminal acetyl group; acetylglutathione, for example, forms a different radical from that formed by glutathione (see later discussion).

Chloroacetylalanine (see Fig. 2) appears to form the free methyl radical since it gives a quartet with component spacings of 23 gauss. However, the radical here may be of some such form as

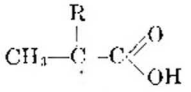

where R has no coupling nuclei. If this is true, the quartet patterns with spacings of 23 gauss does not provide an unambiguous identification of the free methyl radical.

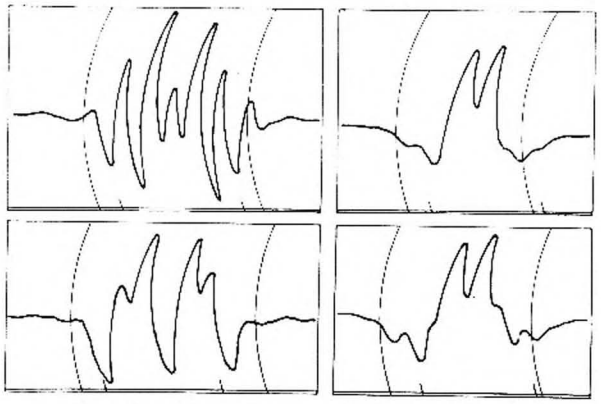

Acetyl-DL-leucine. Chloroacetyl-L-leucine.

Fig. 6.—Electron spin resonance of X-irradiated acetyl peptides. Upper curves for 300°K; lower for 77°K.

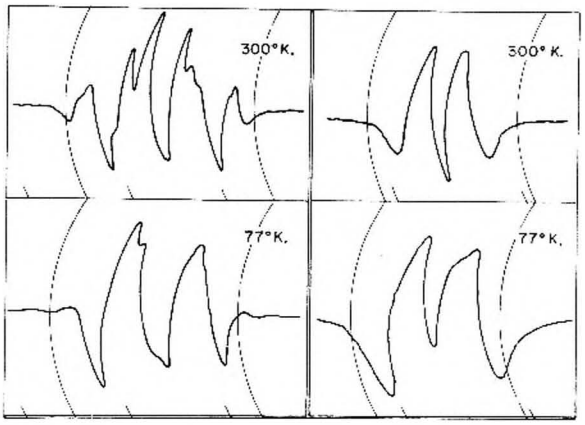

Fig. 7.—Electron spin resonance of some X-irradiated acetyl peptides at different temperatures.

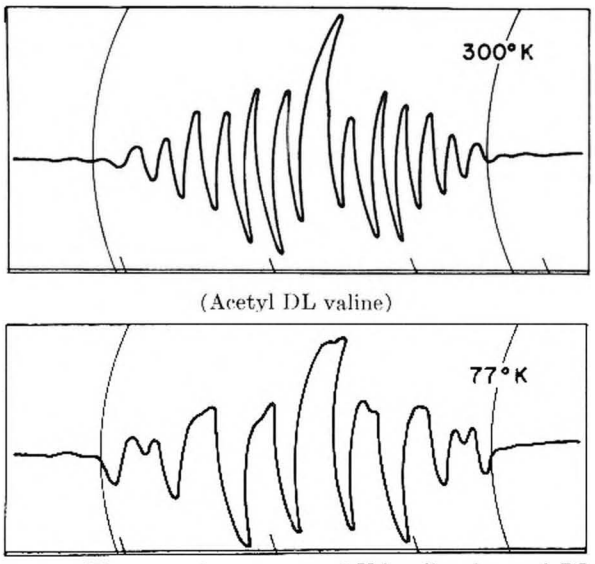

Fig. 8.—Electron spin resonance of X-irradiated acetyl DL valine.

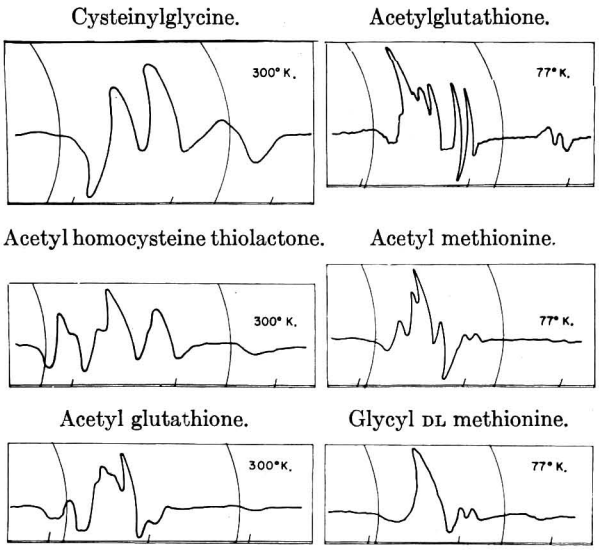

Fig. 9.—Electron spin resonance of some X-irradiated peptides containing sulfur.

Acetylalanine, when X-irradiated, gives a sextet pattern of component spacing of only 20 gauss. Possibly the radical here is not C_2H_5 but some other radical in which there are 5 hydrogens which accidentally have approximately equal couplings.

In acetylvaline, R = $(CH_3)_2(HC)$–. When this compound was irradiated with X-rays a remarkable paramagnetic resonance consisting of some 18 hyperfine components spread over 200 gauss was observed. The hyperfine structure appears to be a set of 9 doublets (see Fig. 8) with approximately Gaussian intensity distribution if the interference evident in the central region is caused by the superposition of a resonance from a second radical. This set of 9 components apparently arises from a radical which has 8 protons with equal coupling to the electron spin, with a 9th one of somewhat less coupling. At liquid air temperature the coupling of the 9th proton is reduced to about one fourth the coupling of the other eight, and the set of nine doublets becomes convincingly evident. One would expect the direct dipole–dipole interaction to be largely averaged out by the spreading of the odd electron wave function, to allow odd electron density to be around many protons. Thus, we attribute the 200 gauss spread almost completely to population by the odd electron of the 1s orbital of the protons. Since complete population of these orbitals would give a total spread of 504 gauss,[9] we know that the odd electron has about 200/504 or $^2/_5$ of its density in 1s orbitals of the hydrogens.

The incomplete resolution of the acetyl valine pattern makes the above assignment uncertain. The observed curve for room temperature fits as well or better the theoretical pattern of a radical with eight coupling hydrogens, six equivalent ones each with splitting of 23 gauss, a seventh with 43 gauss splitting and an eighth with 13 gauss splitting. At 77°K. splitting by the six equivalent hydrogens are altered to 27 gauss each and the others to 50 and 11 gauss. Probably the radical is

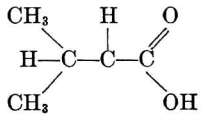

or has some form similar to this.

Interestingly, when the temperature of X-irradiated acetylvaline is reduced further to that of liquid helium, the pattern changes completely. No longer is there evidence for the equivalent coupling of a larger number of protons; unequal coupling of protons in different groups is evident.

Glutathione

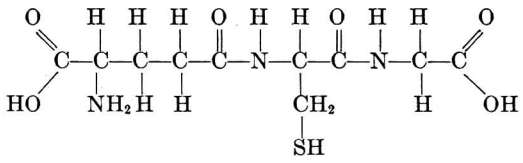

is a tripeptide of glutamic acid, cysteine and glycine. As is shown in the accompanying paper on amino acids, when this tripeptide is irradiated it gives no evidence of the quintet of glutamic acid nor of the glycylglycine doublet but rather a field-dependent pattern like that of cystine, cysteine or the many proteins which contain these amino acids in their residues.

It has been previously emphasized[2] that the sulfur group, which is the common group characterizing these compounds, must be the group suffering the electron loss upon ionization. The sulfur hydrazyl or the disulfide group in the side chains of peptides or proteins evidently acts as a protective agent to other parts of the molecule since in many of these substances no evidence is obtained for radicals produced by any other group. Cysteinylglycine follows this behavior in giving only the characteristic cysteine or cystine-like resonance.

Acetylglutathione and acetylhomocysteine thiolactone are evidently exceptions to the above rule. Although their patterns (See Fig. 9) do appear to have the cystine-like resonance as a component, both show evidence for another pattern superimposed. The acetyl compounds may be more difficult to "protect" than the usual peptides composed completely from amino acids.

At liquid air temperatures the cysteine-like resonance of acetylglutathione became more prominent possibly because of a smearing out of the other component. The components become sharper at the lower temperature, and a doublet splitting barely apparent at room temperature becomes resolvable. This doublet splitting, which is not understood, was not observed for cysteine, cystine or glutathione.

Acetylleucine gives a symmetrical pattern with unequal spacing, which indicates a radical with unequal H coupling. At the temperature of liquid nitrogen the pattern becomes a bit simpler and appears to be a doublet of about 45 gauss separation with an additional doublet splitting of about 15 gauss superimposed. This pair of doublets is also evident at room temperature, but with other interfering lines. Furthermore, a similar gross doublet of about 45 gauss separation was observed for acetylglutamic acid at both room temperature

(9) R. Livingston, H. Zeldes and E. H. Taylor, *Phys. Rev.*, **94**, 725 (1954).

and 77°K. and in chloracetylglycylglycine at 77°K. Although in these compounds the secondary structure of the gross doublet may differ, the large doublet splitting, 45 gauss, indicates strong coupling by a single proton in each of the radicals formed.

When X-irradiated *in vacuo* and observed at room temperature glycylmethionine and acetylmethionine both give as their primary pattern a triplet similar to that of X-irradiated glycine. In both there is evidence for a very weak component of the cysteine-like resonance, with the doublet splitting at low temperature like that for acetylglutathione. See Fig. 8. The latter component may arise from an impurity of –SH or –S–S– links in the methionine. It seems more probable that the triplet for both these compounds may form a radical of the type $XSCH_2$, which would have the principal forms

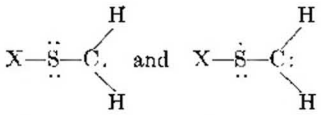

This indicated exchange would be strong because S and C have the same electronegativity, 2.5. It would be equivalent to a "three-electron bond"

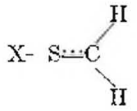

which has about half the strength of a normal bond. This extra stabilization should cause the loss of an H^+ from the CH_3 rather than the loss of the $(CH_3)^+$ from the S in the ionized molecule.

When glycylmethionine is X-irradiated in air rather than *in vacuo*, the resonance is primarily a sharp singlet rather than a triplet (Fig. 5). The oxygen may tie onto the above radical to convert it to

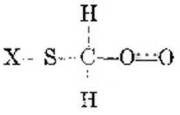

as described for glycyl and alanylphenylalanine. This oxygen effect is in contrast to that observed for the –SH or –S–S– compounds the resonances of which are killed by air.

ELECTRON SPIN RESONANCE STUDIES OF RADIATION DAMAGE TO AMINO ACIDS[1]

BY HOWARD SHIELDS AND WALTER GORDY

Department of Physics, Duke University, Durham, North Carolina

Received December 17, 1957

The earlier investigation of radiation damage to certain amino acids with the method of electron spin resonance has been extended to all the basic amino acids. Most amino acids when X-irradiated were found to have characteristic resonance patterns, each different from those found for the other amino acids. For most of them the characteristic pattern arises from hydrogen nuclear coupling with the electron spin. However, cysteine, cystine and glutathione gave very similar resonance patterns. For these compounds the structure of the resonance appears to arise mainly from an anisotropy in the g-factor rather than from nuclear interactions. The common pattern of these sulfur-containing amino acids suggests that the odd electron is mainly localized on the sulfur. The absence of resolvable structure for the resonances of X-irradiated tyrosine and trytophan suggests that the odd electron giving the resonance may be migrating within the unsaturated rings of these substances. The evidence indicates that the tyrosine and tryptophan rings, in addition to sulfur groups, may in certain combinations act as protective agents to prevent radiation damage to other parts of the molecule. Tentative identifications of the free radicals produced by irradiation of a few of the acids are made from the structure of the resonances.

Earlier reports have been made on the paramagnetic resonance of free radicals produced by ionizing radiations in certain of the amino acids.[2] The present paper represents a somewhat more complete report on these studies which are still in progress. Several additional amino acids have been examined. No results are yet available on the X-ray dosage required to produce a given number of radicals although experiments are in progress which should give such information for certain of these compounds.

The present measurements were mostly at 23,000 Mc./sec. although some of the results were checked at 9,000 and at 3,700 Mc./sec. The paramagnetic resonance spectrometer was similar to that employed by Beringer[3] for the study of paramagnetic gases. It has a bolometer detector with a phase-sensitive, lock-in amplifier and an automatic Esterline-Angus recorder. Small amplitude magnetic modulation of the resonance at 42 c.p.s. was employed with the lock-in amplifier tuned to the modulation frequency. This arrangement gives the signal as the first derivative of the line-shape curve. For some recordings the amplifier was tuned to the second harmonic of the modulation frequency. This arrangement gives the signal as the second derivative of the line-shape curve.

Glycine, Alanine, Valine and Leucine.—In the first report[2] the resonances produced by X-irradiation of glycine and alanine were shown to have hyperfine structure arising from interaction of the electron spin with various numbers of hydrogen nuclei. The principal resonance of glycine appears

(1) This research was supported by the United States Air Force through the Air Force Office of Scientific Research of the Air Research and Development Command and by the Office of Ordnance Research, Department of the Army. Reproduction in whole or in part is permitted for any purpose of the United States Government.

(2) W. Gordy, W. B. Ard and H. W. Shields, *Proc. Natl. Acad. Sci.*, **41**, 983 (1955).

(3) R. Beringer and J. G. Castle, Jr., *Phys. Rev.*, **78**, 581 (1950).

to be a triplet due to two hydrogens with equivalent coupling, that of alanine a quintet due to four hydrogens with equivalent or nearly equivalent coupling.

Irradiated samples of both alanine and glycine have been heated to temperatures near the melting point without destruction of their resonances. Both have had appreciable water added—though they were not dissolved in it—without destruction of the resonances. Irradiated samples of both glycine and alanine which had been left in the open air for a period of about two years were found to have strong resonances. Although thermodynamic arguments can be given for the formation of the charged radical[2] $(C_2H_4)^+$ from ionized alanine, it seems surprising that positively charged radicals would remain stable under the above conditions. Indeed it seems surprising that any simple hydrocarbon free radical would do so.

Hydrogen exchange between carbons, which has been suggested as one possible explanation of the apparently equivalent coupling in the free ethyl radical[4] produced by X- or ultraviolet irradiation of $(C_2H_5)_2Hg$ at 77°K., also provides a possible mechanism for the equalization of the couplings of an even number of 4 or more protons without the postulation of static geometrical symmetry of the charged radicals such as $(C_2H_4)^+$. Thus, the quintet of X-irradiated alanine and other compounds might arise from a radical of the form RC_2H_4 in which the H atom exchange between the two forms

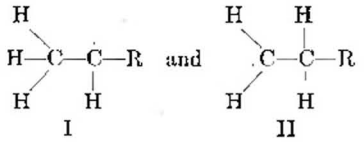

I and II

occurs at a frequency short as compared with the lifetime in the spin states. In agreement with the previous work on polycrystalline materials, observations on single crystals of alanine[5] and valine indicate that the anisotropic components in the H couplings are very small compared with isotropic components at room temperature and that the couplings of the four protons, if not equal, are very nearly so. The proton exchange would tend to reduce and to equalize the orientation-dependent coupling of the four protons, in accordance with observations.

It may be, however, that a radical such as either I or II above might accidentally have equivalent or nearly equivalent coupling of all four protons without the dynamic symmetry produced by proton exchange. As explained in the accompanying paper, contributing structures of the form III or IV

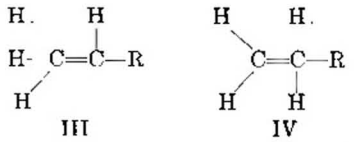

III IV

could equalize the coupling in the radicals I and II, respectively, without proton exchange between I and II. The contributions of each of the three equivalent forms of III, or of each of the two forms of IV, would have to be about 4.5% to equalize the couplings and account for the observed component spacings. Possibly hyperconjugation as indicated by III and IV and proton exchanges indicated by I and II both occur in the same radical.

The resonance curve for polycrystalline alanine is not a perfectly symmetrical quintet but has an additional splitting evident mainly on one outside component. The single crystal studies[5] have already shown that this splitting is caused by the super position of symmetrical quintet patterns of slightly different H couplings and slightly different g-factors. In other words, it has been shown that both the nuclear couplings and the g-factors depend slightly upon the orientation of the crystal axis in the magnetic field. This observation proves that the radicals are not tumbling freely. However, the couplings of the four protons remain equal, or approximately so, for different orientations. This indicates that the coupling is primarily of the Fermi type, or that rapid hydrogen exchange averages out the effects of difference in angle of the various CH bonds with the applied field for a given orientation of the radical.

Interestingly, β-alanine, which has the amino group attached to the second carbon does not give

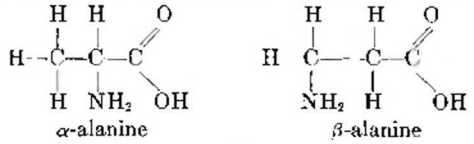

α-alanine β-alanine

the α-alanine quintet as the primary pattern but does show it as a secondary pattern upon prolonged irradiation. See Fig. 1.

The primary pattern for β-alanine is not as stable nor as well resolved as that for α-alanine. We cannot guess the nature of the radical from the incompletely resolved pattern, but the shape of the pattern suggests N^{14} coupling.

In contrast to the valines and leucines (see below) no differences could be detected in the resonances of irradiated D-, L- and DL-alanines.

The resonances for X-irradiated D- and L-valine are the same, but that for DL-valine appears to differ from them. This difference, however, may be only one of relative component spacing. Compare Figs. 2 and 3. There are uncertainties arising from incomplete resolution of the patterns. The best resolution is obtained with low amplitude modulation (lower curves of Fig. 2), but stronger modulation (as in Fig. 3) is needed to detect the weak, outer components. The higher modulation indicates that both D- and L-valine have symmetrical patterns of nine components with gaussian, or approximately gaussian, intensity distribution and a g-factor of 2.00. With lower modulation, Fig. 2, each component of the set of 9 is partially resolved into a doublet or triplet. The pattern for DL-valine is similar but somewhat better resolved because of the wider spacing of the substructure. However, the outer components for DL-valine could not be detected, and it is not certain that they exist.

(4) W. Gordy and C. G. McCormick, *J. Am. Chem. Soc.*, **78**, 3243 (1956).

(5) A. van Roggen, L. van Roggen and W. Gordy, *Bull. Am. Phys. Soc.*, **1**, 268 (1956).

α-Alaine. β-lAanine.

Fig. 1.—Electron spin resonance curves of X-irradiated α-alanine and β-alanine. The samples in the powdered form were observed at room temperature in air at a frequency of 23,000 Mc./sec. The g-factor for the center of the resonance pattern is 2.00. The scale markers at the base of the figure are 68 gauss apart. The curves represent first derivatives of the actual absorption contours and were obtained by small amplitude modulation of the resonance frequency with a phase-sensitive, lock-in amplifier tuned to the modulation frequency. They were recorded on curved coördinate paper with an Esterline–Angus recorder. Except for specified variations, these conditions apply to the other figures of this paper.

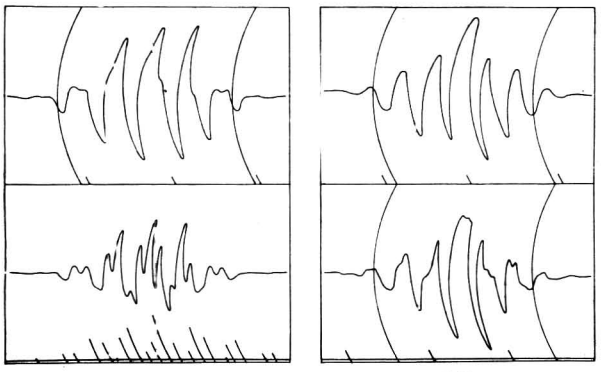

DL-Valine. L-Valine.

Fig. 2.—Electron spin resonance curves for valine at 9000 Mc./sec. These curves represent second derivatives of the actual absorption curves. The modulation amplitude is greater for the upper curves than for the lower ones. The bars in the lower left figure represent the theoretical pattern for an organic free radical with 6 hydrogens, each producing splitting of 26 gauss and 2 additional ones producing splitting of 33 gauss each. Very weak outer components are not shown.

The best resolved pattern of DL-valine can be fitted within experimental error to that of a radical having sets of six and two hydrogens with equivalent couplings. The set of six split the resonance into a septet with component spacing of 26 gauss, and the equivalent pair split the components of the septet further into triplets of component separation of 33 gauss. The theoretical pattern for this type of radical is indicated by bars below the observed patterns for DL-valine in Fig. 2. It is seen to agree very well with the observation. The pattern for D- or L-valine appears to arise from a similar radical but with the equivalent pair of protons having a coupling more nearly equal to that of the six, and with coupling constants slightly lower. These differences may arise from effects of the different internal crystalline fields. The DL-valine has a different crystalline form from that of L- or D-valine. The patterns for D- and L-valine appear to have a secondary resonance near

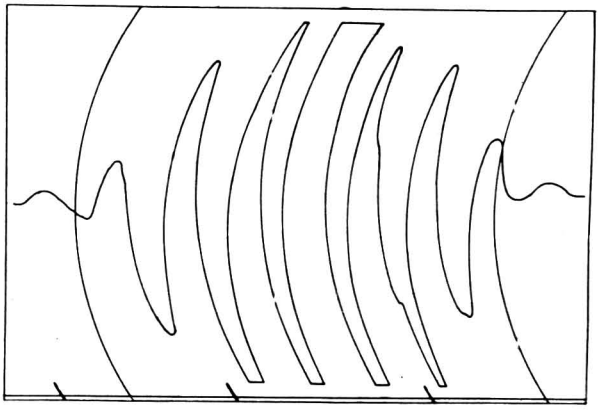

D-Valine.

Fig. 3.—Electron spin resonance at 9000 Mc./sec. for X-irradiated D-valine with sufficient modulation and amplifier gain to show the weak outer components. The curve represents the second derivative of the absorption contour. A radical with 8 hydrogen nuclei coupling equally to the electron spin would have in the strong-field case a 9 component hyperfine structure with relative intensities: 1, 8, 28, 56, 70, 56, 28, 8, 1.

the center, but this may be a confusing effect of the incomplete resolution of the substructure.

The radical $(CH_3)_2CCH_2COOH$, with sets of 6 and 2 equivalent hydrogens, can be made from valine by the loss of NH_2 and the shift of a proton between carbons. It may give rise to the observed patterns. The large isotropic coupling of the eight proton spins to the odd electron spin can be explained by treating the radical as a hybrid of the forms of type II, III and IV below.

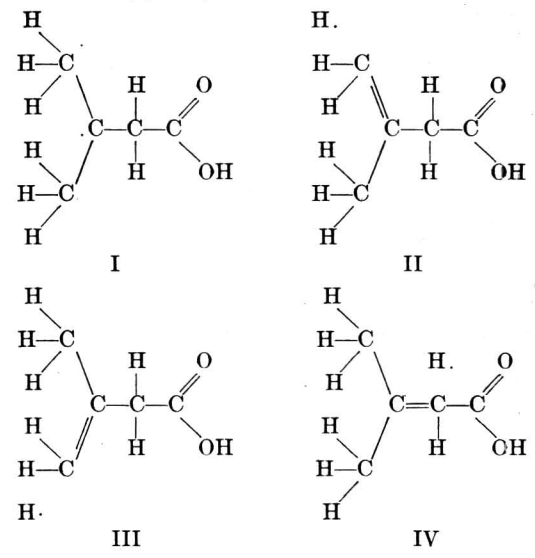

I II III IV

The anisotropic direct dipole–dipole interaction between the proton and electron spin in such a radical would be insignificant, in accordance with the observations. The couplings indicate that the odd electron has about 5% of its density in the 1s orbital of each of the six equivalent protons and therefore that forms II and III contribute about 15% each to the ground state of the molecule. The contribution of form IV is of the same order of magnitude as those of II and III. This resonance would tend to cause the four carbons of the $(CH_3)_2CCH_2$ group to lie in a plane with the three CC

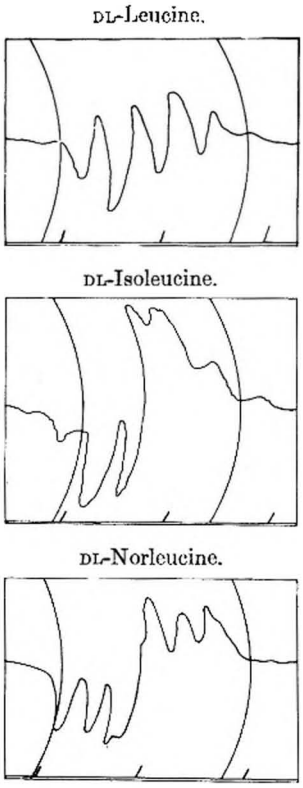

Fig. 4.—First derivative electron spin resonance curves for various isomeric forms of leucine after X-irradiation.

bonds at approximately 120° apart. The cage in which the radical is trapped could easily distort the form of this group and influence the relative contributions of the various structures and hence the relative nuclear couplings. This effect might account for the principal differences of the patterns for DL-valine from those of D- or L-valine.

Of course the various contributing structures mentioned here are not real. The hypothetical structures I to IV are useful, however, in showing how the electron spin density is spread out around the various hydrogens in the actual structure. Furthermore, the specific radical mentioned may not be the one observed, but we believe that it is very similar to the one observed. For example, the observed radical might be $(CH_3)_2CCH_2R$ or $(CH_3)_2CHCHR$, where R is any group which has no coupling nuclei.

Norvaline gives no observable resonance with the X-ray dosage which produced strong resonance in valine and other amino acids. No observable resonance could be produced when it was irradiated in either air or a vacuum. We must conclude that in contrast to other amino acids studied, the radicals produced in norvaline are very short lived.

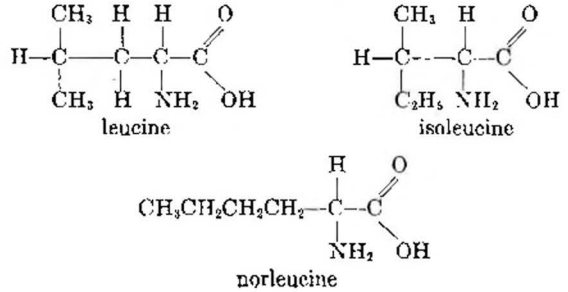

Leucine, norleucine and isoleucine give entirely different resonance patterns (see Fig. 4). These bear out the results on valine and other molecules that isomeric arrangement is highly significant in the determination of radiation effects on molecules. The resonances of leucine, isoleucine and norleucine all have patterns arising from proton hyperfine structure. However, the patterns are complex with incompletely resolved structure, and no attempt will be made to assign a specific radical to them.

Amino Acids Containing Sulfur.—The studies on single crystals of cystine prove that the asymmetric pattern originally obtained for polycrystalline cystine is caused by an orientation dependence of the g-factor as earlier assumed. Figure 5 shows the resonances obtained for some selected orientations. Figure 5 also shows the resonance of the same crystal later crushed into a polycrystalline form. Figure 6 shows the powdered cystine reso-

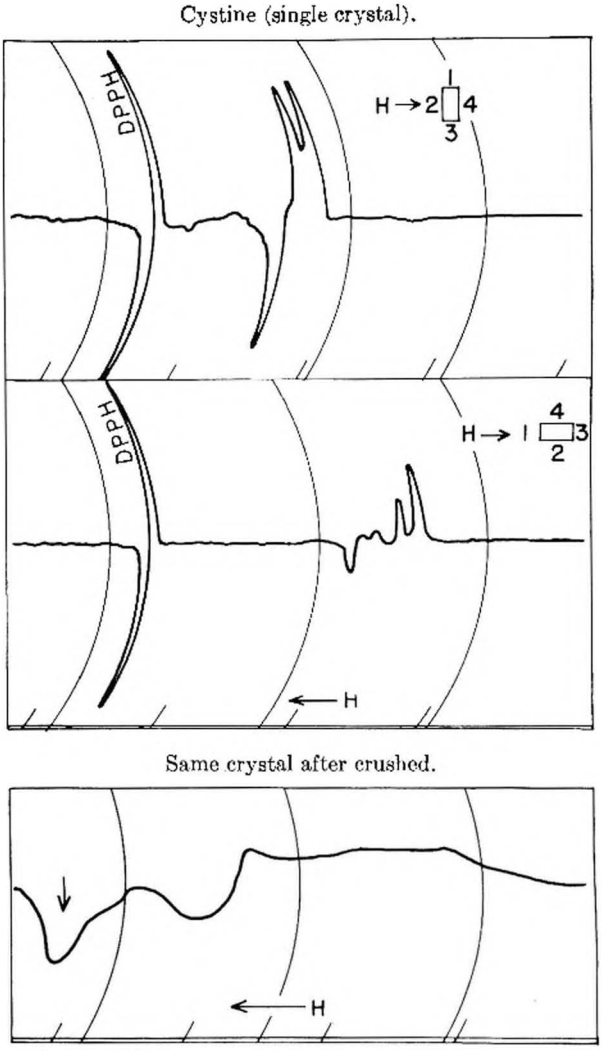

Fig. 5.—The upper curves show the electron spin resonance at 23,000 Mc./sec. of an X-irradiated single crystal of cystine for two different orientations of the crystal in the magnetic field, with the sharp resonance of diphenyl picryl hydrazil (DPPH) superimposed. The lower curve shows the resonance of the same crystal after it was crushed into the polycrystalline form. The arrow in the lower curve shows where the DPPH resonance (g = 2.0036) would fall.

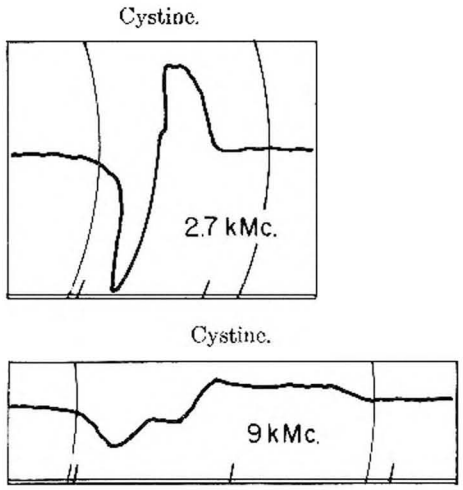

Fig. 6.—Electron spin resonance of X-irradiated powdered cystine at two different frequencies.

nance observed at different microwave frequencies (and hence with different magnetic fields). As expected for a resonance which has different g-values for different orientations, the pattern is more spread out at the higher frequencies. This marked field-dependence of the g-values arises, we think, from a residual spin orbital coupling. A significant residual spin orbital coupling would be expected if the odd spin were mainly localized on an SS link or a single S atom.

Figure 7 compares the resonance of X-irradiated cysteine at 23,000 Mc. with that for X-irradiated cystine. The only reproducible difference in the two patterns is a small difference in the field dependence. (That for cystine is slightly more spread out.) Probably this slight difference in the patterns arises from a difference in the internal crystalline fields rather than from a difference in the radicals themselves. Cysteine is a monomer which contains the SH link whereas cystine is a dimer joined by the disulfide bond. The formulas for them are

X—SH
cysteine

X—S—S—X
cystine

where X = $CH_2CH(NH_2)COOH$ in each.

In Fig. 7 is also given the resonance of X-irradiated, reduced glutathione

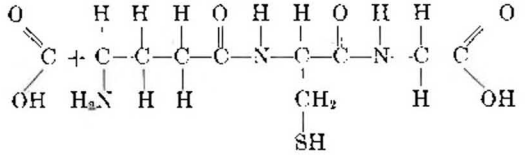

and oxidized glutathione. The reduced glutathione gives the same pattern as that of cysteine. In the accompanying paper glycylglutathione is shown to give the same resonance. The resonance of oxidized glutathione may be the same as that of cystine but with an impurity pattern superimposed, perhaps one caused by the formation of a complex with oxygen. We think that the extra bump may be due to an impurity because it was higher in a lower priced sample.

The resonance of X-irradiated homocystine

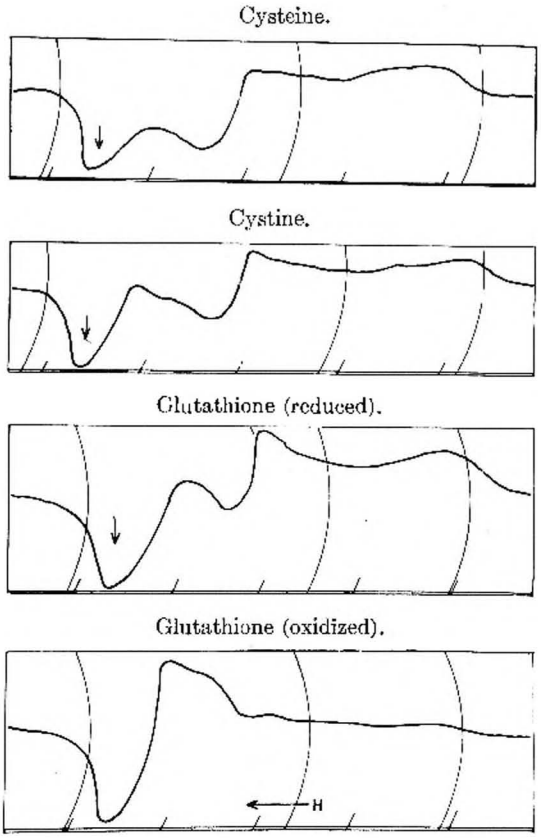

Fig. 7.—Comparison of resonances at 23,000 Mc./sec. of free radicals produced by X-irradiation of cystine, cysteine and glutathione. Arrows indicate position for g-factor of free electron spin.

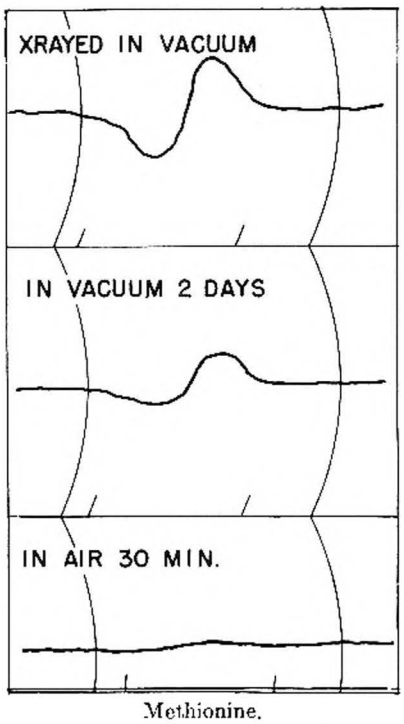

Methionine.

Fig. 8. -Electron spin resonance of radicals produced by X-irradiation of methionine, showing effects of air on the rate of decay.

X—CH_2—S—S—CH_2—X
homocystine

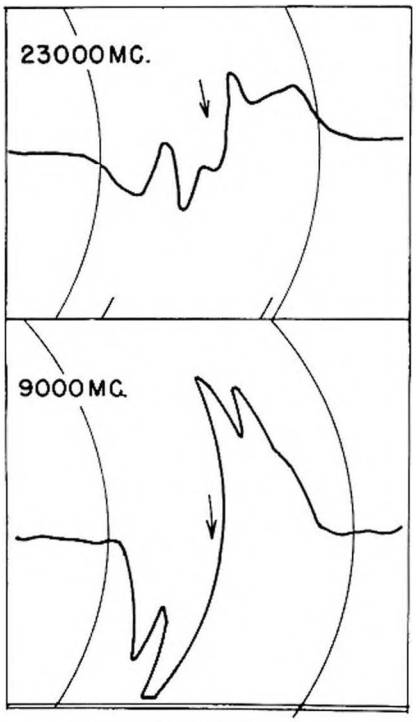

Lanthionine.

Fig. 9.—Electron spin resonances of X-irradiated lanthionine at two different frequencies. Arrows show position for g-factor of free electron.

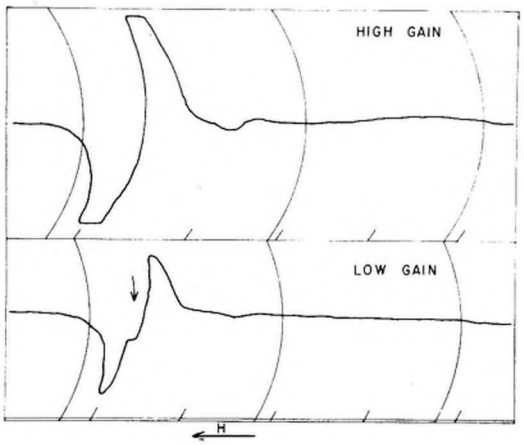

Djenkolic acid.

Fig. 10.—Electron spin resonance of X-irradiated djenkolic acid at 23,000 Mc./sec. Arrow indicates g factor of free electron.

which is not shown, is the same as that for cystine.

The structural formulas for methionine, lanthionine and djenkolic acid are

$X—CH_2—SCH_3$	$X—S—X$	$X—S—CH_2—S—X$
methionine	lanthionine	djenkolic acid

where again X represents the group $CH_2CH(NH_2)$-COOH. These compounds when X-irradiated do not give the characteristic cysteine or cystine resonance despite their close structural similarity to these compounds. Compare Figs. 8, 9 and 10. Note, however, that the structural differences occur in groups connected to the sulfur. For example, methionine is like homocysteine except that the H attached to the S of the latter is replaced by CH_3 in the former. Lanthionine is like cystine with one less sulfur. Djenkolic acid is like cystine with a CH_2 inserted between its two sulfurs. Contrast these small structural changes, which cause large changes in the resonance, with the larger structural difference in cystine and glutathione which leads to no observable difference in the resonance. Since the resonance is sensitive to the substitution only when it involves atoms bonded to the sulfur, we believe that these comparisons indicate that the odd spin density in all these cases is mainly on the sulfur. However, we are left with the problem of accounting for the similarity of the resonances for the -SH and –S–S– compounds and the differences of these from those of methionine, lanthionine and djenkolic acid, which have two carbons attached to each sulfur.

It originally was suggested[2] that the radical produced by radiation of cystine is of the form

$$X—S\cdots S^+—X$$

Since the additional three-electron bond made possible by the removal of an electron from sulfur would strengthen rather than weaken the SS link, it was suggested that this link may not be broken by ionization but may form a low energy trap for the positive charge or electron hole. The fact that cysteine gives the same type of resonance now makes this interpretation questionable, although not disproved. To form the same radical after ionization, cysteine would have to lose the SH hydrogen to become $X–S^+$ (which is not a free radical) and then dimerize with a neighboring X-SH to form $X–S\cdots S^+–X$. The simpler and seemingly more probable event would be the loss of H^+ upon ionization to form the neutral radical $X–S\cdot$. Cystine could form the same radical if the SS link is broken after ionization. Thus we do not know whether the common resonance of cysteine and cystine is due to $X–S\cdot$ or to $X–S\cdots S^+–X$, but we think it is one or the other. To clear up the uncertainty, we hope later to make measurements on the S^{33} nuclear coupling in a sample with S^{33} concentrated. A further discussion of this case is given elsewhere.

The principal resonance of irradiated djenkolic acid is a doublet similar to that of glycylglycine. There is evidence, however, that a field-dependent component like the cystine resonance is superimposed on the doublet. The doublet may arise from the radical, X–S–CH–S–X, which should have the principal resonating structures

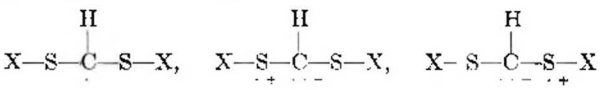

It is evident that these structures are equivalent to a switching three-electron bond between the C and S. Such bonding should be significant here because C and S have essentially the same electronegativities.

The weak cystine-like resonance in djenkolic acid could arise from an impurity of cystine or cysteine, or it might arise from a small concentration of the radical X–S·, formed from the djenkolic acid.

The spin resonance of X-irradiated methionine is a fairly broad singlet which of course may have un-

resolvable structure. A possible occurrence in ionized methionine would be the loss of $(CH_3)^+$ from the S to form the radical $X–CH_2–S\cdot$. If this is the radical formed in methionine, the radical in homocysteine cannot be formed by the breaking of the SS link because the patterns of homocystine and methionine would then be the same, would arise from the same radical. This conclusion suggests that the radical which gives the cystine-like resonance is $X–S\cdot\cdot S^+–X$, or that the one for methionine is not $X–CH_2–S\cdot$. If the unresolved structure of the methionine resonance is a triplet, the radical may be $X–S–CH_2$. However, methionine has a different oxygen effect than has glycylmethionine, which has a resolvable triplet resonance only when X-irradiated *in vacuo*. See the paragraph below. It is of interest that methyl sulfide, when X-irradiated, gives a triplet resonance.

The resonance of X-irradiated lanthionine is apparently complicated by having a proton hyperfine structure plus a field dependence. See Fig. 9. It is difficult to make a guess from the observed pattern about the identity of the radical. The resonance bears no resemblance to that of cystine.

The resonances of many of the sulfur compounds are killed by oxygen. The rapid quenching of the resonance of methionine by air is illustrated by Fig. 8. Interestingly, the resonance of glycylmethionine, which is similar to that of methionine, is not quenched by air but is converted from a triplet to a singlet.

Amino Acids with Rings.—Phenylalanine

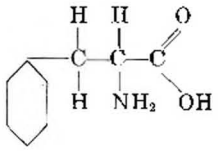

appears to give an incompletely resolved triplet when X-irradiated. However, the gaussian intensity distribution is not certain. See Fig. 11. A triplet might arise from the radical

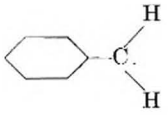

The unpaired electron of this radical would migrate in the ring, but the ring hydrogens should only broaden the components of the triplet caused by the two hydrogens outside the ring.

Tyrosine is like phenylalanine except that an OH is substituted for an H on the ring. The resonance of tyrosine (Fig. 12) is, however, a moderately broad singlet rather than a triplet as is obtained for phenylalanine. *Ortho*, *para* and *meta*-tyrosine were all examined and each found to give the singlet. It seems probable that tyrosine would lose a proton upon ionization to form the radical

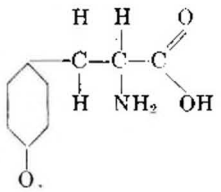

This radical would be stabilized by migration of the odd electron around the ring as indicated by the possible contributing structures

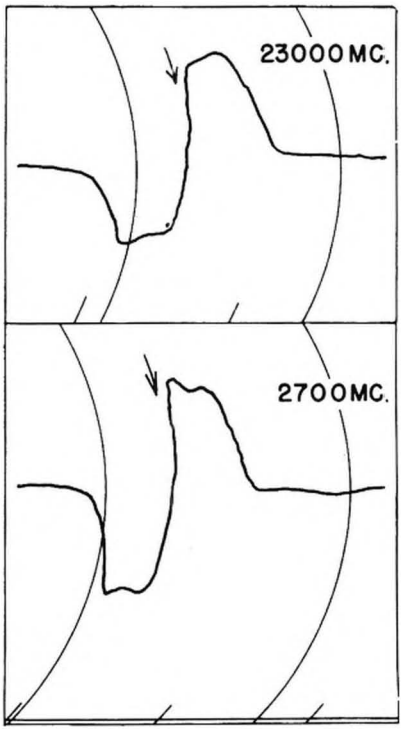

Phenylalanine.

Fig. 11.—Electron spin resonance of X-irradiated phenylalanine at two different frequencies. Arrows indicate position for free electron spin.

Tyrosine.

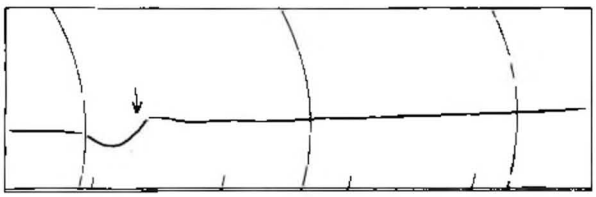

3,5-Diiodotyrosine.

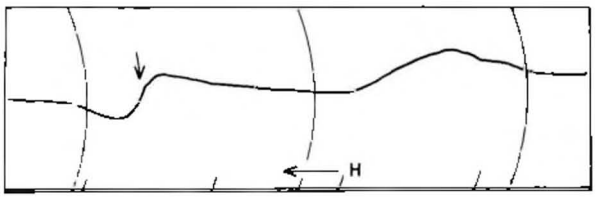

Tryptophan.

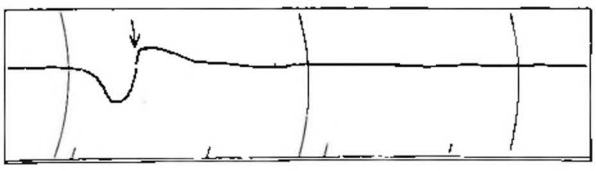

Fig. 12.—Electron spin resonance of X-irradiated tyrosine, diiodotyrosine, and tryptophan at 23,000 Mc./sec. Arrows show position for free electron spin resonance.

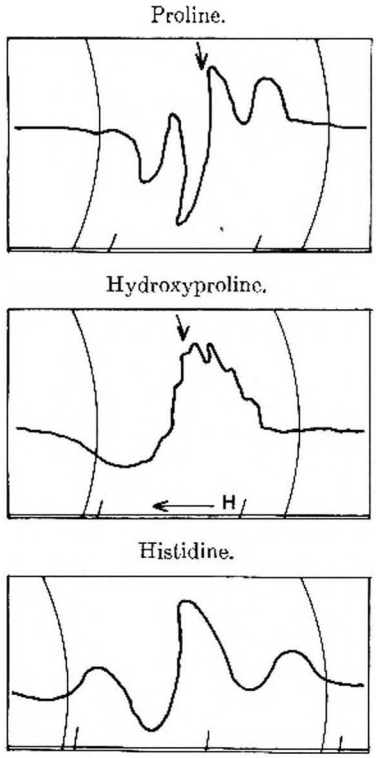

Fig. 13.—Electron spin resonance of X-irradiated proline, hydroxyproline and histidine.

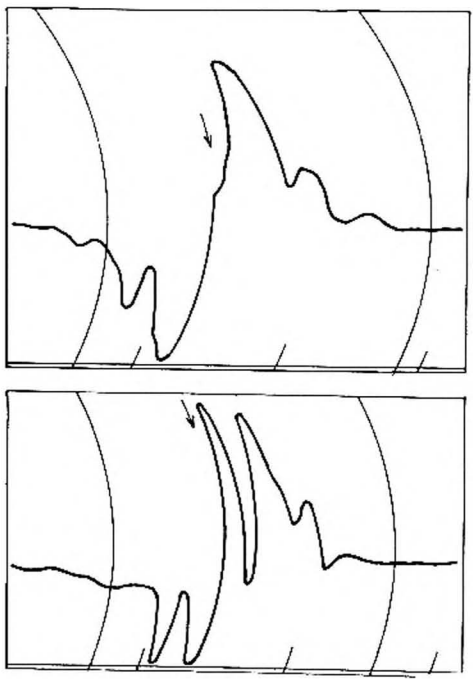

Fig. 14.—Electron spin resonance of X-irradiated serine and threonine.

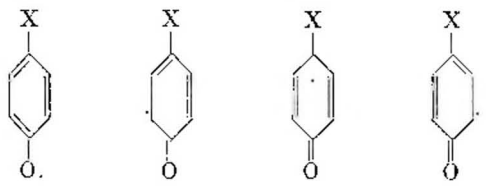

but the ring protons would not likely give a resolvable structure in the solid state.[6] Here X represents $CH_2CH(NH_2)COOH$.

The tyrosine ring should provide a good sink for an electron hole. Since in a biological system the lost proton might be regained, it seems that tyrosine like cysteine would be useful as a protective agent against damaging effects of radiation. As a constituent of proteins it should tend to prevent the breaking of the polypeptide backbone structure by ionization. The phenylalanine ring might likewise provide a sink to prevent breakage of a polypeptide chain. However, the damage to the phenylalanine residue, if the above interpretation of its resonance is correct, would be more severe than that to tyrosine.

The resonance of 3,5-di-iodotyrosine is more complicated than that of tyrosine itself. It is spread out over about 200 gauss with bend points near each end. However, the spreading is almost the same at 9000 as at 23,000 Mc./sec. This suggests that the spreading may arise partly from an orientation-dependent iodine hyperfine structure which cannot be resolved in the polycrystalline sample used and partly from anisotropy in the g-factor.

The resonance of X-irradiated tryptophan

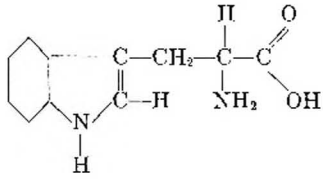

is a broad singlet like that of tyrosine. See Fig. 12. The radical which causes this resonance might be formed by the loss of the NH proton. The odd electron could then migrate around in both rings. This migration could be described in terms of resonance or the switching of bonds as is described above for tyrosine. Tryptophan should thus act as a protective agent in the manner proposed for tyrosine.

Proline and hydroxyproline

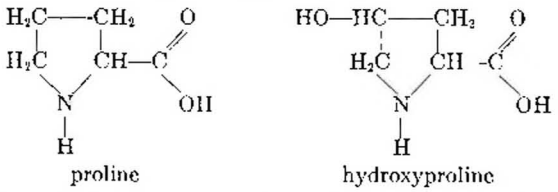

respond differently to X-irradiation. See Fig. 13. Proline gives a resonance with five peaks, but the two outer components are too weak to fall into a gaussian distribution of intensities. The resonance might be classified as a triplet with very weak shoulders, like that of irradiated glycine.

The resonance of hydroxyproline has an incompletely resolved nuclear hyperfine structure of several components. From the difference in the number of coupling protons we suspect that the ring is broken in proline but not in hydroxyproline. We shall not speculate on what the particular radical may be in either case.

(6) The component spacings of the hyperfine structure in various semiquinones observed in solution are only about 2 gauss. See, for example, J. E. Wertz, *Chem. Revs.*, **55**, 917 (1955).

Histidine (base free)

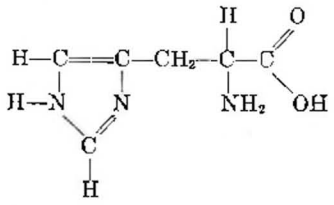

when X-irradiated gives a triplet resonance with a total spread of about 100 gauss. See bottom curve of Fig. 13. The triplet splitting is greater and the resolution more nearly complete than that for glycine or other substances from which we have obtained triplet hyperfine structure caused by protons. It seems possible that the radical formed may be

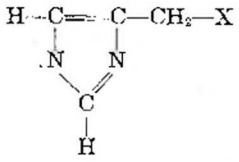

where X represents $CH(NH_2)COOH$, and that the triplet arises from the CH_2 protons outside the ring. The large coupling of the two protons could result from total contributions of about 100/504, or 20% of the two equivalent structures of the form

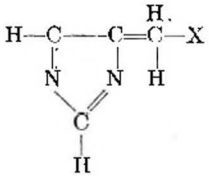

to the ground state of the molecule. The resonance of histidine monohydrochloride is similar to that of base free histidine except that each of the triplet components gives evidence of an unresolved structure.

Serine and Threonine.—Figure 14 gives the first derivative curves for the spin resonance of free radicals produced by X-irradiation of serine and threonine.

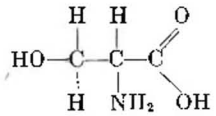

serine

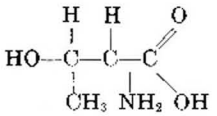

threonine

The curves given are for the L compounds. These are the same as for the corresponding D compounds. No studies were made of the DL series.

Both curves of Fig. 14 show hyperfine structure arising from three or more hydrogen nuclei. For both the resolution is incomplete, and there is complexity which may arise from the superposition of patterns of more than one radical and/or the unequivalent coupling of the hydrogens. It is not possible to ascertain the specific radicals from the patterns.

In the earlier work a simple doublet of 35 gauss separation was obtained by X-irradiation of serine hydrochloride. It is interesting that the HCl completely changes the radical formation of serine. The pattern given for threonine in the earlier work is less complete and more poorly resolved than that in Fig. 14.

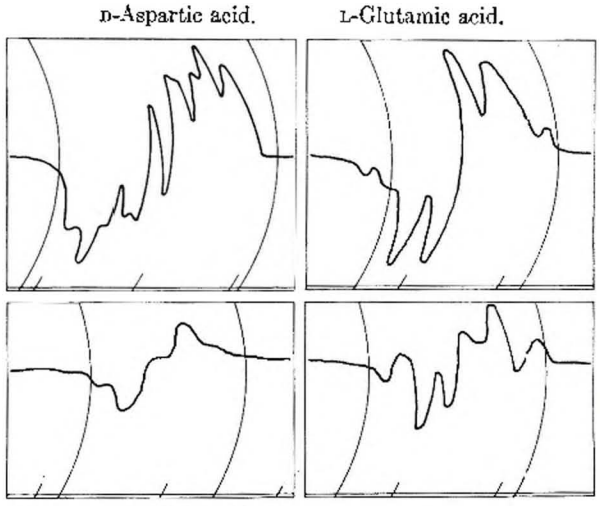

Fig. 15.—Electron spin resonance of X-irradiated aspartic acid and asparagine, glutamic acid and glutamine.

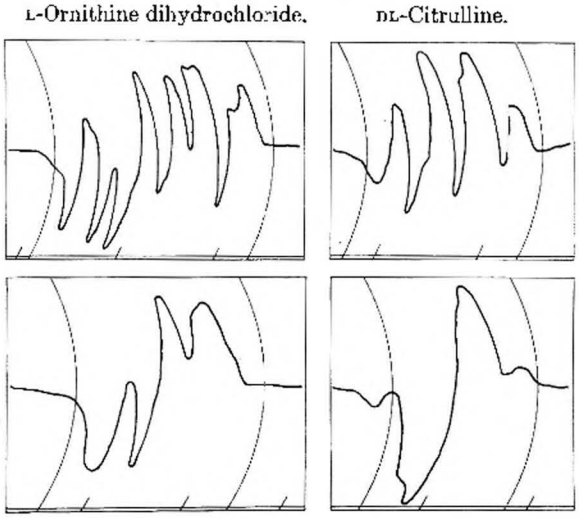

Fig. 16.—Electron spin resonance of X-irradiated ornithine, lysine, citrulline and arginine.

Aspartic Acid, Asparagine, Glutamic Acid and Glutamine.—The resonance produced by X-irradiation of each of these compounds has a complex structure apparently arising from interaction of the electron spin with hydrogen nuclei. See Fig. 15. By comparison of the patterns for the four compounds

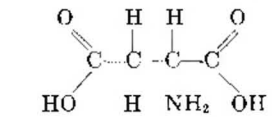

aspartic acid

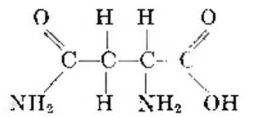

asparagine

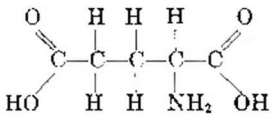

glutamic acid

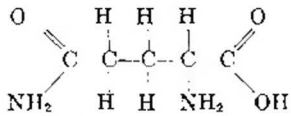

glutamine

one sees that qualitative changes in the resonance patterns are obtained either by substitution of NH_2

for OH or by an increase of the chain length with a CH_2 group. Again the specific radicals cannot be assigned.

Ornithine, Lysine, Arginine and Citrulline.—In the electron spin resonance curves for X-irradiated ornithine hydrochloride, $NH_2(CH_2)_3CHNH_2COOH$-(HCl), and lysine hydrochloride, $NH_2(CH_2)_4$-$CHNH_2COOH$(HCl), one again sees the qualitative differences caused by an increase of one CH_2 group in the chain. See Fig. 16. (Compare with asparagine and glutamine above.) Figure 16 also gives the resonances of X-irradiated arginine and citrulline. All these resonances are complex and give evidence for the existence of more than one radical and for unequivalent coupling of protons in the same radical.

In France Combrisson and Uebersfeld[7] have investigated with electron spin resonance the effects of atomic pile irradiation on a number of amino acids. They reported a triplet resonance for several amino acids and no observable signal for others. We do not yet know the causes for the differences between our observations and theirs, but they must arise from differences in the experimental conditions or in the methods of irradiation.

(7) J. Combrisson and J. Uebersfeld, *Compt. rend. Acad. Sci. (Paris)*, **238**, 1397 (1954); J. Uebersfeld, thesis for degree of doctor of physical science, University of Paris, 1956.

EQUILIBRIA IN AQUEOUS SOLUTIONS OF COPPER(II) CHELATES WITH α,α'-DIPYRIDYL, *o*-PHENANTHROLINE AND ETHYLENEDIAMINE[1]

BY L. B. RYLAND, G. S. RONAY AND F. M. FOWKES

Shell Development Company, Emeryville, California

Received December 23, 1957

The equilibria of species in solutions of the 1:1 chelates of cupric nitrate with α,α'-dipyridyl, *o*-phenanthroline or ethylenediamine have been investigated by potentiometric titration with sodium hydroxide. Equilibria have been calculated from the sodium hydroxide consumption in solutions of different cupric chelate concentration at constant *p*H. It was found that in solutions of the 1:1 chelate of cupric ion and dipyridyl (containing 0.1 *M* KNO_3 to maintain constant ionic strength), the system studied in greatest detail, three species are present in measurable quantities: an acidic species A, $DipyCu(H_2O)_2^{++}$; an uncharged but water-soluble basic species B_2, $DipyCu(OH)_2^{\circ}$; and a dimeric species $(B_1)_2$, DipyCu 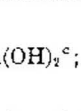 CuDipy^{++}.

Presumably a species B_1, $DipyCu(H_2O)OH^+$, also exists but not in measurable concentrations. In acidic solutions species A predominates, in neutral solutions species $(B_1)_2$ predominates, and in alkaline solutions species B_2 predominates; species $(B_1)_2$ increases in concentration at the expense of other species with increase in the over-all concentration of copper chelate. At 25° for the equilibrium $2A \leftrightarrows (B_1)_2 + 2H^+ + 2H_2O$, $K_{\alpha 2} = 10^{-10.74}$, and for the equilibrium $A \leftrightarrows B_2 + 2H^+$, $K_A = 10^{-16.28}$. Analogous constants for solutions of the 1:1 chelate of cupric ions and *o*-phenanthroline are $K_{\alpha 2} = 10^{-10.86}$ and $K_A = 10^{-17.0}$. In both systems the constants increase with temperature; $\Delta H_{\alpha 2}$ is 8.2 and 8.3 kcal./mole and ΔH_A is 5.4 and 4.2 kcal./mole for the dipyridyl and *o*-phenanthroline chelate, respectively.

Introduction

The hydrolysis of hydrated metal ions has been studied in some detail by others[2-6] who have shown that hydrated metal ions such as cupric, uranyl, bismuth and scandium hydrolyze to form basic ions and dimers or polymers of the basic ions. A similar investigation has been undertaken with hydrated chelated metal ions.

The present investigation has been confined to the 1:1 chelates of cupric ion with α,α'-dipyridyl or with 1,10-*o*-phenanthroline which are of interest as catalysts in hydrolysis reactions.[7] The object of the investigation is to identify the various species in such solutions and to determine the appropriate equilibrium constants as a function of concentration, *p*H and temperature. A few results with ethylenediamine are appended.

(1) (a) Presented at the 128th Meeting of the American Chemical Society in Minneapolis, Minnesota, September, 1955; (b) this paper reports work done under contract with the Chemical Corps, U. S. Army, Washington 25, D. C.

(2) K. J. Pedersen, *K. Danske Videnskabernes Selskab*, **20**, No. 7 (1943).

(3) F. Graner and L. G. Sillen, *Acta Chem. Scand.*, **1**, 631 (1947).

(4) S. Ahrland, *ibid.*, **3**, 374 (1949).

(5) M. Kilpatrick and L. Pokras, *J. Electrochem. Soc.*, **100**, 85 (1953).

(6) S. Hietanen and L. G. Sillen, *Acta Chem. Scand.*, **8**, 1607 (1954).

(7) T. Wagner-Jauregg, *et al.*, *J. Am. Chem. Soc.*, **77**, 922 (1955).

(8) *Cf.* A. E. Martell and M. Calvin, "Chemistry of the Metal Chelate Compounds," Prentice-Hall Publ., Inc., New York, N. Y., 1952.

Experimental Details

Materials.—The α,α'-dipyridyl was certified reagent grade from Fisher Scientific Company and its melting point indicated a purity of 99.9%. The 1,10-*o*-phenanthroline monohydrate was manufactured by the G. Frederick Smith Chemical Company. The ethylenediamine monohydrate was obtained from Eastman Kodak Company (No. 1915) and had a purity of 97.2% by acid titration. The cupric nitrate and potassium nitrate were standard reagent grade chemicals. Solutions for titration were maintained free of CO_2 and contained 0.1 *M* KNO_3 and 4.75% of propylene glycol.

Apparatus. Potentiometric titrations were made with a Precision-Shell Dual AC Titrometer, using a jacketed titration beaker through which thermostated water was passed to give temperature control.

Discussion of Results

Equilibria of Species in Solutions of 1:1 Cupric Dipyridyl Nitrate.—The stability of the 1:1 chelate is sufficient[8] that it is treated as an undissociable entity. The titration of this chelate with sodium hydroxide (Fig. 1) shows that it loses two hydrogen ions in two steps. Designating the minimum

hydration necessary to explain the observed reactions, we write

$$DipyCu(H_2O)_2^{++} \rightleftarrows DipyCu(H_2O)OH^+ + H^+ \rightleftarrows DipyCu(OH)_2^0 + 2H^+$$

which we abbreviate to

$$A \rightleftarrows B_1 + H^+ \rightleftarrows B_2 + 2H^+$$

giving rise to equilibrium constants

$$K_{A_1} = \frac{[B_1][H^+]}{[A]},\ K_{A_2} = \frac{[B_2][H^+]}{[B_1]},\ K_A = \frac{[B_2][H^+]^2}{[A]}$$

The family of curves in Fig. 1 cross at one mole of sodium hydroxide per mole of chelate, which occurs at *p*H 8.1. At this ratio [A] = [B_2], so from the definition of K_A we see that the *p*H of the "crossover" is $pK_A/2$. The *p*H of the crossover is independent of concentration, but at any *p*H below or above it the titration curves shift with increase in concentration toward an hydroxyl to copper ratio of 1.0. This means that species B_1 forms a dimer or polymer.

The formation of polymers of B_1 can be written as

$$nA \rightleftarrows (B_1)_n + nH^+ + nH_2O$$

$$K_{\alpha n} = \frac{[(B_1)_n][H^+]^n}{[A]^n}$$

The equilibrium constants have been determined from the titration data (in the *p*H range of 6–7.5 where [B_2] is small compared with [A]) in the following manner. For any point in a titration curve let Y equal the total equivalents per liter of hydroxide consumed up to that point

$$Y = [B_1] + 2[B_2] + \sum_{n=2}^{\infty} n[(B_1)_n] \qquad (1)$$

Substitution of equilibrium constants gives

$$Y - 2[B_2] = K_{A_1}\frac{[A]}{[H^+]} + \sum_{n=2}^{\infty} nK_{\alpha n}\frac{[A]^n}{[H^+]^n} \qquad (2)$$

From this series we may determine K_{A_1} and the $K_{\alpha n}$ values if we know [A] as a function of *p*H. The value [A] is calculated from the initial concentration of copper chelate $[A]_i$

$$[A] = [A]_i - Y + [B_2] \qquad (3)$$

in which [B_2] is closely approximated by

$$[B_2] = K_A\frac{([A]_i - Y)}{[H^+]^2}$$

and pK_A is obtained by doubling the *p*H of the "crossover."

Substitution of (3) into (2) gives

$$Y - 2[B_2] = K_{A_1}\left(\frac{[A]_i - Y + [B_2]}{[H^+]}\right) + \sum_{n=2}^{\infty} nK_{\alpha n}\left(\frac{[A]_i - Y + [B_2]}{[H^+]}\right)^n \qquad (4)$$

By plotting the logarithm of $Y - 2[B_2]$ *vs.* the logarithm of ($[A]_i - Y + [B_2]$) as in Fig. 2 the resulting line has a slope of $\bar{n}$, the average number of B_1 units in the aggregating species, and from the coördinates of a point in a section of given n, $K_{\alpha n}$ may be calculated from

$$\log K_{\alpha n} = \log\frac{(Y - 2[B_2])}{n} - n\log\frac{([A]_i - Y + [B_2])}{[H^+]} \qquad (5)$$

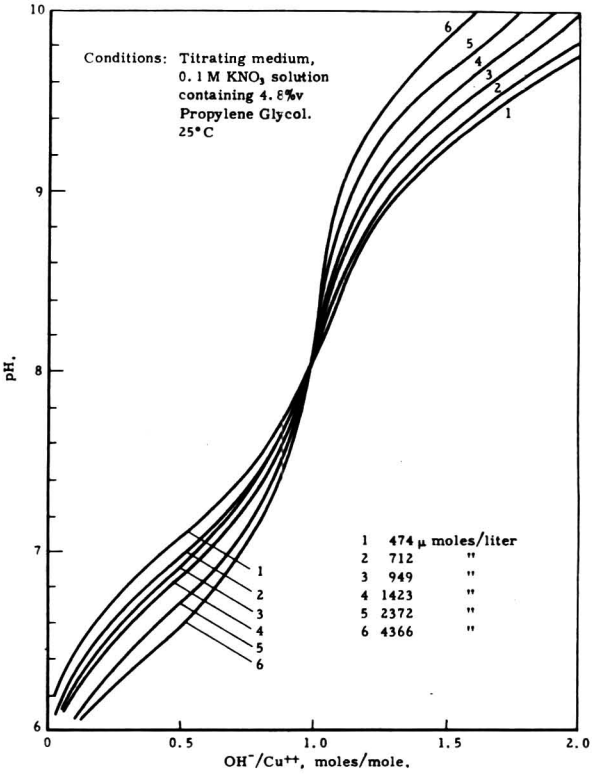

Fig. 1.—Titration of 1:1 dipyridyl cupric nitrate at various concentrations with sodium hydroxide.

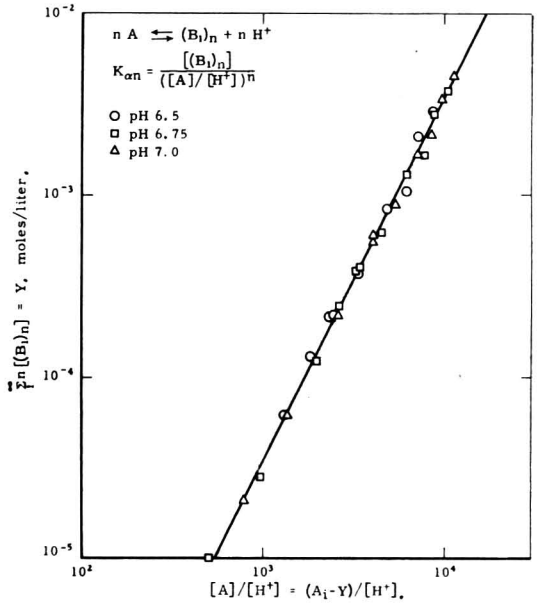

Fig. 2.—Hydrolysis of the 1:1 cupric dipyridyl nitrate at 25°, *p*H 6.5 to 7.0, where "A" represents DipyCu $(H_2O)_2^{++}$, and B_1 DipyCu$(H_2O)OH^+$.

In several cases [B_2] turned out to be negligible and log Y *vs.* log ($[A]_i - Y$) is plotted.

At *p*H 9 or above, where [B_2] is large and [A] very small, we may use a similar treatment by considering addition of acid to a solution of species B_2

$$nB_2 + nH^+ \rightleftarrows (B_1)_n$$

$$K_{\beta n} = \frac{[(B_1)_n]}{[B_2]^n[H^+]^n}$$

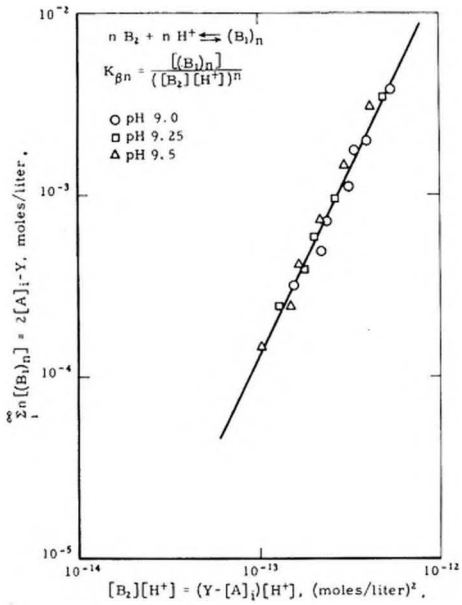

Fig. 3.—Hydrolysis of the 1:1 cupric dipyridyl nitrate at 25°, pH 9.0 to 9.5, where B_2 represents DipyCu(OH)$_2$.

By using the above expression in equation 1 we obtain Y (total hydroxide consumed) as a function of $[B_2]$

$$Y = 2[B_2] + \frac{[B_2][H^+]}{K_{A_2}} + \sum_{n=2}^{\infty} nK_{\beta n}[B_2]^n[H^+]^n \quad (6)$$

$[B_2]$ is determined from experimental measurements by

$$[B_2] = Y - [A]_i + [A]$$

in which $[A]$ is usually negligibly small, but can be closely approximated by

$$[A] \approx \left(\frac{2[A]_i - Y}{K_{\alpha 2}}\right)^{1/2} [H^+]$$

In terms of experimentally determined quantities, equation 6 becomes

$$(2[A]_i - 2[A] - Y) = (Y + [A] - [A]_i)\frac{[H^+]}{K_{A_2}} + \sum_{n=2}^{\infty} nK_{\beta n}(Y + [A] - [A]_i)^n[H^+]^n \quad (7)$$

This relation is used for determination of $\bar{n}$ and $K_{\beta n}$ by plotting $\log (2[A]_i - 2[A] - Y)$ *vs.* $\log (Y + [A] - [A]_i)[H^+]$, as in Fig. 3. The slope gives $\bar{n}$ and the coördinates give $K_{\beta n}$ at any pH or concentration, for

$$\log K_{\beta n} = \log \frac{(2[A]_i - 2[A] - Y)}{n} - \bar{n} \log (Y + [A] - [A]_i)[H^+] \quad (8)$$

Determination of $K_{\alpha n}$ and $K_{\beta n}$ allows calculation of K_A (provided $\bar{n}$ is the same in both pH regions), for

$$\frac{K_{\alpha n}}{K_{\beta n}} = \frac{K_n K_{A_1}{}^n}{K_n / K_{A_2}{}^n} = (K_{A_1}K_{A_2})^n = K_A{}^n \quad (9)$$

This is especially useful in these systems where $[B_1]$ is immeasurably small so that K_n, K_{A_1} and K_A are indeterminable, but $K_{\alpha n}$, $K_{\beta n}$ and K_A can be determined accurately.

Equilibria at 25°.—From the titration curves shown in Fig. 1, values of Y and $[A]_i - Y$ were determined at pH 6.5, 6.75 and 7.0 for all eleven concentrations (these are listed in Table I[9]). The $\log Y$ *vs.* $\log ([A]_i - Y)/[H^+]$ relation derived from equation 4 is shown in Fig. 2. A constant slope of 2.0 over the whole range of concentration shows that $(B_1)_2$ is the only form of B_1 present in measurable concentrations. This may be represented as

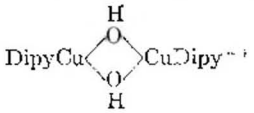

Furthermore, in the region of higher pH, the plot of titration data according to equation 7 in Fig. 3 also shows a constant slope of 2.0 and shows that in this pH region, also, the only form of B_1 is the dimer $(B_1)_2$. The presence of other species should be evident in Figs. 2 and 3 by curvature at either end of the straight lines to higher values of $\Sigma n[(B_1)_n]$. The presence of species B_1 would curve the lower end of the line upward and the presence of $(B_1)_3$ or higher polymers would curve the upper end upward. Of course, some B_1 must be present, but the maximum value of K_{A1} consistent with the data of Fig. 2 is about $10^{-5.7}$. The equilibrium constant $K_{\alpha 2}$ is found by equation 5 to be 1.8×10^{-11} or $10^{-10.74}$, $K_{\beta 2}$ is found by equation 8 to be $10^{+21.83}$, and K_A is found by equation (9) to be 5.2×10^{-17} or $10^{-16.28}$. The pH of the crossover should be $pK_A/2$ or 8.14; the observed crossover is actually pH 8.1.

Equilibria at 0 and 41.2°.—Titrations were made at 0 and 41.2° with 5×10^{-3} and 5×10^{-4} mole/liter of copper chelate (Fig. 4[9]). Values of Y were determined at pH 6.25, 6.50, 6.75, 7.0, 7.25, 8.5, 8.75, 9.0 and 9.25 (Table II[9]). In calculating Y, the free hydroxyl ion concentration at 0 and 41.2° was calculated from the pH measurement and using $10^{-14.95}$ and $10^{-13.7}$, respectively, for the dissociation constant of water. The graph of $\log Y$ *vs.* $\log ([A]_i - Y)/[H^+]$ at 0° gives a straight line of slope 1.8 to 2.0 ($\bar{n}$) and it is found that

$$K_{\alpha 2} = 6.5 \times 10^{-12} = 10^{-11.19}$$

For the data at pH 8.75 – 9.25, $\log (2[A]_i - 2[A] - Y)$ was plotted *vs.* $\log (Y - [A]_i + [A])$. A straight line of slope 1.9 to 2.0 and a $K_{\beta 2}$ of $10^{+21.85}$ were obtained. By equation 9

$$K_A = \left(\frac{K_{\alpha n}}{K_{\beta n}}\right)^{1/n} = 10^{-16.52}$$

so the $pK_A = 16.52$. This checks with the pK_A of 16.5 obtained by doubling the pH of the crossover (pH 8.25).

At 41.2°, we obtained $\bar{n} = 1.85$, and $K_{\alpha 2} = 10^{-10.32}$. This $\bar{n}$ is considered to be within experimental error of 2.0. The data obtained at pH 8.5, 8.75, 9.0 and 9.25 when plotted according to equation 7 give $K_{\beta 2} = 10^{+21.62}$ and $K_A = 10^{-15.92}$. The pK_A of 15.92 checks the value of 15.90 obtained by doubling 7.95, the pH of the crossover.

Temperature Coefficients of $K_{\alpha 2}$ and K_A.—When the values of $\log K_{\alpha 2}$ and $\log K_A$ are plotted *vs.*

(9) At the request of the Editor, Tables I–III and Figs. 4–6 are omitted but are available from the authors, or as photoprints or microfilm (Document No. 5520) for $1.25 from the ADI Auxiliary Publications Project, Photoduplication Service, Library of Congress, Washington 25, D. C.

$1/T$ the three points do not give a straight line, but rather a curve with increasing slope at higher temperatures. The slopes at 25° give $\Delta H_{\alpha 2}$ = 8.2 kcal/mole, and ΔH_A = 5.4 kcal/mole.

Equilibria of Species in Solutions of Copper *o*-Phenanthroline (1:1) Nitrate.—As in the case of copper dipyridyl, several species of copper *o*-phenanthroline exist in aqueous solutions

A—*o*-$PhCu(H_2O)_2^{++}$
B_1—*o*-$PhCu(H_2O)(OH)^+$
B_2—*o*-$PhCu(OH)_2$
$(B_1)_2$—(*o*-$PhCuOH)_2^{++}$

The equilibria between these species are as shown previously. The titration curves at 25 and 41.2° with 5 and 10 × 10^{-4} moles/liter of chelate are shown in Fig. 5,[9] the values of Y at pH 6.5, 6.75, 7.0, 7.25 and 7.5 are shown in Table III,[9] and the graphs of log Y *vs.* log ($[A]_i - Y$) are shown in Fig. 6.[9]

At 25°, $\bar{n}$ is found to be 2.0 throughout the whole range of pH values and concentrations, and $K_{\alpha 2}$ = 1.27 × 10^{-11} = $10^{-10.90}$. The pH of the cross-over is 8.50 so K_A = $10^{-17.00}$.

At 41.2°, $\bar{n}$ is also 2.0 for the whole range of pH values and concentrations, and $K_{\alpha 2}$ = 5 × 10^{-11} = $10^{-10.30}$. The pH of the cross-over is 8.35; thus, K_A = $10^{-16.7}$. From the values of $K_{\alpha 2}$ and K_A at 25 and 41.2°, one may calculate $\Delta H_{\alpha 2}$ = 8.3 kcal./mole, and ΔH_A = 4.2 kcal./mole.

Comparison of Equilibrium Constants.—In Table IV are shown the equilibrium constants at various temperatures for copper dipyridyl (1:1) nitrate and copper *o*-phenanthroline (1:1) nitrate. The tendency to dimerize to species $(B_1)_2$ is about the same, but the *o*-phenanthroline chelate is definitely the weaker acid as evidenced by the lower value of K_A. The acidity of 1:1 metal chelates undoubtedly is influenced by the basicity of the ligand; as the basicity (or pK_a) of ligands increases, the acidity of the chelates should decrease. Thus in comparing dipyridyl (pK_a=4.4) with *o*-phenanthroline (pK_a 5.0) as ligands for cupric ion, it is found that the *o*-phenanthroline chelate is the weaker acid.

TABLE IV

EQUILIBRIUM CONSTANTS FOR COPPER DIPYRIDYL AND COPPER *o*-PHENANTHROLINE IN 0.1 *M* KNO_3

Constant	Temp., °C.	Copper dipyridyl	Copper *o*-phenanthroline
$K_{\alpha 2}$	0	0.65 × 10^{-11}	.....
	25	1.8 × 10^{-11}	1.27 × 10^{-11}
	41.2	4.8 × 10^{-11}	5 × 10^{-11}
K_A	0	3.0 × 10^{-17}	.....
	25	5.2 × 10^{-17}	1.0 × 10^{-17}
	41.2	12.0 × 10^{-17}	2.0 × 10^{-17}

Equilibria of Species in Solutions of 1:1 Cupric Ethylenediamine Nitrate.—In all of the foregoing work the solutions contained 0.1 *M* sodium nitrate to keep activity coefficients of the metal chelate ions constant over wide ranges of concentration. However, in the case of the ethylenediamine chelate, addition of salt caused formation of a copper-containing precipitate so in this system salt could not be used and activity coefficients were not constant. Plots of the data as in Figs. 2, 3 and 6 have a very wide scatter of points. Nevertheless, the titration curves appear similar, with a cross-over at pH 8.6 (indicating a pK_A of 17.2) and the value of $K_{\alpha 2}$ is estimated to be about $10^{-11.6}$.

Acknowledgment.—The authors wish to thank Dr. J. N. Wilson for advice and encouragement and Mrs. Helen B. Heppe and Mr. Sherwood C. Beckley for assistance in obtaining precise titration curves.

HYDROGEN OVERPOTENTIAL ON ELECTROPLATED COPPER-TIN ALLOYS

BY I. A. AMMAR AND H. SABRY

Department of Chemistry, Faculty of Science, University of Cairo, Cairo, Egypt

Received August 30, 1957

Hydrogen overpotential has been measured on electroplated Cu, Sn and Cu–Sn alloys, in 1.0 *N* HCl at 30°. Six alloys ranging in composition from 12 to 80% Sn have been studied. The overpotential has been measured in the current density range 10^{-2} to 3 × 10^{-6} amp./cm². The results have been analyzed statistically and the 95% confidence limits, for the mean overpotential values, have been calculated. Attempts have been made to explain the overpotential–alloy composition relation through the dependence of overpotential on the heat of adsorption of hydrogen on the alloy.

Introduction

Overpotential studies on alloys are numerous. Thus Newbery[1] observed that the overpotential η was higher for Pb–Hg and Zn–Hg alloys than the corresponding values for the components. Fischer[2] measured η on a number of alloys and found it to be independent of the composition of the alloy and equal to that of the component with the lower overpotential. Harkins and Adams[3] found the overpotential on monel metal to be lower than the corresponding values for the components. For Cu–Ni alloys, Raeder and co-workers[4,5] observed a gradual change from the overpotential on Cu to that on Ni. Sharp maxima and a flat minimum were, however, observed for the other alloys studied by the above authors.[4,5] DeKay Thompson[6] studied the relation between the overpotential and composition of brass, and observed a sharp minimum between 15

(1) E. Newbery *J. Chem. Soc.*, **109**, 1051 (1916).
(2) P. Fischer, *Z. physik. Chem.*, **113**, 326 (1924).
(3) W. Harkins and H. Adams, THIS JOURNAL, **29**, 205 (1925).
(4) M. Raeder and J. Brun, *Z. physik. Chem.*, **133**, 15 (1928).
(5) M. Raeder and D. Efjestad, *ibid.*, **A140**, 124 (1928).
(6) M. DeKay Thompson, *Trans. Electrochem. Soc.*, **59**, 115 (1931).

and 18% Cu. He observed no connection between η and the equilibrium diagram of the alloy. DeKay Thompson and Kaye[7] observed a maximum between 40 to 80% Fe for the overpotential on Ni–Fe alloys at low polarizing current densities in KOH solutions. For Cr–Ni alloys, a minimum in the overpotential–alloy composition relation was observed between 20 and 30% Cr at high polarizing current densities.[8] Croatto and Da Via[9] observed a rise in η with the increase of Sb and Cd contents in Pb–Sb and Pb–Cd alloys when two phases were present.

No general conclusions, as to the relation between η and the alloy composition, could be drawn from the results of the above authors. Furthermore, no close connection between the overpotential–alloy composition relation and the equilibrium diagram or the lattice structure of the alloy could be established.[6,7] The aim of the present investigation is, therefore, to study the relation between overpotential and alloy composition for electroplated Cu–Sn alloys, with careful attention paid to the recent advances in the technique of hydrogen overpotential measurements,[10] and to attempt an explanation for the results obtained. The lack of rigorous experimental techniques in the older work emphasizes the need for the present investigation. Statistical analysis must be used, therefore, in order to establish the overpotential results with certainty. The use of electroplated Cu-Sn alloys is justified by the ease with which they are prepared in a reproducible fashion, and by the occurrence in the literature of reliable data for the overpotential on both Cu[11,12] and Sn.[13]

Experimental

The experimental technique was similar to that previously described for electroplated cathodes.[14] Electroplating was carried out in a cell fitted with water-sealed ground glass joints. The plating and the overpotential cells were made of arsenic-free glass and were cleaned with a mixture of Analar HNO_3 and H_2SO_4 acids followed by conductivity water. A platinum wire, sealed to glass, was used as a substrate for electroplating, and was cleaned in the above manner. After plating the electrode was washed several times with conductivity water and was immediately inserted in its position in the previously cleaned overpotential cell (water-sealed taps and ground glass joints). The cell was completely filled with conductivity water and this was displaced by pure hydrogen before the electrolyte was introduced. The electrolyte was 1.0 *N* HCl and was purified by pre-electrolysis[15] on an auxiliary electrode, of the same alloy as the test cathode, at about 4×10^{-2} amp./cm.^{2} for 20 hours. A platinized platinum electrode, in the same solution and at the same temperature as the test cathode, was used as a reference. In this manner the overpotential was measured directly. The direct method and the rapid technique were employed.[16] The temperature was kept constant at 30 ± 0.5° with the help of an air thermostat. The apparent surface area was used for the calculation of the current density.

The cathodes employed were electroplated Sn and Cu–Sn alloys. The overpotential on electroplated Cu was previously investigated.[11] Six compositions for Cu–Sn alloys were studied: 12, 28, 42, 55, 67 and 80% Sn. Tin was plated from a stannate bath[16] operated at 80 ± 1°. Deposition was carried out at a current density of 2×10^{-2} amp./cm.^{2} for 20 minutes. The compositions (in g./l.) of the various baths used for the deposition of Cu–Sn alloys are given in Table I, together with the appropriate cathodic current density employed.[17] The use of potassium salts in place of sodium salts, in some baths, is justified by the fact that potassium salts increase the stability of the bath.[17,18] Baths which were kept for some time were, therefore, prepared from potassium salts. For the deposition of the alloys containing 42% Sn, this bath was used[17]

Sodium stannate, $Na_2SnO_3 \cdot 3H_2O$	100 g./l.
Sodium hydroxide, NaOH	10 g./l.
Cuprous cyanide, CuCN	11.5 g./l.
Sodium cyanide, NaCN	28.5 g./l.
Cathodic current density	3×10^{-2} amp./cm.^{2}

For the decomposition of all alloys studied, the temperature was kept constant at 65 ± 1° and deposition was carried out for 20 minutes. To ensure the constancy of the bath composition during alloy deposition, two copper and tin anodes were used.[17] The composition of the plated alloy was checked by analysis, and when the plating conditions were kept as constant as possible variations only of the order of 1 to 2% in the composition of the alloy were ob-

TABLE I

% Sn	$SnCl_4 \cdot 5H_2O$	NaOH	KOH	Cu(CN)	NaCN	KCN	Current density, amp./cm.^{2}
12	80	80	..	36	56	..	3×10^{-2}
28	118	..	180	12	29	..	2
55	118	97	..	12	29	..	3
67	118	..	136	12	29	..	2
80	170	..	174	4	..	27	2

TABLE II[a]

Electrode	N	3.3 × 10^{-3} amp./cm.^{2} η	σ	$\pm L$	10^{-3} amp./cm.^{2} η	σ	$\pm L$	3.3 × 10^{-4} amp./cm.^{2} η	σ	$\pm L$
Cu	15	299	7	15	261	6	13	233	5	11
12% Sn	8	429	6	15	372	7	16	328	7	15
28%	8	433	9	21	384	6	14	347	4	10
42%	12	386	9	20	333	9	20	288	10	19
55%	10	396	8	18	349	7	15	311	6	13
67%	7	389	7	18	337	6	14	293	6	14
80%	7	500	5	11	446	5	11	396	5	12
Sn	15	633	2	5	580	2	4	530	3	6

[a] Values of $\bar{\eta}$, σ and L are approximated to the nearest mv.

TABLE III

Electrode	b (mv.)	σ	$\pm L$	$(\bar{i}_0)$, amp./cm.^{2}	σ	$\pm L$
Cu[a]	125	1	3	1.9×10^{-5}	3.7×10^{-6}	8.0×10^{-6}
12% Sn	108	1	3	3.9×10^{-7}	2.6×10^{-8}	6.2×10^{-8}
28%	107	2	5	2.3	3.1	7.2
42%	102	2	4	4.6	1.9	4.1
55%	104	1	3	3.5	1.1	2.4
67%	105	2	5	4.0	1.9	4.8
80%	106	2	4	7.7×10^{-8}	2.3×10^{-8}	5.6×10^{-8}
Sn	107	1	3	4.2×10^{-9}	5.3×10^{-10}	1.1

[a] Only the higher Tafel line slope and the corresponding i_0 value are included (*cf.* ref. 11).

(7) M. DeKay Thompson and A. Kaye, *ibid.* **60**, 229 (1931).
(8) M. DeKay Thompson and G. Sistare, *ibid.*, **78**, 259 (1940).
(9) U. Croatto and M. Da Via, *Ricerca Sci.*, **12**, 1197 (1941).
(10) J. O'M. Bockris, *Chem. Revs.*, **43**, 525 (1948).
(11) S. Wakkad, I. A. Ammar and H. Sabry, *J. Chem. Soc.*, 5020 (1956).
(12) J. O'M. Bockris and N. Pentland, *Trans. Faraday Soc.*, **48**, 833 (1952).
(13) A. Hickling and F. Salt, *ibid.*, **36**, 1226 (1940); **37**, 333 (1941); J. O'M. Bockris and S. Ignatowicz, *ibid.*, **44**, 519 (1948); K. Pecherskaya and V. Stender, *J. Appl. Chem., Russ.*, **19**, 1303 (1946).
(14) I. A. Ammar and S. A. Awad, THIS JOURNAL, **60**, 837 (1956).
(15) A. Azzam, J. O'M. Bockris, B. Conway and H. Rosenberg, *Trans. Faraday Soc.*, **46**, 918 (1950).
(16) W. Blum and G. Hogaboom, "Principles of Electroplating and Electroforming," McGraw-Hill Book Co., Inc., New York, N. Y., 1949, p. 328.
(17) R. Angles, F. Jones, J. Price and J. Cuthbertson, *J. Electrodepositor's Tech. Soc.*, **21**, 19 (1946); Tin Research Inst. (London), publications and private communications.
(18) F. Lowenheim, *Trans. Electrochem. Soc.*, **84**, 195 (1943).

served. Analar grade reagents were used for the preparation of the various baths.

Results

Hydrogen overpotential is measured in the current density range 10^{-2} to 3×10^{-6} amp./cm.^{2}, in 1.0 N HCl solution at 30°. The results are statistically analyzed. For this reason, a new electrode and a new solution are used to measure each individual Tafel line. The mean Tafel line is computed from at least seven individual measurements. To show the accuracy of the results, the mean over-potential $\bar{\eta}$, the corresponding error σ, the 95% confidence limits $\pm L$,[19] and the number of individual measurements N are given in Table II for electroplated Cu, Sn and Cu–Sn alloys at three different current densities, *i.e.*, 10^{-2}, 10^{-3} and 10^{-4} amp./cm.^{2}. The results for Cu plated from a cyanide bath, taken from a previous investigation,[11] are included here for comparison. The mean values for the Tafel line slope $\bar{b}$, and for the exchange current ($\bar{i}_0$) are given in Table III together with their standard errors and confidence limits. The mean Tafel lines for electroplated Cu, Sn and Cu-Sn alloys are shown in Fig. 1. It is clear from this figure that in most cases the overpotential tends to a stationary value at the low current density range, and this is attributed to the dissolution of the electrode.[23] In Fig. 2 the mean overpotential is plotted against the composition of the alloy for 3.3×10^{-3}, 10^{-3} and 3.3×10^{-4} amp./cm.^{2}.

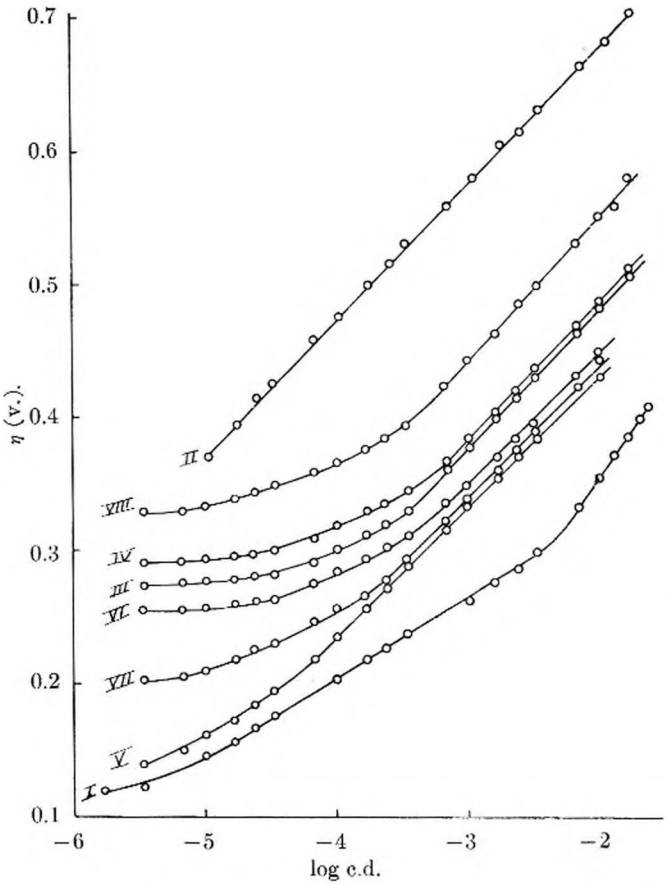

Fig. 1.—Mean Tafel lines for electroplated Cu, Sn and Cu-Sn alloys in 1.0 N HCl at 30°: I, Cu; II, Sn; III, 12% Sn; IV, 28% Sn; V, 42% Sn; VI, 55% Sn; VII, 67% Sn; VIII, 80% Sn.

Discussion

Previous work on the kinetics of the cathodic hydrogen evolution reaction on Cu in HCl solutions has indicated that the slow discharge of H^+ ions is rate determining.[12,21] This conclusion has been based on the value of the Tafel line slope, and on the fact that the capacity of the electrode-solution interface is independent of frequency.[12] This indicates a small coverage of the metal surface with adsorbed H atoms and hence a rate-determining slow discharge has been favored. For Sn cathodes, also in HCl solutions, the transfer coefficient α is found to lie between 0.4 and 0.45.[13,22] In the present investigation a value of $\alpha = 0.56$ is calculated from the mean slope of the Tafel lines on Sn (*cf.* Table III) according to $b = 2.303\ RT/\alpha F$. Since a rate-determining catalytic desorption is characterized by a value of $\alpha = 2$ in the current density range studied in the present investigation, the overpotential results on Sn may be explained by a rate-determining slow discharge or a slow electrochemical mechanism.[23] Distinction between the two alternatives could not be made directly since the evaluation of the stoichiometric number or the elec-

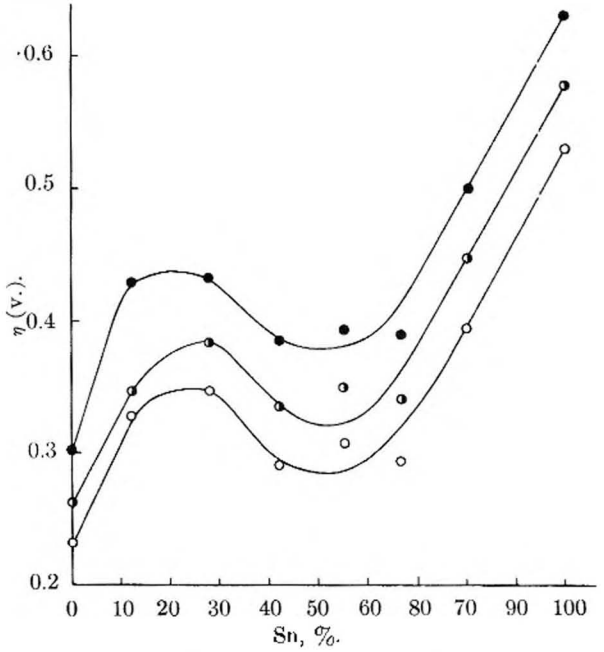

Fig. 2.—Relation between overpotential and alloy composition at: ●, 3.3×10^{-3}; ◑, 1.0×10^{-3}; ○, 3.3×10^{-4} amp./cm.^{2}

(19) O. Davies, "Statistical Methods in Research and Production," Oliver and Boyd, London, 1949.

(20) J. Kolotyrkin and A. Frumkin, *Compt. rend. acad. sci., U.R.S.S.*, **33**, 445 (1941).

(21) N. Petland, J. O'M. Bockris and E. Sheldon, *J. Electrochem. Soc.*, **104**, 182 (1957).

(22) J. O'M. Bockris, "Electrochem. Constants," Natl. Bur. Standards, No. 524, 1953, p. 243.

(23) J. O'M. Bockris and E. C. Potter, *J. Electrochem. Soc.*, **99**, 169 (1952).

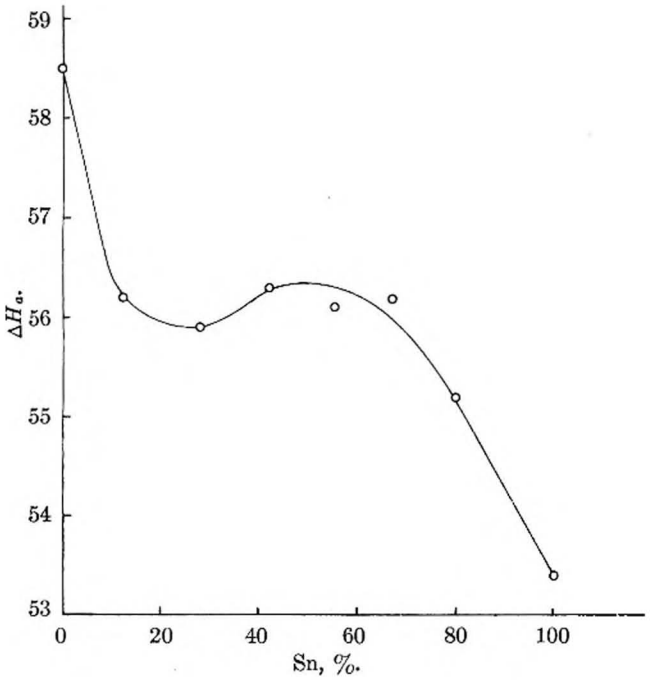

Fig. 3.—Relation between ΔH_a (kcal./gram atom) and the alloy composition for a rate-determining slow discharge mechanism.

tron number[23] has been hindered by the dissolution of the electrode at low current densities.

The results of the present investigation on electroplated Sn are in good agreement with those of Pecherskaya and Stender[13] also on an electroplated Sn electrode. Although the values of α and b for electroplated electrodes agree with those obtained for electrodes in the form of a wire (Bockris[13] and Hickling[13]), yet the overpotential results on the former are numerically smaller than those on the latter. This may be attributed to a large true surface area for electroplated electrodes as compared to electrodes in the form of a wire. Thus, at a constant apparent current density (using the apparent surface area), the true current density is smaller in the case of electroplated Sn than in the case of a tin wire. Hence, the overpotential will be numerically smaller on the former as compared to the latter.

The dependence of hydrogen overpotential on the nature of electrode material has been investigated by Rüetschi and Delahay[24] for a rate-determining slow discharge mechanism. They have observed a linear relation between η, for values numerically greater than 0.1 v., and the heat of adsorption of atomic hydrogen on the metal. It is worthwhile to consider the treatment of the above authors in an attempt to explain the relation between overpotential and the alloy composition for Cu–Sn alloys studied in the present investigation; the assumption being now made that the slow discharge controls the rate of hydrogen evolution for Cu, Sn and Cu–Sn alloys (*cf.* the values of b in Table III). It is noteworthy that two slopes are obtained for Cu plated from a cyanide bath, and this has been attributed to the heterogeneity of the electrode surface.[11] Now, the exchange current for the hydrogen evolution reaction is given by[24]

$$i_0 = K_1 \exp[-\Delta H_0^*/RT) \quad (1)$$

where K_1 includes the standard entropy of activation ΔS_0^* at the reversible potential, and ΔH_0^* is the standard heat of activation at the same potential. When ΔS_0^* is independent of electrode material as it has been suggested by Rüetschi and Delahay,[24] and when the other terms in K_1 are the same for a number of metals, *i.e.*, the rate-determining reaction, the electrolyte concentration and the temperature are the same, i_0 will change with ΔH_0^* from one metal to another. In comparing the overpotential at two different electrodes, it has been shown that the difference between the values of ΔH_0^* is approximately equal to the difference between the heats ΔH_a of adsorption of hydrogen on the two metals when the slow discharge is rate determining on both cases, thus[24]

$$[(\Delta H_0^*)_1 - (\Delta H_0^*)_2] \simeq -[(\Delta H_a)_1 - (\Delta H_a)_2] \quad (2)$$

and consequently

$$\Delta H_0^* \simeq \text{const.} - \Delta H_a \quad (3)$$

From (1) and (3) one gets

$$i_0 \simeq K_2 \exp[\Delta H_a/RT] \quad (4)$$

and K_2 is independent of electrode material. The relation between η and ΔH_a can be deduced when the cathodic current density i is given by

$$i = i_0 \exp[-\alpha\eta F/RT] \quad (5)$$

and thus from (4) and (5) at constant i one gets

$$\eta \simeq K_3 + (\Delta H_a/\alpha F) \quad (6)$$

and K_3 is independent of electrode material if α is independent of electrode material. Equation 6 can, in principle, be used to calculate approximate values of η for a metal on which the slow discharge is rate determining, when K_3 and ΔH_a are estimated. Values of ΔH_a for Sn and Cu–Sn alloys, calculated according to (6) and taking ΔH_a for Cu as 58.5 kcal./gram atom,[24] are shown in Fig. 3. However, Fig. 3 can only indicate that if the slow discharge is rate-determining the heat of adsorption of hydrogen decreases with the increase of Sn content in the alloy up to about 28% Sn. This is followed by a slight increase of ΔH_a above 28% Sn, and then it decreases considerably above 67% Sn. It is known[25] that alloys having the composition 39 to 60% Sn are mixtures of the superlattices ϵ and η' phases which correspond to the formulas Cu_3Sn and Cu_5Sn_5, respectively.[25,27] From 0 to 39% Sn, the alloy is a mixture of the superlattice ϵ and the solid solution α-phase.[25] For compositions higher than about 61% Sn the alloy is a mixture of the superlattice η' and Sn.[25] From this, and on the assumption that the slow discharge is rate-determining, Fig. 3 indicates that ΔH_a decreases with the tin content of the alloy except in the region where the mixture of the two superlattices ϵ and η' is formed. The above discussion could have been

(24) P. Rüetschi and P. Delahay, *J. Chem. Phys.*, **23**, 195 (1955).

(25) G. Raynor, Inst. Metals Annotated Equilibrium Diagram Series, No. 2 (1944).

(26) J. Bernal, *Nature*, **122**, 54 (1928).

(27) A. Westgren and G. Phragmen, *Z. Metallkunde*, **18**, 279 (1926); *Z. anorg. Chem.*, **175**, 80 (1928).

checked had it been possible to get some direct information as to the relation between ΔH_a and the alloy structure.

The authors wish to express their thanks to Prof. J. Horiuti and Prof. J. O'M. Bockris for helpful discussions.

HYDROGEN OVERPOTENTIAL ON MERCURY IN PERCHLORIC ACID SOLUTIONS

BY I. A. AMMAR AND M. HASSANEIN

Department of Chemistry, Faculty of Science, Cairo University, Cairo, Egypt

Received January 13, 1958

Hydrogen overpotential has been measured on Hg in 0.1, 1.0, 2.0 and 5.0 N $HClO_4$ at 25°. The observed Tafel line slopes are numerically greater than the theoretical value of 0.12 v. expected for a slow proton discharge or a slow electrochemical desorption. Electrocapillary curves have been measured in the same solutions, and the components of the charge of the double layer have been calculated. The Tafel line slopes have been related to the structure of the interface at the cathodic branch of the electrocapillary curves.

Introduction

Criteria for establishing the mechanism of hydrogen evolution on the cathode have been recently formulated.[1-3] These include the Tafel slope, the electron number and the stoichiometric number. Tafel slopes associated with the three important mechanisms, namely, slow discharge, electrochemical desorption and catalytic combination are $(2 \times 2.303RT/F)$ for the first, $(2 \times 2.303RT/3F)$ and $(2 \times 2.303RT/F)$ for the second, $(2.303RT/2F)$ and ∞ for the third. Side reactions, due to the presence of trace impurities, often vitiate the kinetics of hydrogen evolution and the experimental slope is different from what is theoretically expected. However, in some studies, carried out under rigorous experimental conditions, breaks in the Tafel line are observed in the current density range where contributions from resistance overpotential, concentration polarization and ionization of adsorbed atomic hydrogen are diminishingly small and can be neglected.[4-6] The break in the Tafel line is sometimes attributed to a complex mechanism in which the rate is controlled by more than one step.[5] In other cases, the occurrence of two slopes has been explained on the basis that the potential at the Gouy–Helmholtz boundary is dependent on the electrode–solution p.d. when the electrode potential is near to that of the electrocapillary maximum.[6] Specific adsorption of H_3O^+ ions on Ag cathodes also has been suggested.[4] In this case, the increase of the Tafel slope with increase of cathodic polarization is due to the decrease of the symmetry factor, for the discharge step, as a consequence of the approach of the initial state to the cathode surface.

Anomalies in the shape of the Tafel lines for Hg in concentrated solutions of HCl and HBr are attributed to the adsorption of anions at the low current density range.[7] This causes a decrease in the overpotential at low current densities as compared to the values obtained by extrapolating the Tafel line from high to low current densities. Adsorption of anions has been confirmed by calculating the surface concentration of anions with the aid of the Gibbs adsorption equation. A marked increase in the surface concentration of anions, with decrease of current density, leads to the appearance of an inflection in the Tafel line. Adsorption of both anions and cations has been studied by measuring electrocapillary curves for Hg in HCl solutions of different concentrations.[8] On the cathodic side of the electrocapillary curve, the charge in dilute solutions is due largely to an excess of hydrogen ions. In concentrated solutions, however, there is an actual repulsion of hydrogen ions but the charge is due to the much greater repulsion of Cl^- ions.[8] On the anodic side Cl^- ions are attracted, and in dilute solutions the charge is carried chiefly by the excess of these ions. At the electrocapillary maximum the adsorption of both ions is equal and the net charge is zero.

The aim of the present investigation is to extend the studies of adsorption of anions and cations on Hg to solutions of perchloric acid, and to study the overpotential in these solutions with particular attention to the Tafel line slope. Hence, the relation between the Tafel slope and the extent of adsorption may be elucidated. Perchloric acid is chosen because overpotential studies on Hg in this acid are very few.[3]

Experimental

The electrolytic cell was used to measure hydrogen overpotential as well as electrocapillary curves. It was constructed of arsenic-free glass and water-sealed taps and ground glass joints. The cell had four compartments for the cathode, anode, pre-electrolysis electrode and reference electrode. The reference electrode was a platinized platinum electrode in the same solution as the mercury cathode. A Luggin capillary was used to connect the cathode and reference electrode compartments. Overpotential was measured on a mercury cathode in the form of a pool at the bottom of the cathode compartment. This mercury was introduced from a reservoir attached to the bottom of the cathode compartment. For the measurements of electro-

(1) J. O'M. Bockris and E. C. Potter, *J. Electrochem. Soc.*, **99**, 169 (1952).

(2) J. O'M. Bockris, *Ann. Revs. Phys. Chem.*, 5, 477 (1954).

(3) J. O'M. Bockris, "Electrochem. Constants," Natl. Bur. Standards, No. 524, 1953, p. 243.

(4) J. O'M. Bockris and B. Conway, *Trans. Faraday Soc.*, **48**, 724 (1952).

(5) I. A. Ammar and S. Awad, THIS JOURNAL, **60**, 837 (1956).

(6) J. O'M. Bockris, I. A. Ammar and A. K. Huq, *ibid.*, **61**, 879 (1957).

(7) Z. Iofa, *Acta Physicochim., U.R.S.S.*, **10**, 903 (1939).

(8) M. Devanathan, Ph.D. Thesis, London, 1951.

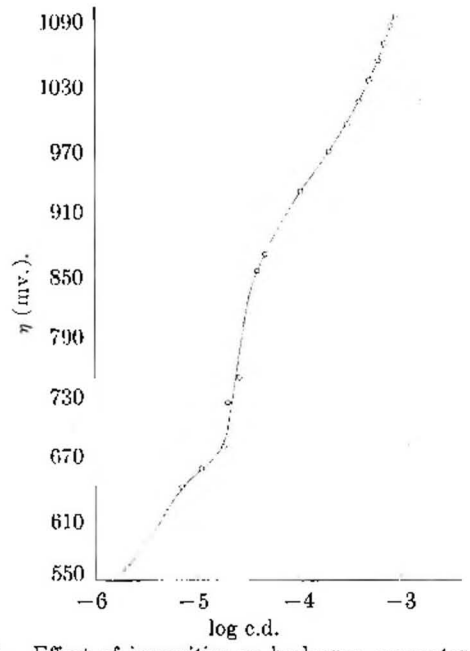

Fig. 1.—Effect of impurities on hydrogen overpotential on Hg in 0.1 N $HClO_4$.

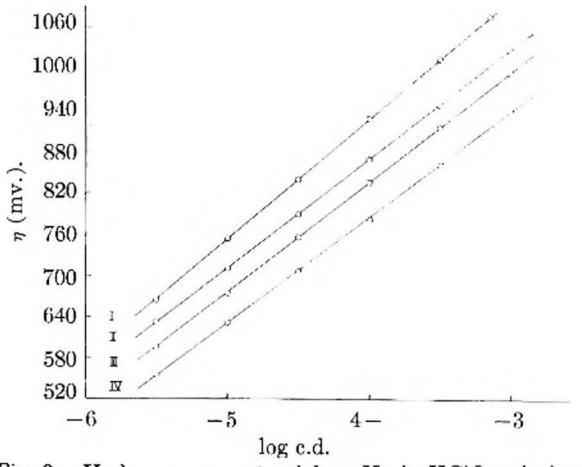

Fig. 2.—Hydrogen overpotential on Hg in $HClO_4$ solutions at 25°: I, 0.1 N; II, 1.0 N; III, 2.0 N; IV, 5.0 N.

capillary curves, a capillary electrometer[8,9] was placed at the top of the cathode compartment by means of a ground glass joint. The electrometer consisted of a reservoir sealed at both ends to two ground glass joints. One of these joints was sealed to the measuring capillary and the other was used to connect the electrometer to the pressure control system. A platinum contact was sealed to the side of the reservoir. The internal radius of the measuring capillary was 1/100 mm. and high sensitivity was obtained by making the bore taper vary slightly toward the end of the capillary.[8] The anode and the pre-electrolysis electrodes were two platinum discs, 1 cm.^{2} each, sealed to glass. The pre-electrolysis electrode could be lowered into the solution, without introducing air, by means of a ground glass joint (*ca.* 12 cm. long). Purified hydrogen was introduced into the four compartments of the cell and was allowed to escape to the atmosphere *via* bubblers filled with conductivity water.

Commercial hydrogen was purified by passage through a glass furnace kept at 450°, containing Cu. CO_2 was removed by soda lime and the gas was dried by silica-gel. Mercury was purified by distillation in an all-glass apparatus under reduced pressure as that produced by a water pump, and was then electrolyzed In this process of electrolysis, the mercury to be purified was made the anode in a saturated solution of mercurous nitrate acidified with nitric acid; the cathode being a drop of mercury previously purified by electrolysis. The mercury anode, with a current density of 10^{-1} amp./cm.^{2} applied to it, was kept vigorously stirred by a mechanical stirrer. The resulting mercury was washed several times with conductivity water, dried by sucking the water from its surface, and it was finally distilled under reduced pressure. Conductivity water used in the present investigation had a specific conductivity of *ca.* 5×10^{-7} ohm^{-1} cm.$^{-1}$. It was prepared from distilled water by further distillation with $KMnO_4$ and KOH, and impurities in the steam were removed by partial condensation in a series of 4 traps. The remaining steam was then condensed and collected. The resulting water was deoxygenated by pure hydrogen. Perchloric acid solutions were prepared from the "Analar" grade acid by appropriate dilutions and were pre-electrolyzed,[10] in the electrolytic cell at 10^{-2} amp./cm.^{2} for 20 hours using the platinum pre-electrolysis electrode.

The cell was cleaned with a mixture of concentrated "Analar" HNO_3 and H_2SO_4 acids. It was then washed with conductivity water. The capillary electrometer was cleaned with streaming concentrated "Analar" HNO_3 by suction applied to the upper end of the reservoir. In a similar manner air and conductivity water were passed alternately through the capillary for several hours, after which the reservoir and the rest of the apparatus except the capillary were dried by careful heating with a small flame. The reservoir was half filled with pure mercury and was placed in its position in the electrolytic cell. The cell was filled completely with conductivity water and this water was displaced by pure hydrogen. Perchloric acid solution was introduced into the cell as previously described.[5] The solution was divided between the anode and the pre-electrolysis electrode compartments. The pre-electrolysis electrode, with a p.d. applied to it, was lowered into the solution and pre-electrolysis was continued with purified hydrogen passing into the solution. After pre-electrolysis, part of the pre-electrolyzed solution was introduced into the cathode compartment over the surface of the mercury pool (already connected to the polarizing circuit through a side Pt contact) and another part was transferred to the reference electrode compartment. Tafel lines were then traced from high to low current densities. Current densities were calculated using the apparent surface area of the mercury pool.

For the measurements of electrocapillary curves, the mercury in the capillary was polarized and its potential was measured against the reversible hydrogen electrode. Pressure was applied *via* a mercury manometer on the mercury in the reservoir to bring the meniscus in the capillary to the tip. The difference (h_m) in the levels of mercury in the two limbs of the manometer was recorded with a long focus cathetometer. The pressure was then released to let the mercury rise in the capillary. The potential was adjusted to another value and the same procedure was repeated. When the whole of the electrocapillary range had been covered, the height (h_c) of mercury in the electrometer from the tip of the capillary and the height (h_s) of the solution (also from the tip) were measured. The temperature of the cell and that of the mercury manometer (both were thermostated) were also recorded. The interfacial tension was calculated from the measured heights according to[8,9]

$$\gamma = (rg/2)\rho_{T_1}[h_c + h_m(\rho_{T_2}/\rho_{T_1}) + h_s(\rho_S/\rho_{T_1})]$$

where ρ_{T_1} is the density of Hg at the temperature T_1 of the cell, ρ_{T_2} is the density of Hg at the temperature of the manometer and ρ_S is that of the solution at T_1. The constant $(rg/2)$ was obtained by calibrating the capillary in 1.0 N HCl at 25° and taking γ at the electrocapillary maximum as 422.6 dyne cm.$^{-1}$.[9]

Results and Discussion

Two slightly different techniques were employed in the measurements of overpotential. In the first, the overpotential was measured directly after introducing the pre-electrolyzed solution to the cathode and the reference electrode compartments, and the rapid technique was used.[10] An example of the

(9) R. Parsons and M. Devanathan, *Trans. Faraday Soc.*, **49**, 673 (1953).

(10) A. Azzam, J. O'M. Bockris, B. Conway and H. Rosenberg, *ibid.*, **46**, 918 (1950).

Tafel lines thus obtained is shown in Fig. 1 for 0.1 N $HClO_4$ at 25°. It is clear from this figure that the overpotential is not linear to the logarithm of the current density over the entire current density range studied. The reproducibility of results was also poor. In the second technique the mercury cathode was polarized at about 5×10^{-3} amp./cm.^{2} in the previously pre-electrolyzed solution, and the potential was measured as a function of time till a constant potential was attained. The Tafel line was then rapidly traced to low current densities. With this technique the overpotential was linear to the logarithm of the current density and the reproducibility was improved. This technique was used, therefore, to measure Tafel lines in 0.1, 1.0, 2.0 and 5.0 N $HClO_4$ at 25°. It is possible to attribute the behavior of the Tafel line shown in Fig. 1 to the occurrence, on the surface of Hg, of a thin oxide film which can be cathodically reduced, and hence the shape of the Tafel line is improved after cathodic polarization.

For each concentration studied several Tafel lines were measured in separate experiments and the mean line was computed. The mean Tafel lines are shown in Fig. 2. The standard error and the 95% confidence limits[11] for the mean overpotential results also were calculated. The confidence limits did not exceed ±12 mv. The mean Tafel line slopes, computed from the slopes of separate Tafel lines, are 0.17 v. for 0.1 N and 0.16 v. for 1.0, 2.0 and 5.0 N $HClO_4$; the average deviation being less than 0.01 v. for each value. It is clear that the values given above are higher than the theoretical value of 0.12 v. associated with the slow discharge mechanism and the electrochemical desorption at high cathodic polarization.[1] The fact that the interface Hg–$HClO_4$ is characterized by high Tafel line slopes was confirmed by measuring Tafel lines: (i) on Hg in 0.1 N HCl using exactly the same technique as that for $HClO_4$ solutions, and (ii) on Ag in 0.1 N $HClO_4$. The results at 25° are shown in Fig. 3 from which it is clear that the Tafel line slope for Hg in 0.1 N HCl is 0.10 v. and that for Ag in 0.1 N $HClO_4$ is 0.11 v. Previous work on hydrogen overpotential on Hg in $HClO_4$[12] has indicated the occurrence of a region of decreased overpotential resulting in the anomalous behavior of Tafel lines, and this is not related to any kind of depolarization.[13] In the present investigation overpotential measurements in 0.1 N $HClO_4$ were extended to 10^{-7} amp./cm.^{2}. The results of three experiments at 35° are shown in Fig. 4 from which it is clear that the overpotential tends to a stationary value at the lowest current density range.

Electrocapillary curves were measured in 0.1, 1.0, 2.0 and 5.0 N $HClO_4$ at 25°. Measurements were repeated, at least five times, for each concentration. The results were reproducible to ±0.5 dyne cm.$^{-1}$ at the maximum and to ±1.0 dyne cm.$^{-1}$ at the ends of the curve. The mean results are shown in Fig. 5. The charge density q of the mercury surface was calculated by graphical differentiation of the electrocapillary curve according to

$$(d\gamma/dE) = -q$$

The results are given in Fig. 6. The surface excess of anions $\Gamma-$ was calculated according to[14]

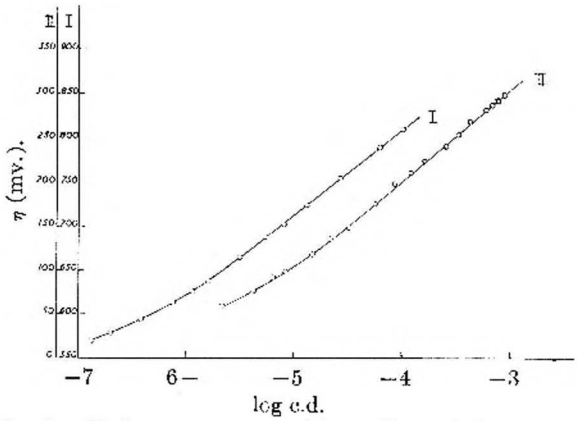

Fig. 3.—Hydrogen overpotential on Hg and Ag at 25°: I, Hg in 0.1 N HCl; II, Ag in 0.1 N $HClO_4$.

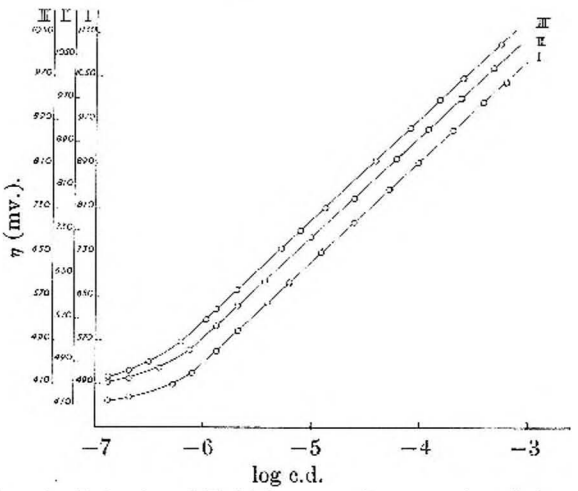

Fig. 4.—Behavior of Tafel lines on Hg in 0.1 N $HClO_4$ at low current densities.

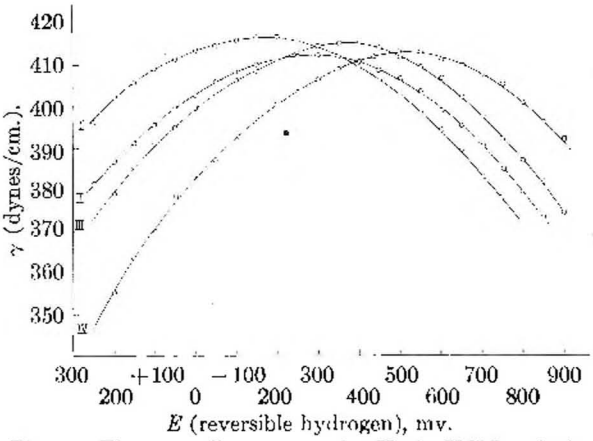

Fig. 5.—Electrocapillary curves for Hg in $HClO_4$ solutions at 25°: I, 0.1 N; II, 1.0 N; III, 2.0 N; IV, 5.0 N.

(11) O. Davies, "Statistical Methods in Research and Production," Oliver and Boyd, London, 1949.

(12) Z. Iofa and A. Frumkin, *J. Phys. Chem., U.S.S.R.*, **18**, 268 (1944).

(13) Since reference 12 is not available in this country, a comparison between the present results and those of Iofa and Frumkin[12] could not be attempted beyond what is given in *C. A.*, **39**, 3209 (1945).

(14) D. C. Grahame, *Chem. Revs.*, **41**, 441 (1947).

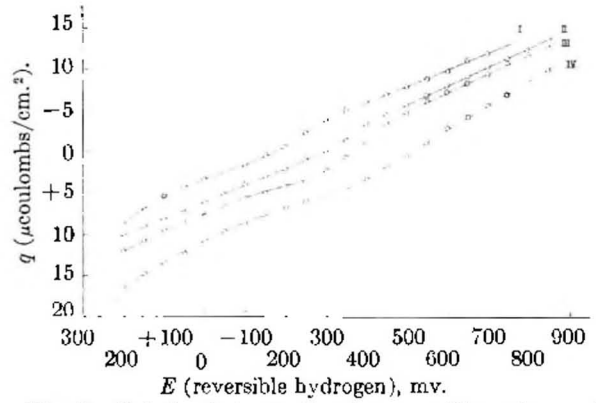

Fig. 6.—Relation between the charge on Hg surface and the potential E: I, 0.1 N; II, 1.0 N; III, 2.0 N; IV, 5.0 N $HClO_4$.

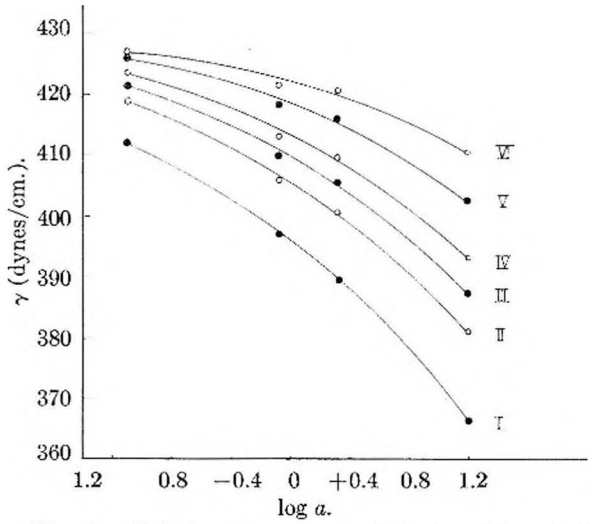

Fig. 7a.—Relation between γ and the logarithm of the activity of $HClO_4$: I, 200 mv.; II, 100 mv.; III, 50 mv.; IV, 0 mv.; V, −100 mv.; VI, −200 mv.

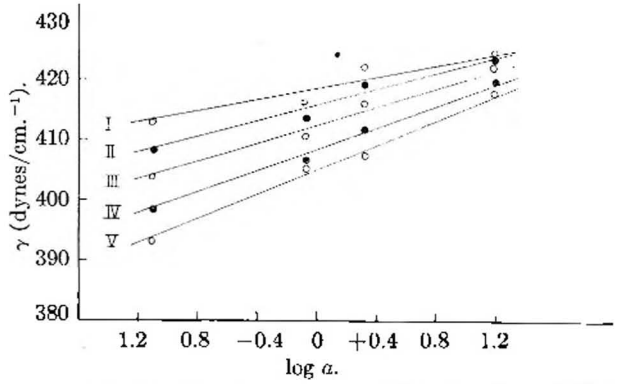

Fig. 7b.—Relation between γ and the logarithm of the activity of $HClO_4$: I, 500 mv.; II, −550 mv.; III, −600 mv.; IV, −650 mv.; V, −700 mv.

$$(d\gamma/d\mu)_{E^+} = -\Gamma-/\nu_-$$

where μ is the chemical potential of the electrolyte, and $\nu-$ is the number of anions resulting from the dissociation of one molecule of the electrolyte. The surface excess of cations was calculated from the total charge and $\Gamma-$. The relation between γ and log a, where a is the activity of $HClO_4$, is shown in Fig. 7. The components of the charge of the double layer, at different potentials, are given in Table I for 1.0 and 2.0 N $HClO_4$. The positive sign for the perchlorate ions represents a repulsion of these ions from the double layer, the negative sign indicates adsorption, and *vice versa* for hydrogen ions. It is clear from Table I that on the anodic branch of the electrocapillary curves both ClO_4^- and H^+ ions are attracted but the charge of the double layer is due to the much greater attraction of ClO_4^- ions. On the cathodic branch both ions are repelled and the charge of the double layer is due to the much greater repulsion of ClO_4^- ions.

TABLE I[a]

E	1.0 N		2.0 N	
(m.v.)	ClO_4	H^+	ClO_4	H^+
200	−29.7	19.7	−36.1	24.1
100	−25.4	17.1	−30.7	21.2
50	−22.2	14.8	−27.6	18.9
00	−19.2	13.0	−24.6	16.6
−100	−14.9	11.0	−20.2	14.5
−200	−10.7	8.5	−14.4	10.1
−500	7.6	−2.1	7.6	−3.0
−550	10.9	−4.2	10.9	−4.9
−600	12.2	−4.2	12.2	−5.1
−650	14.9	−5.8	14.9	−6.6
−700	17.0	−7.0	17.0	−7.7

[a] Values are given in microcoulombs/cm.².

It is not possible to explain the occurrence of Tafel line slopes of *ca.* 0.16 v. on the basis of simple theories of hydrogen overpotential. This slope is a property of the system studied and is not due to trace impurities since it is obtained under pure conditions and it is reproducible. Suppose the hydrogen evolution reaction is controlled by the proton discharge or by the electrochemical desorption at high cathodic polarization. Under this condition the expression for the slope is given by[6]

$$\frac{\partial\,\Delta\phi}{\partial \log i_c} = \frac{-2.303RT}{F[\lambda\beta + (1-\lambda\beta)(\partial\phi_2/\partial\Delta\phi)]}$$

where β is the symmetry factor, λ is the electron number and ϕ_2 is the potential at the outer Helmholtz plane. When $(\partial\phi_2/\partial\Delta\phi) = 0$ the above equation simplifies to the expression previously given by Bockris and Potter.[1] Under this condition the slope of 0.16 v. indicates a value of 0.4 for β when the proton discharge is rate determining and 0.2 for the slow electrochemical desorption. These values are smaller than the values usually observed for the above mechanisms. For the symmetry factor to decrease, with the position of the activated complex unchanged, the initial state of the reaction must be shifted toward the electrode surface.[4] However, Table I indicates that repulsion of both H^+ and ClO_4^- ions takes place in the potential range where the slope of 0.16 v. is observed (*cf.* Fig. 2). Hence the difference between the above value and the theoretical value of 0.12 v. observed for other systems may be attributed to the effect of $(\partial\phi_2/\partial\Delta\phi)$. Accordingly the present results indicate that $(\partial\phi_2/\Delta\phi) \simeq -0.25$ when $\lambda\beta = 0.5$. It has been shown[6] that when chloride ions are specifically adsorbed on W in 0.1 N HCl $(\partial\phi_2/\partial\Delta\phi)$ has a positive value. The negative value observed in the present investigation for $(\partial\phi_2/\partial\Delta\phi)$ may be ac-

counted for by the repulsion of both H^+ and ClO_4^- ions which is experimentally observed at the cathodic branch of the electrocapillary curve. On concluding, one may note that for Hg in acid solutions the slow proton discharge is more probable than the slow electrochemical desorption.[15]

The authors wish to express their thanks to Prof. A. R. Tourky for his interest in this work.

(15) B. Conway and J. O'M. Bockris, *J. Chem. Phys.*, **26**, 532 (1957).

AN APPARATUS FOR THE INVESTIGATION OF RAPID REACTIONS. THE KINETICS OF THE CARBONIC ACID DEHYDRATION[1]

BY PAUL G. SCHEURER, ROBERT M. BROWNELL AND JAMES E. LUVALLE[2]

Technical Operations, Arlington Laboratory, Arlington, Mass.

Received January 15, 1958

A brief description of a flow machine constructed for the investigation of rapid reactions of photographic interest is given. Details are given of those parts of the instrument which are different from other machines that have been described in the literature. The latter portion of the paper presents data obtained on the dehydration of carbonic acid. This reaction was utilized to test the performance of the machine. The energy of activation was found to be 16.1 kcal./mole, $\Delta S^* = 36$ e.u. and $\Delta F^* = 5.9$ kcal./mole. First ionization constants and the heat of ionization were computed for carbonic acid at each temperature. The computed heats showed good agreement with Roughton's measured values.

I. Introduction

Reactions with half-lives of one minute or less may be investigated by the capacity flow method of Denbigh,[3] the continouus flow method of Hartridge and Roughton[4] or the accelerated and stopped flow methods of Chance.[5] The capacity flow method is excellent for reactions with a half-life of a few seconds to several minutes. The stopped flow method may be used for reactions with a half-life down to 0.4 to 0.7 millisecond. The methods used for solution kinetics can, of course, be used for gaseous kinetics with suitable modifications.[6] A flow machine for solution kinetics with some new features has been constructed and tested. This paper will give a brief description of the flow machine and discuss the data obtained with it on the dehydration of carbonic acid.

II. The Flow Machine

Figure 1 is a block diagram of the stopped flow apparatus. The machine may be separated for convenience into three parts; the mechanical drive, the mixing and observation cells and the electronic observation system. The mechanical drive consists essentially of a variable speed lead screw drive[7] powered by a ½ h.p. enclosed motor which propels four fluid displacement pistons in cylinders of twenty-five, twenty-five, fifty and one hundred milliliter capacity, respectively. The inside diameter of the cylinders slightly exceeds the diameter of the pistons. The pistons have self-aligning end connectors and ride in spaced bearings one of which is a tapered gland ring for sealing the cylinder head against fluid pressure. A circular gland nut allows for initial and subsequent adjustment due to wear. The bearings and glands are machined from "Rulon," a self-lubricating material. Roller trip microswitches prevent over-run of the carriage. The motor is powered from a separate line to avoid interaction with the electronic equipment and the control console. Rotation of the lead screw operates a "Metron" tachometer head, while acceleration of the displacement driver plate is recorded by a rack-driven potentiometer and associated electronic circuitry. Tubing running to the cylinders and solenoid valves is fabricated from 0.125" o.d. and 0.062" i.d. full-annealed type number 304 stainless steel. Weatherhead "Ermeto" swedge type fittings are used on all transitions to valves and cylinders. The Skinner solenoid valves have stainless steel bodies and synthetic rubber inserts which are spring loaded in the plungers of the three way valves. It was necessary to break the stainless tubing connections between the solenoid valves and the mixing chamber with a short length of polyethylene tubing to absorb mechanical shock to the observation cell.

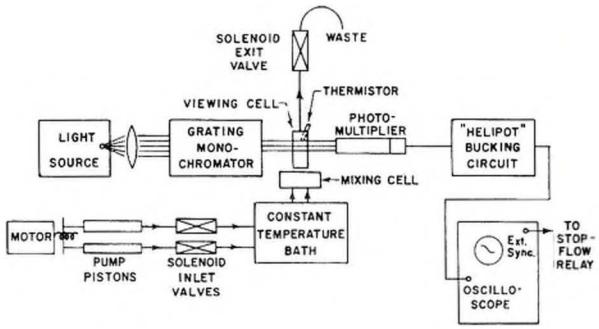

Fig. 1.—Block diagram of stopped flow apparatus.

A schematic diagram of the motor and solenoid controls is given in Fig. 2. The single phase Doerr motor was coupled to the displacement pistons through a hydraulic speed control. Three double-pole-double-throw relays (RE_1, RE_2 and RE_3) were used for the forward and reverse connections and also were utilized in the control of the solenoid valves. The normally open pair of contacts of RE_2 close during reverse motion to ensure that solenoid valves SV1, SV2, SV3 and SV4 connect their respective pump cylinders to the reservoirs. A normally closed pair of contacts of the forward relay, RE_1, maintains the exit solenoid valve, SV5, closed at all times other than during forward motion. The solenoid valves are operated from a d.c. supply using a germanium diode bridge and a resistance-capacitance filter. This ensures high speed closure of the valves and reproducibility of closing time. The speed of closure is increased by

(1) This research was supported by the United States under Contract AF 18(600)-371 monitored by the Office of Scientific Research. Reproduction in whole or in part is permitted for any purpose of the United States Government.

(2) To whom inquiries concerning this paper should be sent.

(3) (a) K. G. Denbigh, *Trans. Faraday Soc.*, **40**, 352 (1944); (b) B. Stead F. M. Page and K. G. Denbigh, *Discs. Faraday Soc.*, **2**, 263 (1947); (c) K. G. Denbigh, M. Hicks and F. M. Page, *Trans. Faraday Soc.*, **44**, 479 (1948); (d) F. M. Page, *ibid.*, **49**, 1033 (1953).

(4) (a) H. Hartridge and F. J. W. Roughton, *Proc. Roy. Soc. (London)*, **A104**, 376 (1923); (b) H. Hartridge and F. J. W. Roughton, *Proc. Cambridge Phil. Soc.*, **23**, 450 (1926); (c) G. A. Milliken, *Proc. Roy. Soc. (London)*, **A155**, 277 (1936).

(5) (a) B. Chance, *J. Franklin Inst.*, **229**, 455, 613, 737 (1940); (b) *Rev. Sci. Insts.*, **18**, 601 (1947); (c) *ibid.*, **22**, 619 (1951).

(6) (a) F. Raschig, *Z. angew. Chem.*, **18**, 281 (1905); (b) T. D. Stewart and E. R. Edlund, *J. Am. Chem. Soc.*, **48**, 1014 (1923); (c) H. S. Johnston and D. M. Yost, *J. Chem. Phys.*, **17**, 386 (1949).

(7) W. R. Ruby, *Rev. Sci. Instr.*, **26**, 460 (1955).

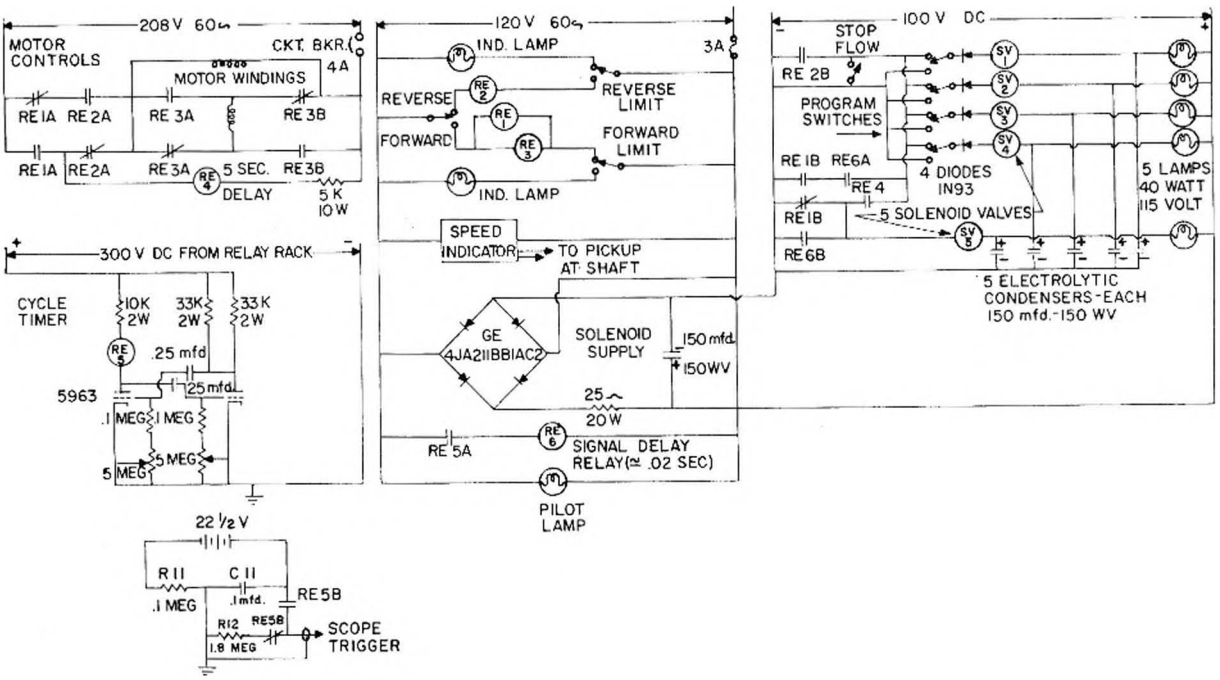

Fig. 2.—Schematic of motor and solenoid controls.

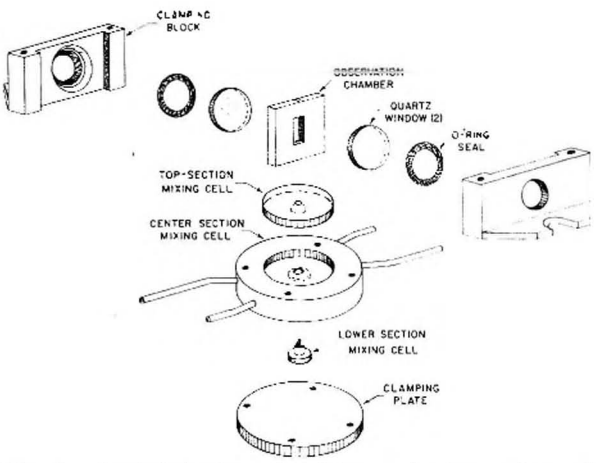

Fig. 3.—Exploded view of mixing and observation cell assembly.

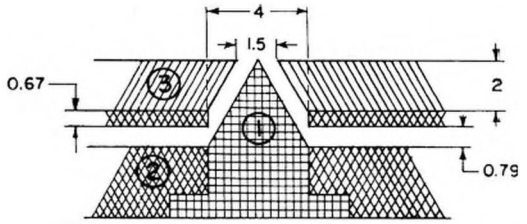

Fig. 4.—Mixing cell (side view) dimensions are given in mm. Cell has been drawn 5× actual size.

the momentary application of overvoltage to the solenoid as it discharges a 150 microfarad condenser. The solenoids are held closed by their rated voltage. A current-limiting lamp in series with each solenoid holds the power dissipation of each solenoid below its rated maximum. Diodes are used in series with the solenoids to prevent interaction. RE_2 also operates RE_6. During the forward thrust of the drive the programmed valves open and close in accordance with the operation of RE_6. It was important that the input solenoid valves be operated discontinuously so that they would not get hot and raise the temperature of the reactants. The time delay relay RE_4 is used to ensure that the valves are energized only during motion of the displacement pistons. The programming switches enable the operator to set up the desired sequence of operations. If necessary, three mixers may be cascaded. Upon the usual operational procedure, only the mixing unit immediately connected to the observation cell is used.

The mixing cell and the observation cell were assembled as one unit (Fig. 3), with the mixing cell below the observation cell. The mixing cell, Fig. 4, was made in three parts from Lucite and press fitted. The 60° cone section, 1, was inserted from below into the main section, 2, with the four tangential jets and the base of the cone at the same level. Section 3 with a 60° cone shaped hole was inserted from the top so that the lower cone was centered in the upper conical shaped hole. The dimensions of the mixing cell could be varied easily by changing the dimensions of the upper and lower sections. The mixing cell in current use has a volume of 0.016 cm.^{3} The volume between the mixing cell and the observation cell was 0.032 cm.^{3} and the volume of the observation cell was 0.078 cm.^{3}. Thus at a flow of 7.4 cm.^{3}/sec. it would take 15.1 milliseconds after mixing to fill the observation cell. The time of travel for an element of fluid, dx, from the exit of the mixing cell to the center of the slit would then be ten milliseconds. An excellent discussion of errors arising from different types of fluid flow, slit length and distance from the point of mixing already has appeared in the literature.[4,6,8] The observation cell was of stainless steel with quartz windows. The dimensions of the observation cell were 2.00 mm. deep by 3.95 mm. wide by 9.82 mm. high. The optimum design would have the cross sectional area of the observation cell just equal to the cross sectional area of the exit to the mixing chamber. However, at least ten mixing cells were constructed before a unit that mixed properly was obtained; hence the observation cell is too large for the final mixing unit. The first mixing cells were designed similar to those of W. R. Ruby.[7] All of these failed to give good mixing.

The test for complete mixing was very simple. A 10% ammonium sulfate solution was mixed with water. Failure to obtain complete mixing caused the index of refraction to vary throughout the cell, this variation appearing as an apparent difference in light absorption. At 200 r.p.m. (1.8 cm.^{3}/sec.) and all higher velocities of flow, mixing was completed before the fluid reached the observation cell.

(8) S. L. Friess and A. Weissberger, Editors—"Technique of Organic Chemistry," Vol. VIII, "Investigation of Rates and Mechanisms of Reactions," Interscience Publishers, Inc., New York, N. Y., 1953, Chapter X.

III. Electronics and Optics

A Sorenson Nobatron power supply was modified by the addition of an auxiliary choke, 0.04 henry, 30 amperes, to reduce the noise level. This supply furnished the power for the tungsten lamp.

The Bausch and Lomb hydrogen arc was supplied by a bridge selenium rectifier which fed a voltage regulator with six type 6080 series regulator tubes and a 5651 reference tube. A flow switch was inserted in the water line to the hydrogen arc to protect the arc in case of water pressure failure. The E.M.I. 6256B and 6295B photomultiplier tubes were supplied by a power supply rather than batteries. In order to keep the signal output of the photomultipliers in the high sensitivity range of the C.R.O. during the reaction, it was necessary to buck out the initial output voltage at the start of a reaction, or the final output voltage at the end of the reaction. Figure 5 shows the circuit utilized. Adjustment of R_1 for a given reference light level is used to bring point A to zero potential. This then becomes the C.R.O. reference point. The reference light level is expressed as a voltage referred to point A.

$$V = \frac{D}{1500} \times \frac{R_3}{R_2} = 0.004D$$

where D is the vernier reading on the 1500 division Helipot, R_1 and V is the voltage.

The light from the tungsten lamp or the hydrogen arc was passed through a Bausch and Lomb grating monochromator with a dispersion of 33 Å./mm. The over-all sensitivity varied with wave length and was of the order of 0.01 to 0.02 optical density unit per centimeter of oscilloscope deflection with the tungsten lamp at a slit opening of 0.1 mm. (380 to 640 mμ). The sensitivity with the hydrogen arc was of the order of 0.004 to 0.005 optical density unit per centimeter of oscilloscope deflection with a slit opening of 1.58 mm. (240 to 400 mμ). The sensitivity of the apparatus could be increased by employing a Tektronix differential preamplifier (Tektronix Type 53/54D) provided the noise level in the present apparatus could be lowered. Obviously, operation of the photomultiplier at liquid nitrogen temperature would be one way to decrease the noise level.

Preceding stopped flow measurement, a variable timing device (see Fig. 2), periodically energized the solenoid valves, causing them to deliver reactant solutions at convenient time intervals alternately to the mixing cell and the reservoir bottles. When the solenoid valves are energized to shift flow from the mixing cell to the reservoir bottles, the sweep mechanism of the oscilloscope is triggered so that the sweep of the C.R.O. starts prior to the closing of the valves. Thus a small portion of the continuous flow curve is always observed prior to the stopped flow curve. Several traces could thus be observed during one full discharge cycle of the displacement pistons.

IV. Performance

An investigation of the dehydration of carbonic acid[9] was made to determine the performance of the flow machine prior to utilizing it on some reactions of photographic interest. The stopped flow method was used for these experiments.

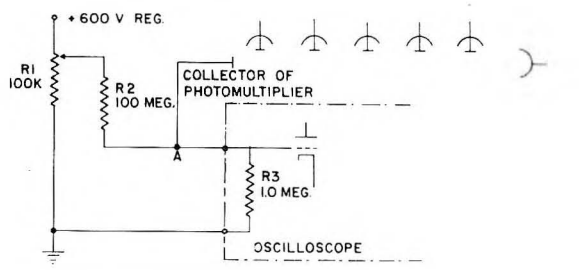

Fig. 5.—Circuit for bucking photomultiplier current for initial and final light levels.

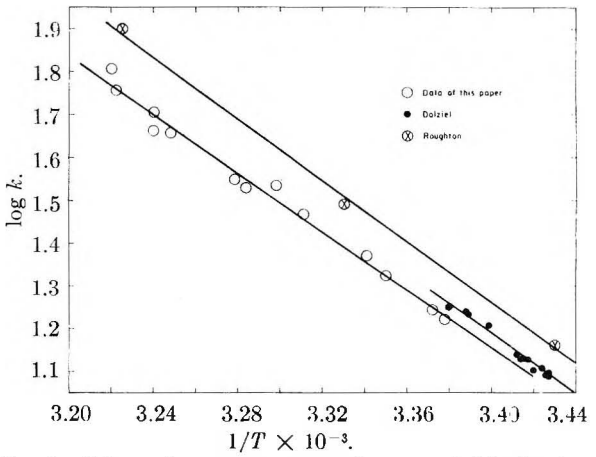

Fig. 6.—Effect of temperature on the rate of dehydration of carbonic acid.

The data obtained with this instrument have been compared with the results of Dalziel[9a] and Roughton[9b] in Fig. 6 and Tables I and II. The data of Fig. 6 were used to obtain the energies of activation given in Table I. The energies of activation agree within the experimental error. The values calculated from the equilibrium constants for the first ionization given in Table II were computed from the rate constants and pH_0 by the methods outlined by Dalziel[9a] and Roughton.[9b] The heats of ionization were computed by the method of Harned and his co-workers,[10] using the equations[10]

$$\log K_1 = \log K_{max} - p(t - \theta)^2 \quad (1)$$

$$\Delta H_1 = -4.6pRT^2(t - \theta) \quad (2)$$

TABLE I

COMPARISON OF ENERGY OF ACTIVATION

	ΔE, kcal./mole
This work	16.1
Roughton[9b]	16.5
Dalziel[9a]	16.9

(9) (a) K. Dalziel, *Biochem. J.*, **55**, 79 (1953); (b) F. J. W. Roughton, *J. Am. Chem. Soc.*, **63**, 2930 (1941); (c) A. R. Olson and P. V. Youle, *ibid.*, **62**, 1027 (1940); (d) F. J. W. Roughton, *Proc. Roy. Soc. (London)*, **155A**, 269 (1936); (e) R. Brinkman, R. Margolia and F. J. W. Roughton, *Phil. Trans. Roy. Soc.*, **A232**, 65 (1933); (f) F. J. W. Roughton, *Proc. Roy. Soc. (London)*, **126A**, 474 (1930); (g) M. N. J. Dirken and H. W. Mook, *J. Physiology*, **70**, 382 (1930); (h) R. N. J. Saal, *Rec. trav. chim.*, **47**, 264 (1928).

(10) (a) H. S. Harned and N. D. Embree, *J. Am. Chem. Soc.*, **56**, 1050 (1934); (b) H. S. Harned and R. A. Robinson, *Trans Faraday Soc.*, **36**, 973 (1940).

TABLE II

DEHYDRATION SPECIFIC RATE CONSTANTS, $(pH)_0$, FIRST IONIZATION CONSTANTS AND THE HEATS OF IONIZATION FOR CARBONIC ACID

$t°$, °C.	k, sec.$^{-1}$	$(pH)_0$	$K_{H_2CO_3}$[a]	$-\Delta H$, cal.
0.0	1.97[9b]	...	$(2.5 \pm 0.3)^{9b} \times 10^{-4}$	1710 ± 105^{9b}
17.90	14.6[9b]	...	...	1240 ± 50^{9b}
23.0	18.1	3.56	$2.4\ (2.4) \times 10^{-4}$	800
23.5	19.0	3.69	1.8 (1.78)	800
25.5°	23.0	3.72	1.7 (1.66)	890
26.3°	25.6	3.69	1.8 (1.78)	760
27.0°	31.0[9b]			960 ± 130^{9b}
29.0°	32.0	3.80	1.4 (1.38)	680
30.2	37.7	3.76	1.5 (1.52)	650
31.5	37.0	3.79	1.4 (1.41)	620
32.0	38.6	3.81	1.4 (1.35)	610
34.8	49.6	3.85	1.2 (1.23)	540
35.6	50.1	3.85	1.2 (1.23)	520
35.6	55.0	3.82	1.3 (1.32)	520
36.67	80.0[9b]			450 ± 12^{9b}
37.3	62.1	3.81	1.3 (1.35)	490
37.5	70.8	3.76	1.5 (1.51)	480

[a] The values in parentheses were used for the calculation of $-\Delta H$.

where p is a constant for any given acid and θ is the temperature corresponding to K_{max}. Roughton has estimated K_{max} to occur at 55° for carbonic acid.[9b] Assuming Roughton's value of 55° for θ, a plot of $(t - \theta)^2$ was made against log K_1 and the slope of the best straight line was used as a value for p ($p = 3.18 \times 10^{-5}$). This value of p was used in equation 2 to compute values of ΔH. The values of ΔH obtained directly by Roughton are also included in Table II. The agreement is certainly within the experimental error. The results of these experiments show that this flow machine may now be utilized for the investigation of previously unstudied reactions.

Acknowledgment.—The electronics were designed and built by R. Smythe and D. Forrant. The mechanical system was designed by E. Gariepy.

THE ENTROPY OF FUSION OF LONG CHAIN HYDROCARBONS

BY R. H. ARANOW, L. WITTEN AND

RIAS, Inc., 7212 Bellona Avenue, Baltimore 12, Maryland

DONALD H. ANDREWS

The Johns Hopkins University, Baltimore 18, Maryland

Received January 22, 1958

An analysis is made of the high entropy of fusion of long chain paraffins attributing that entropy to the onset at melting of freedom of the molecule to undergo hindered rotation about each carbon to carbon bond. The theoretical results are compared with the experimental observations. The entropy of fusion of heavy paraffins yields information concerning the rotational energy levels of the molecules. An empirical relationship is stated connecting the energy levels of the molecule with the melting temperature of the molecule.

I. Introduction

The entropy of fusion of long chain paraffins increases by a factor very close to R ln 3 for each additional CH_2 group added to the chain. The high values for the entropy of fusion of long chain paraffins have long been known and have been attributed[2a,b] to the onset at melting of freedom of the molecule to change from one molecular configuration to another by rotations around carbon to carbon bonds. There are three potential minima for rotation about each carbon to carbon bond and this yields a factor R ln 3 for the entropy increase per mole on addition of a carbon–carbon bond. In this paper we examine this proposal more carefully and make comparisons with experimental results. For paraffins with an even number of carbons the R ln 3 factor checks rather well with experiment, although with deviations which will be discussed later. Many paraffins with an odd number of carbons undergo a phase change in the solid state, a few degrees of temperature below the melting point. The entropy of fusion of these paraffins yields a factor less than $2R$ ln 3 for an additional two CH_2 groups. However, if the entropy change at the pre-melting transition is added to the entropy change of fusion, the resulting total entropy change is indeed $2R$ ln 3 for each additional pair of CH_2 groups. Deviations from the R ln 3 rule can be expected to yield information concerning the excited states of the molecule and indeed they do so as will be shown.

In the next section we give a theoretical analysis of fusion for a simplified model of paraffins. In section III we discuss theoretically the model and its correspondence with the real molecule making detailed comparisons between experiment and theory.

II. Fusion of a Simple Model of Paraffins

In this section we shall not discuss the real molecular configurations of paraffin but instead a fictional model in which there is also a threefold barrier to rotation around bonds. Our fictional model consists of parallel symmetrical triangles which are stacked along a straight line through their centers to form a linear chain, which straight

(1) Much of this work is based on a thesis submitted by R. H. Aranow in partial fulfillment of the requirements of a Ph.D. degree at the Johns Hopkins University. This research was supported in part by the United States Air Force through the Air Force Office of Scientific Research of the Air Research and Development Command under contract number AF 18(600)-765.

(2) (a) I. Langmuir, *J. Am. Chem. Soc.*, **54**, 2798 (1932); (b) S. Mizushima, "Structure of Molecules," Academic Press, New York, N. Y., 1954, p. 111.

line acts as an axis about which each triangle can rotate. The energy of interaction of two neighboring triangles is such that it is minimal when the apices of one triangle project to points between the apices of the neighboring triangle. There are consequently three positions of potential minimum for each triangle with respect to a neighbor. The fictional model and the real molecule are comparable when we consider the rotation around one bond at a time, *i.e.*, interactions between distant neighbor triangles of the model are neglected and interactions between distant parts of the molecule are neglected.

As each triangle in the model rotates, there are three potential minima in the allowed 2 π radians of rotation. This is of course the case in the real molecule as well for rotations about each carbon–carbon bond. The basic remark concerning the interpretation here being discussed for the entropy of fusion is the following. In the solid or crystalline state, the molecules are all in the fully extended orientation and are held rigidly in this orientation by interactions with neighboring molecules; there can be no rotation about carbon to carbon bonds. At melting and in the liquid state interactions with neighbors are not so constraining and these rotations are permitted.

Figure 1a shows the potential energy curve seen by a triangle (or by a CH_2 group) as it rotates with respect to one neighbor above the melting point. There are three potential minima and maxima not all at the same levels for the molecules. The figure shows schematically by E_0 and E_1 the energy levels of the lowest and first excited groups of states. Each group of states contains three energy levels due to the shape of the potential; the spreads ΔE_0 and ΔE_1 of these groups of states are small compared with $E_1 - E_0$. Henceforth, we shall neglect the spreads and treat E_0 and E_1 as triply degenerate energy levels. The partition function Z for a liquid molecule represented by the simplified model can now be stated as

$$Z_{liq} = A_l(3e^{-E_0/kT} + 3e^{-E_1/kT} + \ldots)^{n-1} \quad (1)$$

A_l is a factor which will be discussed later, k is the Boltzmann constant, T the absolute temperature and n the number of triangles in the chain or the number of carbons in the molecule. We assume each bond between triangles contributes the quantity in the parentheses to the partition function; henceforth we shall include only the two energy dependent terms explicitly stated above and neglect the possibility of higher energy states being excited. The end groups behave somewhat differently than the interior groups, but we ignore this also. The contribution of a single triangle-triangle bond is taken with an exponent $(n - 1)$ to give the partition functions for the whole chain; one is subtracted from n because there are $(n - 1)$ triangle–triangle bonds in the model or carbon–carbon bonds in the molecule. The factor A_l is introduced to represent the contribution to the liquid partition function from all considerations except the internal rotations which constitute the theme of this paper.

In the solid state the conditions are different and are as portrayed in Fig. 1b. The potential curve

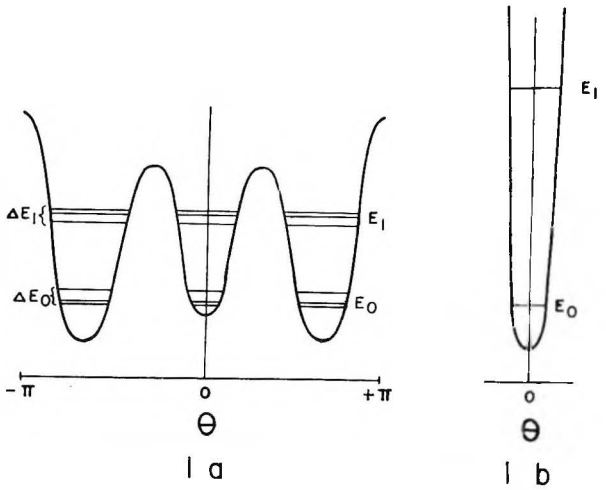

Fig. 1.—Potential energy curve and energy levels for rotation around a triangle to triangle bond in simplified model: θ represents the relative angular position of two triangles about the axis of the model. If the apices of the triangle differ somewhat from each other, the potential minima and maxima are not at the same levels. (a) represents conditions in liquid state; (b) represents conditions in solid state.

has only one minimum and the walls go effectively to infinity because of the action of the neighboring molecules. The energy level E_0 of the solid will be assumed to be the same as that of the ground state of the liquid. This assumption is reasonable since the shape of the potential curve near the minimum in the solid should be about the same as the shape of the three minima in the liquid. Moreover, it is reasonable to believe that the zero level torsional oscillation is so small as to be effectively insensitive to the surrounding molecules. However, it will be assumed that the first excited state E_1 of the solid is much higher than that in the liquid and that it is ignorable at the temperatures which concern us. This assumption is reasonable since the action of the neighboring molecules in the solid is expected to squeeze the walls of the potential together making the potential wall much narrower and raising the energy levels. These assumptions are made only for the sake of simplicity; the analysis, however, can be carried out readily if the assumptions are dropped.

The partition function for the solid can now be stated as

$$Z_{sol} = A_s(e^{-E_0/kT})^{n-1} \quad (2)$$

where A_s is a factor similar to A_l. The entropy S takes the form

$$S = \frac{\partial}{\partial T}(kT \ln Z_{sol}) \quad (3)$$

The entropy of fusion ΔS can now be given as

$$\Delta S_{fusion} = \frac{\partial}{\partial T} kT (\ln Z_{liq} - \ln Z_{sol}) \quad (4)$$

$$\Delta S_{fusion} = \frac{\partial}{\partial T} kT \ln \left(\frac{Z_{liq}}{Z_{sol}}\right) \quad (5)$$

From (1), (2) and (5)

$$\Delta S_{fusion} = \frac{\partial}{\partial T}\left\{kT\left[(n-1)\ln 3 + \ln\frac{A_l}{A_s} + \ln(1 + e^{-E_0/kT})^{n-1}\right]\right\} \quad (6)$$

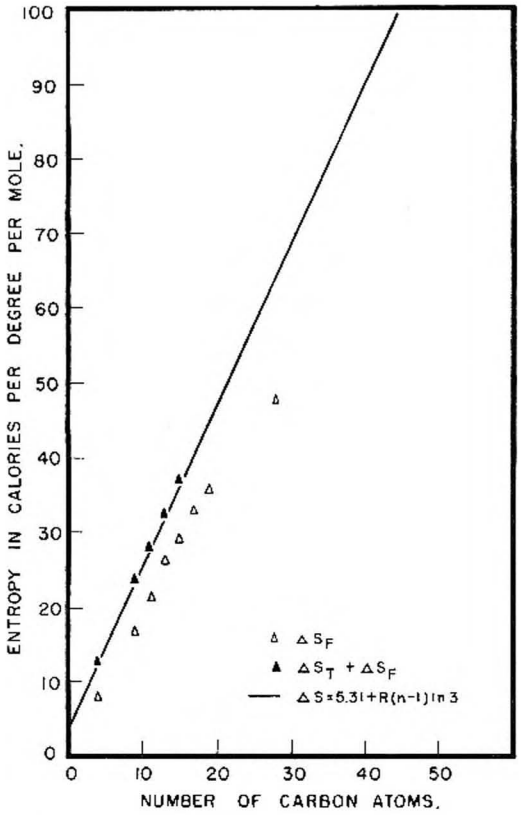

Fig. 2.—Entropies of fusion and of transition for n-hydrocarbons with an odd number of carbons: ΔS_F = entropy of fusion; ΔS_T = entropy of transition.

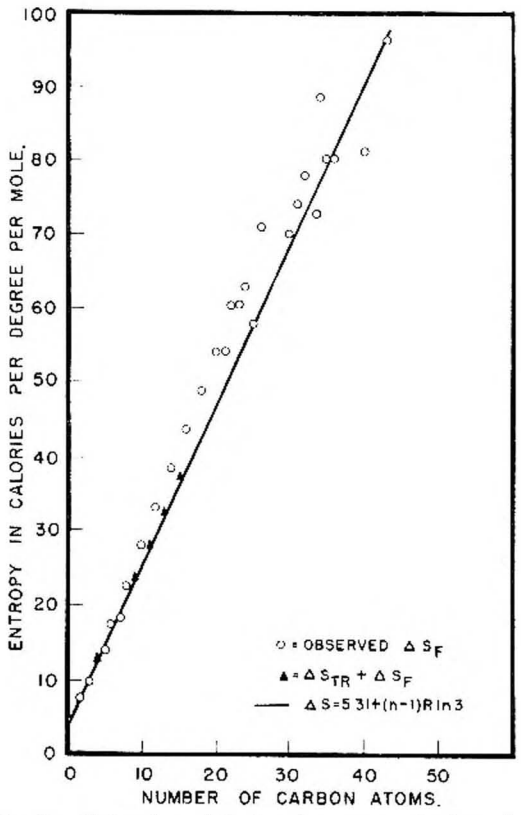

Fig. 3.—Entropies of fusion for even n-hydrocarbons; entropies of fusion plus transition for odd n-hydrocarbons.

where $E_{10} = E_1 - E_0$.

$$\Delta S_{fusion} = k(n-1)\ln 3 + \frac{\partial}{\partial T}\left(kT \ln \frac{A_1}{A_0}\right) + \frac{\partial}{\partial T}\{kT(n-1)\ln(1+e^{-E_{10}/kT})\} \quad (7)$$

The second term on the right is now assumed to be a constant, independent of n, the first term gives the main dependence of the entropy of fusion, the third term gives a correction which is temperature dependent and which can be used in conjunction with experimental results to yield information regarding energy levels.

III. Comparison with the Real Molecule

The real molecule differs from the model considered in the preceding section in that a CH_2 group cannot rotate independently of the rest of the molecule. Consequently, the simplified expressions 1 and 2 for the partition functions must be modified. The modifications will alter the functional form perhaps very much, but the expressions 1 and 2 are probably still good approximations to the true partition functions. Another source of discrepancy is that for real molecules changing configurations give rise to serious inhibitions to many rotational states due to steric hindrances where parts of the molecule interfere physically with the motion of other parts. Such steric hindrances are completely ignored in the model.

Calling the second term on the right in expression 7, C, we can rewrite the expression to get the entropy of fusion per mole

$$\Delta S_{fusion} = C + R(n-1)\ln 3 + R(n-1)\ln(1+e^{-E_{10}/kT}) + RT(n-1)\frac{\partial}{\partial T}\ln(1+e^{-E_{10}/kT}) \quad (8)$$

R is the gas constant and the entropy of fusion is now given per mole. The entropy of fusion and E_{10} for ethane is known. Consequently, we can find C for ethane and assume that C remains fixed for all the paraffins. The entropy of fusion ΔS of ethane is 7.59 cal. per degree per mole; the energy level of the first excited state is 275 cm.$^{-1}$ [3]; consequently, one can calculate C to be 5.31 cal. per degree per mole.

Figure 2 shows how the hydrocarbons with an odd number of carbons fit into the theory. It is seen that the entropy of fusion falls below the expected theoretical curve. However, a few degrees below fusion there was a phase transition with a corresponding entropy increase. If this transition is considered as a partial melting, the total entropy of fusion must be considered as being the sum of the observed entropy of fusion and of the transition entropy. This sum, the filled triangles, does fit the theoretical curve very well (assuming that only the ground state is appreciably occupied). Two molecules, one having seventeen carbon atoms and the other nineteen, are shown only with open triangles. The transition entropy data for these molecules is not yet available. We can predict the existence of these transitions and also the entropy change to be expected at the transition, this being

(3) G. Herzberg, "Infrared and Raman Spectra," 2nd ed., D. Van Nostrand Co., New York, N. Y., 1950, p. 344.

the distance from the corresponding triangles to the full line on Fig. 2.

Figure 3 gives the experimental results for the entropy of fusion of a long list of hydrocarbons.[4,5] The open circles represent molecules with even numbers of carbons. The filled triangles are the same as those of Fig. 2. The line drawn is given by the first two terms of expression 8. We see that even molecules lie regularly above the line; deviations from the line are due to the last two expressions of equation 8. Consequently, we can learn something about the excited energy levels of even hydrocarbons by studying these deviations in detail.

On Fig. 3 as on Fig. 2, the full triangles fall right on the line; there is apparently no deviation due to excited states. However, the "melting" here occurs in two steps at two different temperatures. This introduces complications which mask the effect of the excited levels and are reflected in the specific heat behavior of the odd hydrocarbons between the transition and melting temperatures. The melting and transition phenomena of odd hydrocarbons are worthy of further analysis.

Using the full expression 8, and the experimental results of Fig. 3, the energy level of the first excited torsional state E_{10}/k has been calculated for a number of even hydrocarbons. Those having more than twenty carbon atoms have been ignored because the data scatter and probably are not sufficiently reliable for this purpose. The curve in Fig. 4 shows also two experimental values for E/k for propane[6] and the value for ethane.[3] There are two values for propane because there are two carbon–carbon bonds and the carbon atoms do not form a linear chain. In general, for the real n-carbon molecule there are $n-1$ levels for the first excited state, each level being triply degenerate, the $n-1$ splitting arises because of the non-linearity of the carbon chain and the resulting perturbation about the model we have been considering. The level we have been calling E is thus an "average" energy level. An experimental "average" energy level can be taken for propane and we see that it fits an extrapolation of the energy levels found by our calculation for the longer molecules. Figure 4 also shows the rocking frequency found for $C_{64}H_{130}$,[7] and it appears that the values found by our technique for the average first excited state will approach this value from below as one should expect.

On Fig. 5 we repeat the calculated values of Fig. 4. Now, ask the question: if we know E/k can we predict at what temperature the paraffin will melt? The answer is given empirically in the following way. If T_m is the melting temperature, it is given by the relationship $3T_m = E/k$. The statement can also be inverted, if we know the melting temperature of a paraffin can we calculate the "average" value E of the first excited state. The result is given by the same relationship $3T_m = E/k$. Figure 5 shows this empirical relationship by showing in addition to the calculated values of E/k, the values of $3T_m$ for a number of hydrocarbons—T_m being the observed melting temperature.

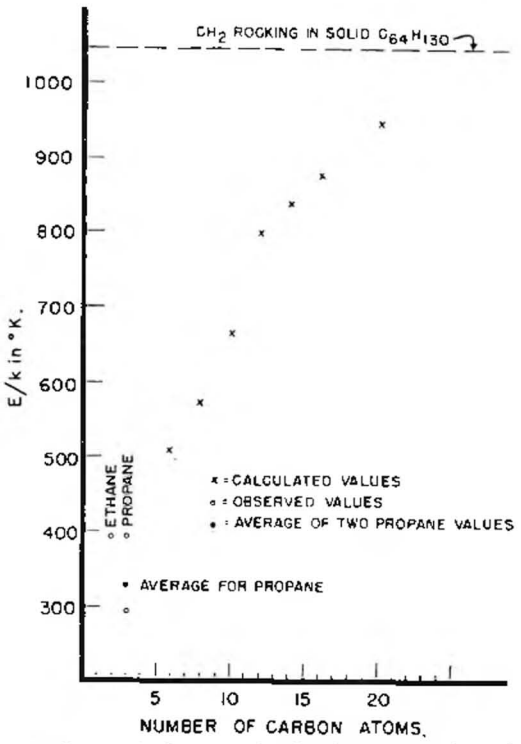

Fig. 4.—First excited energy levels of even n-hydrocarbons.

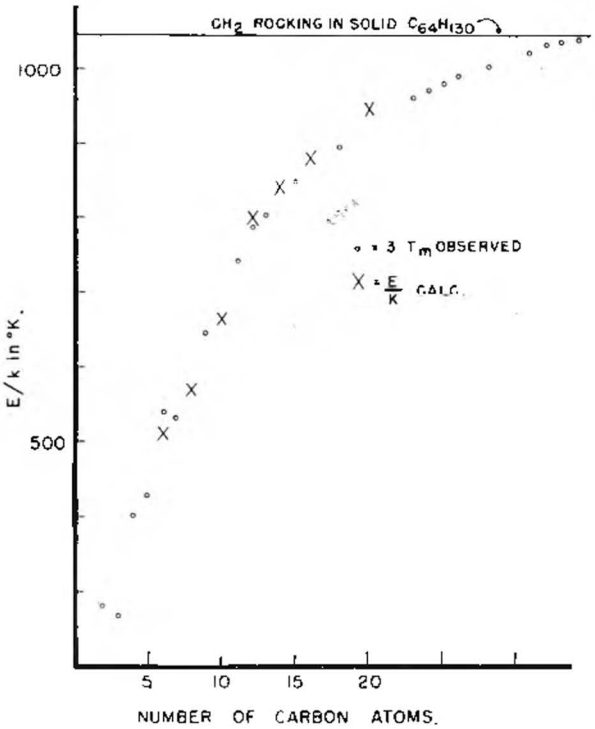

Fig. 5.—Criterion for melting of n-hydrocarbons.

IV. Conclusions

The onset of hindered rotations at melting is consistent with the behavior of the Raman spectra[8]

(4) J. Timmermans, "Les Constantes Physique des Composes Organiques Cristallises," Masson, Paris, 1953.

(5) H. L. Finke, M. E. Gross, G. Waddington and H. M. Huffman, *J. Am. Chem. Soc.* **76**, 333 (1954).

(6) Ref. 3, p. 360.

(7) S. Krimm, C. Y. Liang and G. B. B. M. Sutherland, *J. Chem. Phys.*, **25**, 543 (1956).

(8) G. J. Szasz, N. Sheppard and D. H. Rank, *ibid.*, **16**, 704 (1948).

and heat capacity[5] of liquid paraffins, *i.e.*, the predominant internal behavior is that of a torsional oscillator, not a free rotator. The heat capacity in the liquid is approximately the same as in the solid. If free rotation of internal bonds had begun at melting, the heat capacity contribution per bond would have dropped from approximately R cal. per degree (for classical torsional oscillator) to $R/2$ cal. per degree (free rotator). The onset of torsional oscillation with high probability to shift from one position of potential minima to another reconciles heat capacity and Raman spectra with data indicating that there are many configurations for long chains in the liquid.[9]

Experiments with an analogous compound,[10] 2-dibromo-2,2-difluoroethane, indicate that the isomeric forms consistent with hindered rotations can be observed in the liquid state but only one form is observed in the solid state.

It is reasonable to believe that the long chain fluorocarbons should exhibit the same fusion entropy behavior as the hydrocarbons. If the increase per CF_2 group is $R \ln 3$ we would thus have confirmation that the effect of structure is the dominant factor in determining the entropy of fusion of long chain molecules.

(9) E. J. Hennelly, W. M. Heston and C. P. Smyth, *J. Am. Chem. Soc.*, **70**, 4102 (1948).

(10) R. F. Kagarise, *J. Chem. Phys.*, **24**, 1264 (1956).

THE HYDROGENATION OF BENZENE OVER COPPER-NICKEL ALLOYS

BY W. KEITH HALL AND P. H. EMMETT[1]

Mellon Institute, Pittsburgh, Pa.

Received February 10, 1958

A kinetic study of the hydrogenation of benzene over a series of copper nickel alloy catalysts has been carried out with a view to providing data for critical tests of theories relating catalytic activity to properties of the solid state. The isothermal activity data obtained, as expected from earlier work, showed a sharp decrease near the critical alloy composition of 60 atom % copper where the d band of the metal is just filled. However, the activation energy data obtained concomitantly showed that the observed changes in activity did not reflect changes in the activation energies, but came about through overpowering "compensations" by the frequency factors. A possible interpretation of this result is advanced.

Introduction

The hydrogenation of benzene over copper-nickel alloys has been studied by a number of workers.[2-4] In all of these cases, catalytic activities have been determined either at a given temperature,[4] or the catalytic activities have been compared by seeking the temperature at which a given conversion is obtained.[2,3]

In recent years, workers in the field have become interested in relating catalytic activity to the electronic properties of the solid state. These attempts have been stimulated by a series of papers by Dowden[5-8]; the theoretical development contained in one of these[6] clearly indicates that in order to sort out the various electronic variables which may be affecting the course of the catalytic reaction, it is necessary to determine both activation energies and frequency factors. According to this development, if a positive ion is involved in the catalytic mechanism, then over a series of homogeneous solid solutions of copper and nickel, the frequency factor would be expected to fall as copper is alloyed with nickel (*i.e.*, as the partially empty d-band of the nickel is filled) so that at the critical composition of 60% copper–40% nickel, its value would be only a very small fraction of that of pure nickel; because of a scarcity of holes, the number of sites/cm.^{2} available for ion formation would be severely limited. Simultaneously, since the work function of copper is less than that of nickel, the activation energy of the hydrogenation reaction might be expected to increase as copper is alloyed with nickel. The combined operation of these two factors is in such a direction that the over-all reaction rate would be expected to fall sharply at or near the critical composition. Such behavior was indeed observed by Reynolds[4] in isothermal determinations of the rates of hydrogenation of benzene and styrene over copper–nickel alloys. Since it was apparent that a more critical test of these ideas could be obtained by determination of both the absolute activities and the activation energies for benzene hydrogenation over a similar series of alloys, the present work was undertaken.

Long, Fraser and Ott[2] discovered quite several years ago that a number of alloy systems could be formed by coprecipitation of the oxides, and then reduction with hydrogen. Of particular interest are their studies of the catalytic activity of three copper–nickel alloys containing 28, 54 and 79 atom % copper, respectively, in the benzene hydrogenation. Using five-cc. samples of the metal oxides, these workers found that on reduction the pure nickel catalyst had the highest activity. The sample containing 28 atom % copper was the least active alloy; the activity rose slightly as the percentage of copper increased to 54 and then 79%. Pure copper, of course, did not hydrogenate benzene. No surface area values were obtained on these samples. Emmett and Skau[3] studied the hydrogenation of benzene over copper catalysts sub-

(1) Dept. of Chemistry, Johns Hopkins University, Baltimore, Maryland.

(2) J. H. Long, J. C. W. Fraser and E. J. Ott, *J. Am. Chem. Soc.*, **56**, 1101 (1934).

(3) P. H. Emmett and N. J. Skau, *ibid.*, **65**, 1029 (1943).

(4) P. W. Reynolds, *J. Chem. Soc.*, 265 (1950).

(5) D. A. Dowden, *Research*, **1**, 239 (1947).

(6) D. A. Dowden, *J. Chem. Soc.*, 242 (1950).

(7) D. A. Dowden, *Ind. Eng. Chem.*, **44**, 977 (1952).

(8) D. A. Dowden and P. W. Reynolds, *Disc. Faraday Soc.*, **8**, 172 (1950).

stantially free of nickel and catalysts in which small amounts of nickel had been deliberately incorporated. They found that on the pure copper catalysts the reaction did not take place at 200°. With the addition of as much as 0.001% nickel, however, small activities were observed, and on catalysts containing as much as 1% nickel, substantial activities were obtained at space velocities of approximately 100. These data point out the fact that the benzene hydrogenation over copper–nickel alloys persists almost over to pure copper and that the fall in activity between 1% nickel and pure copper represents a percentage decrease in activity as large as that observed by Reynolds as the *d*-band fills.

Iron–cobalt and palladium–silver alloys were also studied[3] in the same reaction. With the former, it was found that the catalytic activity decreased as the iron was alloyed with cobalt even in those instances in which the face-centered cubic structure of cobalt was largely maintained. A similar decrease in rate was noted in the work of Reynolds[8] for the styrene hydrogenation as the iron content of a nickel–iron alloy was increased. With the palladium–silver system,[3] the activity fell off, as silver was alloyed, much as with the copper–nickel system. Surface areas were quoted on all samples, but unfortunately activation energies were not obtained.

It should be noted that the activation energies reported herein are apparent activation energies defined as the temperature coefficient of the fractional conversion. For the sake of brevity, the word "apparent" will be understood henceforth. No attempt was made to calculate apparent frequency factors, but the trends of this parameter with composition were inferred from the behavior of the activation energies and the total absolute rates per unit catalyst area.

Experimental

In the present work, eleven catalysts were prepared, spanning the composition range between pure nickel and pure copper rather uniformly. The mode of preparation followed by Best and Russell[9] was fairly closely adhered to. Calculated amounts of analytical reagent grade $Cu(NO_3)_2 \cdot 3H_2O$ and/or $Ni(NO_3)_2 \cdot 6H_2O$ were dissolved in water and diluted to correspond to about 5 g. of NiO and/or CuO per hundred ml. of solution. Only distilled water which had been further purified by running through an ion-exchange column so that its conductivity indicated a total ionic concentration of less than 0.5 part per million (as Na^+) was used and only stainless steel, Coors porcelain, and Monel metal equipment were employed to minimize pickup of traces of alkali. The ionic constituents were not allowed to contact stainless steel, to avoid possible contamination with iron. In a typical preparation, the solution of the mixed metal ions was made in a large porcelain evaporating dish and was stirred rapidly with a Monel stirrer at room temperature while powdered chemically pure ammonium bicarbonate was added until a permanent turbidity just formed. Then, 2.2 moles of the bicarbonate per mole of metal ion was added as rapidly as possible, and the suspension was stirred for 10 to 20 minutes. The dish was then covered and allowed to stand overnight while the precipitate settled; this was then washed by decantation with small amounts of hot water until the washings became colorless, indicating the absence of ions of copper and/or nickel and hence that the nitrate ion had been largely removed. The dish was then made part of a steam-bath and water was evaporated until the raw catalyst became a pasty solid with the consistency of putty. This was then transferred to a smaller, clean evaporating dish and further dried in an oven at 110° overnight. The dried precipitate was broken with a stainless steel spatula and forced through a No. 6 screen; the material retained on a No. 10 screen was separated to be used in the experiments. This fraction was kept in an evaporating dish in the muffle furnace for two hours at 400°, during which time its color changed from bluish green to brown or black as the basic carbonates were converted to the oxides. This treatment also ensured removal of traces of nitrate, ammonia and carbon dioxide left from the decantation washing. The finished raw catalysts were stored in sealed metal cans until needed.

Several samples of each catalyst were analyzed for total nickel and total copper to provide data for the composition variable in the studies. These data are listed in Table I. Qualitative tests were made for iron using SCN^-. Although this test is extremely sensitive, the results were al negative. A polarographic analysis of Catalyst III for sodium ion established that it contained less than 0.005% as Na_2O. The remaining samples were rated by their emission spectrograms as one, two and three, with one indicating the lowest amount and three being the order of the alkali in Catalyst III. The nickel used in the preparation was supplied by Fisher Scientific Company and was of analytical reagent grade and "low in cobalt." The atom per cent. of nickel given in Column 5 of Table I were calculated on the assumption that upon reduction only copper and nickel are left. In the same way, the values for the % oxygen given in column 4 were obtained by difference. In all cases, this residual oxygen was found to be higher than for the stoichiometric composition of MeO where Me represents both nickel and copper. The most pronounced deviation occurred with Catalyst X, where it corresponded to a composition of $MeO_{1.07}$. Since these figures were obtained by difference and may include any bound water, carbon dioxide or ammonia not released by heating in air to 400° for several hours, too much significance cannot be attached to them. Oxides of this system, however, are seldom stoichiometric and nickel oxide, at least, varies over a range of composition nearly as great as that indicated. The data listed in columns 6 and 7 showed that the alkali content of these catalysts was extremely low and was, in fact, barely at the limit of detectability by ordinary methods.

TABLE I

SUMMARY OF ANALYSES MADE ON RAW CATALYSTS

Catalyst no.	Cu, %	Ni, %	O,[a] %	Atom % Ni in reduced catalyst	Rating[b] Na	Rating[b] K
VIII	0	76.77	23.23	100.0	1	nil
V	12.40	64.27	23.33	84.8	2	1
VI	22.37	54.17	23.46	72.4	2	1
VII	37.24	40.07	22.69	53.8	..	..
IX	43.85	33.82	22.33	45.5	2	nil
X	50.84	24.51	24.65	34.3	2	1
IV	63.18	15.10	21.72	20.6	..	..
XI	67.76	10.80	21.44	14.7	nil	1
III	73.15	5.70	21.15	7.8	3	nil
II	78.79	0	21.21	0	..	..
I	79.14	0	20.86	0	..	..

[a] Oxygen is given by difference. For comparison, stoichiometric NiO is 21.42% oxygen and stoichiometric CuO is 20.12% oxygen. [b] Polarographic analysis of Catalyst III showed that the total alkali was less than 0.005%. Emission spectrograms were made of the other catalysts and compared to that from Catalyst III. They were rated 1, 2 and 3 with 1 being the lowest amount and 3, the highest.

The hydrogen used in this work, both for reduction and for hydrogenation, came from tanks of high purity hydrogen supplied by the Air Reduction Sales Co. It was further purified, however, by passing through a train consisting of a Deoxo purifier, anhydrous magnesium perchlorate, platinized asbestos at 375°, more anhydrous magnesium perchlorate, and finally a trap containing about 25 g. of high area charcoal. The latter was thermostated at −195°. The hydrogen used, therefore, was as pure as could be obtained

(9) R. J. Best and W. W. Russell, *J. Am. Chem. Soc.*, **76**, 838 (1954).

by ordinary means. This was important, as it was discovered early in the work that these catalysts were particularly sensitive to small amounts of poisons, as evidenced by a rapid decline in activity with throughput, before the charcoal trap was added. The benzene was from a special lot of sulfur-free, high purity material made by the Jones and Laughlin Steel Co. It was freed from water and other possible oxygenated materials by passage through a column of dry silica gel. Freezing point, refractive index, infrared, ultraviolet and mass spectrometric analyses made on this sample failed to locate any trace of an impurity.

The raw catalysts, consisting of the mixed oxides of copper and nickel, were loaded into Pyrex glass reaction vessels and attached to an all-glass high vacuum system of the conventional type. Both the inlet and the exit arms were protected from mercury vapor by a rolled leaf of 23 carat gold foil at the points of attachment. The tube was maintained in a vertical position and so arranged that a furnace, which could be controlled to ±0.3° by a conventional thyratron circuit, could be raised around it. Reduction was carried out by passing purified hydrogen over the catalyst at a space velocity of approximately 5,000 cc. of gas per cc. of catalyst per hour and at temperatures between 150 and 350°. The reduction was started at 150° and continued at this temperature for about one-half hour. At the moment the reduction was initiated, as evidenced by condensation of excess water in the exit line, the catalysts were observed to glow visibly momentarily. During the half-hour period, the bulk of the water was removed from the catalyst and its volume decreased to about one-half its original volume. After this treatment, the furnace was removed, and the tube was tapped so that a coherent catalyst bed was re-formed. The furnace was then replaced, and the thyratron circuit set to control at 350°. The temperature rose from 150° to this value over a period of about an hour. Reduction at 350° was continued for a 16 to 18-hour period. At the end of this time, the furnace was again lowered, and the catalyst tube was removed from the system and weighed to obtain a measure of the extent of the reduction. This was obtained by comparing the observed weight loss with that expected from the analysis of the raw catalyst. In almost all cases, the observed loss was found to exceed 98% of that expected. The tubes were then replaced on the rack and the reduction continued for a period of two hours in those cases in which the calculated extent of reduction exceeded 98%, but for an additional overnight period in those instances in which the calculated extent of reduction appeared to be less than 98%. Subsequent reductions were carried out at somewhat lower temperatures, never exceeding 250°.

Catalyst testing in the hydrogenation reaction could be carried out over the freshly reduced catalyst by simply lowering the furnace temperature to the desired level at the end of the final reduction. Then, by reversing two three-way stopcocks, the hydrogen stream could be by-passed through the benzene saturators so that the composition of the gas passing over the catalyst became approximately 9:1 = hydrogen:benzene. The flow rate was now controlled at 50 cc. of hydrogen per minute per g. of catalyst to within 2%. The reduced catalyst weights were in the range of from one to three g.

The hydrocarbon products were removed from the exit gas stream by passing the gases from the catalyst through small, detachable, glass traps immersed in liquid nitrogen. The samples were collected over periods of time ranging from 10 to 20 minutes. The benzene–cyclohexane mixtures obtained in this way were analyzed to determine the extent to which the reaction had proceeded. This was usually done by measuring the refractive index of the liquid and referring to a calibration curve made with the benzene used and with spectroscopically pure cyclohexane. In a few instances, however, samples of the liquid obtained at fairly high conversions (20 to 35%) were also analyzed by infrared spectroscopy and by passing aliquots through a gaseous chromatographic column filled with supported dioctyl phthalate. In all cases the analyses agreed quite well and gave no evidence of the presence of either of the cyclohexenes or of cracked products, thus justifying the reliability of the refractive index measurements.

Each sample obtained yielded a point on a log conversion *vs.* $1/T$ curve, the temperature datum for which was obtained by measuring the output of a calibrated chromel–alumel thermocouple with a Leeds and Northrup portable potentiometer. The thermocouple was positioned in close contact with the glass wall of the thermocouple well of the catalyst tube, in the center of the annular shaped catalyst bed. Additional data were obtained by changing the temperature between collections by from 5 to 25° before the next collection was started. The progress of the changes in temperature could be followed visually as the output of the thermocouples plotted on a Speedomax chart, the sensitivity of which was about 1.2 millivolts or about 30° for full scale response. Sample collections were made only when this guide indicated that the temperature was perfectly constant and that the catalyst was in steady-state operation. In almost all cases, the data were obtained at successively higher temperatures followed by at least one or two repeat points at lower temperatures to ensure that gross changes in catalyst activity with time were not occurring.

Data derived from the activation energy plots obtained in this work are collected in Table II. Since the flow rate per g. of metal was maintained constant, specific activities could be obtained by division of the fractional conversions obtained at selected temperatures by the specific surface areas in $m.^2/g.$ Under these conditions, satisfactory conversions could be obtained for all catalysts except copper-rich Catalyst III and pure copper Catalyst II at temperatures below 220°. Due to the reversibility of the reaction, this was the highest temperature that was feasible to use without consideration of the effects of back reaction. A figure for the activity of Catalyst III could just be measured. Its activation energy was obtained after lowering the flow by a factor of four. In the case of Catalyst II, however, there was no evidence of any conversion at 220° even at a flow one-tenth that used for the remainder of the catalysts.

Table II

Summary of Experiments with the Hydrogenation of Benzene

Catalyst no.	Nickel atom %	Apparent activation energy, kcal./mole	Catalyst activity % of benzene converted at 135°	161.8°	Specific surface area, $m.^2/g.$	Specific activities at 135°	161.8°
VIII	100.0	13.2	9.6	30.0	0.82	11.7	36.6
		13.1	11.2	30.0	1.01	11.1	29.7
V	84.8	18.8	25.5	99.9	1.57	16.2	63.6
VI	72.4	18.4	25.5	99.9	1.48	17.2	67.5
VII	53.8	18.7	22.5	93.0	1.82	12.4	51.1
IX	45.5	18.5	15.0	58.0	1.67	9.0	34.7
X	34.3	16.4	4.0	13.8	0.88	4.5	15.7
IV	20.6	15.5	2.3	7.4	0.93	2.5	8.0
XI	14.7	14.1	1.7	4.9	1.04	1.6	4.7
III	7.8	12.5	0.0	<1.0	0.57	0.0	1.7
II	0.0	..	0.0	0.0	0.33	0.0	0.0

The reaction is exothermic, and it was impossible to control it above about 25% conversion even though the all-glass catalyst vessels were constructed in such a way that the catalyst was contained in a thin annular space about two mm. thick between the tube wall and the thermocouple well. The nature of the phenomenon was as follows: at conversions of around 12% of the entering benzene to cyclohexane, the temperature in the thermocouple well exceeded that of the furnace by about two degrees and at twice this conversion, the temperature differential was nearly five degrees; attempts at slightly higher conversions resulted in complete conversion and measurable temperature differentials of over 50°.

The catalysts were quite sensitive to small traces of poisons. Usually during the four to six-hour period required to make the measurements, about 5% of the catalyst activity was lost. Since effects varying over several orders of magnitude were being investigated, however, this was deemed satisfactory. For assurance against serious poisoning, all data reported herein were checked at least twice by repeating the testing procedure after an additional overnight reduction in pure hydrogen.

After the catalyst testing had been completed, each sample was reduced for several hours and then evacuated at approximately 100° for three or four hours until a pressure of better than 5×10^{-5} mm. had been attained. Surface area measurements were then made on each catalyst

using the BET[10] method, the cross-sectional area of the nitrogen adsorbate being taken as 16.2 A.^{2} These data were used to calculate specific activities.

Finally, after the adsorption measurements had been made, some of the catalyst samples were sealed off under vacuum, opened under benzene, and subjected to X-ray analysis for determining the lattice parameters. The results of these experiments have been described elsewhere.[11] It will be sufficient to state here that these data were found to be in excellent agreement with the data of Owen and Pickup[12] obtained on alloys that had been melted. Hence, the data obtained tend to substantiate the conclusion of Long, Fraser and Ott[2] to the effect that catalysts prepared in this manner are fairly homogeneous solid solutions of copper and nickel in the face-centered cubic alloy phase.

Results

The results obtained in this study are summarized in Figs. 1 and 2. Figure 1 shows that the present work is in qualitative agreement with that of Reynolds[13] (broken curve), but that there are two marked differences. The first of these is that Reynolds observed the sharp drop in activity at about 70% nickel, whereas in the present work the abrupt drop in activity occurs at about 40% nickel in much better agreement with the hypothesis that the activity should fall as the hole in the d band is filled. The other important difference is that Reynolds found pure nickel to be the catalyst of maximum activity, with the alloys falling to successively lower activities as copper was alloyed with nickel. In the present work, the maximum activity appeared on the alloy containing about 75% nickel while pure nickel was only about as active as the catalyst with 45% nickel. It is, of course, impossible to establish categorically the cause for these discrepancies. A partial explanation, however, may be found in the following facts: Reynolds studied the hydrogenation over skeletal Raney catalysts that had been either exhaustively extracted with alkali or surface etched by the foraminate process (surface activation with flowing dilute hot alkali). The starting materials were ternary alloys of copper, nickel and aluminum. By either process of activation, it probably was impossible to remove completely. As the interstitial aluminum ions have contributed electrons into the d-band of the nickel, it is not surprising that these catalysts behaved as if they contained more copper than the amount actually present. With regard to the lower activity of the pure nickel catalyst observed in the present work, a similar argument may be advanced. Alternatively, Fig. 1 shows that the difference obtained at 135° between the activity of the pure nickel catalyst and the one containing 27.6% copper is not nearly so pronounced as that obtained at 161.8°, and extrapolation of these data to 100° eliminates the maximum altogether. Since Reynolds' data were obtained at 100° and since at this temperature both sets of data indicate that nickel has the highest activity, one would conclude that perhaps no actual discrepancy between the two sets of data exists.

(10) S. Brunauer, P. H. Emmett and E. Teller, *J. Am. Chem. Soc.*, **60**, 309 (1938).

(11) W. K. Hall and L. Alexander, *J. Phys. Chem.*, **61**, 242 (1957).

(12) E. A. Owen and L. Z. Pickup, *Z. Krist.*, **88**, 116 (1935).

(13) Data taken from Table VI of ref. 4 were plotted as the dashed line of Fig. 1, after multiplying the per pass conversions by 0.75 (for convenience) and calculating the % nickel as (100 − %Cu).

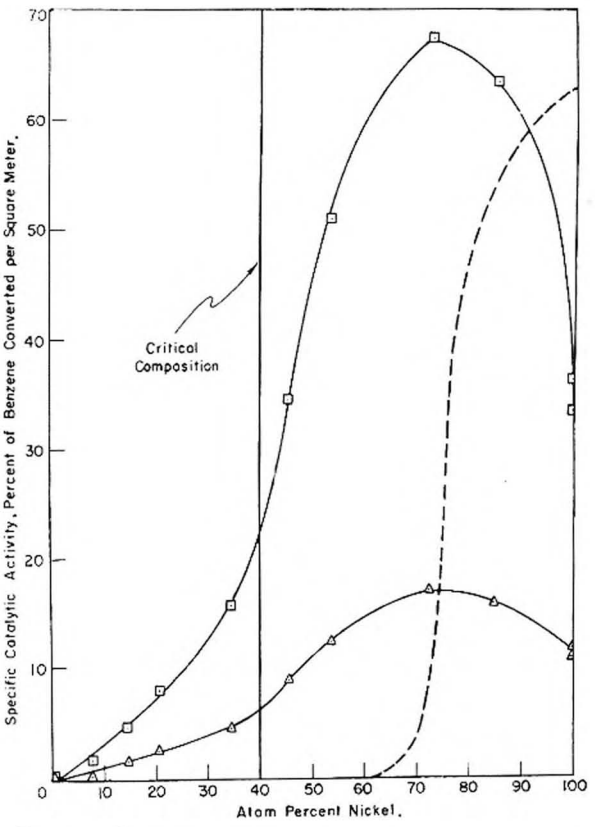

Fig. 1.—Catalytic activity of a series of copper-nickel alloys in the hydrogenation of benzene: ⊡, data for 161.8°; △, data for 135.0°. The dashed line is taken from data of Reynolds[13] (see text).

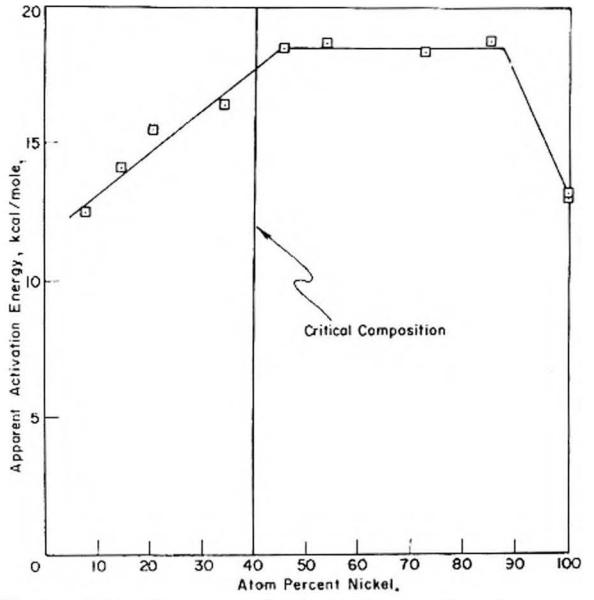

Fig. 2. Activation energy for the hydrogenation of benzene for a series of copper-nickel alloys.

Discussion

The principal thesis developed by Dowden[5–8] was that in a heterogeneous reaction, where an ion formed from reactant gas is important to the rate-determining step, a term containing the work function, φ, will appear as part of the apparent activation energy. It was further argued that changes

in the factor, $\exp(\pm a\varphi/RT)$ ("a" is an arbitrary constant), of the rate expression might be expected to outweigh all other changes as the composition variable of a series of alloys is altered; in this connection, Dowden paid particular attention to hydrogenation reactions (including benzene) over copper–nickel alloys. (The sign of the exponential will, of course, depend upon the reaction mechanism and in particular whether a positive or negative ion is involved.) Finally, it was noted that if positive ions are important to the reaction mechanism, the frequency factor may be expected to undergo a drastic decrease as the hole in the d-band nears complete filling.

In the present work, the apparent activation energy is discontinuous with composition, *i.e.*, it first increases then decreases as copper is alloyed with nickel. Stated another way, the *simple* hypothesis advanced by Dowden does not appear to be operative; hence, an alternative explanation must be sought.

Several possibilities present themselves. One is that the reaction mechanism is different over the nickel than over the copper–nickel alloy catalysts; this may be dismissed for lack of evidence. Another is that the work functions of the surfaces of the catalysts, covered with gas in steady state reaction, do not vary continuously with composition as would be expected from the band theory of metals. This possibility cannot be dismissed because it is well known that work functions of gas covered surfaces frequently differ from those of the corresponding clean surfaces by as much as 35 kcal./mole.[14] Furthermore, the relative order of work functions is frequently changed by the adsorption process.[15] Finally, the possibility that the value of this parameter may go through a maximum (or minimum) between the pure nickel catalyst and the 84.8% nickel catalyst, seems particularly reasonable in view of a poisoning and/or promoting effect (respectively) found for hydrogen for the ethylene hydrogenation reaction over these same catalysts, as reported in a following paper. This then seems to be the most likely place that the simple theory can be in error, and offers a simple, although as yet untested, hypothesis for the interpretation of our data. Furthermore, it avoids the necessity of assuming that the mechanism changes between nickel and the alloy catalysts as would be required to explain the maximum in the activation energy found for the nickel-rich alloys. In this connection, it should be pointed out that the nickel catalyst was retested starting with a completely new sample of catalyst to ensure without reasonable doubt that the activity and activation energies obtained for this catalyst were indeed lower than those found for the nickel-rich alloys. The excellent reproducibility found both for the activity and for the activation energy is taken as proof of the validity of these points.

The single criterion which best describes all of our data is that the observed changes come about through an overcompensation of changes in apparent activation energy, by changes in frequency factor. The correct rate expression must account for this fact. Such effects are well known; for example, Schwab[16] has written

$$\ln C = \ln C_0 + (1/h)E_a \qquad (1)$$

as a general law of heterogeneous catalysis; C is the frequency factor, E_a the apparent activation energy of the Arrhenius equation and C_0 and h are constants. More recently, Cremer[17] has reviewed this subject. Adopting this view, it becomes evident that with respect to the data obtained in the present work, at least, the electronic factors controlling the behavior of the reaction as a function of composition also lead to the "law of compensation."

J. H. deBoer[18] has discussed in some detail the changes of work function with surface coverage. He has found that for low coverages the change in work function should be proportional to the surface coverage. This has been verified experimentally for the case of the adsorption of cesium on tungsten.[19] At higher coverages, this simple relationship breaks down and deBoer pictures the positive ion on the sparsely populated surface surrounded by atoms of cesium. At still higher coverages, atoms are adsorbed with their dipoles reversed due to polarization effects, so that the change in work function goes through a maximum. The situation is complicated further by the fact that the work function now becomes a function of temperature. In this connection, deBoer[20] recently pointed out that a strong analogy exists between the variation of the constant A of the Richardson equation for thermionic emission

$$i = AT^2 \exp[-\phi/kT] \qquad (2)$$

and the relation established by Schwab[17] for the variation of frequency factor with activation energy, *viz.* (1). In (2), i is the current passed per cm.^{2}, ϕ is the work function of the surface at temperature T, and k is the Boltzman constant. The constant A can be evaluated by statistical thermodynamical methods; it turns out that for a pure metal, it should have a value of 120 amp./cm.^{2} deg.^{2}. It is found,[15] however, that with cesium adsorbed on tungsten, the value of A falls to 3.26 and with oxygen on the same metal, it has a value of 5×10^{11}. Richardson,[21] himself, established that

$$\phi = a \log A_\theta + b \qquad (3)$$

held for the experimental observations available at the time (ϕ_θ and A_θ are defined as in (2), but at constant coverage θ; a and b are constants). This relationship has been interpreted by Schottky[22] and somewhat differently by Zwikker[23] as due to a temperature dependence of the dipole moments in the double layer.

(14) J. C. P. Mignolet, *Disc. Faraday Soc.*, **8**, 105 (1950).

(15) (a) C. W. Oatley, *Proc. Phys. Soc.*, **51**, 518 (1939); (b) J. H. deBoer, "Electron Emission and Adsorption Phenomena," Clarendon Press, 1935, p. 149 ff.

(16) G. M. Schwab, *Proc. XI Intern. Congr. Pure and Appl. Chem., London* (1947).

(17) E. Cremer, "Advances in Catalysis," Vol. VI, Academic Press, New York, N. Y., 1955, p. 75 ff.

(18) J. H. deBoer, ref. 15b, p. 80 ff.

(19) J. B. Taylor and I. Langmuir, *Phys. Rev.*, **44**, 432 (1933).

(20) J. H. deBoer, *Disc. Faraday Soc.*, **8**, 208 (1950).

(21) O. W. Richardson, *Proc. Roy. Soc. (London)*, **A91**, 524 (1915).

(22) W. Schottky, "Handbuch der Experimentalphysik," Vol. 13, 1928, p. 164.

(23) C. Zwikker, *Physik. Z.*, **30**, 578 (1929).

As yet there is no agreement as to the exact interpretation of this relationship. The important experimental fact is, however, that just as in the Richardson equation the pre-exponential factor, A, varies over many orders of magnitude as the work function for surfaces on which gas is adsorbed, so also in catalysis the frequency factor in the kinetic rate expression may be expected to vary with the activation energy which, in turn, contains the work function. Furthermore, it operates in such a direction that if the activation energy is increased, the frequency factor will be increased and if the activation energy is decreased, the frequency factor will be decreased, regardless of whether the adsorbing ion is a positive ion or a negative ion.[20] Needless to say, this offers the simplest and most straightforward correlation of the data presented herein.

Acknowledgment.—Thanks are due to Professor H. S. Frank of the University of Pittsburgh for many helpful discussions in the course of this work, which was sponsored by the Gulf Research & Development Co. as a part of the research program of the Multiple Fellowship on Petroleum.

THE HEATS OF COMBUSTION AND FORMATION OF HEXACYCLO[7:2:1:$0^{2:5}$:$0^{3:10}$:$0^{4:8}$:$0^{6:12}$]DODECANE. TWO TECHNIQUES FOR THE COMBUSTION CALORIMETRY OF VOLATILE SOLIDS

BY WARD N. HUBBARD, F. R. FROW AND GUY WADDINGTON[1]

Contribution No. 72 from the Thermodynamics Laboratory, Petroleum Experiment Station, Bureau of Mines, U. S. Department of the Interior, Bartlesville, Oklahoma

Received February 17, 1958

The heat of combustion of solid hexacyclo[7:2:1:$0^{2:5}$:$0^{3:10}$:$0^{4:8}$:$0^{6:12}$]dodecane was determined; $\Delta Ec°_{298.15} = -1616.83 \pm 0.23$ kcal. mole^{-1}. From this value the standard heat of formation was calculated; $\Delta Hf°_{298.15}$(solid) $= +12.06 \pm 0.27$ kcal. mole^{-1}. Two new techniques for the combustion calorimetry of volatile solids are described.

Introduction

The recently synthesized compound[2] hexacyclo-[7:2:1:$0^{2:5}$:$0^{3:10}$:$0^{4:8}$:$0^{6:12}$]dodecane[3] (hereinafter called hexacyclododecane) is a saturated hydrocarbon having a "cage" structure and undoubtedly possesses appreciable strain energy. Heat of formation values for estimating strain energy in this and related molecules are lacking. Because of current interest in molecules with "cage" and bicyclic structures the heat of combustion of hexacyclododecane was determined in this Laboratory.

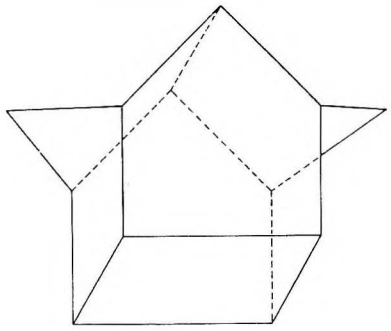

Introduction of samples into the combustion bomb required special techniques because the compound is too volatile to weigh directly in a crucible. The techniques developed may be applicable to combustion calorimetry of other slightly volatile solid substances.

(1) Inquiries concerning this paper should be addressed to J. P. McCullough, Petroleum Experiment Station, Bureau of Mines, P. O. Box 1321, Bartlesville, Oklahoma.

(2) S. Winstein and L. deVries, unpublished. Presented by S. Winstein at the 18th Conference of the International Union of Pure and Applied Chemistry, Zurich, Switzerland, July 20–28, 1955.

(3) For mention of the systematic name see *Chem. Ind.*, 562 (1954).

Experimental

Material.—The sample of hexacyclododecane was prepared and specially purified by L. deVries under the direction of Professor S. Winstein, Department of Chemistry, University of California at Los Angeles. The purification included treatment with permanganate to remove unsaturated impurities, three recrystallizations from pure acetone, and, finally, sublimation at reduced pressure. The melting range, 168.1–168.6°, was not reduced by further treatment.

Crystals of hexacyclododecane are highly disordered at room temperature.[4] Consequently, it is reasonable to assume that the cryoscopic constant is small. Calculations based on the observed melting range and the estimate that the cryoscopic constant is in the range of 0.02–0.002 deg.$^{-1}$ led to the conclusion that the purity of the sample was in the range of 99.0–99.9 mole %. The average mass of carbon dioxide produced in the combustion experiments was 99.99% of that calculated from the mass of sample if the sample was assumed to be pure $C_{12}H_{14}$. Thus, the composition and the heat of combustion of whatever impurity was in the sample probably did not differ grossly from that of hexacyclododecane.

Apparatus and Procedure.—Most of the apparatus and procedures used in this investigation have been described. A tantalum-lined bomb, Ta-1,[5] was used in a rotating-bomb calorimetric system, BMR 1,[6] but the bomb was not rotated during the experiments. The calorimetric procedures were similar to those described in ref. 6 for the combustion calorimetry of liquid organic sulfur compounds. However, only 1.0 ml. of water was introduced into the bomb, and the bomb was purged to remove air before charging with oxygen. Also, because unusually violent combustion tended to dislodge the baffle from the crucible, the baffle was tied in position with platinum wire. Special techniques discussed later were necessary for weighing the sample because of the high volatility of hexacyclododecane.

After the calorimetric part of an experiment, carbon dioxide was determined in the bomb gases. Gas issuing from

(4) Communicated by Professor J. D. McCullough, Department of Chemistry, University of California at Los Angeles.

(5) W. N. Hubbard, J. W. Knowlton and H. M. Huffman, THIS JOURNAL, **58**, 396 (1954).

(6) W. N. Hubbard, C. Katz and G. Waddington, *ibid.*, **58**, 142 (1954).

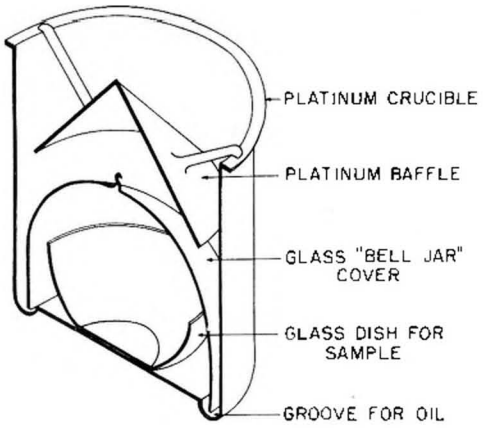

Fig. 1. - The covered sample technique.

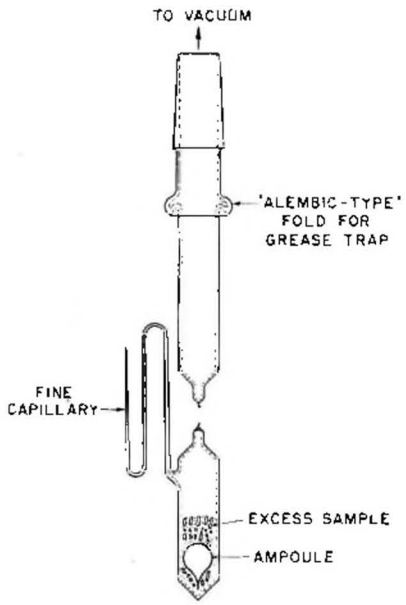

Fig. 2.—System for filling ampoules with a volatile solid.

the carbon dioxide absorption train was tested for carbon monoxide, and no significant amount was found. To determine the amount of nitric acid formed, the solution remaining in the bomb was titrated with standardized NaOH solution to the brom cresol green end-point.

Calibration.—The energy equivalent of the calorimetric system was determined from combustion experiments with benzoic acid, N.B.S. Standard Sample 39g, which was certified to evolve 26.4338 ± 0.0026 abs. kj. per gram mass by combustion under specified conditions.[7] For the conditions of the calibration experiments, which were essentially those of ref. 7, a value of 26.4343 abs. kj. per gram mass was used. From 22 experiments, the energy equivalent of the calorimetric system, ε (calor.), was found[8] to be 3892.6 ± 0.1$_5$ cal. deg.$^{-1}$.

Special Techniques for Volatile Solids.—Hexacyclododecane is a solid at room temperature and is volatile enough that it cannot be weighed directly in a crucible. Two special techniques for containing the sample were used.

In one technique, illustrated in Fig. 1, the sample was contained in a thin glass dish over which was placed a thin glass "bell jar" cover. The dish and cover were made by passing a glowing 0.01-inch-diameter platinum wire through thin-walled Pyrex glass bulbs of appropriate size and shape. Kindling oil in the groove at the bottom of the crucible formed an effective seal for preventing escape of vapors. The mass of sample was obtained by difference from appropriate weighings. The total mass of dish and cover was 0.1 to 0.2 g. A filter paper fuse dipped into the oil outside the cover.

In the second technique, the sample was contained in a Pyrex glass ampoule. An ampoule and excess sample were placed in a filling tube, as shown in Fig. 2. The filling tube was evacuated and sealed. The sample was melted, and the long, fine capillary side arm was broken so as to admit air slowly to the filling tube, forcing the sample into the ampoule. When the ampoule was filled, the tube was inverted and allowed to cool with the stem of the ampoule upright until the sample solidified. The ampoule was removed by cracking open the filling tube. It was found easier to remove the ampoule from the filling tube and excess compound from its outer surface when the solid was warm and somewhat plastic.

The stem of the ampoule was not sealed. Constancy of weight of the filled ampoule showed that (a) all excess compound had volatilized from its outer surfaces and (b) the capillary stem of the ampoule was small enough to prevent significant volatilization from within.

Results

Four satisfactory combustion experiments were made with the covered-sample and six with the ampoule technique. The results are presented in Table I. The values of $-\Delta Ec^\circ/M$ for $C_{12}H_{14}$ are in terms of the defined calorie equal to 4.1840 absolute joules and apply to the idealized combustion reaction

$$C_{12}H_{14}(c) + 15^1/_2O_2(g) = 12CO_2(g) + 7H_2O(liq) \quad (I)$$

with all reactants and products in their appropriate standard state.[9] The amount of reaction was determined both from the mass of hexacyclododecane, m', and from the mass of carbon dioxide in the products (after correction for CO_2 produced by combustion of fuse and oil). The amounts of carbon dioxide from hexacyclododecane are listed in Table I, both as mass in grams and as per cent. of the amount calculated from the mass of sample.

In addition to the ten satisfactory experiments, twelve more were attempted. One of these was rejected because of a calorimetric uncertainty. The other eleven showed signs in varying degree of violent fragmentation of the sample upon ignition. Usually violent combustion reactions occurred with both the covered-sample and ampoule techniques. Apparently this behavior depends on the nature of the compound rather than on the technique employed to contain the sample in the combustion bomb. Previous experience in this Laboratory has indicated that compounds with appreciable strain in the molecule may not react as smoothly in the combustion bomb as those with less strain.

Two conclusions may be drawn from the values of $-\Delta Ec^\circ/M$ in Table I. First, a comparison of the values obtained separately by the covered-sample and the ampoule techniques shows that either method can give reliable results. Second, a comparison of the values based on mass of hexacyclododecane with those based on mass of carbon dioxide in the products shows that determination of the amount of reaction by either means leads to results that are in accord. However, much better

(7) (a) NBS certificate for Standard Sample 39g; (b) R. S. Jessup *J. Research Natl. Bur. Standards*, **36**, 421 (1946).

(8) The uncertainty given is the standard deviation of the mean. See Chapter 14, "Experimental Thermochemistry," F. D. Rossini editor, Interscience Publishers, Inc., New York, N. Y., 1956, pp. 297–320.

(9) W. N. Hubbard, D. W. Scott and Guy Waddington, Chapter 5, "Experimental Thermochemistry," F. D. Rossini, Editor, Interscience Publishers, Inc., New York, N. Y., 1956, pp. 75–128.

TABLE I

RESULTS OF COMBUSTION EXPERIMENTS[a,b]

	a. Covered sample technique						b. Ampoule technique			
m', g.	0.27663	0.40127	0.46756	0.41210	0.64100	....[f]	0 51866	0 48061	0.53095	....[f]
$\Delta t_c = t_f - t_i - \Delta t_{corr.}$, deg.	2.00000	1.99974	1.99998	2.00395	2.00111	2.00483	1.99877	1.99843	1.99816	2.00064
ε(calor.)$(-\Delta t_c)$, cal.	7785.22	7784.21	7785.14	7800.60	7789.54	7804.02	7780.43	7779.11	7778.06	7787.71
ε(cont.)$(-\Delta t_c)$, cal.	9.66	9.62	9.58	9.62	9.55	9.59	9.55	9.57	9 55	9.60
$\Delta E_{ign.}$, cal.	1.35	1.35	1.35	1.35	1.35	1.35	1.35	1.35	1.35	1.35
$\Delta E'_{dec.}$ (HNO_3) cal.	0.60	0 63	0 81	0 23	0.26	0.31	0.38	0.25	0.26	0.28
ΔE cor. to st. states,[d] cal.	2 94	3.17	3.28	3.19	3.55	3.36	3.30	3.30	3.38	3.24
$-n''\Delta Ec°$(auxiliary oil), cal.	4947 76	3673.84	2995.58	3579.44	1227.73	2449.63	2469.60	2857.22	2342.16	3218 07
$-n'''\Delta Ec°$(fuse), cal.	15.69	14.87	15.81	15.61	15.73	15 30	15.38	15.57	15.77	15.42
$n'\Delta Ec°(C_{12}H_{14})$, cal.	2826 54	4099.97	4777.89	4210.40	6550.47	5343.66	5299.91	4910.99	5424.69	4558.95
$-\Delta Ec°/M(C_{12}H_{14})$based on m' cal. g.$^{-1}$	10217.76	10217.48	10218.78	10216 93	10219.14	.....	10218.48	10218 24	10216.95	.....
Average			10217.74					10218.20		
CO_2 from $C_{12}H_{14}$: mass, g.	.....[e]	1.33958	1.55996	1.37495	2.13960	1.74474	1.73046	1.60432	1 77137	1.48917
% theoretical	.....	100.027	99.987	99.971	100.014	.....	99.969	100 015	99.968	.....
$-\Delta Ec°/M(C_{12}H_{14})$based on CO_2 formed, cal. g.$^{-1}$	.....	10214.74	10222.05	10220.02	10217.75	10221.70	10221.68	10216.86	10220 71	10217.29
Average			10218.92					10219.22		

[a] The symbols and abbreviations used in this table are those used in ref. 6, except as noted. [b] Auxiliary data: ε(calor.) = 3892.61 cal. deg.$^{-1}$; ν(bomb) = 0.340 l.; $\Delta Ec°$(auxiliary oil) = 10,984.8 cal. g.$^{-1}$; $\Delta Ec°$(fuse) = 3923 cal. g.$^{-1}$; estimated physical properties of $C_{12}H_{14}$ at 25° ρ = 1.11 g. cc.$^{-1}$, C_p = 0.3 cal. deg.$^{-1}$ g.$^{-1}$, $(\partial E/\partial P)_T$ = −0.0024 cal. g.$^{-1}$ atm.$^{-1}$. [c] ε_i(cont.)$(t_i - 25°) + \varepsilon_f$(cont.)$(25° - t_f)$. [d] Items 81–85, incl., 87–91, incl., 93 and 94 of the computation form of ref. 5. [e] CO_2 determination uncertain. [f] m' determination in doubt.

precision is obtained if the amount of reaction is based on the mass of hexacyclododecane.

The average of all values based on mass of hexacyclododecane is 10,218.0 ± 0.29[7] cal. g.$^{-1}$; the average of all values based on mass of carbon dioxide in the products is 10,219.2 ± 0.87[8] cal. g.$^{-1}$. These average values were combined by weighting them inversely as the square of the standard deviation of the mean to give 10,218.1 ± 0.28[8] cal. g.$^{-1}$ as the accepted value. The over-all standard deviation is 0.73 cal. g.$^{-1}$, and the uncertainty interval is 1.46 cal. g.$^{-1}$. (See reference of footnote 8 for discussion of propagation and combination of errors.)

From the value −10,218.1 cal. g.$^{-1}$ for $\Delta Ec°/M$ and the molecular weight of $C_{12}H_{14}$, 158.232 g. mole^{-1},[10] the calculated value of $\Delta Ec°_{298.16}$ for equation 1 is −1616.83 kcal. mole^{-1}. The value of $\Delta Hc°_{298.16}$ for equation 1 is −1618.90 kcal. mole^{-1}. From this value of $\Delta Hc°_{298.16}$ and values of the heats of formation of carbon dioxide[11] and water,[12] the standard heat of formation, $\Delta Hf°_{298.16}$ of solid hexacyclododecane according to the reaction

$$12C(\text{graphite}) + 7H_2(g) = C_{12}H_{14}(c) \qquad (II)$$

was found to be +12.06 ± 0.27 kcal. mole^{-1}. The assigned uncertainty is the uncertainty interval.[8]

(10) 1951 International Atomic Weights, E. Wichers, *J. Am. Chem. Soc.*, **74**, 2447 (1952).

(11) E. J. Prosen, R. S. Jessup and F. D. Rossini, *J. Research Natl. Bur. Standards*, **33**, 447 (1944).

(12) D. D. Wagman J. E. Kilpatrick W. J. Taylor, K. S. Fitzer and F. D. Rossini, *ibid.*, **34**, 143 (1945).

CRYOSCOPY OF THE LiCl–KCl EUTECTIC MELT CONTAINING ALKALI HALIDES AND ALKALI TITANIUM FLUORIDES AS SOLUTES[1,2]

BY G. J. JANZ, C. SOLOMONS, H. J. GARDNER, J. GOODKIN AND C. T. BROWN

Department of Chemistry, Rensselaer Polytechnic Institute, Troy, N. Y.

Received February 21, 1958

The cryoscopic behavior of NaCl, LiF, NaF, KF, Li_2TiF_6, Na_2TiF_6, and K_2TiF_6 in the LiCl–KCl eutectic melt is reported. In the regions of dilute concentrations, the behavior of the alkali halides is in accord with complete dissociation, the deviations from thermodynamic ideality being attributed to solid solution formation, and for LiF, in addition, an activity coefficient of 2. The cryoscopy of the alkali titanium fluorides similarly is in accord with a primary dissociation to form the alkali fluoride and titanium tetrafluoride in the melt. The results are discussed in the light of the various theories and models of ionic mixtures.

Introduction

Freezing point measurements yield information about the natures and activities of the molecular and ionic species and the modes and degrees of dissociation occurring in a solute–solvent system. The present communication reports the results of cryoscopic studies in the LiCl–KCl eutectic mixture (m.p. 354°) containing as solutes NaCl, LiF, NaF, KF, Li_2TiF_6, Na_2TiF_6 and K_2TiF_6.

The theoretical principles of cryoscopy in molten salts have been the subject of a recent review,[3] it will be sufficient for the present to survey briefly

(1) Part II of a series of communications on the Constitution of Chloride Melts Containing Titanium. (Part I, see ref. 7, this paper.)

(2) This work was supported by the Office of Naval Research, Metallurgy Branch, under Contract Nonr-591(06).

(3) G. J. Janz, C. Solomons and H. J. Gardner, *Chem. Revs.*, in press (1958).

the basic principles. The approach usually used in molten salt cryoscopy is that of Hoenen,[4] who in 1913 developed a rigorous thermodynamic treatment for the effects of various types of solute species on pure salts and on various phase point mixtures, *e.g.*, eutectic mixtures, of salts. The basic conclusions from this theory are that in very dilute solutions, addition of a species as solute which is already present as a result of the dissociation of the solvent should cause no change of freezing point; and that in fully dissociated molten salts, or other fully dissociated solvents, this behavior should be observed over the entire concentration range. The freezing point depression in dilute solution is given by

$$\Delta T_f = nk_f m_2 \qquad (1)$$

where n is the number of *foreign* particles.

The thermodynamic aspect of the effects of *common* and *foreign* ions has been given a structural interpretation. Temkin,[5] investigating molten slags, showed that the basic freezing point equation 1 is obeyed if the activity of a salt M_iA_i in a mixture is given by the relation

$$a_{M_iA_i} = \frac{n_{M_i^+}}{\Sigma_i n_{M_i^+}} \times \frac{n_{A_i^-}}{\Sigma_i n_{A_i^-}} = N_{M_i^+} N_{A_i^-} \qquad (2)$$

where the *ion fractions*, $N_{M_i^+}$, $N_{A_i^-}$, are given by the ratio of the amount of a given ionic species to the total amount (gram-ions) of ions of the same sign in the system. The Temkin model, statistically interpreted, corresponds to an ionic mixture in which the anion is surrounded by cations, and *vice versa*, the anions being randomly distributed among themselves, and similarly the cations. Deviations from ideality, *i.e.*, from the Temkin model, arising from restrictions in mixing have been considered by Flood, Forland and Grjotheim.[6] For ionized systems an insight on the relative degrees of ionic and covalent bonding between nearest neighbors is possible from such structural concepts. An aim of the present investigation has been a study of the applicability of these concepts to ionic mixtures of alkali halides, with special reference to the cryoscopy of fluorides in small amounts in a chloride environment. The complex salts, M_2TiF_6, were selected to gain some insight on the dissociation processes of these salts in a chloride melt. The relatively low melting point (354°) of the LiCl–KCl eutectic mixture simplifies the experimental problems; a quantitative interpretation of the cryoscopic results was made possible by the recent determination in this Laboratory of accurate values of the heat of fusion and cryoscopic constant[7] of this solvent.

Experimental

Materials.—The alkali halides, LiCl, NaCl, KCl, LiF, NaF and KF, were Fisher reagent grade chemicals, used without further purification. The salts were dried *in vacuo* using the stepwise temperature increase with argon flush technique previously described in detail.[8] The final drying temperatures for LiCl, NaCl, KCl, LiF, NaF and KF, were 450, 420, 300, 600, 450 and 400°, respectively. The dried salts were stored in sealed ampoules until required for use. The Li_2TiF_6 was prepared[9] in this Laboratory from TiO_2, HF and Li_2CO_3. Recrystallization from dilute aqueous HF solution gave a product of 99.3% purity, by titanium and fluorine analysis. The Na_2TiF_6 and K_2TiF_6, supplied by the Kawecki Chemical Company, were used without recrystallization. Titanium analyses showed the purity of the sodium and potassium salts to be 99.5 and 99.8%, respectively. The salts were dried following the procedure for the alkali halides,[8] preliminary weight loss studies having shown the final temperatures should be 300, 350 and 465° for the lithium, sodium and potassium salts, respectively. The dried salts were stored in sealed ampoules until required for use.

The *eutectic mixture*, 58 mole % LiCl, 42 mole % KCl, was prepared from the dried salts, filtered molten, and treated with dry HCl gas in the manner described in an earlier communication in this series.[7] The melting point of the eutectic prepared in this manner was reproducible at 354.3–354.4°.

Apparatus.—An all-glass vacuum and gas transfer system constructed for work with controlled atmospheres was used in the present investigation. Details of the cryoscopic assembly are the subject of another communication[10]; it is sufficient to note that a reciprocating spiral stirrer with a magnetic solenoid control was used to ensure efficient attainment of equilibrium between the solid and liquid phases. An apparatus designed in this Laboratory[11] for automatically recording the cooling curve, and capable of measuring small temperature changes (1–5°) in the region of the melting temperature (354.3°) of the eutectic with an accuracy of ±0.02°, was used in the later measurements. A manual Rubicon precision potentiometer and a stop-watch were used for the earlier experiments. A platinum/platinum–10% rhodium thermocouple was used as a temperature sensing device. Absolute temperatures of the molten salt samples were measurable with an accuracy of ±0.3°, the limits being those of the N.B.S. calibration of the platinum/platinum–10% rhodium thermocouple used.

Procedure.—The eutectic mixture (approximately 80 g.) was weighed into the inner tube of the cryoscope in a drybox, and the cryoscope was assembled. It was evacuated and refilled twice with dry, pure argon to remove all oxygen. An atmosphere of argon was left in the cell. The eutectic was caused to melt by raising the furnace temperature slowly, and the stirrer was put into operation. By adjustment of a "Variac" autotransformer, which supplied current to the Leeds and Northrup Company "Micromax" strip-chart recorder-controller whose operation kept the molten eutectic at a temperature constant within ±2°, the furnace was allowed to cool slowly. The melt was thus caused to cool and, finally, to freeze. When the temperature of the solid and liquid mixture had remained constant for a sufficient length of time, usually not less than 5–7 minutes, the "Variac" was readjusted to allow the solid to melt again, and another cooling curve was taken. In general, two successive cooling curves obtained on a given sample did not differ by more than 0.02°.

Once reproducibility of the freezing point of the eutectic had been found for the particular sample in use, successive weighed portions of the solute to be studied were added, the procedure described above being carried out for each addition until reproducible freezing points were obtained. As the concentration of the solution increased, the "plateau" in the solvent cooling curve gave way to a slow, linear decrease of temperature during freezing. Extrapolation of the cooling curve back to the point of onset of supercooling gave a value of the freezing point of the mixture sufficiently accurate for the present work.[12] In any one melt, usually 3–5 additions were made, with repeated measurements using fresh melts. With the alkali fluorides, one addition experiments, while more laborious, were used to minimize possible errors from side reactions with the glass walls of the cryoscope.

(4) P. H. J. Hoenen, *Z. physik. Chem.*, **83**, 513 (1915).

(5) M. Temkin, *Acta phys. Chem. URSS* **20**, 411 (1945).

(6) H. Flood, T. Forland and K. Grjotheim, *Z. anorg. Chem.*, **276**, 19 (1954).

(7) C. Solomons, J. Goodkin, H. J. Gardner and G. J. Janz, *J. Phys. Chem.*, **62**, 248 (1958).

(8) H. J. Gardner, C. T. Brown and G. J. Janz, *ibid.*, **60**, 1458 (1956).

(9) G. J. Janz, C. T. Brown and M. R. Lorenz, *ibid.*, **62**, in press (1958).

(10) C. Solomons and G. J. Janz, *Rev. Sci. Inst.*, **29**, 302 (1958).

(11) C. Solomons and G. J. Janz, *Anal. Chem.*, in press (1958).

(12) A. G. Keenan, *J. Phys. Chem.*, **60**, 1356 (1956).

Results

The concentration ranges investigated and the observed freezing point depressions for the seven solutes studied are summarized in Table I and are illustrated for the region of very dilute solutions molality, ($m \leqslant 0.1$) in Fig. 1. In the latter, the dotted lines are predicted from the theory of Hoenen[4] for $n = 1, 2, 3$ and 5, respectively, using the recently determined value of 13.7 ± 0.3 deg. mole^{-1} kg. as the cryoscopic constant for the LiCl–KCl eutectic mixture. The term n is the number of ions from the dissociation of the solute which are "foreign" to those of the ionized, molten salt solvent. Inspection of Fig. 1 shows clearly that in the limit, *i.e.*, as $m \rightarrow 0$, the experimental results approach integral values of n in each case. A comparison of these values with those predicted from possible dissociations of the solute species is made in Table II.

TABLE I

CRYOSCOPIC BEHAVIOR OF SOME ALKALI HALIDES AND ALKALI TITANIUM FLUORIDES IN THE LiCl–KCl EUTECTIC MIXTURE[a]

NaCl							
m (molality)	0.019	0.047	0.059	0.087	0.196	0.401	0.489
Δt (°C.)	.18	.43	.77	.96	2.03	2.98	2.87
LiF							
m	0.014	0.021	0.029	0.055	0.058		
Δt (°C.)	.36	.48	.63	1.00	1.08		
NaF							
m	0.013	0.022	0.045	0 07	0.243		
Δt (°C.)	.33	.41	.91	1.39	4.26		
KF							
m	0.019	0 026	0.034	0.044	0.050	0.062	
Δt (°C.)	.24	.35	.46	.58	.65	.77	
Li_2TiF_6							
m	0.0067	0 022	0.047	0.067	0.117		
Δt (°C.)	.38	1.77	3.03	3.85	5.02		
Na_2TiF_6							
m	0.0033	0.010	0.019	0.055	0.062	0.1020	
Δt (°C.)	.74	.77	1.33	3.48	3.25	5.14	
K_2TiF_6							
m	0.0037	0.0081	0.031	0.066			
Δt (°C.)	.33	.30	.96	2.33			

[a] Limits of error in observations of freezing point depressions, ±0.01°.

The molten mixtures were observed visually during the addition of the solutes. On addition of NaCl, and the three alkali fluorides, the melts remained clear and completely homogeneous. Addition of the alkali titanium fluorides, in the very dilute region, gave clear homogeneous solutions, a transient yellow-orange color in the melt being observed when these salts were first added. As the concentration of the titanium salts increased ($0.05 < m < 0.1$), the formation of some bubbles in the melts was observed. At higher concentrations still, the wall of the Pyrex glass cryoscope was attacked, with the formation of a blue opaque deposit. The measurements were limited to the dilute region to minimize the effects of secondary processes that enter with increasing concentration.

The measurements with the alkali fluorides and alkali titanium fluorides in the eutectic were for the greater part restricted to one addition for each eutectic charge, although it was noted that with care, as many as 5 to 8 additions could be completed before the cryoscopic tube was crazed or cracked by the attack of the alkali fluorides on the glass.

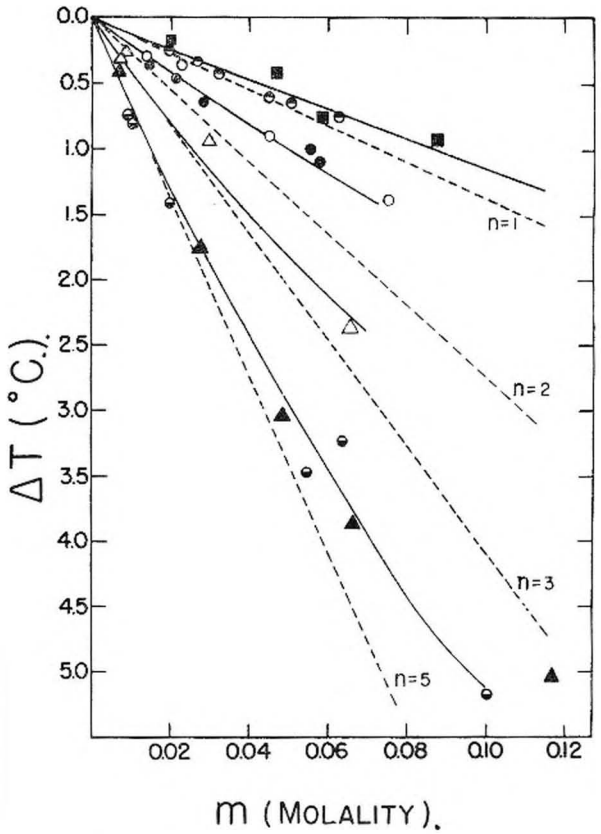

Fig. 1.—Cryoscopic behavior of some alkali halides and alkali titanium fluorides in the LiCl–KCl eutectic melt: theoretically predicted slopes, ---------; experimental results: ■, NaCl; ◉, LiF; ◓, KF; ○, NaF; ▲, Li_2TiF_6; △, K_2TiF_6; ◒, Na_2TiF_6.

TABLE II

COMPARISON OF OBSERVED CRYOSCOPIC n (FOREIGN PARTICLES) AND PREDICTED VALUES IN THE LiCl–KCl EUTECTIC MELT

Solute	Ionizations	Cryoscopic n value[a] Predicted[b]	Obsd.
NaCl	$NaCl = Na^+ + Cl^-$	1	1
LiF	$LiF = Li^+ + F^-$	1	2
NaF	$NaF = Na^+ + F^-$	2	2
KF	$KF = K^+ + F^-$	1	1
Li_2TiF_6	$Li_2TiF_6 = 2Li^+ + TiF_6^{2-}$	1	
	$TiF_6^{2-} = TiF_4 + 2F^-$	2	
	$Li_2TiF_6 = 2Li^+ + 2F^- + TiF_4$	3 (5)[c]	5
Na_2TiF_6	$Na_2TiF_6 = 2Na^+ + 2F^- + TiF_4$	5	5
K_2TiF_6	$K_2TiF_6 = 2K^+ + 2F^- + TiF_4$	3	3

[a] Limiting value as molality approaches zero. [b] From the theory of Hoenen,[4] assuming ideal systems. [c] The value in brackets is predicted if the enhanced value of n observed for LiF is applied as an empirical correction.

Discussion

Alkali Halides.—It can be seen from Fig. 1 that the freezing point depressions for KF are in close agreement with theory[4] over the entire concentration range studied, while the values for NaC

and NaF fall above the theoretically predicted slopes at finite concentrations but approach them in the limit as m approaches zero. For LiF, the observed freezing point depression is twice that predicted from the Hoenen theory assuming an ideal system and, like NaF, the values are less than the limiting value as m increases.

The deviations from the theoretically predicted slopes as m increases may be attributed in part to deviations from ideality, and in some cases in part to the formation of solid solutions, of the type M′F–M″Cl for the fluorides, where M′ is Na, K or Li, and M″ is K or Li, and M′Cl–M″Cl for the case of the chlorides, where M′ is Na in this case, and M″ is as above. The basic freezing point equation 1 may be expressed as

$$\Delta T_f = nkM(1 - \rho) \qquad (3)$$

where ρ, the coefficient of distribution of the solute *between solid and liquid*,[13] is zero in the absence of solid solution formation. Of the solutes investigated, KF is the best behaved, ρ being approximately zero over the entire concentration range investigated, *i.e.*, up to $m = 0.06$, and the properties of the mixture KF–LiCl–KCl in this concentration range accord with the thermodynamic models of Hoenen and Temkin.

From an earlier phase rule study[14] of the NaCl–LiCl–KCl ternary system, the freezing point depression at $m = 0.40$ is estimated to be 1.5°. The agreement with the present value, 2.9°, leaves much to be desired but is as good as could be expected as in phase rule studies temperatures are usually measured with an accuracy of only plus or minus several degrees. The anomalous behavior of LiF is most probably caused by the electrostatic disturbance[5,15] of the small lithium ion produced in the framework of anions. The mechanism of the disturbance is not clear. From the thermodynamic viewpoint, the cryoscopic data for LiF indicate an activity coefficient of 2 as m approaches zero.

Alkali Metal Titanium Fluorides.—Inspection of the cryoscopic behavior of the three alkali metal titanium fluorides in the LiCl–KCl eutectic, in the light of the results for the simple alkali halides, shows that they are in accord with the basic over-all process

$$M_2TiF_6 = 2M^+ + 2F^- + TiF_4$$

where M is Li, Na or K. For Li_2TiF_6 an empirical correction for the "enhanced" cryoscopic effect of LiF must be made. A quantitative analysis of a solution of 0.05 m Li_2TiF_6 in the LiCl–KCl eutectic mixture gave a titanium balance of 99%, with 1% accounted for as volatile titanium. An investigation of the stability of Li_2TiF_6 alone, under high vacuum and elevated temperatures, has been completed recently in this Laboratory.[9] At about 400°, it was found that the thermal dissociation is in accord with the over-all process

$$Li_2TiF_6 = 2LiF + TiF_4$$

The cryoscopy of K_2TiF_6 in molten NaCl has been reported by Petit and Bourlange[16] in the temperature range 800–900°. In dilute solutions the cryoscopic n value found, 5, is in accord with the observations of the present studies, *i.e.*, that the primary dissociation of the salt is

$$K_2TiF_6 = 2K^+ + 2F^- + TiF_4$$

At higher concentrations the n value increased to 8, and it was suggested that the process

$$TiF_4 + 4Cl^- = TiCl_4 + 4F^-$$

may occur in addition to the above so that the over-all reaction in the melt would be

$$K_2TiF_6 + 4NaCl = 2K^+ + 6F^- + TiCl_4 + 4Na^+$$

which is in close accord with the cryoscopic n value of 8 if the limited solubility and the volatility of $TiCl_4$ are taken into account. The secondary process proposed is in effect a solvolysis reaction. No support for this proposed solvolysis has as yet been obtained in this Laboratory; evidence has been obtained, however, that attack of the TiF_4 or other fluorides on the walls of the glass apparatus occurs, particularly if the melts are not rigorously dried, and this causes a gradual increase in the apparent cryoscopic n value. This may be the cause of the results obtained in NaCl melts.[16]

Although for convenience the constitution of the titanium-containing species in these melts has been given as TiF_4 or $TiCl_4$, it is unlikely that an un-ionized molecule could exist in a fused ionic salt.[17] Formation of the complex ion $TiF_4Cl_2^{2-}$ would not affect the interpretation of the cryoscopic data; it would also explain why TiF_4 is retained by the melt even though it sublimes at 283.9° (p = 760 mm.), 70° below the melting point of the eutectic solvent.[18,19] Observations by Hill[20] that $TiCl_4$ is much more soluble in molten NaF than in molten NaCl may be explained similarly through the formation of mixed chlorofluoro ions, *e.g.*

$$TiCl_4 + 2F^- = TiCl_4F_2^{2-}$$

The small solubility of $TiCl_4$ in NaCl may be the result of formation of a small amount of less stable $TiCl_6^{2-}$ ions.

(13) G. Petit, *Compt. rend.*, **239**, 261, 353 (1954).

(14) T. W. Richards and W. B. Meldrum, *J. Am. Chem. Soc.* **39**, 1816 (1917).

(15) E. R. Van Artsdalen and I. S. Yaffe, *J. Chem. Phys.*, **59**, 118 (1955).

(16) G. Petit and C. Bourlange, *Compt. rend.*, **237**, 457 (1953).

(17) K. Grjotheim, *Kgl. Norske Videnksab. Selskabs Skrifter*, Nr. 5, 12 (1956).

(18) W. C. Arsem. Appendix in: F. D. Rossini, P. O. Cowie, F. O. Ellison and C. O. Browne, "Properties of Titanium Compounds," Office of Naval Research Report ACR-17 (October, 1956).

(19) E. H. Hall, J. M. Blocher, Jr., and I. E. Campbell, Battelle Memorial Institute Report of May 1, 1956, to Office of Naval Research.

(20) D. L. Hill, private communication, Feb., 1958.

THE DIFFERENTIAL THERMAL ANALYSIS OF PERCHLORATES. II. THE SYSTEM $LiClO_4$–$LiNO_3$

BY MEYER M. MARKOWITZ

Foote Mineral Company, Research and Development Department, Berwyn, Penna.

Received February 24, 1958

The phase system $LiClO_4$–$LiNO_3$ was found to be of the simple eutectic type with the eutectic at about 172° and at a composition of 53.5 mole % $LiClO_4$, 46.5 mole % $LiNO_3$. In contrast with the other alkali metal perchlorates, which display but a short temperature interval between fusion and rapid decomposition, lithium perchlorate is thermally stable at and above its melting point. Like many other metal salts of oxyacids, the ease of thermal decomposition of perchlorates generally increases as the size of the cation decreases.

A review of the literature reveals that there is a paucity of phase studies of anhydrous systems involving perchlorate salts. This lack of data can be attributed to the thermal instability of most perchlorates at fusion temperatures.[1] In the course of an investigation of the thermal behavior of lithium perchlorate, it was found that this substance exhibited considerable stability at its melting point (247°) and to some temperature beyond. However, differential thermal analyses (DTA),[2] and thermogravimetric analyses,[3] show that lithium perchlorate decomposes at a lower temperature than the other alkali metal perchlorates. Nevertheless, there exists a sufficiently long temperature interval between the melting point and the onset of rapid decomposition of the salt to permit a high temperature phase study involving this compound.

Experimental Procedures

DTA curves were obtained using the arrangement of chromel–alumel thermocouples described by Gordon and Campbell.[2] The recording system consisted of a 10 millivolt span Leeds–Northrup X-Y recorder which allowed for the simultaneous plotting of sample temperature *versus* the temperature differential between the 3.0-g. sample and a similar quantity of ignited alumina, the reference material. By diverting the e.m.f. from the temperature measurement through a 1000-ohm potentiometer which acted as a voltage divider, it was possible to achieve a variable range for the instrument. Because of the small magnitude of the e.m.f.'s originating from the temperature differentials, these were amplified by a Leeds–Northrup zero-center, stabilized d.c. amplifier before passage to the recorder. All temperatures reported here have been corrected by the individual calibrations of the thermocouples used.

Inasmuch as the individual salts and their mixtures have fairly low melting points, a convenient heating arrangement was constructed of an electrically heated 500-ml. three-necked flask containing Mobiltherm 600 as the heating medium. The sample and alumina were contained in small test-tubes held in the side necks of the flask; a mechanical stirrer was inserted in the center neck. The linear heating rate of 5° per minute used in the phase studies was obtained by manual adjustment of the current to the heater.

Anhydrous lithium perchlorate was prepared by neutralization of a solution of lithium hydroxide monohydrate with aqueous perchloric acid followed by prolonged drying of the resulting solution in an oven at 250°, and then final vacuum (1–3 mm.) dehydration of the solid for 8 hours at 160°. The resultant material was analyzed by precipitation as nitron perchlorate.[4] Qualitative tests were negative for the presence of chloride by the addition of silver nitrate, and of chlorate by reduction with sulfurous acid and addition of silver nitrate. Analysis of product: ClO_4^-, 92.3 (calcd., 93.5).

Reagent grade lithium nitrate, dried under vacuum for 6 hours at 160° was analyzed by precipitation as nitron nitrate.[4] Analysis of product: NO_3^-, 87.7 (calcd., 89.9).

The Thermal Behavior of Lithium Perchlorate.—DTA curves of lithium perchlorate extending to about 275° reproducibly showed the appearance of but one endothermic break at 247°, reversible upon cooling. Visual observation confirmed the correspondence of this temperature to fusion of the salt. On occasion a small, reversible endothermic break was evident at about 146°. However, by allowing a continuous stream of dry nitrogen to play on the sample during the DTA run, the 146° break disappeared. X-Ray powder patterns of the salt at 170° in a helium atmosphere showed that no change in structure over that prevailing at room temperature was occasioned past 146°. Apparently then the 146° break must be attributed to the presence of a small amount of lithium perchlorate monohydrate which is known to undergo the transition $LiClO_4 \cdot H_2O \rightleftharpoons LiClO_4 + H_2O$ at 146°[5] in the binary system $LiClO_4$–H_2O. The X-ray patterns and DTA curves of the water-free salt failed to reveal any crystallographic change in lithium perchlorate. This verifies the early microscopic and thermometric work of Vorlaender and Kaascht.[6] Such transitions are, however, characteristic of the other alkali metal perchlorates.[1] This behavior tends to show a similarity of lithium perchlorate to the non-polymorphic, anhydrous alkaline earth perchlorates.

The melting point of 247° found for lithium perchlorate in the present study agrees well with that of 247.7° as reported by Gluyas.[7] The oft-quoted value of 236° probably stems from determinations made with water-contaminated samples.[8]

Maintaining fused lithium perchlorate at 275° for three days gave no indications of decomposition through the absence of chloride and chlorate. This is consistent with the results of Richards and co-workers[9,10] who prepared the compound in a state of high purity by dehydrating the trihydrate during prolonged heating at 300° in a dry air current.

By carrying the DTA of lithium perchlorate to about 725° in a high temperature furnace, the phenomenon of reaction product crystallization in the DTA of inorganic perchlorates[1] was demonstrated. At a heating rate of 15° per minute, the rate of decomposition became appreciable at about 502°. The aspect of the DTA curve was akin to the upper portion of the curve obtained for lithium perchlorate trihydrate by previous workers[2] except that an additional, endothermic break appeared at about 610°. This corresponds closely to the melting point of lithium chloride (614°). No other breaks were observed by cooling and reheating of the final product of the DTA run.

The only heat effect found during the DTA of lithium nitrate carried out to about 275° was that associated with fusion at 257°.

(1) M. M. Markowitz, THIS JOURNAL, **61**, 505 (1957).

(2) S. Gordon and C. Campbell, *Anal. Chem.*, **27**, 1102 (1955).

(3) G. G. Marvin and L. B. Woolaver, *Ind. Eng. Chem., Anal. Ed.*, **17**, 474 (1945).

(4) F. P. Treadwell and W. T. Hall, "Analytical Chemistry," Vol. II, John Wiley and Sons, Inc., New York, N. Y., Ninth English Edition, 1942, pp. 383 384.

(5) J. P. Simmons and C. D. L. Ropp, *J. Am. Chem. Soc.*, **50**, 1650 (1928).

(6) D. Vorlaender and E. Kaascht, *Ber.*, **56**, 1157 (1923).

(7) R. E. Gluyas, Ph.D., Thesis, Ohio State Univ., 1952.

(8) A. Potilitzen, *Chem. Centr.* **61**, I, 72 (1890); *J. Russ. Phys. Chem. Soc.*, **19**, 339 (1887); **20**, 541 (1888).

(9) T. W. Richards and H. H. Willard, *J. Am. Chem. Soc.*, **32**, 4 (1910).

(10) T. W. Richards and M. W. Cox, *ibid.*, **36**, 819 (1914).

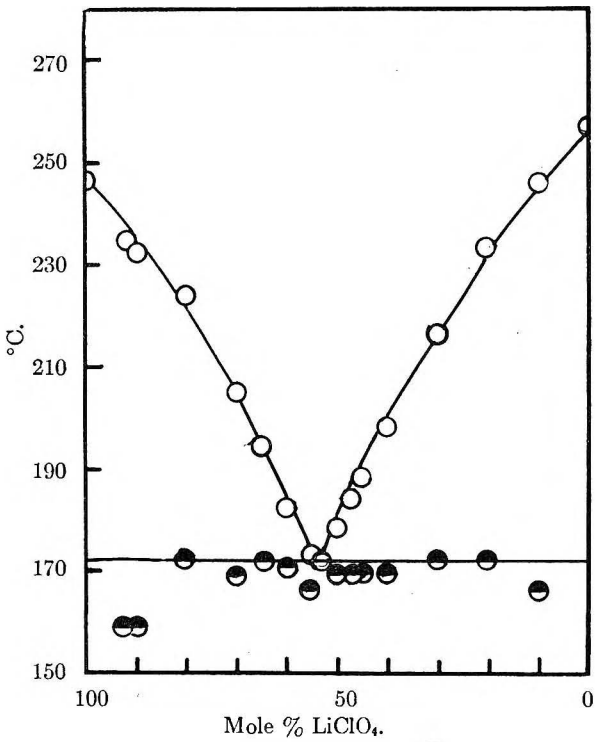

Fig. 1.—The system $LiClO_4$–$LiNO_3$.

The System $LiClO_4$–$LiNO_3$.—The salt mixtures indicated in Table I were subjected repeatedly to DTA with passage of nitrogen gas to minimize any effects due to water absorption By this means the eutectic data and part of the liquidus data of Table I were obtained. For samples numbered 6 through 12, the liquidus temperatures were determined by direct visual observation of the appearance and disappearance of the last traces of solid in the melt.[11] This was necessitated by the inadequate endothermal indications of the liquidus temperature on the DTA curves for samples so close to the eutectic composition. The complete data are incorporated in Fig. 1 from which it is seen that the system is of the simple eutectic type with the eutectic at about 172° and at a composition of 53.5 mole % $LiClO_4$, 46.5 mole % $LiNO_3$. None of the samples gave evidence of decomposition of the perchlorate as shown by the absence of chloride and chlorate in the melts upon analysis.

TABLE I

THE SYSTEM $LiClO_4$–$LiNO_3$

Sample no.	Mole % $LiClO_4$	Mole % $LiNO_3$	Eutectic, cor., °C.	Liquidus, cor., °C.
1	100.0	0.0	..	247
2	91.5	8.5	158	234
3	90.0	10.0	158	232
4	80.0	20.0	172	224
5	70.0	30.0	168	205
6	65.0	35.0	171	194
7	60.0	40.0	170	182
8	55.0	45.0	166	173
9	53.5	46.5	172	Eutectic
10	50.0	50.0	170	178
11	47.5	52.5	171	184
12	45.0	55.0	171	188
13	40.0	60.0	170	197
14	30.0	70.0	172	216
15	20.0	80.0	172	233
16	10.0	90.0	166	246
17	0.0	100.0	..	257

(11) S. T. Bowden, "The Phase Rule and Phase Reactions," The Macmillan Co., London, 1954, pp. 208–211.

Discussion

On the basis of thermogravimetric studies,[3] the temperatures at which the perchlorates of lithium, sodium, and potassium start to undergo appreciable weight losses are about 420, 480 and 500°, respectively. From the present DTA study on anhydrous lithium perchlorate, the temperature interval between salt fusion and the onset of rapid decomposition is from 247 to about 502° or approximately 255°. Similar data[2] for the other anhydrous alkali metal perchlorates are given in Table II for purposes of comparison. The decomposition reactions correspond to the conversion of the alkali metal perchlorate to the chloride plus gaseous oxygen as indicated by an endothermic break on each of the DTA curves.

TABLE II

TEMPERATURE INTERVALS BETWEEN FUSION AND ONSET OF RAPID DECOMPOSITION FOR THE ANHYDROUS ALKALI METAL PERCHLORATES

Compound	Fusion, °C.	Temp. of appreciable reaction rate, °C.	ΔT, °C.
$LiClO_4$	247	502	255
$NaClO_4$	482	571	89
$KClO_4$	588	608	20
$RbClO_4$	612	625	13
$CsClO_4$	589	620	31

A number of points are clearly illustrated by the values given in Table II. Lithium perchlorate has the longest temperature interval between fusion and onset of rapid decomposition; accordingly, it has a true melting point. The other perchlorates cannot possess fixed points of fusion because of the corresponding short temperature intervals. For each perchlorate salt, under comparable experimental conditions, the DTA technique measures the temperature at which the rate of the decomposition reaction becomes appreciable; slow decomposition may, of course, ensue at lower temperatures as indicated by the thermogravimetric studies.[3]

The values of the decomposition temperatures as determined by DTA increase as the radius of the cation of the alkali metal perchlorate. This is an effect that has been noted previously for the alkali metal hydrogen phosphates by similar methods,[12] for various salts of oxy acids containing oxygen bridges such as pyrosulfates[13] and dichromates[14] by equilibrium measurements, and for the alkaline earth carbonates[15] and alkali metal nitrates[16] by vapor pressure measurements. The decrease in thermal stability with decrease in cation size must be related to the increasing polarizing power of the cation and to the increasing crystal energy of the decomposition products with decreasing cation size.[15]

Acknowledgment.—Thanks are extended for the encouragement given the performance of this work

(12) R. K. Osterheld and M. M. Markowitz, THIS JOURNAL, **60**, 863 (1956).

(13) H. Flood and T. Foerland, *Acta Chem. Scand.*, **1**, 781 (1947).

(14) H. Flood and A. Muan, *ibid.*, **4**, 364 (1950).

(15) W. E. Van Arkel, "Molecules and Crystals in Inorganic Chemistry," Interscience Publishers, Inc., New York, N. Y., First English Edition, 1949. p. 118.

(16) M. Centnerszwer, *J. chim. phys.*, **27**, 9 (1930).

by Dr. R. G. Verdieck, Manager of Chemicals Research, Research and Development Department, and by Dr. E. M. Kipp, Director of Research, Foote Mineral Company. Appreciation is also expressed for the cooperation of Dr. Earl Feingold, Atlantic Refining Company, for the X-ray powder patterns of lithium perchlorate under anhydrous conditions.

THE STRUCTURE OF GAS-ADSORBENT CARBONS

BY W. F. WOLFF

Research Department, Standard Oil Company (Indiana), Whiting, Indiana

Received February 26, 1958

Irregularly shaped and layer-type pore structures have both been proposed for gas-adsorbent carbons. In an attempt to distinguish between these structures, the penetration by liquids with different molecular shapes into the pore systems of these carbons has been studied. Conventional nitrogen-adsorption and analytical methods have been applied to the calculation of structural dimensions. The evidence favors a layer-type structure, with a micropore system consisting of molecular-size fissures between relatively large graphitic planes.

Introduction

Despite a long-standing interest in the properties and uses of active carbons,[1] their structure or structures remain obscure.[2] Recent studies in this Laboratory have been directed toward establishing the structure of active carbons used for gas and vapor adsorption. These gas-adsorbent carbons are commonly prepared by the high-temperature steam activation of such dense carbonaceous solids as charred nutshells. In common with other active carbons, they give X-ray patterns indicating graphite-like regions.[3-5] Their adsorption characteristics appear to be associated with a system of remarkably small and uniform pores.[6]

The X-ray evidence is generally interpreted in terms of a structure with irregularly shaped pores, and a surface formed by the exteriors of small imperfect stacks of graphitic planes. Such "crystallites" are presumed to be interconnected by regions having a disordered cross-linked structure.[2,3]

Adsorption studies, on the other hand, suggest a layer-type structure. According to this view, the pore structure is formed by fissures between graphitic planes, and the surface is provided by the graphitic walls of these pores.[7,8]

In an attempt to distinguish between these structures, the molecular-sieve properties of two gas-adsorbent carbons have been investigated. The penetrations of various liquids into the pore structures of the carbons were measured by a nitrogen-desorption technique. By using liquids with suitable molecular shapes it was hoped to observe differences in penetration caused by the shape of the pores. To further define the structure, average pore dimensions, graphitic plane sizes and the amounts of non-carbon constituents were also determined for several such carbons.

Experimental

Commercial active carbons were used without purification. The coconut charcoal was an 8- to 14-mesh product supplied by E. H. Sargent and Company. The coal-based carbon was a 20- to 50-mesh product from Pittsburgh Coke and Chemical Company. A 12- to 20-mesh active carbon from the Burrell Corporation, and other carbons designated either by type or source, also were used.

Liquids employed in the molecular-sieve studies included 2,2,4-trimethylpentane of 99+% purity from Phillips Petroleum Company, titanium tetrachloride of 99.5+% purity from Matheson, Coleman and Bell Company, *n*-dodecane from Humphrey-Wilkinson, and technical α-methylnaphthalene from the Eastman Kodak Company. These liquids were used without further purification. 96% α-Methylnaphthalene, from Reilly Tar and Chemical Corporation, was acid-treated, percolated and distilled to give a product with a cryoscopic purity of 97+%; the principal impurity, as determined from the infrared spectrum, was the β-isomer. Reagent grade carbon tetrachloride from Mallinckrodt Chemical Works was percolated through silica gel.

The liquids were used as nitrogen desorbents in studying the molecular-sieve properties of gas-adsorbent carbons. Fourteen grams of active carbon was weighed to 0.1 g. and heated to 320°, with stirring, under a stream of high-purity dry nitrogen. The dried carbon was cooled, under nitrogen, to room temperature. Twenty-five ml. of the desorbent liquid was then added to the carbon, and the volume of gas evolved during the first 18 hours was measured by water displacement. The volume was corrected for the hydrostatic head and the vapor pressures of water and the desorbent.

Surface areas and micropore volumes of the active carbons were determined by conventional Brunauer-Emmett-Teller (B.E.T.) nitrogen-adsorption techniques.[9] Micropore determinations were made at a relative pressure sufficient to obtain capillary condensation in all pores less than 600 Å. in diameter. The surface tensions of α-methylnaphthalene, *n*-dodecane and titanium tetrachloride were obtained by capillary rise. The surface tension of titanium tetrachloride was measured under a carbon dioxide atmosphere.

Carbon, hydrogen, sulfur and ash were determined by the classical procedures. Oxygen determinations were obtained by a modified Schütze method.[10] A spectroscopic procedure[11] was used to determine metal contents.

Active carbons impregnated with sodium silicate and with silica were used to study the effect of ash on measured oxygen content. Sodium silicate on active carbon was

(1) J. W. Hassler, "Active Carbon," Chemical Publishing Company, Brooklyn, N. Y., 1951, pp. 4–9.
(2) J. J. Kipling, *Quart. Revs.*, **10**, 1 (1956).
(3) J. C. Arnell and W. M. Barss, *Can. J. Research*, **26A**, 236 (1948).
(4) H. Richter, G. Breitling and F. Herre, *Z. angew. Phys.*, **8**, 433 (1956).
(5) H. L. Riley, *Quart. Revs.*, **1**, 59 (1947).
(6) S. Brunauer, "The Adsorption of Gases and Vapors. Vol. I. Physical Adsorption," Princeton Univ. Press, Princeton, N. J., 1943, pp. 159, 166, 345.
(7) P. H. Emmett, *Chem. Revs.*, **43**, 69 (1948).
(8) Reference 6, pp. 176, 207, 357.
(9) Reference 6, pp. 285–299.
(10) I. J. Oita and H. S. Conway, *Anal. Chem.*, **26**, 600 (1954).
(11) A. J. Frisque, *Anal. Chem.*, **29**, 1277 (1957).

prepared by wetting the Burrell carbon with a dilute sodium silicate solution. The product was heated to 390° under nitrogen, cooled and ground to pass a 60-mesh screen. To prepare silica on active carbon, the carbon was wetted with dilute sodium silicate solution, then treated with gaseous HCl until no more heat was evolved. The product was water-washed, dried overnight on a suction filter and ground to pass a 60-mesh screen.

Structure Type. -Five liquids with differing molecular sizes and shapes were used in testing the coconut charcoal and the coal-based carbon for molecular-sieve properties. The nitrogen-desorption technique used was expected to be particularly sensitive to molecular-sieve effects, because at room temperature the nitrogen would presumably be concentrated in the narrowest pores.

The volumes of nitrogen desorbed by the various liquids are listed in Table I, together with the surface tensions and molecular cross-sectional areas[7] of the desorbents. Density measurements have shown that the penetration of a liquid into the micropore structure of an active carbon is largely determined by the surface tension of the liquid,[12] penetration being favored by low surface tension. Vapor adsorption techniques indicate that molecular size also affects the degree of penetration.[7]

TABLE I

NITROGEN DESORPTION FROM GAS-ADSORBENT CARBONS

	Vol. gas desorbed, cc.	Surface tension of desorbent, dynes/cm.	Molecular area of desorbent, Å.²
Coconut charcoal			
n-Dodecane	118	26	57
α-Methylnaphthalene (Technical)	113	40	42
α-Methylnaphthalene (Purified)	110	40	42
2,2,4-Trimethylpentane	106	19	46
Titanium tetrachloride	77	30	35
Coal-based Carbon			
n-Dodecane	82	26	57
Carbon tetrachloride	73	27	32

Although the effectiveness of the desorbents can be explained partially in terms of their surface tensions and molecular areas, certain of the data can be explained by neither factor. Thus, *n*-dodecane desorbs more nitrogen than does 2,2,4-trimethylpentane, even though the dodecane has both a higher surface tension and a greater molecular area. A similar and even more striking example of this type of behavior is given by α-methylnaphthalene and titanium tetrachloride; the liquid with the higher surface tension and molecular area, α-methylnaphthalene, desorbs about 45% more nitrogen than does the titanium tetrachloride.

A third factor, the molecular shape, appears to be involved in determining the degree to which a liquid can penetrate the micropore structure of a gas-adsorbent carbon. The liquids with linear or planar molecular shapes—*n*-dodecane and α-methylnaphthalene –desorbed the most gas. The remaining liquids, with bulky, roughly spherical molecular shapes, apparently were less efficient in penetrating the micropore structures of the carbons. This molecular-sieve action is consistent with the picture that gas-adsorbent carbons have a layer-type structure, with a pore system made up of narrow fissures between graphitic planes, and is not readily explainable in terms of a structure containing irregularly shaped pores. A molecular-sieve effect of this type has been postulated to account for the adsorption characteristics of a Saran charcoal.[13]

The anomalously low apparent densities of gas-adsorbent carbons in carbon tetrachloride[12] can be explained similarly. The interpretation of these results as being a molecular-sieve effect was discounted on the basis that no correlation was observed between average pore diameters and the degree of carbon tetrachloride penetration. However, the significance of the diameter values is open to question, as they were calculated from the total pore volume by the conventional relationship between pore volume and surface area.[14]

Pore Dimensions. -The assignment of dimensions to the pores in active carbon is an arbitrary process, because of the uncertainty as to pore shape.[2] If, however, a layer-type structure is accepted for gas-adsorbent carbons, conventional methods, such as those based on surface–area and pore–volume determinations,[7,14] can be used to obtain average pore widths and pore–width distributions.

If meaningful results are to be obtained from relationships between pore volume and surface area, caution must be used in the choice of both the volume and the area values. Gas-adsorbent carbons generally contain a mixture of very large and extremely small pores, but few of intermediate size. Although the macropores provide much of the total pore volume, almost all of the surface area is in the micropores.[15] Thus, average micropore widths calculated from the micropore volume and either the micropore area or the total surface area have significance. On the other hand, average pore widths calculated from the total pore volume and surface area tell little about the structure.

The interpretation of surface-area measurements for solids containing very small pores is still debatable.[16] Aside from the soundness of the B.E.T. method, the size of the molecule used in determining the area introduces an uncertainty. For example, to measure surface areas with nitrogen by the B.E.T. method, a definite area is assigned to each nitrogen molecule. In pores having such a width that only one nitrogen molecule can fit between the opposing walls, the area assigned to the molecule is only half of that actually covered by the nitrogen, and the calculated width of the pore is double the true value. Thus, if no distinction can be made between molecules adsorbed in pores of these dimensions and those adsorbed on less-confined surfaces, calculation from pore volume and surface area can

(12) R. M. Guest, R. McIntosh and A. P. Stuart, *Can. J. Research*, **24B**, 124 (1946).

(13) J. R. Dacey and D. G. Thomas, *Trans. Faraday Soc.*, **50**, 740 (1954).

(14) M. N. Fineman, R. M. Guest and R. McIntosh, *Can. J. Research*, **24B**, 109 (1946).

(15) M. M. Dubinin, *Quart. Revs.*, **9**, 101 (1955).

(16) P. H. Emmett, "Catalysis," Vol. I, Reinhold Publ. Corp., New York, N. Y., 1954, pp. 40–42, 50, 51.

only give a range of values for the average pore width.

For a system of pores made up of fissures, the average pore width is given by the geometrical relationship[7]

$$W = \frac{2V}{A}$$

where W is the width, V is the pore volume and A is the surface area of the pores. To allow for the uncertainty in the surface-area technique, the equation might be modified to

$$W = \frac{nV}{A}$$

where n lies between 1 and 2. The most probable pore width will lie within the range of values given by this relationship.

The relationship has been used to determine average micropore widths of five commercial gas-adsorbent carbons. As shown in Table II, the average widths lie between 4 and 10 Å. The data are consistent with gas-adsorbent carbons having pores narrow enough to exclude such bulky molecules as carbon tetrachloride.

TABLE II

MICROPORE WIDTHS OF GAS-ADSORBENT CARBONS

Carbon	Surface area, m.²/g.	Av. micropore width, Å.
Pittsburgh	850	7.1 ± 2.4
Sargent	1040	6.3 ± 2.1
Fisher	1090	7.4 ± 2.5
Burrell	1140	7.7 ± 2.6
Columbia	1460	7.0 ± 2.4

From the surface area and pore volume data a rough measure of size distribution in the micropores can be obtained. Unlike most porous solids, gas-adsorbent carbons tend to take up only about a monomolecular layer of adsorbate, with little formation of bimolecular or deeper layers. This behavior has been explained in terms of micropores not more than one or two molecular diameters in thickness.[17] If the fraction of the micropore volume occupied by a complete monomolecular layer of nitrogen is F_m, then

$$F_m = \frac{A}{V} \times 3.53 \times 10^{-4}$$

where A is the specific surface area in m.²/g. and V is the micropore volume in cc./g. The relation is based on the approximation that the surface area of the micropores and the total surface area are identical. The constant is simply the volume of liquid nitrogen required to cover a square meter of surface with a monomolecular film.

The equation provides a simple, though rough, determination of pore-size distribution in the micropores. Because pores less than three molecular diameters in width will hold only monomolecular layers of nitrogen, the value of F_m will be, to some extent, a measure of the fraction of micropores in this size range.

F_m values determined for five commercial gas-adsorbent carbons, sugar charcoal and wood charcoal are given in Table III with similar values calculated from literature data for fourteen other carbons. At least half of the pores in the micropore systems of these active carbons are no more than about two molecular diameters in width. Most of the values calculated from literature data are somewhat higher than those determined in this study, where some intermediate-pore volumes were included in the micropore volumes.

TABLE III

MONOMOLECULAR ADSORPTION IN ACTIVE CARBONS

Carbon	Surface area, m.²/g.	Monolayer fraction of micropore vol., F_m
Pittsburgh	840	0.75
Sargent	1040	.84
Fisher	1090	.72
Burrell	1140	.64
Columbia	1460	.75
Sugar charcoal	310	.66
Wood charcoal	750	.46
Darco[18]	560	.97
Columbia[18]	1400	1.08
Coconut charcoal[14]	640	0.87
Coconut charcoal[14]	750	1.02
Coconut charcoal[14]	900	0.90
Coconut charcoal[14]	1070	.90
Coconut charcoal[14]	1140	.80
$ZnCl_2$-activated wood charcoal[14]	1840	.64
Coal-based carbon[19]	160	.83
Coal-based carbon[19]	400	.79
Coal-based carbon[19]	590	.93
Coal-based carbon[19]	750	.94
Coal-based carbon[19]	1060	.87
Coal-based carbon[19]	1110	.76

Plane Sizes. To estimate plane sizes in the gas-adsorbent carbons, a method based on the determination of carbon and hydrogen contents was used. In a series of regularly shaped aromatic compounds, there is a regular increase in the carbon:hydrogen ratio as the number of aromatic nuclei increase. Thus, for a series of hexagonally developed aromatics (*i.e.*, benzene, coronene, dodecabenzcoronene, etc.) the plane diameter, in ångströms, is given by

$$D = 0.41(C/H) - 2.5$$

where (C/H) is the weight ratio of carbon to hydrogen. If graphitic planes are assumed to be hydrogen-terminated aromatics, this relationship can be used to estimate plane sizes in active carbons. A similar procedure has been used in studying the constitution of coal.[20]

Carbon:hydrogen ratios and calculated plane sizes for five gas-adsorbent carbons are given in Table IV. The ratios for the first three coconut-based carbons are uniform and correspond to average plane diameters of 35 to 40 Å. The remaining two, however, have about half this diameter. These are probably minimum values, because irregularly shaped aromatic molecules and the presence of any

(17) S. Brunauer, P. H. Emmett and E. Teller, *J. Am. Chem. Soc.*, **60**, 309 (1938).

(18) L. C. Drake and H. L. Ritter, *Ind. Eng. Chem., Anal. Ed.*, **17**, 787 (1945).

(19) E. O. Wiig and S. B. Smith, THIS JOURNAL, **55**, 27 (1951).

(20) D. W. VanKrevelen and H. A. G. Chermin, *Fuel*, **33**, 79 (1954).

non-aromatic hydrogen are not accounted for by the above equation. Termination by hydrogen-free oxide groups, however, will tend to have a compensating effect.

TABLE IV

AVERAGE PLANE SIZES IN GAS-ADSORBENT CARBONS

Carbon	Carbon: hydrogen ratio	Av. plane diameter, Å.
Sargent A	105:1	41
Sargent B	100:1	39
Sargent C	89:1	34
Burrell	56:1	20
Pittsburgh	48:1	17

The evidence that gas-adsorbent carbons have plane diameters of 20–40 Å., or more, is in reasonable accord with estimates based on X-ray data, which have been interpreted in terms of average crystallite diameters ranging from 20 to 50 Å.[3,5] This general agreement supports the validity of calculations based on carbon and hydrogen content and the underlying assumption that the edges of the graphitic planes are predominantly terminated by hydrogen. On the other hand, much of the work dealing with the mechanism of carbonization has been interpreted in terms of a structure containing little or no hydrogen at the plane edges.[21,22] Results of paramagnetic-resonance studies of carbons[23] can be interpreted in terms of an intermediate structure that is largely saturated but contains a small percentage of non-functionally terminated edge atoms.

Non-carbon Constituents.—Non-carbon constituents—hydrogen, oxygen and mineral matter—are found in all active carbons, presumably bound to the edge atoms of the graphitic planes.[2] To obtain an estimate of the relative importance of these constituents in determining the structures of gas-adsorbent carbons, four commercial carbons were analyzed. The analyses are given in Table V.

On a weight basis, the most important non-carbon constituent is the mineral matter. However, because it can be leached out under relatively mild conditions,[2] it seems to have little effect on the structure of the carbon.

The weight concentration of oxygen is somewhat greater than that of hydrogen in most cases. On a molar basis, however, the amounts of oxygen range from only one-nineteenth to one-eighth of the amount of hydrogen. Oxygen-containing terminating groups and several oxide structures[2] have been postulated as important constituents of certain carbons; they evidently play a lesser but significant role in conventional gas-adsorbent carbons.

The oxygen values may be somewhat high, because of partial reduction of the mineral matter during the determination. To measure the probable magnitude of this effect, direct oxygen determinations were obtained for a carbon before and after impregnation with typical ash constituents, silica and sodium silicate. The data, given in Table VI, indicate that a partial reduction of the mineral matter does take place, but oxidation of the carbon during the impregnation step is not completely precluded.

TABLE V

ANALYSES OF GAS-ADSORBENT CARBONS

(Weight %)

	Sargent A	Sargent C	Burrell	Pittsburgh
Carbon	95.2	94.7	94.4	77.8
Hydrogen	0.91	1.07	1.70	1.62
Oxygen	.94	2.12	1.46	2.25
Sulfur	.09	...	...	...
Ash, total, as oxides	3.9	2.4	3.8	18.44
Aluminum	0.13	...	...	...
Calcium	.77	...	...	...
Iron	.07	...	...	...
Magnesium	.27	...	...	...
Manganese	.01	...	...	...
Potassium	.29	...	...	...
Silicon	1.2	...	...	...
Sodium	0.26	...	...	...

TABLE VI

EFFECT OF ASH ON OXYGEN DETERMINATION

(Weight %)

	Ash	Oxygen
Active carbon	7.0	1.68
Silica-on-active carbon	9.6	1.88
Sodium silicate-on-active carbon	12.0	2.02

Discussion

Integration of the results of the present study with the results and views developed by earlier workers suggests a structure for gas-adsorbent carbons. They appear to be formed of large particles, or regions, which are made up of stacks of graphitic planes or groups of such stacks. The graphitic planes generally have average diameters greater than 40 Å. and are almost entirely terminated by functional groups—principally hydrogen. The macropores of gas-adsorbent carbons may be considered either as interstices between graphitic particles or channels through graphitic regions. On the other hand, the micropores are fissures within the graphitic regions and are bounded by essentially parallel graphitic planes. The micropores provide almost all of the surface area of the carbon; most of them are less than 10 Å. in width.

This structure provides a satisfactory basis for explaining the adsorption characteristics of gas-adsorbent carbons. Indeed, most of the structural details have been developed from studies of adsorption phenomena. However, the consistency of this structure with the results of X-ray studies must be considered.

With the assumed layer-type structure, both surface-area and X-ray data for typical active carbons give reasonably consistent values, about 10 Å., for the average thickness of the graphitic walls that bound the micropores.[7] On the other hand, a pos-

(21) H. L. Riley, *Chemistry & Industry*, **58**, 391 (1939).

(22) H. T. Pinnick, "Proceedings of the First and Second Conferences on Carbon," The Waverly Press, Baltimore, Md., 1956, pp. 3–6.

(23) D. J. E. Ingram, "Investigations on the Trapping of Free Electrons in Carbon," presented at the Conference on Industrial Carbon and Graphite, London, September, 1957; R. C. Pastor, J. A. Weil, T. H. Brown, and J. Turkevich, "Proceedings of the International Congress on Catalysis, Philadelphia, Pa., 1956," Academic Press Inc., New York, N. Y., 1957, pp. 107–13.

sible inconsistency is shown by the results obtained on prolonged steam activation of a commercial gas-adsorbent carbon.[3] During activation, the X-ray-determined average crystallite size remained essentially constant, while the B.E.T. surface area doubled. According to the proposed structure, a change in surface area of this magnitude should incur a large increase in the number, depth or width of the fissures in the graphitic sections. Correspondingly, the distance between fissures and thus the heights of the crystallites would be markedly reduced. Yet, only a minor reduction in average crystallite height was observed.

The discrepancy could be caused by difficulties in interpreting the X-ray data. X-Ray patterns given by active carbons show broad peaks, characteristic of amorphous solids, that may be caused by the presence of small, highly ordered crystallites within the less-ordered solid. The sizes of the crystallites are calculated from the amount of broadening.

The broadening need not, however, be caused by regions with the degree of order usually assumed in calculating crystallite heights. Relatively large bundles of graphitic planes also could cause it if they were in a sufficiently disordered or strained state.[24] This requirement appears to be satisfied by the stacks of planes that form the basic units in the proposed structure. The disorder in such stacks presumably would include variations in interplanar distances and deviations of the planes from parallelity.

Probable sources of disorder include the fissures that make up the micropore system, the mineral matter, cross-linking between planes, and the functional groups terminating the graphitic planes. Planes terminated only by hydrogen can be stacked with an interplanar distance of the order observed in graphite.[25] However, most functional groups will tend to increase the thickness of the plane at its edge. Thus, the interplanar spacing would be expected to differ with the number and type of functional groups, and perhaps with the sizes of the planes. These considerations are consistent with the X-ray evidence that active carbons generally have interplanar distances greater than that of graphite.[26]

(24) B. E. Warren, *J. Chem. Phys.*, **2**, 551 (1934).

Conclusion

The proposed structure for gas-adsorbent carbons seems to be in reasonable agreement with data obtained by adsorption, X-ray and other techniques. The same structural considerations presumably apply, in different degrees, to other forms of graphitic carbon.

Additional work is required to further test the proposed structure. Critical attention should be given to the premises that the graphitic planes are terminated by functional groups, and that the X-ray patterns of the carbons measure a degree of disorder more than size.

Acknowledgment.—The author wishes to thank G. S. John for helpful discussions and R. F. Waters for determining the surface areas and micropore volumes.

(25) J. M. Robertson and J. G. White, *J. Chem. Soc.*, 607 (1945).
(26) W. R. Ruston, *Fuel*, **32**, 52 (1953).

THE WATER WETTABILITY OF METAL SURFACES[1]

BY DONALD J. TREVOY AND HOLLISTER JOHNSON, JR.

Communication No. 1946 from the Kodak Research Laboratories, Eastman Kodak Company, Rochester, N. Y.

Received February 27, 1958

Low contact angles with water may be obtained on the surfaces of chemically reactive metals by a process involving chemical cleaning with powerful oxidizing acids, followed by electropolishing to restore smoothness to the etched specimens. By using highly refined handling techniques, contact angles in the range, 0–11°, were obtained on aluminum, brass, copper, magnesium, nickel, stainless steel and zinc. The low contact angles are considered a good indication that organic contamination was virtually absent from the electropolished surfaces. The possibility of spurious inorganic contamination, apart from the normal oxide film, also was considered, and, in the case of copper electropolished in phosphoric acid, the residual phosphate on the surface was estimated by coulometric reduction and shown to be much less than a monolayer. The preparatory technique used in this study is applicable to a wide variety of metals and alloys and serves to demonstrate experimentally the inherent water wettability of clean metal surfaces. It also provides a means of preparing clean, smooth substrates on which fatty acids or other compounds may be deposited and their behavior observed in determining wettability and adhesion. Mechanical polishing, followed by exhaustive rinsing with hot or cold redistilled organic solvents, was not effective in producing low contact angles on metal surfaces.

Introduction

The idea has been expressed by Adam,[2] and shared intuitively by many others, that all clean, smooth metal surfaces should be well wet by water and should, therefore, exhibit zero contact angles. With few exceptions, the quest for such surfaces in the laboratory, however, has not been a rewarding one. In the case of platinum, it is well known that flaming or drastic chemical cleaning may produce excellent water wettability, but these techniques are not applicable to the more reactive metals and alloys. Intensive effort over a period of several decades by Bartell and co-workers to produce "clean" metal surfaces was culminated in 1953[3] by the preparation of evaporated films of silver and gold which showed initial advancing contact angles in the range 0-10°. In 1955, Zisman and co-

(1) Presented at the 131st Meeting of the American Chemical Society, Miami, Fla., April 7–12, 1957.

(2) N. K. Adam, "The Physics and Chemistry of Surfaces," Oxford University Press, New York, N. Y., 1941, p. 186.

(3) F. E. Bartell and J. T. Smith, THIS JOURNAL, **57**, 165 (1953).

workers reported contact angles of 4° on steel and stainless steel prepared by mechanical abrasion,[4] but few wettability data have been published by the Zisman group on metal surfaces other than platinum. This exclusion of the more reactive metals from wettability experimentation is probably the direct result of difficulty in producing smooth, clean surfaces having reproducible properties.

The aims of the present work are therefore two-fold: first, to establish experimentally the hydrophilic nature of metal surfaces in general and, second, to provide a convenient means of producing smooth, clean specimens for subsequent adsorption of fatty acid or other adsorbate and further wettability study. The clean surface then becomes only a stepping-stone to the contaminated surface for which both the nature and the amount of contamination are known.

For purposes of this presentation, a clean metal surface is defined as one which is essentially free of non-gaseous organic contamination or spurious inorganic contamination. No attempt has been made to eliminate either the normal oxide film, which is almost invariably present on a metal surface in air, or adsorbed gases, such as nitrogen, oxygen, water and carbon dioxide.

Preparation of specimens by abrasion plus solvent rinsing did not prove satisfactory, and was replaced by drastic chemical cleaning, followed by electropolishing to restore smoothness. If properly carried out, this technique has the unique advantage of producing a surface which is not only free of organic matter, but is also extremely smooth, thereby avoiding the complication of roughness in measuring and interpreting contact angles. In the present paper, preparatory techniques and contact angles with water are reported for seven metals or alloys; aluminum, brass, copper, magnesium, nickel, stainless steel and zinc.

Experimental

Measurement of Contact Angles.— Contact angles were measured by the captive-bubble method introduced by Taggart, Taylor and Ince,[5] which involves observing the angle at the liquid–solid–gas junction while holding a bubble in contact with the specimen which is completely submerged in the liquid. The bubble is formed initially by use of a special glass pipet bent up at the lower end and fitted at the upper end with a small rubber bulb from an eye dropper. By means of a screw which operates a slide to raise or lower the bubble holder, the liquid is caused to advance or recede across the surface. After the system has come to rest, the angle is observed by use of a protractor eyepiece on a microscope. The angles measured are therefore the static advancing and static receding angles. Beginning with the bubble squeezed down against the specimen almost to the point of escape, the bubble holder is raised in arbitrary increments of 0.006 inch between each observation until the bubble is free from the surface. The bubble holder is then lowered stepwise in the same manner until the bubble escapes. With a bubble holder having an inside diameter of 0.25 inch, there results a series of eight or more readings for both advancing and receding angles. For a uniform surface, the angles do not vary greatly through each group of readings, and an average value for each group is computed.

Measurements also were made by the sessile-drop method,[6] in which a drop of liquid is placed on a plane, horizontal specimen, and the angle at the solid–liquid–gas junction is observed by use of the optical system just described. Again, by adding liquid to the drop from a pipet and allowing the system to come to rest, one may observe a static advancing angle; and, by withdrawing liquid from the drop, a static receding angle is obtained. With the sessile-drop method, there is little assurance that the gas near the liquid–solid–gas junction is saturated with respect to the vapor of the liquid, and angles obtained by the two methods do not always agree.

Preparation of Specimens by Abrasion and Solvent Rinsing.—First attempts to prepare clean metal surfaces involved abrasion, followed by solvent rinsing. A variety of abrasives were tried, and quite elaborate solvent rinsing devices were developed. In one of these devices, freshly distilled solvent at the boiling point was caused to impinge upon the metal specimen in the form of a high-velocity jet. These methods were not effective, however, in producing a high degree of water wettability on small specimens of aluminum, copper, magnesium, platinum, silver, titanium and zinc. Furthermore, the contact angles observed were not reproducible, suggesting that the specimens were still contaminated to varying degrees with organic matter.

Chemical Cleaning of Specimens.—Chemical treatment with strong oxidizing acids was an effective preparatory treatment for mechanically polished surfaces of platinum, stainless steel and titanium, and reproducible contact angles of 5–7°, advancing and receding, were obtained by the bubble method. In the case of platinum, it was necessary to measure the contact angles immediately after cleaning, because the angles increased on exposure to laboratory air, as reported many years ago by Pockels.[7] This effect was not observed with stainless steel or titanium on storage for several weeks.

Chemical Cleaning and Electropolishing.—When it became evident that abrasion followed by solvent rinsing did not produce clean, smooth metal surfaces, and because drastic chemical treatment caused etching of the surface of the more reactive metals, a three-step procedure was developed which shows great promise and has applicability to a wide variety of metals and alloys. First, the specimen, usually a square of metal 1 inch by 1 inch by $^1/_{16}$ inch, is rinsed with an organic solvent to remove gross contamination. Then it is placed in a strong oxidizing acid, at a temperature and for a time suitable to the particular metal involved, to remove final traces of organic contamination by degradation. Many of the metals and alloys commonly used are etched or roughened considerably by this drastic treatment. Smoothness is restored by electropolishing the specimen in a liquid medium from which undesirable organic contamination is carefully excluded.

Electropolishing is a process of anodic dissolution in which a smoothing action occurs. The composition of the electrolyte and the conditions under which electropolishing will occur are rather critical and not well understood, but from the abundant literature on the subject one can usually find workable techniques for polishing most metals and alloys. In selecting bath compositions for the present work, organic addenda were avoided where possible. In essence, one needs only a beaker in which to electropolish small metal specimens; but, after working with the technique a short while, requirements become evident which demand a somewhat more elaborate setup. The all-glass polishing apparatus shown in Fig. 1 provides movement of electrolyte over a wide range of velocity by use of a glass circulating pump, and also allows convenient heating or cooling of electrolyte when necessary. The apparatus is rigorously cleaned with dichromate–sulfuric acid cleaning solution before use, and electrodes are suspended from the open top in either horizontal or vertical arrangements in the electrolyte. The volume of solution required is about 580 ml. Direct current for electropolishing is provided by a power supply which delivers a full-wave, rectified, unfiltered, continuously variable potential in the range 0–25 v., with a current capacity to 25 amp.

The electropolished surface is not only free of crystal fragments, smeared metal, recrystallized metal, and abrasive inclusions, but it also displays, when viewed in the electron microscope, a degree of smoothness which exceeds that usually obtained by other means. This characteristic is, of course, highly desirable in a wettability study, and the fact

(4) H. W. Fox, E. F. Hare and W. A. Zisman, National Research Laboratory Report 4569, July 29, 1955, Washington, D. C.

(5) A. F. Taggart, T. C. Taylor and C. R. Ince, Am. Inst. Mining Met. Engrs., (Milling Methods), Tech. Pub. 204, 1929.

(6) E. Kneen and W. W. Benton, THIS JOURNAL, **41**, 1195 (1937).

(7) A. Pockels, *Physik. Z.*, **15** 39 (1914).

that electropolished surfaces often exhibit, on a macro scale, a slight waviness does not detract from their excellence in the present application. All of the electropolished surfaces appear as brilliant mirrors to the eye but some surface detail is usually evident in electron micrographs. This detail may take the form of ridges bounding extremely smooth areas, or one may observe a slight, general roughness characterized by asperities about 100 Å. high. Although none of the surfaces is a perfect atomic plane, the order of smoothness attained is very high and is probably sufficient to eliminate roughness as a variable in the contact-angle measurement.

Handling Techniques.—Extraordinary handling techniques were necessary to obtain low contact angles on sensitive metals such as copper, and the steady lowering of angles obtained on copper is believed to be the direct result of a progressive refinement in cleaning and handling procedure. All glassware was cleaned in fresh dichromate–sulfuric acid cleaning solution and held with stainless steel tongs during rinsing, care being taken that at no time did a liquid bridge occur along the tongs from the hand to the glassware. Metal specimens were handled with glass tongs fashioned from Pyrex glass rod which were treated with cleaning solution directly before each use. All water used for rinsing glassware and specimens, or for measuring contact angles, was double-distilled, the second distillation being done in a block tin still with a partial condenser. The specific conductance of this water was about 0.6×10^{-6} mho, no provision being made for elimination of carbon dioxide absorbed from the air. The water was dispensed from an all-glass system actuated by a glass-covered solenoid valve. During the drying period, glassware was allowed to drain onto other clean glassware previously prepared, or onto a thick pad of new filter paper. These extreme precautions in the washing, rinsing and drying of glassware, and in the handling of specimens cannot be overemphasized, and are believed to be largely responsible for the success achieved in producing hydrophilic metal surfaces.

Sources and Specifications of Metals and Alloys.—Aluminum, Lurium 5, half-hard, Fromson Orban Co., Inc., 205 East 42nd Street, New York 17, New York. Brass, commercial, yellow, cold-rolled, 1/4 hard temper, ASTM Spec. No. B36, Alloy 6, Eastman Kodak Company, stock item. Copper, photoengravers', Edes Manufacturing Co., Plymouth, Mass. Magnesium, "Zomag," photoengravers', Rolled Plate Metal Co., Brooklyn, New York. Nickel, 99.99%, International Nickel Company, New York, New York. Stainless Steel, AISI Type 316, annealed, cold finished, Eastman Kodak Company, stock item. Zinc, "Zomo," photoengravers', Rolled Plate Metal Co., Brooklyn, New York.

Detailed Preparation of Metal Specimens.—In the following paragraphs, cleaning and polishing methods are described fully for the metals and alloys tested to date.

Aluminum.—Specimens of high-purity aluminum, 1 inch × 1 inch × 1/16 inch, were rinsed with acetone, cleaned for 1 minute in dichromate–sulfuric acid solution at room temperature, and electropolished in the sulfuric acid–phosphoric acid bath described by Basinska, Polling and Charlesby.[8] Horizontal electrodes with a stainless-steel cathode were used, and polishing was continued for 12 minutes at 110° with gentle flow of electrolyte, and a constant current of 10 amp. at a potential of about 6.3 v. Immediately after removal from the polishing bath, the specimen was rinsed with redistilled water. It was then rinsed with 10% *o*-phosphoric acid, a procedure which will be discussed in more detail later, and finally with more water. This rinsing procedure was duplicated for all of the metals mentioned in the succeeding paragraphs except magnesium and nickel.

If contact angles were to be measured by the bubble method, the wet specimen was placed immediately in the contact-angle cell. If angles by the sessile-drop method were desired, the specimen was given a further rinse in redistilled ethanol to remove the water and thereby to avoid excessive oxidation while drying. The ethanol for this purpose was made continuously available by a special still which operated under total reflux. Before adopting the ethanol rinse as a standard procedure, it was established experimentally that the contact angles were not altered by the ethanol.

(8) S. J. Basinska, J. J. Polling and A. Charlesby, *Acta Metallurgica*, **2**, 313 (1954).

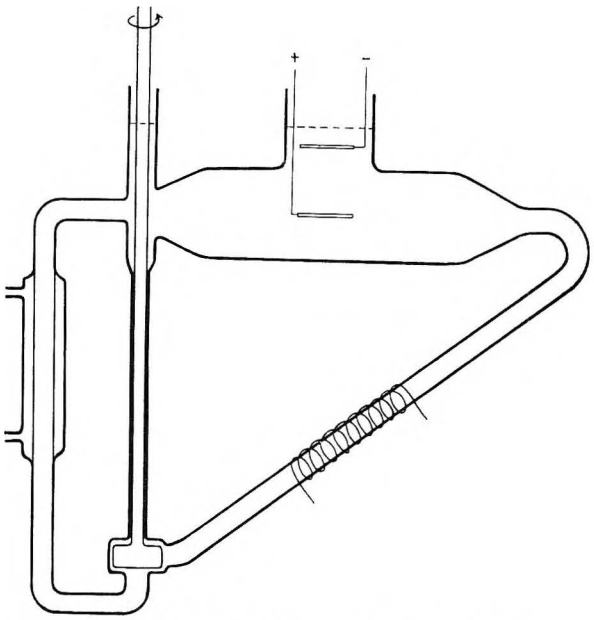

Fig. 1.—All-glass electropolishing apparatus.

Brass.—Specimens of yellow brass were rinsed with acetone, dried, and immersed in hot (80–90°), fresh, dichromate–sulfuric acid cleaning solution for 1 minute before polishing. Electropolishing was done in 63 weight % aqueous *o*-phosphoric acid[9] at room temperature. The brass anode and stainless-steel cathode were suspended horizontally about 3 cm. apart by specimen holders made from platinum wire. Typical polishing conditions were 2.0 v., 0.4 amp., at room temperature. The circulating pump was operated briefly after 5 minutes to remove the dark, solid film which formed during the early part of the polishing period, then polishing was continued without movement of electrolyte for 15 minutes.

Copper.—Specimens of copper were polished in the same bath and by the same technique used for brass.

Magnesium.—Photoengravers' magnesium was immersed for 1 minute in dichromate–sulfuric acid cleaning solution, or in 25% nitric acid, at room temperature. It was then electropolished to a brilliant finish in the bath of Jacquet[10] which consisted of 215 cm.^{3} of 85% o-phosphoric acid, 348 cm.^{3} of absolute ethanol, and 18 cm.^{3} of water. The bath was operated at room temperature using a double, vertical, stainless-steel cathode, a vertical anode supported by a platinum-wire holder, and an applied potential of 1.5 v. which produced a current of 0.07 amp. Polishing time was 1 hour. Following Jacquet's recommendation, the potential was applied before introducing the specimen into the solution, and the specimen was removed while the potential was still being applied. No rinse in 10% *o*-phosphoric acid was used because it produced rapid dissolution and roughening of the surface.

Nickel.—The 71 weight % sulfuric acid bath of Wensch[11] was effective in polishing nickel. Specimens were held horizontally by an expendable holder made from stainless-steel wire, and polishing was continued for 20 minutes at 5.5 v., 7.5 amp., with gentle flow of electrolyte, and in the temperature range 22–32°. Since nickel sulfate is quite soluble, no special rinse was used.

Stainless Steel.—The sulfuric acid–phosphoric acid bath of Faust[12] was used to polish stainless steel. With horizontal electrodes polishing was continued for 3.5 hours, the potential being adjusted in the range, 2.2–2.4 v., to produce a constant current of 0.70 amp. During the first hour of the polishing operation the specimen was periodically flushed *in situ* to avoid pitting.

Zinc.—Specimens of zinc were polished in the same bath

(9) P. A. Jacquet, *Compt. rend.*, **201**, 1473 (1935).

(10) P. A. Jacquet, *Rev. gén. élec.*, **54**, 239 (1945).

(11) G. W. Wensch, *Metal Progress*, **58**, 735 (1950).

(12) C. L. Faust, U. S. Pat. 2,334,698 (Nov. 23, 1943) and U. S. Pat. 2,334,699 (Nov. 23, 1943).

and by the same technique used for magnesium. Polishing was continued for 1 hour at 2.2 v., 0.19 amp., at room temperature. Immediately after removal from the polishing bath, the specimens were rinsed rapidly with distilled water to minimize attack by the polishing solution. This was followed by the usual rinse with 10% *o*-phosphoric acid and finally with more water.

Results

Contact angles measured by the bubble method, using air bubbles and redistilled water, fell in the range 5.0-9.1° for all the metals studied and are collected in Table I. It is readily apparent from inspection of columns 2 and 4 that the observed values were quite reproducible for different specimens of the same metal. Of the seven metals reported, copper appeared to lose wettability most readily by contamination, but with careful technique eight specimens prepared over a period of three days gave mean angles of 7-8° advancing and receding, with only one slightly higher measurement (13.5°) in a total of about sixty observations.

TABLE I

CONTACT ANGLES OF WATER ON ELECTROPOLISHED METAL SURFACES BY THE CAPTIVE BUBBLE METHOD

	Contact angle, °			
	Advancing		Receding	
Metal	Independent specimens	Mean values	Independent specimens	Mean values
Aluminum	7.5	6.8	7.2	6.6
	7.6		7.5	
	6.8		5.9	
	6.0		6.1	
	6.1		6.5	
Brass	8.0	7.5	7.1	7.0
	7.1		6.9	
	7.3		6.9	
Copper	7.7	7.3	6.7	7.5
	7.8		5.9	
	6.4		6.5	
	7.4		7.6	
	7.1		9.1	
	8.3		8.1	
	6.4		8.4	
	7.0		7.9	
Magnesium	5.9	5.7	5.4	5.4
	5.5		5.7	
	5.9		5.5	
	5.0		5.2	
	6.4		5.4	
Nickel	5.8	6.1	6.1	6.4
	6.0		7.0	
	6.3		5.9	
	6.1		6.5	
Stainless steel	8.5	8.2	8.1	8.0
	8.3		8.4	
	7.8		7.6	
Zinc	5.0	6.1	5.6	6.0
	5.9		5.7	
	7.3		6.8	

Values of contact angles measured by the sessile-drop method are given in Table II and again were highly reproducible from specimen to specimen of the same metal. On some of the metal surfaces, no recession was observed when water was withdrawn from the drop, and the receding angles by the drop method were therefore considered to be zero for these metals.

TABLE II

CONTACT ANGLES OF WATER ON ELECTROPOLISHED METAL SURFACES BY THE SESSILE DROP METHOD

	Contact angle, °			
	Advancing		Receding	
Metal	Independent specimens	Mean values	Independent specimens	Mean values
Aluminum	4.1	4.6	0.0	0.0
	4.1		0.0	
	4.9		0.0	
	5.3		0.0	
Brass	10.4	10.5	0.0	0.0
	9.6		0.0	
	10.1		0.0	
	10.9		0.0	
Copper	9.6	9.6	4.2	3.9
	9.6		3.2	
	9.7		4.3	
Magnesium	0+	0+	0.0	0.0
	0+		0.0	
	0+		0.0	
Nickel	7.3	7.1	3.0	2.8
	6.9		2.1	
	7.2		3.4	
Stainless steel	4.3	5.4	0.0	0.0
	5.6		0.0	
	5.6		0.0	
	6.1		0.0	
Zinc	8.9	8.5	0.0	1.2
	8.6		2.0	
	8.1		1.5	

Discussion

Our inability to obtain low contact angles on metal surfaces by abrasion and rinsing with organic solvents is not surprising in view of Langmuir's observation[13] in 1938 that hot benzene was not adequate in removing the last traces of stearic acid from a chromium surface. More recent evidence by Hackerman and Cook[14] corroborates this early observation and suggests that at least a fraction of the final monolayer is chemisorbed rather than physically adsorbed to the solid surface.

Other experiments, to be described later, demonstrate that a rather small fraction of a monolayer of organic molecules is sufficient to increase the contact angle of water on many metal surfaces. In the present experiments, utilizing chemical treatment followed by electropolishing, it therefore seems likely that virtually complete elimination of organic matter has been achieved.

The possibility of contamination of an electropolished surface by inorganic salts from the polishing bath is not so readily dispensed with. This is particularly serious in the case of phosphoric acid polishing baths, since many metal phosphates are relatively insoluble in water. To minimize the deposition during rinsing of phosphate salts on metals polished in such media, it has been customary after polishing to interpose a rinse with 10% *o*-phosphoric acid between two water rinses. In

(13) I. Langmuir, *Science*, **87**, 493 (1938).

(14) N. Hackerman and E. L. Cook, THIS JOURNAL, **56**, 524 (1952).

the case of copper, it was possible to estimate the amount of phosphate remaining on the surface by coulometric reduction of the inorganic surface film in an oxygen-free electrolyte. This work has been reported elsewhere by Lambert and Trevoy.[15] Allen[16] used a similar rinsing technique to eliminate phosphate contamination from electropolished copper, and claimed to produce specimens having no phosphate residue. Our reduction experiments, which are believed to be more sensitive than Allen's, indicated a residual phosphate film having an average thickness of 1.3 Å. based on the apparent area of the specimen, even under optimum polishing and rinsing conditions. Without question, this residual phosphate represents much less than a monolayer, however, and evidence is presented in the publication cited that the phosphate probably resides in depressions in the surface or edges of the specimen, and is not uniformly distributed. It is concluded that the observed low advancing contact angles reported for electropolished copper are truly characteristic of a copper surface carrying the normal cuprous oxide film. Although no coulometric data are available for the other metals, it is probable that the rinsing technique which is effective for copper is effective for these also, and that the reported contact angles are representative of surfaces which are substantially free of both organic and spurious inorganic contamination. Magnesium is one exception for which the possibility of phosphate contamination has not been eliminated.

Mean values reported in Table I for contact angles measured by the bubble method vary only from 5.4 to 8.2°, and all values in this range represent a high degree of water receptivity or hydrophilic character. While it is difficult to differentiate between a contact angle of about 4 and 0°, because of the problem of aligning a cross-hair with a curved surface which makes a very small angle with the solid at the point of intersection, the values usually observed are larger than 4°. As viewed in the microscope, these angles are clearly non-zero. It is not known whether they are due to some artifact or are characteristic of the oxide surface itself. On a uniform solid surface, it is commonly observed that the angles vary slightly, but in a regular manner, as the bubble holder is raised or lowered. The advancing angles decrease as the bubble holder is raised while the receding angles increase as the bubble holder is lowered. Typical values for an electropolished zinc surface are: for the advancing contact angle, 7.5, 8.4, 6.9, 6.0, 5.2, 4.7, 5.2, 3.4°; for the receding angle, 2.5, 3.9, 3.2, 4.3, 5.5, 3.8, 4.7, 5.5°. These variations are not attributable to variations in the solid surface, and apparently are associated with the geometry of the bubble as distorted by the solid surface. In both cases, the lower angles are obtained when the bubble is only slightly distorted from a spherical shape, and it is possible that the lower values are closer to the true angles, and that the true angles may in fact be zero. This suggests the use of a very large bubble which would enable one to scan an appreciable area of the surface with little distortion of bubble shape.

Mean values reported in Table II for contact angles measured by the sessile-drop method varied from 0° to 10.5°, again representing a high degree of water-receptivity. This is a wider variation in values, however, than was obtained by the captive-bubble method, and may well be due to adsorption of organic molecules from the air. The observed angles are not identical for different metals, possibly because the metals have different capacities for capture of impinging organic molecules. In using the bubble method, the usual procedure was to transfer the rinsed specimen directly to the contact-angle cell without drying, thereby avoiding opportunity for direct adsorption of contaminants from the air.

On extended storage in laboratory air, no large loss of wettability was observed on any of the electropolished surfaces prepared in this study, but tests are incomplete. Since chemically cleaned platinum has shown a substantial loss in water-receptivity on exposure to laboratory air, it therefore seems likely that the sticking coefficient of organic molecules impinging on a metal surface is much greater for platinum than for many other metals.

(15) R. H. Lambert and D. J. Trevoy, *J. Electrochem. Soc.*, **105**, 18 (1958).

(16) J. A. Allen, *Trans. Faraday Soc.*, **48**, 273 (1952).

THE FAR INFRARED SPECTRA OF CF_3CH_3, CF_3CH_2Cl, CF_3CHCl_2 AND CF_3CCl_3[1]

BY EDWARD CATALANO AND KENNETH S. PITZER

Contribution from the Department of Chemistry, University of California, Berkeley 4, California

Received March 8, 1958

The infrared absorption spectra of the series of substituted ethanes CF_3CH_3, CF_3CH_2Cl, CF_3CHCl_2 and CF_3CCl_3 were measured in the range of 150–450 cm.$^{-1}$ by the use of a grating spectrometer and a CsI prism spectrometer. In some cases bands were observed which had not appeared in the Raman spectra of the substances. The necessary revisions of the vibrational assignment are discussed together with the probable values of the barriers to internal rotation.

The infrared and Raman spectra of the series of substituted ethanes CF_3CH_3, CF_3CH_2Cl, CF_3CHCl_2 and CF_3CCl_3 were measured or reviewed in Nielsen, *et al.*, and Cowan, *et al.*[2–5] Since their infrared measurements do not extend to the lower frequency fundamentals of these molecules, we have measured the spectra in the 150–450 cm.$^{-1}$ range. This range is of particular interest in connection with the torsional motion and the low frequency bending vibrations. Also, the low frequency vibrations are especially important in thermodynamic calculations for these substances.

Experimental

The samples were provided by the E. I. du Pont de Nemours Co., and had been carefully purified. Two spectrometers were used: the grating instrument described by Bohn, *et al.*,[6] and a Perkin–Elmer 12C spectrometer with a CsI prism. The various spectra are shown on Figs. 1–4. The instrument employed is indicated as well as the number of lines per inch on the grating where pertinent. Both instruments were calibrated with the spectrum of water vapor.

Discussion

Before considering the interpretation of the individual spectra a few general remarks seem appropriate. The torsional frequency has been particularly difficult to locate in spectral studies of this type because of its zero or very low intensity in many cases. Many published assignments of this mode have been incorrect. However, this motion has one unique characteristic which makes it possible to identify the mode in some cases where it would otherwise be ambiguous. This is the very large anharmonicity which is very apparent for any CH_3 torsion. The spectra of CH_3CCl_3[7] and CH_3CH_2F[8] show this very clearly. The hot bands are separated by about 15 cm.$^{-1}$ and decrease successively in intensity by a factor of about $1/e$ (at room temperature). This characteristic is used in locating the torsion mode in CH_3CF_3. However, when both rotating groups contain two or more heavy atoms, the torsional frequency is typically about 100 cm.$^{-1}$ or smaller and the anharmonicity is correspondingly smaller than for CH_3 torsion. The natural band width, even of the Q branches, seems to obscure the hot band sequence in the case of the heavier groups.

The approximate product rule for substitution of similar atoms[9] is very useful in checking the reasonableness of assignments. Its use is mentioned several times. For this purpose the moments of inertia need be known only approximately. Consequently these values will not be discussed except in the case of CF_3CH_3 where there is a surprisingly large discrepancy between two investigations.

The spectral assignments are correlated on Fig. 5 which shows the region 0–600 cm.$^{-1}$. The selected values of the torsional frequencies are far from certain; they yield for the potential barrier about 3000 cal./mole for CF_3CH_3 and about 6000 cal./mole for the other three compounds. A more gradual trend might have been expected and, indeed, the present values may well be in error.

In view of remaining small uncertainties it seems hardly wise to revise the published thermodynamic functions[2,10] for these molecules. One can readily correct for the changes in frequencies or internal rotation barriers which are introduced by our study.

CF_3CH_3.—The spectrum in Fig. 1 shows a single strong band at 365 cm.$^{-1}$ which agrees exactly with the published work.[4,10] We agree with the assignment of this band to the CF_3 rocking motion.

The torsional mode would be inactive in this molecule as a fundamental but we may hope to detect it in some combination such as proved possible in CH_3CCl_3.[7] The frequency 238 cm.$^{-1}$ was suggested by Nielsen, *et al.*,[2,4] on this basis, but their assignment seems unlikely to us because no hot bands were observed. A re-examination of their spectra shows one distinct sequence of three bands of appropriately diminishing intensity at 1186, 1172 and 1155 cm.$^{-1}$. No satisfactory interpretation has been given previously for these bands which range from medium to weak in intensity. We propose the interpretation 970 + torsion with the 0–1, 1–2 and 2–3 transitions in torsion. The corresponding difference bands fall in range 740–780 cm.$^{-1}$ which is free from strong absorption. The detail in this region is confused, however, and the probable cause is overlapping with the sum bands of 541 + torsion. If we ignore any additional anharmonicity in the combination band, the torsional level separations become 216, 202 and 185 cm.$^{-1}$ which correspond exactly to the sequence calculated for a cosine barrier of 3040 cal./mole with the

(1) This research was a part of the program of Research Project 50 of the American Petroleum Institute.

(2) J. R. Nielsen, C. Y. Liang and D. C. Smith, *J. Chem. Phys.*, **21**, 1060 (1953).

(3) J. R. Nielsen, C. Y. Liang, R. M. Smith and D. C. Smith, *ibid.*, **21**, 383 (1953).

(4) J. R. Nielsen, H. H. Claassen and D. C. Smith, *ibid.*, **18**, 1471 (1950).

(5) R. D. Cowan, G. Herzberg and S. P. Sinha, *ibid.*, **18**, 1538 (1950).

(6) C. R. Bohn, N. K. Freeman, W. D. Gwinn, J. L. Hollenberg and K. S. Pitzer, *J. Chem. Phys.*, **21**, 719 (1953).

(7) K. S. Pitzer and J. L. Hollenberg, *J. Am. Chem. Soc.*, **75**, 2219 (1953).

(8) E. Catalano and K. S. Pitzer, THIS JOURNAL, **62**, 873 (1958).

(9) K. S. Pitzer and E. Gelles, *J. Chem. Phys.*, **21**, 855 (1953).

(10) D. C. Smith, G. M. Brown, J. R. Nielsen, R. M. Smith and C. Y. Liang, *J. Chem. Phys.*, **20**, 473 (1952).

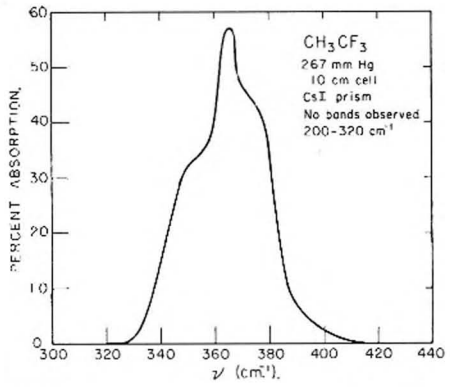

Fig. 1.—The infrared spectrum of CF_3CH_3.

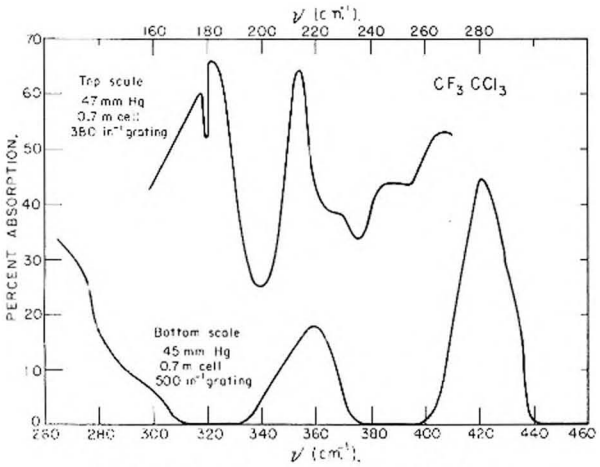

Fig. 2.—The infrared spectrum of CF_3CCl_3.

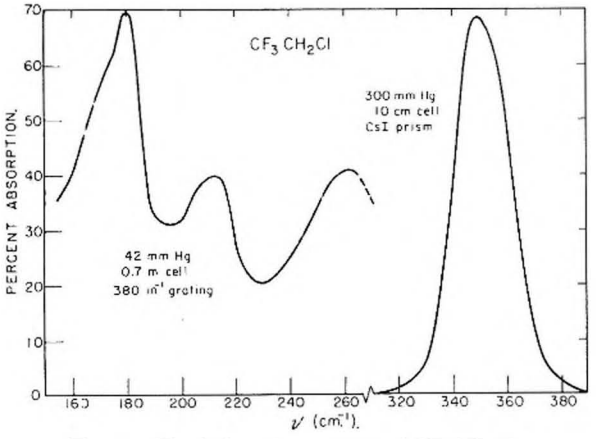

Fig. 3.—The infrared spectrum of CF_3CH_2Cl.

reduced moment of inertia 5.11×10^{-40} g. cm.^{2} given by Nielsen, *et al.* While the evidence for this barrier is not conclusive by any means, it does seem to us the most likely value on the basis of available evidence.

This barrier value is just enough lower than that assumed by Nielsen, Claassen and Smith[4] to yield good agreement with the experimental entropy value of Russell, Golding and Yost.[11] Also the moments of inertia are now known more accurately from the microwave investigation of Thomas,

(11) H. Russell, Jr., D. R. V. Golding and D. M. Yost, *J. Am. Chem. Soc.*, **66**, 16 (1944).

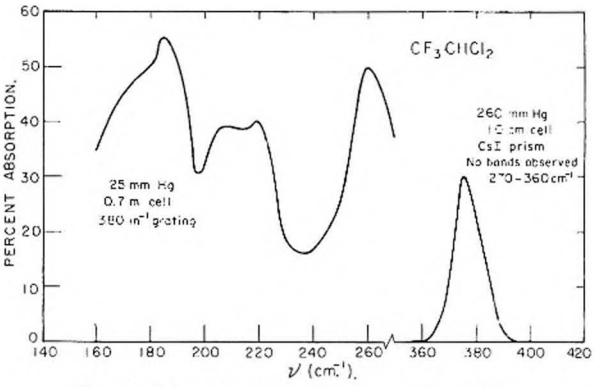

Fig. 4.—The infrared spectrum of CF_3CHCl_2.

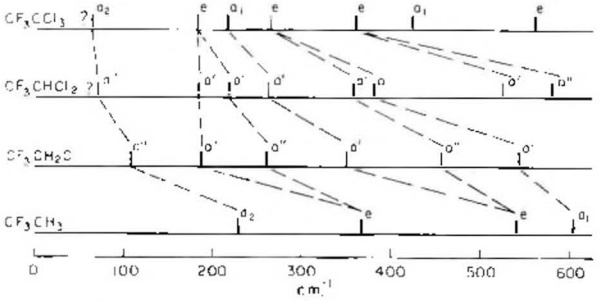

Fig. 5.—A correlation of the low frequency vibrations for the series $CF_3CH_xCl_y$.

Heeks and Sheridan.[12] If we modify the thermodynamic calculations of Smith, *et al.*,[10] in these two respects, the entropy near room temperature is increased by 0.30 cal./deg. mole which was just the discrepancy between the earlier calculation and the experimental value.

CF_3CCl_3.—The spectrum is shown in Fig. 2 and the frequencies are listed in Table I along with those from the Raman spectrum of Nielsen, Liang, Smith and Smith.[3] The assignment of these authors was clear-cut except for the torsion and one totally symmetric mode. They assigned the latter to a weak infrared band at 490 cm.$^{-1}$ The new spectrum contains a previously unobserved strong band at 214 cm.$^{-1}$ which is now assigned as an A_1 fundamental. Product rule correlations with CH_3-CF_3 and CH_3CCl_3 clearly indicate that the 490 value is much too large and that 214 cm.$^{-1}$ is in the expected range.

TABLE I

INFRARED AND RAMAN SPECTRA OF CF_3CCl_3 TO 450 CM.$^{-1}$

Infrared	Raman[3]	Assignment
182s	182s,dp	E fundamental
214s		A_1 fundamental
248w,sh		182 + torsion
265m	265s,dp	E fundamental
359m	367m,dp	E fundamental
422s	429vs,p	A_1 fundamental

Evidence was sought for the torsional frequency. The shoulder at 248 cm.$^{-1}$ may be assigned as a sum of 180 + torsion, yielding 68 cm.$^{-1}$ for the torsion frequency. Then the band at 490 cm.$^{-1}$, previously assigned as a fundamental, may be ascribed to the superposition of 265 + 214 = 479 and

(12) L. F. Thomas, J. S. Heeks and J. Sheridan, *Z. Elektrochem.*, **61**, 935 (1957).

561 − 68 = 493. Thus, we believe that 68 cm.$^{-1}$ is a likely value for the torsional frequency but it cannot be regarded as certain. This frequency corresponds to a cosine potential barrier of approximately 6000 cal./mole.

CF_3CH_2Cl.—The infrared spectrum in the low frequency range is shown in Fig. 3. The strong band at 350 cm.$^{-1}$ was reported by Nielsen, Liang and Smith[2] at ~355 cm.$^{-1}$. We did not find the weak band they reported at 330 cm.$^{-1}$ although we cannot claim it definitely absent because of an interference with a line due to a trace of H_2O. The lower frequency portion of the spectrum is new. The strong band at 180 cm.$^{-1}$ is presumably the same fundamental as is observed at 191 cm.$^{-1}$ in the Raman spectrum of the liquid. The 11 cm.$^{-1}$ shift is larger than is usually observed. The band at 212 cm.$^{-1}$ is probably the overtone of the torsion observed at 109 cm.$^{-1}$ in the Raman effect. The 260 cm.$^{-1}$ band could be accounted for by difference combinations but it seems more likely to be the fundamental previously assigned to 330 cm.$^{-1}$.

While the vibrational assignment of Nielsen, Liang and Smith is undoubtedly correct in most features, it seems to us unlikely at a few points. The approximate product rule was applied to Cl for H substitution from CF_3CH_3 and the results tended to confirm the need of some revision. The revisions we thought most likely in view of trends from other molecules, however, are in conflict with the polarization data for the Raman spectrum. For example, the CH_2 symmetrical bending frequency is usually near 1450 and the CH_2 twisting near 1300 cm.$^{-1}$; whereas, in this case the polarization values require the reverse. In view of these difficulties we shall not attempt a complete assignment.

CF_3CHCl_2.—The spectrum for this substance is given in Fig. 4. All of the bands correspond to those observed in the Raman spectrum by Nielsen, Liang and Smith,[2] who also observed the 376 cm.$^{-1}$ band in the infrared. We have not examined their assignment as a whole but agree with respect to all of the low frequency bands in our spectrum. We doubt, however, that the torsional fundamental is as high as the 141 cm.$^{-1}$ value they select. This value would appear more reasonable for the overtone and we tentatively select a value of about 72 cm.$^{-1}$ for the fundamental.

REACTIONS OF FRESHLY FORMED SURFACES OF SILICA

BY R. E. BENSON AND J. E. CASTLE

Contribution No. 464 from The Central Research Department, Experimental Station, E. I. du Pont de Nemours and Company, Wilmington, Delaware

Received March 14, 1958

The rupture of silicon-to-oxygen bonds in silica has been shown to produce active sites that are capable of reacting with olefins and with alcohols. These reactions can be effected by grinding silica in the presence of organic liquids or by simple mixing of the organic materials with silica that has been ground and stored in an inert atmosphere. A probable mechanism for these reactions is presented.

Several phenomena have been observed that suggest that certain freshly formed surfaces have unusual properties. For example, atomic nitrogen has been detected in the triboluminescent glow produced during fracture of sugar crystals.[1] The grinding of silica in air has been reported to give atomic oxygen,[2] and sugar has been stated to be adsorbed from aqueous solution by freshly ground quartz.[3] The adsorbed sugar was not removed by washing with water and only a small portion was removed by washing with alcohol. Effects observed on grinding quartz in the presence of alcohol and other organic compounds recently have been reported[4] with reference to our work[5] which is now described in detail. Our study was undertaken to examine the reactivity of freshly formed surfaces toward organic reagents.

It was found that grinding fused silica in the presence of certain organic compounds produced silica powders having chemically combined organic groups. In the instance of styrene, a hydrophobic and organophilic product containing organic material equivalent to 1% styrene and having a weight median diameter of 0.4 μ was obtained, using conventional ball-milling techniques. Analytical data, including surface area determinations, indicated that approximately one-half of the surface was covered by organic product and that the degree of polymerization of styrene was about 10. The organic material was not removed by solvent extraction or vacuum drying and was largely retained after refluxing in water in the presence of a wetting agent. Similar, though less organophilic, products were obtained by grinding fused silica with such vinyl monomers as chloroprene, butadiene, 2-methyl-5-vinylpyridine and β-dimethylaminoethyl methacrylate. The products derived from the two vinyl monomers that contained basic groups could be dyed with conventional acid dyes to give colored silica powders that were washfast. This effect offers striking visual evidence of surface modification.

When fused silica was ground in 1-butanol a hydrophobic and organophilic powder was also obtained. In contrast to styrene-modified silica, this product became hydrophilic on refluxing with water. Products having less organophilic properties were obtained from hydrocarbons including

(1) F. G. Wick, *J. Opt. Soc. Am.*, **27**, 275 (1947); H. Longchambon, *Compt. rend.*, **174**, 1633 (1927); **170**, 691 (1923).

(2) W. A. Weyl, *Research*, **3**, 230 (1950).

(3) Von W. Engel and L. Holzapfel, *Kolloid Z.*, **119**, 160 (1950).

(4) H. Deuel and R. Gentile, *Helv. Chim. Acta*, **39**, 1586 (1956).

(5) L. M. Arnett, M. F. Bechtold and R. E. Benson, U. S. 2,728,732 (December 27, 1955).

TABLE I

BALL-MILLING EXPERIMENTS

Reactants	Time, hr.	Organophilic test[a]	Particle size,[b] μ	Analyses, % Original product C	Original product H	Hydrolyzed product C	Hydrolyzed product H	Organophilic test after hydrolysis
400 g. fused silica 460 ml. styrene	70	+++(Be)[a]	1.2 (2.24 m.²/g.)	1.53 (1.05)	0.20 (.14.[d]	0.86	0.18	+++(Be)[a]
400 g. fused silica 300 g. styrene	48	+++(Be)	0.74 (3.7 m.²/g.)	1.46 (1.08)	.18 (.15)[d]	.93	.17	+++(Be)
60 g. fused silica 100 ml. α-methylstyrene	48	+++(Be)	0 30 (9.1 m.²/g.)	1.09	.17			
100 g. fused silica 112 ml. β-dimethylaminoethyl methacrylate	48	+(Be)		0.35	.13	.16	.17	+(Bu)(dyed)
50 g. fused silica 75 ml. 2-methyl 5-vinylpyridine	48	+(Be)		.63	.15	.39	.18	+(Bu)(dyed)
100 g. fused silica 100 ml. methyl methacrylate	46	++(Bu)		.21	.11			
100 g. fused silica 125 ml. acrylonitrile	66	+(Bu)		.12	.09			
50 g. fused silica 38.3 g. chloroprene	40	++(Be)	6.3	.26	.19			
110 g. fused silica 80 ml. butadiene	7 (−70 to −30°)	++(Be)		.25	.12[c]			
50 g. fused silica 50 ml. 1-butanol	15	+++(Bu)	14 5	.13	.11	.08	.11	−(Bu)
100 g. fused silica 178 ml. 2-octanol	20	+++(Bu)		.05	.08			+sl.(Bu)
50 g. fused silica 50 ml. toluene	15	+(Be)		.08	.10			+(Be)
100 g. fused silica 180 ml. benzene	60	++(Bu)		.40	.14			
100 g. fused silica 180 ml. cyclohexane	60	+(Bu)		.29	.08	.17	.10	+(Bu)
100 g. fused silica 150 ml. cyclohexylamine	20	++(Bu)		.45	.13	.11	.11	+(Bu)
100 g. fused silica 200 ml. acetic acid	60	−(Bu)		.22	.07	.10	.11	−(Bu)
100 g. fused silica 200 ml. tetrahydrofuran	20	++(Bu)		.28	.09	.28	.11	+(Bu)
400 g. glass sand 800 ml. styrene	24	−++(Be)		.47	.08			

[a] Organophilic test is based on partitioning product between water and immiscible organic liquid (Be = benzene, Bu = 1-butanol). In this test a small amount of the product is placed in a test-tube and 5 ml. of water is added. The mixture is shaken and an equal volume of the indicated organic liquid is added. The mixture is shaken again, allowed to stand, and the location of the silica product is observed. +++, entire product goes to liquid–liquid interface; ++, major portion of product goes to liquid–liquid interface; +, about one-third of product goes to liquid–liquid interface; −, little, if any, of product goes to liquid–liquid interface. [b] From surface area measurement[7] (BET method). [c] Poor fracture. Analysis was made on material that suspended readily in benzene. [d] Data for product extracted with benzene in Soxhlet apparatus for 24 hours.

benzene, toluene and cyclohexane. The organic content of these products was considerably less than those derived from styrene.

In extension of this reaction, it also was found that polishing a large quartz crystal in styrene resulted in the formation of a hydrophobic surface as indicated by wetting-angle measurements.

These reactions promoted by fracture are believed to occur on highly reactive sites formed by rupture of silicon-to-oxygen bonds. Life studies of these active centers indicated that they were capable of reacting with styrene and with 1-butanol for more than 260 hours after formation, if kept in an inert atmosphere. However, they were essentially unreactive toward aromatic and saturated aliphatic hydrocarbons unless these materials were present during fracture.

Experimental

Materials and Method.—Fused silica (4–8 mesh) was obtained from the Amerisil Company. In most experiments "Burundum" cylinders (available from U. S. Stoneware Company) were used as the grinding aid. Unless otherwise noted, vinyl monomers containing the usual stabilizing agents were used in this investigation.

In the general procedure, the fused silica and grinding aid were placed in a conventional porcelain ball mill and covered with the organic liquid. The vessel was flushed with nitrogen, sealed and rotated for the indicated time. The vessel was opened, solvent was added, and the product was decanted from the grinding aid. The solid was suspended in a hot solvent that was suitable for removal of any low molecular weight polymer present and was isolated by centrifugation. This extraction was repeated twice. The product was dried in air and finally in a vacuum oven at 130° for 24 hours. The analytical data for these products are given in Table I.

Hydrolysis studies were conducted in the presence of a wetting agent (usually "Triton" X-100). After being refluxed in water for 24 hours, the product was isolated by filtration or centrifugation. The solid was dried in air and washed with fresh solvent that had been used for the extraction process. The analytical data are recorded in Table I.

In many cases it was difficult to avoid some loss of fine particles since they tended to centrifuge or filter poorly. Undoubtedly these small particles had a proportionately higher organic content than the bulk of the material. Thus, loss of this finely divided material may account in part for the lower carbon values that were obtained after some extractions and, particularly, after hydrolysis experiments.

Particle Size Measurements.—Particle size was determined by nitrogen absorption (BET method).[8] In one instance, the weight median particle diameter, as determined by microscopic examination, was 3.8 μ but nitrogen absorption measurements indicated a weight median di-

(8) S. Brunauer, P. H. Emmett and E. Teller, *J. Am. Chem. Soc.*, **60**, 309 (1938).

ameter of 0.76 μ (3.6 m.²/g.). Examination of the product with an electron microscope showed it to be composed of aggregates of small particles that were not visible with a light microscope, thus explaining the discrepancy in particle size measurements.

The extent of surface coverage was determined by the method of Shapiro and Kolthoff.[7] The styrene-modified silica powder having a surface area of 3.6 m.²/g. and containing 0.8% styrene was found to have a hydroxyl area corresponding to 1.5 m.²/g. This indicates that approximately one-half of the surface is covered by organic material and that the degree of polymerization of styrene is about 10, based on the area covered.

Life Study of Active Sites. Fused silica was ground in a helium atmosphere. A portion of the solid was removed at the indicated time intervals and added under helium to test-tubes containing various liquids. The resulting mixtures were agitated for 24 hours in the absence of grinding. The products were removed by filtration, washed with suitable solvents, and allowed to dry. The styrene product was extracted twice with warm benzene. The results obtained with silica powder that had been aged for periods of 1–260 hours are summarized in Table II. The surface sites remained active to styrene and to butanol for more than 260 hours after formation as indicated by positive organophilic tests. For control purposes, a portion of the ground silica was aged in moist air for 24 hours and then added to styrene and to butanol. The resulting products were not organophilic.

TABLE II

LIFE OF ACTIVE SITES[a]

Time	Organic compd.	Organophilic test (Hc)	Analyses, % C	H
After 1 hr.	Styrene	++	0.26	0.17
	Ethylbenzene	−	.05	.06
	Toluene	−	.08	.09
	Acrylonitrile	Slightly +	.04	.08
	1-Butanol	+++		
After 120 hr.	Styrene	+		
	1-Butanol	++		
After 260 hr.	Styrene	Slightly +		
	1-Butanol	+		
Control		−	< .05	.05

[a] Silica was ground under helium and added to the reagents at the indicated time intervals. The resulting mixture was agitated in the absence of grinding for 24 hours.

Similar results were obtained when quartz was ground under helium and added to various organic liquids.

Polishing of Quartz Crystals in the Presence of Styrene.—A quartz crystal (2 cm. square) was polished by rubbing against a glass surface with a silicon carbide–styrene paste. The polished crystal was placed in a beaker containing warm benzene, washed by decantation several times, and then carefully wiped dry. For control purposes another quartz crystal was polished in a similar manner using a paste of silicon carbide in water. The crystal which had been polished in the presence of styrene had a wetting angle with water of 55° compared to a wetting angle of 13° for the control. An unpolished quartz crystal that had been allowed to stand under styrene and then washed with benzene had a wetting angle of 27°. These data indicate that the surface of the quartz crystal that had been abraded in the presence of styrene had been modified. Electron diffraction studies of these crystals were not conclusive, but a less pronounced quartz pattern was found for the styrene-polished crystal than for either the water-polished crystal or the unpolished crystal that had merely stood under styrene. Since the depth of covering is important in electron diffraction studies, it is possible that more of the surface was covered with styrene than was indicated by wetting angle measurements.

Dyeing of Silica Powders Prepared by Grinding Silica in the Presence of Basic Vinyl Monomers.—The silica powder obtained from the grinding of silica in the presence of 2-methyl-5-vinylpyridine was refluxed for 4 hours with 100 ml. of a 0.5% solution of a conventional blue dye of the acid type at a *p*H of 1. The product was removed by filtration, washed with water, acetone and finally with water. The solid was washed with warm water containing "Triton" N-100, with water, and finally with acetone. The product was a light blue powder. A light red silica powder resulted when the methylvinylpyridine–silica product was treated with a conventional red dye. Similar results were obtained when the product derived from silica and dimethylaminoethyl methacrylate was treated with these dyes.

In control experiments, unmodified silica was subjected to the above dyeing conditions and subsequently washed with water and solvent to give a colorless powder. In addition, attempts to dye styrene-modified silica powders under these conditions were unsuccessful.

Discussion

During the fracture of silica, silicon-to-oxygen bonds are broken, and Weyl[8] has postulated the formation of fragments of the type

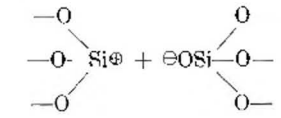

on the surface of the particles. Weyl has pointed out that it is not possible for these fragments to stabilize themselves through loss or gain of electrons in an inert atmosphere. In our work it has been shown that the sites formed by rupture of silicon-to-oxygen bonds by grinding in an inert atmosphere have an appreciable life. Thus, they are capable of reacting with styrene and with 1-butanol for more than 260 hours after formation. These organic compounds are chemically combined, as indicated by failure to remove the organic material by solvent extraction or by vacuum drying.

In addition, the silica product derived from styrene retained its hydrophobic properties after treatment with water, while the product derived from butanol became hydrophilic. These results indicate that styrene is bonded through carbon-to-silicon bonds which are not sensitive to water, whereas 1-butanol is bonded through hydrolyzable silicon-to-oxygen bonds. These data are consistent with a mechanism involving attack of the electrophilic reagent $\equiv O_3Si^{\oplus}$ on styrene to yield $\equiv O_3Si\text{–}CH_2CH(C_6H_5)\text{–}$ which can react further with styrene$^{\ominus}$ according to well-established, acid-catalyzed polymerization mechanisms[8] to give $\equiv O_3Si(CH_2CH(C_6H_5))_nCH_2\overset{\oplus}{C}HC_6H_5$. Termination can occur by reaction of the growing chain with $\equiv O_3SiO^-$ on the surface of the particle, or disproportionation, etc. In the case of 1-butanol, attack of the electrophilic reagent would yield the ester derivative $\equiv O_3SiOC_4H_9$ which would hydrolyze to give 1-butanol with subsequent loss of hydrophobic character for the silica powder.

A mechanism involving free-radical processes is less attractive since vinyl monomers containing reagents known to inhibit free-radical polymerization have been used in this study. In addition, it would be expected that radical attack on 1-butanol would occur on carbon rather than on the oxygen atom. Furthermore, the monomers that are most effective for surface modification are those

(7) I. Shapiro and I. M. Kolthoff, *J. Am. Chem. Soc.*, **72**, 776 (1950).

(8) L. P. Hammett, "Physical Organic Chemistry," McGraw-Hill Book Co., Inc., New York, N. Y., 1940, p. 307.

that are known to undergo polymerization catalyzed by electrophilic reagents.

On the basis of data available, it is not possible to indicate a mechanism by which surface modification takes place when silica is ground in the presence of hydrocarbons such as benzene and cyclohexane. In view of the energy required to break the silicon-to-oxygen bond it seems probable that under grinding conditions highly reactive sites are formed. Thus, temperatures of short duration approaching 1000° have been noted during friction of silica surfaces[9] and the ball-milling of quartz in a calorimeter has indicated quartz to have a specific surface energy of 107,200 ergs/sq. cm.[10] In view of these high energy requirements, it appears probable that a dual thermal-ionic process is operating during the grinding of silica in the presence of various organic compounds.

(9) F. P. Bowden, *Nature*, **166**, 330 (1950).
(10) A. K. Schellinger, *Science*, **111**, 693 (1950).

VOLUME EFFECTS ON MIXING IN THE LIQUID Bi–$BiCl_3$ SYSTEM[1]

BY F. J. KENESHEA, JR., AND DANIEL CUBICCIOTTI

Stanford Research Institute, Menlo Park, California

Received March 14, 1958

Volume effects upon mixing in the liquid Bi–$BiCl_3$ system have been determined by measuring the density as a function of temperature for various mixtures. A pycnometric method was used for the density measurements. There is a decrease in the total volume of the system on mixing. In the salt-rich mixtures the partial molar volume of $BiCl_3$ is approximately the same as the molar volume, and increases with increasing temperature; the partial molar volume of bismuth is much less than the molar volume and decreases with increasing temperature. In the metal-rich mixtures the partial molar volume of $BiCl_3$ is much less than the molar volume, and the partial molar volume of bismuth is about the same as the molar volume. These effects are interpreted in terms of an interstitial type of solution; in the salt-rich solutions, for example, the added bismuth atoms or ions are pictured as entering into the octahedral holes in the chloride quasi-lattice. It also has been found that the expansivity of the salt-rich solutions exhibits negative deviations from additivity, which is found to be due to the negative expansivity of the bismuth in solution. Such behavior is in accord with the proposed solution mechanism.

Introduction

In recent years several papers have reported studies on the solubility of metals in their molten salts.[2] In order to understand the nature of such solutions we have been measuring certain of their thermodynamic properties. In this respect we recently have reported results[3] of vapor pressure measurements in the Bi–$BiCl_3$ system. The present report describes the results obtained on the measurement of molar volume and volume changes on mixing in the Bi–$BiCl_3$ system. This is a convenient system to handle because of the low melting points of bismuth and $BiCl_3$ and because the mixture is compatible with Pyrex. The phase diagram has been investigated by several workers,[4] with some differences in results. In general, however, there is agreement on the presence of a miscibility gap existing approximately between 0.40 and 0.95 mole fraction of bismuth at 320°, and the existence of a solid in this composition range below 320°. In the course of conductivity studies on Bi–$BiCl_3$, Aten[5] measured densities of some of the mixtures. His results, however, showed a non-linear variation with temperature which in the case of pure $BiCl_3$ was not in agreement with Voigt and Biltz[6] and Jaeger and Kahn.[7] It was thought that more accurate density values, and hence volume changes, were desired and thus the present study was carried out.

Experimental

A pycnometric method was used to measure the densities of liquid Bi–$BiCl_3$ mixtures as a function of temperature. Essentially this consisted of measuring the volume of a known weight of the liquid at a particular temperature and its change in volume with temperature.

The pycnometer (Fig. 1) consisted of a Pyrex bulb of 5-cc. capacity to which was attached a 10-cm. length of precision bore tubing with an i.d. of 0.3488 cm. An index mark was scratched at the upper end of the stem and the volume to the mark was measured by weighing the pycnometer with and without water at room temperature. From the weight of the water, corrected for buoyancy, and the known density, the volume was calculated. In making a density measurement on the salt-rich mixtures, bismuth metal was weighed into the pycnometer and purified $BiCl_3$ was distilled into the bulb through the stem under a reduced pressure of 5 mm. of dry air or nitrogen. The pycnometer was then sealed off at the top of the stem.

For the metal-rich mixtures the bismuth was filtered into the pycnometer and heated under vacuum to remove occluded gases. It was necessary to tap the pycnometer gently during this operation to free the gas bubbles which tended to remain trapped in the bulb between the liquid metal and the glass. The $BiCl_3$ was then distilled into the metal under 5 mm. of dry N_2. The final sealing off was done under one-half atmosphere of dry N_2 and the pycnometer was transferred to the furnace without allowing the metal to solidify since expansion on cooling would crack the glass bulb.

The pycnometer was placed in a vertical position in an aluminum block inside a furnace (Fig. 1) and the height of the liquid level and the index mark on the stem were measured by sighting through a slit provided in the furnace wall

(1) (a) This work was made possible by the financial support of the Research Division of the United States Atomic Energy Commission. (b) Presented in part at the 130th National Meeting of the American Chemical Society, Miami, Florida, April, 1957.

(2) (a) D. Cubicciotti, *J. Am. Chem. Soc.*, **74**, 1198 (1952); (b) M. A. Bredig, H. R. Bronstein and Wm. T. Smith, Jr., *ibid.*, **77**, 1454 (1955); (c) K. Grjotheim, F. Grönvold and J. Krogh-Moe, *ibid.*, **77**, 5824 (1955); (d) J. D. Corbett, S. von Winbush and F. C. Albers, *ibid.*, **79**, 3020 (1957).

(3) D. Cubicciotti, F. J. Keneshea, Jr., and C. M. Kelley, THIS JOURNAL, **62**, 463 (1958).

(4) (a) B. G. Eggink, *Z. physik. Chem.*, **64**, 449 (1908); (b) L. Marino and R. Becarelli, *Atti accad. nazl. Lincei*, **25**, 326 (1916); (c) M. A. Sokolova, G. G. Urazov and V. G. Kuznetsov, *Khim. Redkikh Elementov, Akad. Nauk S. S. S. R., Inst. Obshchei i Neorg. Khim.*, **1**, 102 (1954).

(5) A. H. W. Aten, *Z. physik. Chem.*, **66**, 641 (1909).

(6) A. Voigt and W. Biltz, *Z. anorg. allgem. Chem.*, **138**, 277 (1924).

(7) F. M. Jaeger and J. Kahn, *Proc. Acad. Sci. Amsterdam*, **19**, 381 (1916).

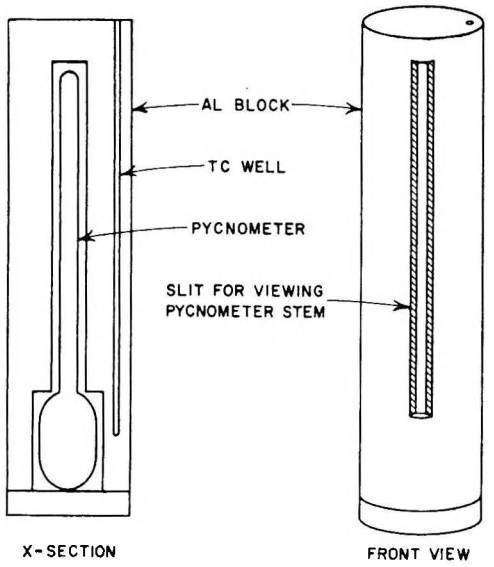

Fig. 1.—Density apparatus used for Bi-$BiCl_3$ mixtures.

and aluminum block. The metal block was used to obtain temperature uniformity and the slits in both the furnace wall and in the aluminum block were covered with Pyrex plate glass to prevent unwanted air currents. The furnace consisted of two semi-cylindrical Hevi Duty resistance heating elements, 8 in. long, insulated with fire brick.

The height of the liquid column of the pure $BiCl_3$ and salt-rich Bi–$BiCl_3$ mixtures was measured with a cathetometer within ±0.005 cm. For the bismuth and metal-rich mixture, heights were measured within ±0.001 cm. by means of a traveling microscope. Although liquid $BiCl_3$ was a reddish-yellow color when heated, it was transparent enough so that the bottom of the meniscus could be observed. The slight difference between the shapes of the menisci of $BiCl_3$ and H_2O (used for calibration) was estimated to introduce less than 0.05% error in the densities. The $BiCl_3$-rich mixtures were quite opaque and the bottom of the meniscus could not be seen. Thus it was necessary to read the top of the meniscus and to apply a correction for the meniscus height. This height was assumed to be the same as for pure $BiCl_3$ and was determined by direct measurement on $BiCl_3$. The meniscus in the case of bismuth and the bismuth-rich solution was approximately the same shape as mercury in glass, and hence the bulbs for these measurements were calibrated with mercury.

The densities were calculated in the following way. The volume of the liquid was computed by subtracting the volume of that portion of the stem which contained no liquid from the total volume of the pycnometer measured to the index mark. Corrections were made for expansion of the glass with temperature. The liquid volume was thus calculated from the expressions

$$V_t^p = V_0^p[1 + \alpha_g(t - t_0)]$$
$$V_t^l = V_t^p - \pi r^2(h_i - h_l)$$

where

V_t^p = vol. of pycnometer at temperature t
V_0^p = vol. of pycnometer at room temperature
α_g = cubical coefficient of thermal expansion for Pyrex = $3 \times 32.5 \times 10^{-7}$ °C.$^{-1}$ [8]
t = temperature of measurement, °C.
t_0 = room temperature, °C.
V_t^l = volume of liquid at temperature t
h_i = height of index mark
h_l = height of top of liquid column
r = inner radius of stem

After the height measurements were made, the pycnometer and contents were weighed and the tip of the stem was broken off. Care was taken not to lose any glass. The metal–salt mixture was melted out of the bulb and the glass was washed out with HNO_3, rinsed with water, dried and weighed. The weight of the metal–salt mixture was then obtained by difference. Since the weight of the added bismuth metal was known, the weight of the $BiCl_3$ in the mixture could be determined and the composition calculated. In some instances the amount of chloride was determined gravimetrically (as AgCl) to calculate compositions. The total weight of the Bi–$BiCl_3$ mixtures was corrected for buoyancy. The densities were then calculated from the mass and the volume.

Temperatures were measured to the nearest 0.1° by either chromel–alumel or Pt–Pt:10% Rh thermocouples. The thermocouples were calibrated against National Bureau of Standards samples of tin, lead and zinc according to procedures recommended by the NBS. The thermocouple was situated in a well in the aluminum block such that the end was next to the bulb portion of the pycnometer. In order to prevent condensation in the vapor space above the liquid, the top part of the stem was maintained at a temperature 4 to 6° higher than the temperature of the bulk of the liquid. The temperature over the length of the bulb portion, which contained the major part of the liquid, did not vary by more than ±0.5°. The furnace current was controlled either manually or by a modified Wheelco "Amplitrol" controller. Sufficient time was allowed for the contents of the bulb to reach temperature equilibrium. Only those readings were accepted which remained constant over a 15-min. period after reaching temperature. The amount of material in the vapor space above the liquid was estimated to be negligible.

The $BiCl_3$ was the analytical reagent grade pretreated by bubbling HCl through the molten salt. The salt was then distilled three times under 5 mm. of dry air or N_2, the latter being used for the metal-rich solutions. The final distillation was made directly into the pycnometer. A sample of $BiCl_3$ was analyzed for chlorine by precipitation as AgCl and 33.72% Cl was found, compared with 33.73% theoretical for $BiCl_3$. The bismuth metal was Johnson–Matthey material obtained from Jarrell–Ash and was specified by the manufacturer to have about 15 p.p.m. of various metal impurities by spectroscopic analysis. The bismuth was used without further treatment for the $BiCl_3$-rich solutions. For the bismuth and bismuth-rich solution the bismuth was heated to 350–400° under vacuum and then filtered into the pycnometer through a coarse fritted glass filter under a N_2 atmosphere.

Results

The densities of the various Bi–$BiCl_3$ mixtures studied are shown as a function of temperature in Fig. 2. The data in all cases fit a linear equation of the form $\rho = a - bt$ where ρ is the density in g./cc., a and b are constants, and t is the temperature in °C. The curves drawn in Fig. 2 were obtained from a least squares treatment of the data. The values of the constants a and b obtained from this treatment are shown in Table I, together with the standard error, defined as the square root of the mean of the squared deviations of the observed density values from the least squares curve.

TABLE I

DENSITY EQUATIONS FOR Bi–$BiCl_3$ MIXTURES

Mole fraction Bi	$\rho = a - bt$ (g./cc.) a	$b \times 10^3$	Standard error (g./cc.)	Temp. range (°C.)
0	4.417	2.20	0.001	239–331
.109	4.614	2.06	.003	289–398
.206	4.866	2.08	.001	267–424
.269	5.068	2.13	.011	295–452
.320	5.236	2.15	.003	310–443
.986	10.386	1.29	.002	329–439
1.000	10.390	1.29	.004	311–442

The density measurements were made over as wide a range as possible between 230 and 450° (the particular range being determined by the amount of material in the pycnometer). The

(8) "Properties of Selected Commercial Glasses," Corning Glass Works, Corning, N. Y., 1957, p. 8.

pressure in the bulb varied between 5 mm. at the lower temperatures and about 1 atm. in the vicinity of 450° due to vaporization of the salt. Since liquid salt compressibilities are of the order of 10^{-6} atm.$^{-1}$,[9] the change of volume with pressure over this range of pressure was of the order of 10^{-4}%, which was small enough to be ignored.

Except for the two solutions at compositions of 0.420 and 0.470 mole fraction of bismuth, all measurements were made on solutions which were single homogeneous phases. According to phase diagram information[4] the 0.420 and 0.470 solutions were measured over the two-liquid phase range. It was not possible to ascertain that two phases were present when making the measurements because the interface was not in the visible portion of the pycnometer stem. Therefore these measurements yielded only the total volumes of the inhomogeneous mixtures in each case. These volumes were divided into the total weights and the ratio plotted in Fig. 2 for comparison with the densities of the homogeneous mixtures. In an inhomogeneous mixture, the total weight divided by the total volume is not the true density, although that ratio is independent of the amount of the mixture at a given over-all composition.

For pure $BiCl_3$ the data of Voigt and Biltz[6] were 0.2–0.5% higher than those of Jaeger and Kahn.[7] The density values observed here for pure $BiCl_3$ were 0.1–0.4% higher than those of Jaeger and Kahn. Aten's[5] data were 1.5% higher than the data of Jaeger and Kahn and, unlike the other three measurements, showed a non-linear variation with temperature. The density observed for pure bismuth was 0.4% lower than literature values[10] over the temperature range investigated.

Using the density data, the molar volumes $\bar{V}$, of the solutions were calculated for various temperatures using the expression

$$\bar{V} = \frac{M_1x_1 + M_2x_2}{\rho}$$

where

M_1, M_2 = molecular weight of $BiCl_3$, Bi
x_1, x_2 = mole fraction of $BiCl_3$, Bi

The molar volumes at 250, 300, 350 and 400° are given as a function of composition in Fig. 3.

In the two-phase region it can be shown that the total volume varies linearly with composition since the density of each phase is constant (at constant temperature). Therefore, in Fig. 3 a straight line (dashed) was drawn through the experimental points measured in the two-phase region. This helped to define the molar volume in the single phase regions.

The partial molar volumes of $BiCl_3$ and bismuth, $\bar{V}_1$ and $\bar{V}_2$, respectively, at a particular composition and temperature, were calculated from the curves of Fig. 3 by the method of intercepts. Some of the results obtained are shown in Table II. The error in the values for the molar volume is estimated to be ±0.1% and is magnified in determining $\bar{V}_1$ and $\bar{V}_2$ because of the extrapolations involved. Thus the error in $\bar{V}_2$ amounts to ±6 cc. at infinite dilution at a temperature of 400°, as indicated in Table II. Values of partial molar volumes for the metal-rich solutions were determined by extrapolating a straight line through only two experimental points. The long extrapolation necessary for $\bar{V}_1$ led to the estimated error of ±15 cc. shown in Table II.

(9) J. O'M. Bockris and N. E. Richards, *Proc. Roy. Soc.* (*London*), **A241**, 44 (1957).

(10) "Liquid Metals Handbook," 2nd ed., U. S. Atomic Energy Commission-Department of the Navy, Washington, D. C., June, 1952 p. 45.

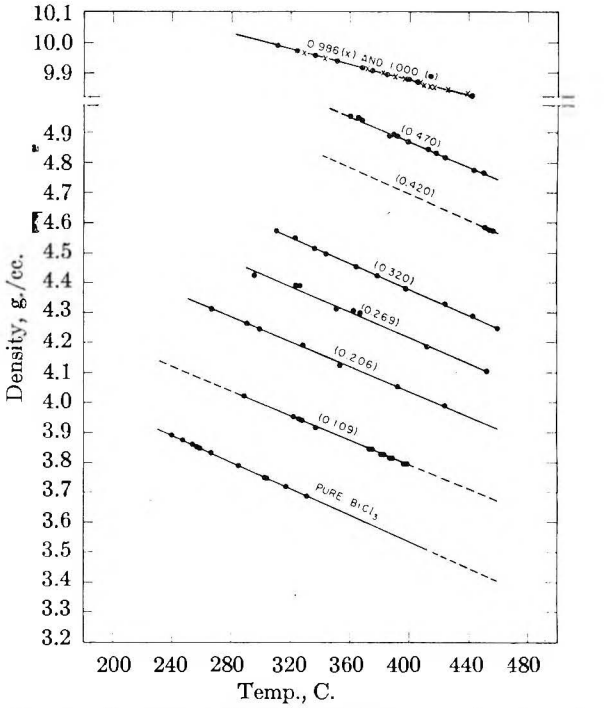

Fig. 2.—Density of Bi–$BiCl_3$ mixtures as a function of temperature. Numbers on curves indicate mole fraction Bi. The 0.420 and 0.470 mixtures were inhomogeneous and hence the volumes indicated are not true densities.

TABLE II

PARTIAL MOLAR VOLUMES IN Bi–$BiCl_3$ MIXTURES

	Mole Fraction Bi			
	0	0.1–0.2	0.3	1.0
	250°			
$\bar{V}_{Bi}$, cc	12 ± 2	15 ± 1	....	....
$\bar{V}_{BiCl_3}$	81.6 ± 0.1	81.3 ± 0.3	....	....
	300°			
$\bar{V}_{Bi}$	10 ± 2	13 ± 1	16 ± 1	20.9 ± 0.1
$\bar{V}_{BiCl_3}$	84.0 ± 0.1	83.7 ± 0.6	82.6 ± 0.6	35 ± 15
	350°			
$\bar{V}_{Bi}$	8 ± 3	12 ± 1	17 ± 1	21.0 ± 0.1
$\bar{V}_{BiCl_3}$	86.5 ± 0.1	86.2 ± 0.2	84.2 ± 0.6	35 ± 15
	400°			
$\bar{V}_{Bi}$	3 ± 6	11 ± 1	15 ± 1	21.3 ± 0.1
$\bar{V}_{BiCl_3}$	89.2 ± 0.1	88.7 ± 0.2	87.2 ± 0.6	35 ± 15

Discussion

It can be seen from these data that when bismuth is mixed with $BiCl_3$ there is a decrease in the total volume. In the dilute solutions of bismuth in $BiCl_3$, $\bar{V}_1$ is approximately the same as $\bar{V}_1$ and increases with increasing temperature, while $\bar{V}_2$ is considerably smaller than $\bar{V}_2$ and decreases with increasing temperature. Thus the solution behaves quite normally with respect to the addition of $BiCl_3$, since the increase in volume during such a process

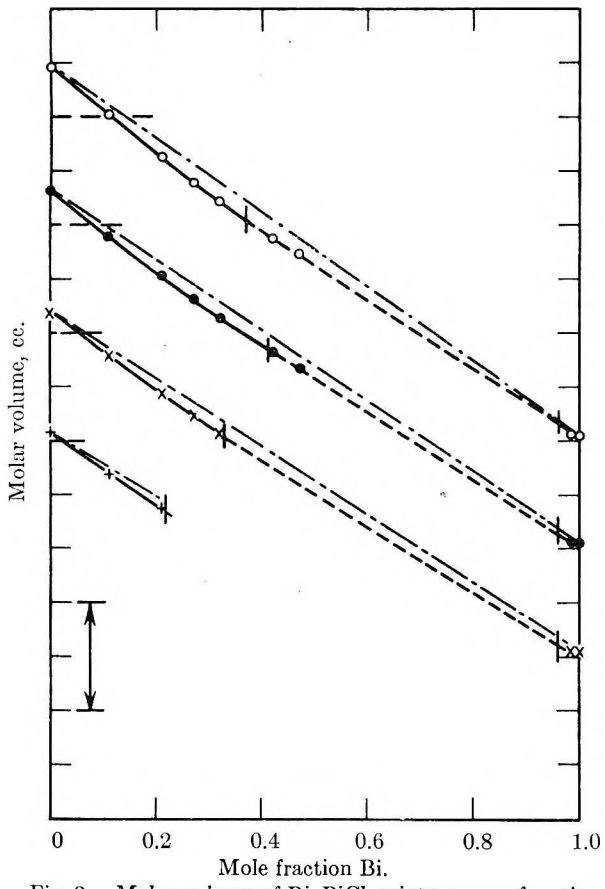

Fig. 3.—Molar volume of Bi–$BiCl_3$ mixtures as a function of composition: ○, 400°; ●, 350°, ×, 300°, +, 250°. |-----|, approximate 2-phase region from phase diagram.[4] Curves are displaced for clarity; the short horizontal line on each curve represents a volume of 80 cc. The vertical arrow represents 20 cc. The upper curve in each case represents additive volumes.

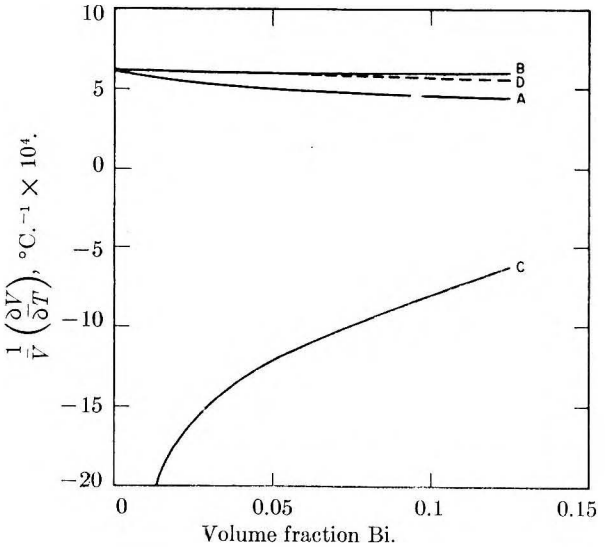

Fig. 4.—Expansivity of Bi-$BiCl_3$ solutions at 400° as a function of volume fraction of added Bi: curve A, $(1/\bar{V})(\partial \bar{V}/\partial T)$; curve B, $(1/\bar{V}_1)(\partial \bar{V}_1/\partial T)$; curve C, $(1/\bar{V}_2)(\partial \bar{V}_2/\partial T)$; curve D, "ideal" expansivity.

corresponds to the volume of $BiCl_3$ added. It is possible to explain the result that $\bar{V}_2$ is smaller than $\bar{V}_2$ by suggesting that when the metal goes into solution, bismuth atoms, or ions formed from ionization of the metal, enter into the interstitial octahedral holes in the liquid quasi-lattice, as has been suggested for other systems.[2] The volume changes involved in such a process can be estimated, assuming that just above the melting point a good deal of short range order is present and that the liquid salt may be approximated by a solid-like structure. Thus, if we make the approximation that the halogen ions in the liquid $BiCl_3$ are arranged in a close-packed lattice, then $^1/_3$ of the octahedral holes which are formed in this array will be occupied by the Bi^{+3} ions of the salt.[11] This leaves a sufficient number of empty octahedral holes to accommodate additional bismuth up to a concentration corresponding to BiCl ($x_2 = 0.667$). If the chloride ions around an octahedral position are regarded as hard spheres just in contact, the maximum radius of a sphere which can be accommodated by an octahedral hole can be calculated to be 0.75 Å. and the volume of such a sphere would be 1.7 (Å.)^3. As a first approximation, we assume the unoccupied holes have this volume, and calculate the volume change accompanying the introduction of bismuth atoms into these holes. From the known radius of bismuth atoms in solid bismuth[12] and from the densities of solid[13] and liquid bismuth, the radius of the bismuth atom in liquid bismuth can be estimated to be about 1.78 Å. The volume of a sphere with this radius is 23.6(Å.)^3. Since this is considerably larger than 1.7(Å.)^3, the introduction of a bismuth atom into a hole will cause the chlorides to be pushed apart to accommodate the bismuth. The change in volume during such a process amounts to 21.9 (Å.)^3 per bismuth atom added, or about 13 cc. per gram-atom of bismuth. This value can be compared with the values found for the partial molar volume of bismuth in the solutions. For a dilute solution at 250°, some 20° above the melting point of $BiCl_3$, the value of $\bar{V}_2$ from Table II is seen to be between 12 and 15 cc., in very good agreement with the calculated volume. On the other hand, if one calculates the change in volume accompanying the addition of one gram-atom of bismuth which is assumed to undergo ionization to Bi^{+3}, a value of about 3 cc. is obtained ($r_{Bi^{+3}} = 1.20$ Å.[12]). This is much smaller than the measured value of 12 cc. at 250°. However, the formation of Bi^{+2} or Bi^{+1} would give calculated values of $\bar{V}_2$ somewhere between 3 and 13 cc. In view of the approximate nature of the calculations involved, one cannot decide on the basis of these figures whether atoms or ions are injected into the interstitial holes. In either case the calculated volume changes are of the correct order of magnitude, lending support to the proposed dissolution mechanism.

The above model is consistent with the observation that $\bar{V}_2$ in the salt-rich mixtures decreases with increasing temperature at constant composition (Table II) since one would expect the liquid lattice to expand with increasing temperature and hence

(11) A. F. Wells, "Structural Inorganic Chemistry," Oxford Press, London, 1945, p. 278.

(12) C. J. Smithells, "Metals Reference Book," Interscience Publishers, Inc., New York, 1949, p. 167.

(13) Ref. 12, p. 413.

to accommodate the bismuth atoms or ions more readily. The change in available volume with temperature may be estimated by assuming that an octahedral hole is equivalent to a cell in the cell model of liquids, and hence the octahedral hole volume has the same temperature coefficient as the cell-free volume of the liquid. Bockris and Richards[9] have found that for a number of molten halides the free volume increases by about a factor of two for a 150° change in temperature. For $BiCl_3$ the octahedral hole volume can be calculated to be about 2 cc./mole and, if this doubles for a 150° change in temperature, then the change in $\bar{V}_2$ should be about 2 cc. This calculated volume change compares fairly well with the experimental decrease of $\bar{V}_2$, (Table II).

For the metal-rich solutions the data show that at 400°, in the range of 0.98 to 1.00 mole fraction of bismuth, $\bar{V}_2 = \tilde{V}_2$ while $\bar{V}_1 = 35$ cc., or 0.4 the molar volume (90 cc.) of $BiCl_3$. If the liquid bismuth lattice is pictured as being composed of Bi^{+3} ions with internuclear distances corresponding to about twice the radius of a bismuth atom,[14] then it is possible to put a Cl^- ion into an octahedral hole in such a lattice with only a small volume expansion. The Bi^{+3} ions which are added along with the Cl^- ions may be assumed to occupy normal lattice positions for bismuth and to become indistinguishable from the original bismuth atoms. The indistinguishability of the added bismuth has support in the observation[15] that the cryoscopic effect of $BiCl_3$ in bismuth corresponds to the addition of only 3 foreign particles, *i.e.*, only the 3 Cl^- ions. Thus part of the volume increase which is produced on adding a mole of $BiCl_3$ to bismuth is due to the addition of a mole of Bi^{+3} having a volume corresponding to the molar volume of bismuth metal, about 20 cc. To this must be added a further volume increase due to the slight expansion brought about by the chlorides. Such a mechanism would thus result in an estimated partial molar volume for $BiCl_3$ between 20 and 90 cc., which is not in disagreement with the observed value of 35 cc.

The concept of filling the octahedral holes in the liquid lattice is useful in discussing the behavior of the thermal expansion of the Bi–$BiCl_3$ solutions. It can be shown that the thermal expansion coefficient of the solution, $\alpha = 1/V(\partial V/\partial T)$, is given by the expression

$$\frac{1}{\bar{V}}\left(\frac{\partial \bar{V}}{\partial T}\right) = \alpha = \left[\frac{x_1\bar{V}_1}{x_1\bar{V}_1 + x_2\bar{V}_2}\right]\frac{1}{\bar{V}_1}\left(\frac{\partial \bar{V}_1}{\partial T}\right) + \left[\frac{x_2\bar{V}_2}{x_1\bar{V}_1 + x_2\bar{V}_2}\right]\frac{1}{\bar{V}_2}\left(\frac{\partial \bar{V}_2}{\partial T}\right) = \phi_1\frac{1}{\bar{V}_1}\left(\frac{\partial \bar{V}_1}{\partial T}\right) + \phi_2\frac{1}{\bar{V}_2}\left(\frac{\partial \bar{V}_2}{\partial T}\right) \quad (1)$$

where ϕ_1 and ϕ_2 are volume fractions. For an ideal solution $1/\bar{V}_1(\partial \bar{V}_1/\partial T)$ and $1/\bar{V}_2(\partial \bar{V}_2/\partial T)$ are equal to the expansivities, α_1 and α_2 of the pure components, and the total expansion coefficient becomes

$$\alpha = \phi_1\alpha_1 + \phi_2\alpha_2 \quad (2)$$

According to this expression, α for an ideal solution is a straight line function of the volume fraction. This is shown by the dashed line (D) in Fig. 4 for a temperature of 400°. The experimentally obtained values for α at 400° shown in Fig. 4 (curve A), were found to exhibit negative deviations from the additivity curve. The contributions of $BiCl_3$ and bismuth to the total solution expansivity, *i.e.*, $1/\bar{V}(\partial \bar{V}/\partial T)$, are also shown in Fig. 4 as curves B and C, respectively. The almost constant value for $BiCl_3$ indicates that the $BiCl_3$ expansivity in solution is the same as in pure $BiCl_3$. On the other hand, the bismuth expansivity in the solution is seen to be negative and it is this contribution which causes the total expansivity to show negative deviations (equation 1). The negative values for $1/\bar{V}_2(\partial \bar{V}_2/\partial T)$ occur because $(\partial \bar{V}_2/\partial T) < 0$, as can be observed in Table II. As suggested before this results from better accommodation of bismuth in the liquid lattice as the temperature increases.

Acknowledgments.—The authors are indebted to Mr. W. Wilson for assistance in the experimental work, to Mr. W. E. Robbins for analytical help, and to Dr. C. M. Kelley for many helpful discussions and suggestions.

(14) Wells, ref. 11, p. 542–3, has pointed out that there are about five effective free electrons per bismuth atom in liquid bismuth, so that such a picture does not seem too unreasonable.

(15) S. J. Yosim and T. A. Milne, Report NAA-SR-1925, Atomics International, Canoga Park, California, July, 1957.

PYROLYSIS OF POLY-α-METHYLSTYRENE[1]

BY DANIEL W. BROWN AND LEO A. WALL

Contribution from the Polymer Structure Section, National Bureau of Standards, Washington 25, D. C.

Received March 19, 1958

The rates of volatilization and the decrease in degree of polymerization have been measured for fractions of poly-α-methylstyrene. The rates increase with initial DP. The DP of the residue decreases moderately. The activation energy is about 65 kcal. per mole of monomer unit produced. The results, interpreted according to the theory of chain degradation, indicate random initiation and a "zip" length of 1340 monomer units produced per chain activated by either initiation or transfer.

Introduction

It has been shown that the yield of monomer from the pyrolysis of poly-α-methylstyrene *in vacuo* is about 95%.[2] The activation energy for the rate of pyrolysis of whole polymer has been reported by various investigators as 45[3] and as 58[4] kcal. per chemical repeating unit. The thermal decomposition behavior of this polymer has not, as yet, been very thoroughly studied. Certain similarities exist between it and polymethyl methacrylate, such as basic structure, simplicity of the pyrolysis products, and low thermal stability. The latter two properties facilitate kinetic studies to some extent. However, certain dissimilarities exist that suggest random initiation, which requires a study of rates of volatilization as a function of polymer chain length.

The present work reports the rates of pyrolysis and the activation energies of fractions whose degrees of polymerization, DP, ranged from 670 to 9530. For several fractions the DP of the residue relative to the initial DP was determined at different conversions.

Experimental

Several viscosity grades of sodium-polymerized whole polymer were obtained from the Dow Chemical Company. Three of them were fractionated by precipitation from benzene with isopropyl alcohol. The intrinsic viscosities of the fractions ranged from 0.31 to 3.19 dl./g. The DP's of five fractions were determined by light scattering measurements using benzene as a solvent. Between DP's of 860 and 4100 the data fit the viscosity relation

$$[\eta] = 1.1 \times 10^{-3} [DP]^{0.57}$$

It was assumed this relation also could be applied without serious error throughout the experimental range of the present degradation experiments, which had DP's ranging from 670 to 9530.

The apparatus was similar to that used by Grassie and Melville[5] in the pyrolysis of polymethyl methacrylate. It consisted of a heated vacuum chamber, a glass bucket that can be lowered into the furnace while the system is evacuated, a thermocouple gage and recorder, and an orifice to permit the buildup of measurable pressure at low rates of pyrolysis.

The principle of operation is that the steady-state pressure produced in the system up-stream of the orifice is determined by the rate of production of volatile material. Since poly-α-methylstyrene produces essentially pure monomer this is substantially equal to the rate of pyrolysis.

The apparatus was calibrated by evaporating α-methylstyrene at constant rates from calibrated capillary tubes. A graph relating the rate of monomer through-put to recorder response was thus obtained. Curvature was found in this graph as a result of the non-linear response of the thermocouple gage to pressure.

A sample of polymer from 12 to 120 mg. was weighed into a glass bucket and dissolved in benzene. After evaporation at room temperature the film was preheated in the evacuated apparatus at 200° for about 20 minutes. This heating removed most of the solvent and did not change the molecular weight. The furnace was then heated to the pyrolysis temperature, the recorder was started, and the bucket containing the sample was lowered into the furnace. After 30 to 60% of the material had been pyrolyzed the bucket was raised again.

The plot produced by the recorder was converted to rate in milligrams per minute *versus* time. A typical curve is shown in Fig. 1. The arrow marks the time at which the thermocouple in the bucket first reached the pyrolysis temperature, 282.5°. The broken portion of the curve therefore represents rates that took place at lower temperatures. Subsequently, any temperature change was less than 0.2°, the smallest change we could observe. The initial small peak is caused by residual solvent. The rate of decomposition at pyrolysis temperature decreases with time because the amount of polymer in the bucket is decreasing.

Curves like that of Fig. 1 were integrated to determine the amount of monomer produced. This was found to be substantially equal to the observed weight loss. By integrating these curves to different times and dividing the weight loss and corresponding rates by the initial weight, curves of rate *versus* conversion like that in Fig. 2 were obtained. All of these curves had a linear portion after the pyrolysis temperature was reached and then tended to level off at high conversions. The linear portion of the plot was extrapolated to zero conversion to obtain values characteristic of the fractions.

Results

The curve in Fig. 2 is typical of all the rate curves. In all experiments the time was noted at which the furnace temperature was attained. No indication of a maximum in the rate was detected after this temperature was reached. The point below 10% conversion in Fig. 5 was obtained at a lower temperature. The leveling off of the rate at high conversion was verified in a number of runs; it is believed to be significant, as will be seen in later discussion. Initial rates obtained by extrapolation are shown in Fig. 3 for a series of polymers of varying D.P. Activation energies calculated from these initial rates were obtained on several polymer fractions, but shortage of material prevented this investigation on other fractions. However, it was ascertained that these activation energies did not change by more than 6 kcal. per chemical repeating unit for the D.P. range of the experimental points shown in Fig. 3.

The relationships of some extrapolated rates are shown in Fig. 4 as a function of reciprocal temperature. The temperature span for most fractions is about 25°. The temperatures could be measured to within about 0.2°. Straight lines were ob-

(1) Presented in part at the 130th Meeting of the American Chemical Society, Atlantic City, N. J., September 16–21, 1956.

(2) S. Straus and S. L. Madorsky, *J. Research Natl. Bur. Standards*, **50**, 165 (1953).

(3) H. H. G. Jellinek, *J. Polymer Sci.*, **3**, 850 (1948); **4**, 1 (1949).

(4) S. L. Madorsky, *ibid.*, **11**, 491 (1953).

(5) N. Grassie and H. W. Melville, *Proc. Roy. Soc. (London)*, **A199**, 1 (1949).

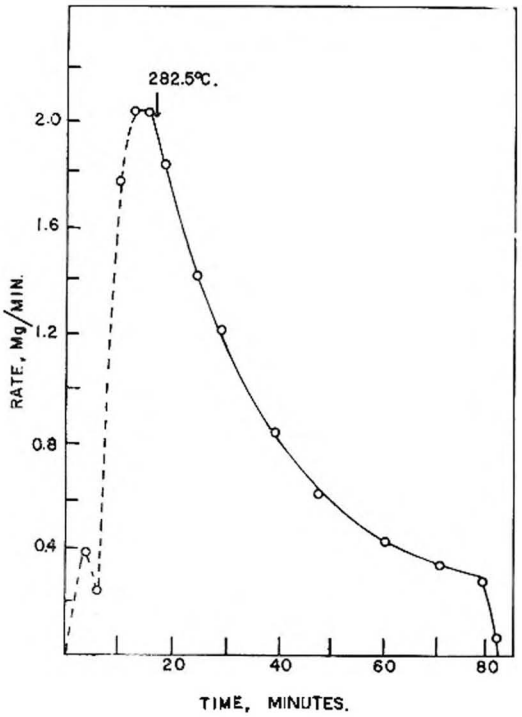

Fig. 1.—Rate of pyrolysis as a function of time. Arrow indicates time at which polymer reached pyrolysis temperature of 282.5°.

tained for most fractions of which sufficient quantity of material was available for a complete study. An uncertainty of 6% in the extrapolated rates covers all departure from straight-line behavior. This may be regarded as the relative reproducibility of the rates, and with the previously mentioned uncertainty in the temperature measurement the results are equivalent to ±4 kcal. in the activation energy. It is clear that the rates increase with initial DP. The increase is less than proportional, though, being only 4-fold for a 15-fold increase in the DP.

The viscosity average DP of the residue relative to the initial DP at different extents of pyrolysis is shown in Fig. 5. True number-average ratios would be somewhat lower since the viscosity-average to number-average ratio is higher for a distribution than for a fraction.

Discussion

The results will be discussed in terms of the following chain-reaction mechanism, which has been developed in a quantitative fashion by Simha, Wall and Blatz.[6-8]

$$\sim CH_2CHXCH_2CHX\sim \xrightarrow{k_1} \sim CH_2CHX\cdot + \sim CHXCH_2\cdot \quad \text{Initiation}$$

$$\sim CH_2CHXCH_2CHX\cdot \xrightarrow{k_2} \sim CH_2CHX\cdot + CH_2{=}CHX \quad \text{Propagation}$$

$$\sim CH_2CHX\cdot + \sim CH_2CHXCH_2CHX\sim \xrightarrow{k_2} \sim CH_2CH_2X + \sim CH_2CX{=}CH_2 + \sim CHX\cdot \quad \text{Intermolecular transfer}$$

(6) R. Simha, L. A. Wall and P. J. Blatz, *J. Polymer Sci.*, **5**, 615 (1950).

(7) R. Simha and L. A. Wall, *ibid.*, **6**, 39 (1951).

(8) R. Simha and L. A. Wall, THIS JOURNAL, **56**, 707 (1952).

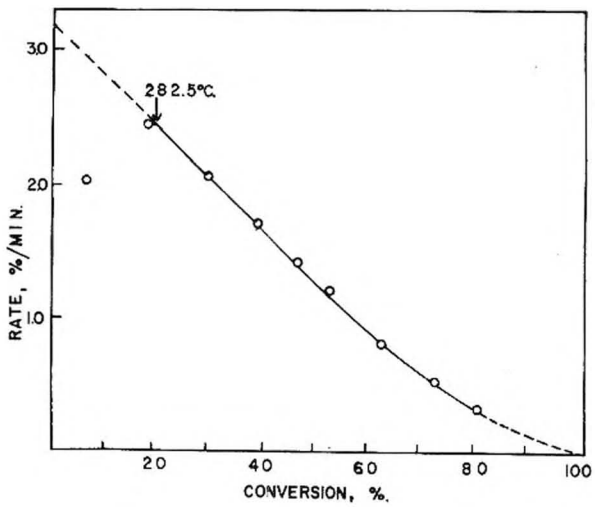

Fig. 2.—Rate of pyrolysis as a function of conversion. Arrow indicates conversion at which polymer reached pyrolysis temperature of 282.5°.

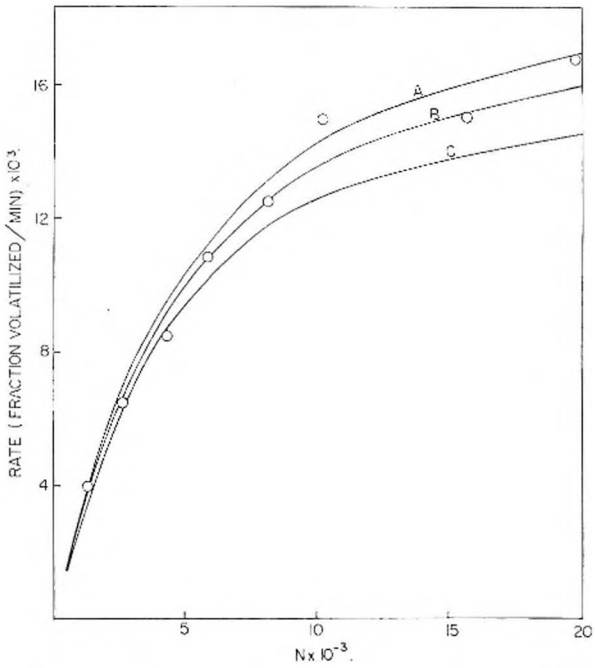

Fig. 3.—Initial rates of volatilization as a function of N, or (2 × DP), for poly-α-methylstyrene fractions. The curves represent theory, equation 3: $\sigma = 0$; $k_1 = 3.42 \times 10^{-6}$; for A, $1/\epsilon = 1476$; for B, $1/\epsilon = 1342$; for C, $1/\epsilon = 1208$.

$$2R \xrightarrow{k_4} 2P \quad \text{Termination}$$

An intramolecular transfer step of the type

$$\sim CHXCH_2CHXCH_2CHX\cdot \xrightarrow{k_3'} \sim CHX\cdot + CH_2{=}CXCH_2CH_2X$$

is also postulated. It, however, is kinetically indistinguishable from the propagation.

Two parameters, $1/\epsilon$ and σ, are used. The former is the ratio of the sum of the rates of propagation, transfer and termination, to the sum of those of transfer and termination. The latter is the number of transfer acts per initiation. If $1/\epsilon >> 1$, monomer is the product of pyrolysis. In

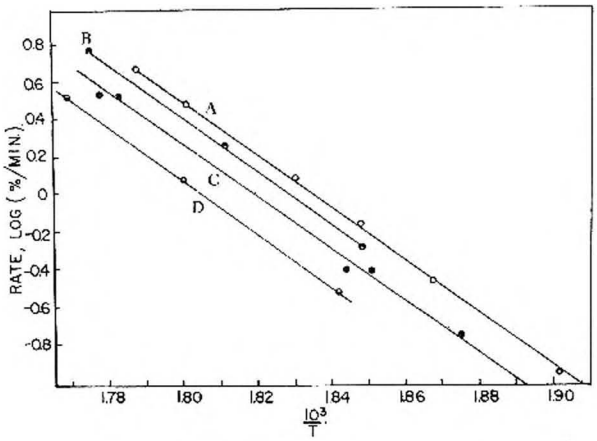

Fig. 4.—Logarithm of the rate of pyrolysis as a function of the reciprocal of the absolute temperature: (A) ○, 345,000 molecular weight; (B) ◓, 258,000 molecular weight; (C) ●, 155,000 molecular weight; (D) ◒, 79,000 molecular weight.

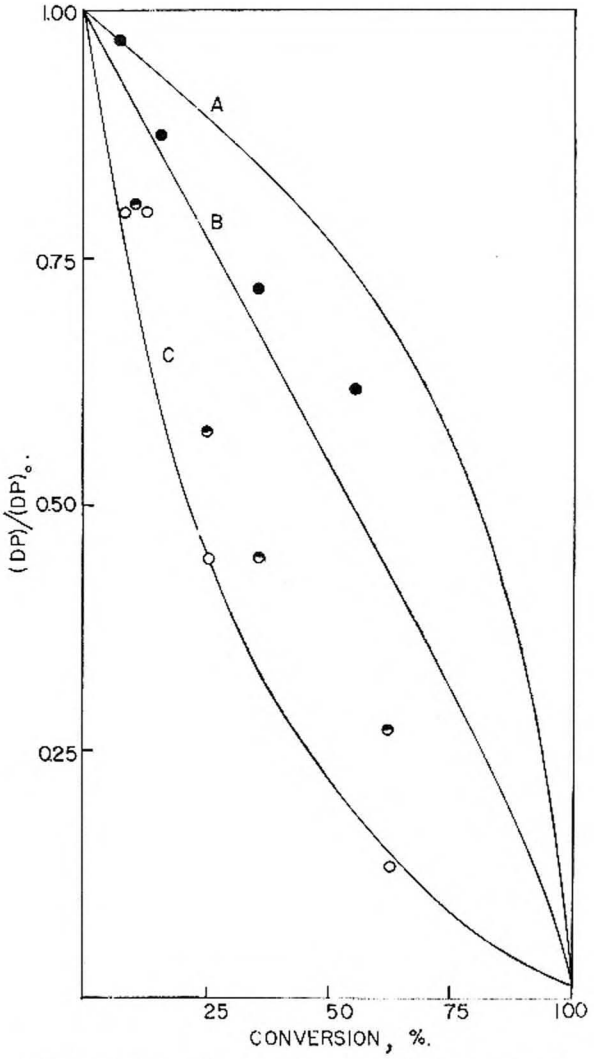

Fig. 5.—Relative degree of polymerization as a function of conversion: ○, 1,120,000 M_n; ◓, 620,000 M_n; ●, 97,000 M_n. The curves are theoretical; $(1/\epsilon - 1)$, for A, = 403, for B, = 268, and for C, = 66.1.

the case of polystyrene deuteration in the α-position of the monomer unit increases the monomer yield[9] and decreases the rate of drop in molecular weight, due to the slower transfer of deuterium atoms.

In the present work with poly-α-methylstyrene, the α-position is blocked by a methyl group and a high monomer yield results indicating again that transfer is small compared to propagation. However, enough transfer acts may still occur *via* the primary or secondary hydrogens of the polymer molecule to compete with the initiation act. There is evidence for transfer of this magnitude in the photoinitiated thermal decomposition of polymethyl methacrylate.[10]

Besides the products, which for this polymer are essentially pure monomer, the important criteria for the mechanism are (1) the variation of the initial rate with N (the average number of carbon atoms in the polymer chain), (2) its variation with conversion, and (3) the change in DP with conversion.

Effect of Molecular Size. The increase in initial rate with N, which is indicative of the mode of initiation, will be discussed first. It differs strongly from earlier results obtained with polymethyl methacrylate by Grassie and Melville[5] and by Brockhaus and Jenckel,[11] whose initial rates are shown in Fig. 6. The former workers interpreted their results as end initiation followed by depropagation which completely consumes radicals of small N; radicals of large N have long enough lifetimes to terminate bimolecularly. The rate, then, should be independent of N at small values of N, and inversely proportional to the square root of N at large values of N. This is equivalent to varying N from $1/\epsilon >> N/2 >> 1$ to $N/2 >> 1/\epsilon >> 1$.[8] Brockhaus and Jenckel do not observe a region in which the initial rate is independent of molecular weight, but find a weak effect at all weights. At high conversion (>30%) they show that the inverse relation reverses, and becomes like that reported here for poly-α-methylstyrene. The reversal was interpreted as indicating an increasing relative contribution of random initiation as a result of the depletion of labile end groups.

With random initiation, when $1/\epsilon >> N/2 >> 1$, the initial rate[12] is given by

$$\left(\frac{dC/dt}{t \to 0}\right) = k_i(1 + \alpha/2)N - k_t(1 + \alpha/2)N^2\epsilon/6 \ldots \quad (1)$$

When $N/2 >> 1/\epsilon >> 1$ the initial rate[9] is

$$\left(\frac{dC/dt}{t \to 0}\right) = 4k_2(k_i/k_t)^{1/2}]/[2(N-1)Q_{N-1}(0)]^{1/2} \quad (2)$$

In the above, k_I, k_2 and k_t are the rate constants for initiation, propagation and termination, respectively, the term $(N-1)Q_{N-1}(0)$ represents the initial concentration of bonds, and the rate dC/dt is the fraction of initial sample removed per unit time.

At small values of N, equation 1 will reduce to its first term, and the rate will be proportional to N. At large values of N the rate is independent of N.

(9) L. A. Wall, D. W. Brown and V. E. Hart, *J. Polymer Sci.*, **15**, 157 (1955).

(10) P. R. E. J. Cowley and H. W. Melville, *Proc. Roy. Soc.* (*London*) **A210** 461 (1951).

(11) A. Brockhaus and E. Jenckel, *Makromolekulare Chem.*, **19**, 262 (1956).

(12) R. Simha, L. A. Wall and J. Bram, to be published.

The less-than-proportional increase with N that is observed implies that $N/2 \approx 1/\epsilon >> 1$. That is, the data obtained cover a transition region in which progressively more radicals terminate before completely depropagating as N is increased, but a substantial portion of radicals completely depropagate before being terminated at all values of N. The general expression[12] for the initial rate is

$$\lim_{t \to 0}(1/k_1)\, dC/dt = (1 + \sigma)(N - 4) - 4S/(N - 1) + [(N - 3)/(N - 1)](\sigma/2)$$

where

$$S = [(1 + \sigma)/4](N - 3 + L)(N - 3 - L + 2) + (2 + \sigma)(1 - (3/4)\epsilon) \quad (3)$$
$$[(1 - \epsilon)/\epsilon^2]\{[(N - 3)/2][\epsilon/(1 - \epsilon)] - 1 - [((L/2) - 1)(\epsilon/(1 - \epsilon)) - 1](1 - \epsilon)^{(N-3)/2 - L/2 + 1}\}$$

Any chain length equal to L or smaller evaporates without decomposition.

The unknown parameters were estimated from equation 1 as follows: The data were plotted in the form $(dC/dt)/N$ *versus* N. A straight line through the points representing the two lowest values of N was extrapolated to $N = 0$. The intercept, $k_1(1 + \sigma/2)$, was $3.42 + 10^{-6}$ min.$^{-1}$; and $1/\epsilon$ was calculated from the slope to be 1342. If radicals disappear bimolecularly throughout the experimental range, ϵ is independent of N, and the calculated value can be applied to the rest of the data. Substitution in equation 3, using $L = 12$, $\epsilon = 1/1342$, and $k_1(1 + \sigma/2) = 3.42 + 10^{-6}$ min.$^{-1}$, yields the middle curve, B, in Fig. 3. Varying ϵ by $\pm 10\%$ gives the other curves. As long as the product $k_1(1 + \sigma/2)$ is not changed, σ and k_1 may have any values without changing the calculated rate. This exceptional agreement between theory and experiments, as shown in Fig. 3, clearly indicates random initiation.

Effect of Conversion.—The curve of rate *vs.* conversion in Fig. 2 tends to level off at higher conversions because low molecular weight material is formed in the residue. This material degrades at a slower rate than the original material, and therefore this curvature is observed. Theoretical curves[12] also show this effect.

Variation in DP with Conversion.—The observed decreases in the relative DP with conversion may be the result of transfer or random initiation. Separation of these two processes will require additional measurements such as the lifetime of the decomposing radicals. The decrease observed with poly-α-methylstyrene is more than that observed with polymethyl methacrylate but less than that with polystyrene. Comparison with theoretical curves[12] constructed for the case of random initiation and $N = 403$ can be made since the ratio $N/(1/\epsilon - 1)$ is the critical quantity. From the theoretical curves A and B, Fig. 5,[12] we estimate that $N/(1/\epsilon - 1) = 403/300$ for our 97,000 molecular weight poly-α-methylstyrene since the experimental data lies between the curves A and B. Since $N = 97{,}000/59$, then $(1/\epsilon - 1)$ is 1230. This result agrees well with that calculated from the dependence of the initial rate on N. The same procedure, using the data for the highest molecular weight fraction (1.12×10^6) and curve C of Fig. 5, gives $(1/\epsilon - 1)$ a value of about 3000; in this case the procedure is not as valid.[12]

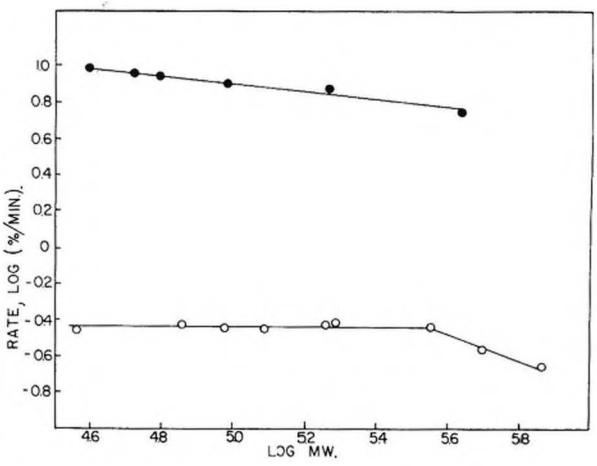

Fig. 6.—Logarithm of initial rates of volatilization as a function of the number-average molecular weights for polymethyl methacrylate: ●, Brockhaus and Jenckel, ref. 9; ○, Grassie and Melville, ref. 5.

Activation Energy.—Unlike previous work[13] with polymethyl methacrylate no definite change was found in the activation energy for depolymerization with increasing molecular weight. Such a change was predicted earlier on theoretical grounds.[14] Although at the higher molecular weights sufficient material was not available to determine precisely the activation energies, a difference of more than 5 kcal. per repeating unit would have been detected. It is concluded, then, that no large change in activation energy occurs with a change in DP.

For small values of N and $\sigma = 0$, $E = E_1$ (equation 1) and for large values of N, $E = E_1/2 + E_2 - E_4/2$ (equation 2). Assuming E to be about 65 kcal, at both limits and E_4 about 20 kcal., *i.e.*, termination is diffusion controlled as found in studies[10] on polymethyl methacrylate, then $E_1 \cong 65$ kcal., and $E_2 \cong 43$ kcal. per unit.

Since the heat of polymerization of α-methylstyrene, H_p, is 9 kcal.,[15] the activation energy for propagation in free radical polymerization, E_p, is 34. This high value may account for the failure of α-methylstyrene to polymerize by this means.

The pre-exponential factors of the rate constants are quite high, of the order of 10^{18}. An abnormally low pre-exponential factor for k_4 has been observed with polymethyl methacrylate.[16] If this low value carries over to poly-α-methylstyrene the high pre-exponential factor may reflect a high ratio of A_1 to A_4. This may imply considerable transfer, relative to initiation, since at low values of N and in the absence of transfer the pre-exponential is simply A_1 and would be expected to be about 10^{13}. High pre-exponential factors, 10^{16}, were observed in the degradation of polymethylene.[16] However, the decompositions of certain small molecules,

(13) S. Bywater, THIS JOURNAL, **57**, 879 (1953).
(14) R. Simha, *J. Polymer Sci.*, **9**, 465 (1952).
(15) D. E. Roberts, *J. Research Natl. Bur. Standards*, **44**, 221 (1950).
(16) L. A. Wall, S. L. Madorsky, D. W. Brown, S. Straus and R. Simha, *J. Am. Chem. Soc.*, **76**, 3430 (1954).
(17) J. H. Raley, F. R. Rust and W. E. Vaughan, *ibid.*, **70**, 1336 (1948).

TABLE I

SUMMARY OF ACTIVATION ENERGIES[a] FOR DEPOLYMERIZATION AND POLYMERIZATION

Polymer	Depolymerization E_0 (over-all) End	E_0 (over-all) Random	E_1 End	E_1 Random	E_2	E_4	Polymerization H_p	Polymerization E_p
Methyl methacrylate	Small N 48 / Large N 32	Large N 58	48	99	18.5	20	13	5.5
α-Methylstyrene		65		65	42.5	(20)[b]	9	33.5
Styrene	58		88		24	(20)	17	7
Ethylene	68		<116		>22 $E_4 \sim 20$	(20)	22	
Tetrafluoroethylene	80		<104		>38	(20)	38	

[a] Values are in kcal.; 1 cal. = 4.185 joules. [b] Values in parentheses are assumed.

di-*t*-butyl peroxide and azomethane[17] have[18,19] the very high pre-exponential values of 10^{16}, suggesting that the 10^{18} found here is real for the simple initiation step.

The observed dependence of initial rate on molecular weight could, it might be argued alternatively, be the result of transfer, competing with terminal initiation. This mechanism has been considered in detail[12] and appears to be unlikely.

Contrary to the suggestion of previous workers,[20] this work, along with other recent work,[11] indicates that end initiation is not exceptionally prevalent in the thermal decomposition of polymers. With the possible exception of polystyrene[20] it appears possible to prepare or purify polymers in a manner which eliminates end initiation or initiation at other "weak" points. The end initiation found in polymethyl methacrylate[11] and in polystyrene[20] appears to be caused by the weak bond beta to a terminal double bond.[11]

Data on the activation energies for the kinetic steps in depolymerization are fairly complete only for polymethyl methacrylate and are given in Table I. However, if we make the reasonable assumption that the activation energy for termination is the same for the other polymers listed in the table as found for polymethyl methacrylate,[10] then some estimates also can be made for the activation energies for initiation in a series of polymers. These estimates are listed in the table along with other related data. The methods of initiation are indicated according to the available evidence and the chain length, N, when the over-all activation energy varies with this quantity. For polyethylene and polytetrafluoroethylene no activation energies are available for propagation in polymerization, and hence inequality signs are shown. Also, since polyethylene decomposes almost entirely by transfer,[15] an estimate based on gas-phase studies[21] is used. Although the values listed in the table are open to considerable question it is still clear that the activation energies for initiation are quite large.

Dissociation energies for the bonds involved are presumably the differences between the values of E_1 and E_4. They are reasonably close to 80 kcal. for the average C–C bond in some instances. The large values for this bond in polyethylene and polytetrafluoroethylene suggest random initiation. The assumption that E_4 is 20 for these polymers can only lead to qualitative conclusions.

Acknowledgment.—The authors wish to express their appreciation to Dr. Donald McIntyre for light-scattering measurements on some of the polymer fractions used in this work, and to Mr. J. K. Draper for assistance in carrying out the pyrolytic studies.

(18) E. W. R. Steacie, THIS JOURNAL, **35**, 1493 (1931).

(19) O. K. Rice and D. V. Sickman, *J. Chem. Phys.*, **4**, 239, 243, 608 (1936).

(20) N. Grassie and W. W. Kerr, *Trans. Faraday Soc.*, **53**, 234 (1957).

(21) F. O. Rice and K. K. Rice, "The Aliphatic Free Radicals," John Hopkins Press, Baltimore, Md., 1935.

MANGANESE CARBONYL: HEAT OF FORMATION BY ROTATING-BOMB CALORIMETRY

BY W. D. GOOD, D. M. FAIRBROTHER[1] AND GUY WADDINGTON[2]

Contribution No. 73 from the Thermodynamics Laboratory, Petroleum Experiment Station, Bureau of Mines, U. S. Department of the Interior, Bartlesville, Oklahoma

Received March 29, 1958

The heat of formation of dimanganese decacarbonyl [$Mn_2(CO)_{10}$] was determined by combustion calorimetry. A rotating-bomb method was employed, and a solution of nitric acid and hydrogen peroxide was used in the bomb to convert all manganese-containing products of combustion to Mn^{++} ion. The combustion reaction was referred by suitable comparison experiments to an aqueous solution of composition $Mn(NO_3)_2 \cdot 10.309H_2O$ as a product. This procedure also minimized errors in reduction of the data to standard states. The results of the calorimetric experiments gave for the reaction $Mn_2(CO)_{10}(c) + 4HNO_3$ (in $16H_2O$) + $6O_2(g) = 2Mn(NO_3)_2$ (in $10.309H_2O$) + $10CO_2(g) + 2H_2O(liq)$ the value $\Delta H°_{298.16} = -777.0 \pm 0.8$ kcal. The derived value for the heat of formation of solid manganese carbonyl from graphite, oxygen gas and manganese metal, $\Delta Hf°_{298.16}$, is -400.9 kcal. mole.$^{-1}$

The thermodynamic properties of metal carbonyls have not been studied extensively by modern calorimetric techniques. Heat of combustion and formation values for carbonyls of chromium,[3,4] molybdenum,[3,4] tungsten[3,4] and nickel[5,6] have been reported. This investigation of dimanganese decacarbonyl [$Mn_2(CO)_{10}$] was part of a continuing program of chemical thermodynamic studies of compounds important in petroleum technology. It also provided additional information about the difficult problem of measuring the heat of combustion of metal organic compounds.

A rotating-bomb method of combustion calorimetry that was developed in this Laboratory[7,8] was used. An earlier study of tetraethyllead[9] showed this method to be applicable to substances like manganese carbonyl that produce a complex mixture of solid products upon combustion in a conventional bomb. Such a mixture is difficult to analyze. Thus, the final thermodynamic state of the combustion process is somewhat uncertain. With the rotating bomb method, a suitable solution is used to dissolve the complex mixture during the combustion period and produce a final state that can be defined readily by chemical analysis.

Experimental

The Combustion Method.—Many exploratory experiments were performed in attempts to find conditions under which the combustion reaction would be complete and produce a well-defined final state. No entirely satisfactory method was found. If oxygen at the normal pressure of 30 atmospheres, a hydrocarbon oil promoter, or both, were used, the combustion reaction formed fused products that were too refractory to be dissolved in a reasonable time by any bomb solution that was investigated. If oxygen at a much lower pressure was used, the combustion reaction gave solid products in a finely divided state suitable for solution. However, a significant amount of "carbon residue" was formed. Since the heat of combustion of this "carbon residue" could be determined in a separate experiment and the appropriate thermochemical correction applied, the conditions were chosen such that readily soluble manganese compounds were formed. All final combustions of manganese carbonyl were done with an initial oxygen pressure of only 5 atmospheres.

Initial Bomb Solution.—The initial bomb solution, selected on the basis of numerous exploratory experiments, contained about 18 wt. % nitric acid and 0.4 wt. % hydrogen peroxide. The nitric acid dissolved the solid bivalent manganese compounds. The hydrogen peroxide, in the presence of nitric acid, reduced manganese compounds of higher valence states (such as Mn_2O_3, Mn_3O_4 and MnO_2) to Mn^{++} ion in solution. Enough solution was required in the bomb to ensure that the crucible, which after the combustion reaction contained a mass of solid manganese compounds, was repeatedly bathed during rotation of the bomb; 50 ml. of solution was adequate and was used in all calorimetric experiments with manganese carbonyl. The amount of hydrogen peroxide in the initial bomb solution was selected to be a safe excess over that needed to reduce all compounds containing manganese in higher valence states to Mn^{++}. Thermochemical corrections, in the range 68–76 calories per combustion experiment, were applied for the decomposition of hydrogen peroxide.

$$H_2O_2(aq) = H_2O(liq) + {}^1/_2O_2(g) \quad \Delta E°_{298.16} = -22.94 \text{ kcal.}$$

The foregoing value of $\Delta E°_{298.16}$ was calculated from data in Circular 500.[10]

Correction for Catalytic Decomposition of Hydrogen Peroxide.—The bomb solution of 18 wt. % nitric acid and 0.4 wt. % hydrogen peroxide was stable in the bomb under the initial experimental conditions. However, after the combustion reaction had occurred, the hydrogen peroxide decomposed slowly because of catalysis by manganous ion. Within the limits of the method used for analysis of the bomb solution and within the range of fractional decomposition of interest, the amount of hydrogen peroxide was found to decrease linearly with time. Insofar as the rate of evolution of energy by the decomposition reaction was constant in the after period, this evolution of energy was accounted for in the calculation of $\Delta t_{cor.}$, the correction to the observed change in temperature in the reaction period.[8] The amount of hydrogen peroxide in the final state of the actual bomb process—the amount appropriate for calculating the thermochemical correction for decomposition—was found by extrapolation back to the midtime of the calorimetric experiment.

Comparison Experiments.—An earlier publication[9] showed how possible errors in rotating-bomb calorimetry of metal-containing compounds could be either avoided or minimized by the use of suitable comparison experiments. Such comparison experiments were used in the present study

(1) U. K. Atomic Energy Authority, Aldermaston, Berkshire, England.

(2) National Research Council, 2101 Constitution Avenue, N. W., Washington 25, D. C

(3) F. A. Cotton, A. K. Fischer and G. Wilkinson, *J. Am. Chem. Soc.*, **78**, 5168 (1956).

(4) K. A. Sharifov and T. N. Rezukhina, *Trudy Inst. Fiz. i Mat., Akad. Nauk Azerbaidzhan S. S. R., Ser. Fiz.*, **6**, 53 (1953); *Referat. Zhur., Khim.*, **1954**, No. 30309; *C. A.*, **49**, 2173 (1955).

(5) A. K. Fischer, F. A. Cotton and G. Wilkinson, *J. Am. Chem. Soc.*, **79**, 2044 (1957).

(6) E. I. Smagina and B. F. Ormont, *Zhur. Obshchei Khim.*, **25**, 224 (1955); *J. Gen. Chem. (U.S.S.R.)*, **25**, 207 (1955)(Engl. translation); *C. A.*, **49**, 11386 (1955).

(7) W. N. Hubbard, C. Katz and G. Waddington, THIS JOURNAL, **58**, 142 (1954).

(8) W. D. Good, D. W. Scott and G. Waddington, *ibid.*, **60**, 1080 (1956).

(9) D. W. Scott, W. D. Good and G. Waddington, *ibid.*, **60**, 1090 (1956).

(10) F. D. Rossini, D. D. Wagman, W. H. Evans, S. Levine and I. Jaffe, "Selected Values of Chemical Thermodynamic Properties," NBS Circular 500, 1952.

of manganese carbonyl. In these experiments the sample was benzoic acid. A second crucible[9] contained liquid $Mn(NO_3)_2 \cdot 10.309H_2O$ enclosed in a thin-walled Pyrex ampoule with a finely constricted neck. The amounts of benzoic acid and manganous nitrate solution and the amount and concentration of the original bomb solution were made such that the final amount of carbon dioxide and the amount and composition of the final bomb solution were substantially the same as for the combustion experiment with manganese carbonyl. The total energy evolution could not be made the same in the two experiments because combustion of benzoic acid produces more energy per unit amount of carbon dioxide produced than does combustion of manganese carbonyl.[11] In the comparison experiments an initial oxygen pressure of 30 atmospheres was used since complete combustion of benzoic acid is not obtained at the much lower oxygen pressure necessary for the combustion experiments with manganese carbonyl. The design of a comparison experiment is illustrated by a numerical example in Table I.

It is seen that, except for oxygen, the amounts of the various substances in the final state were nearly the same in the combustion and comparison experiments. The amounts of oxygen in the final state differed because of the difference in the initial pressures of oxygen.

The use of the comparison experiments allowed the combustion reaction of manganese carbonyl to be referred to $Mn(NO_3)_2 \cdot 10.309H_2O$ as a product. The heat of formation of aqueous manganous nitrate solutions is known, and the value of $\Delta Ec°$ referred to $Mn(NO_3)_2 \cdot 10.309H_2O$ was used to compute the heat of formation of manganese carbonyl. The corrections to standard states were nearly the same for the combustion and comparison experiments, and errors in these corrections nearly canceled in the final value of $\Delta Ec°$. The important correction for dissolved carbon dioxide was not exactly the same in the two experiments because of the differences in total pressures of oxygen required for the reactions. However, any error in this correction was much less than it would have been if comparison experiments had not been used. The calorimetry in the combustion and comparison experiments is similar in enough respects that the procedure was more nearly a substitution method than if no comparison experiments had been performed.

TABLE I

NUMERICAL EXAMPLE TO ILLUSTRATE DESIGN OF COMPARISON EXPERIMENT

Combustion Experiment		Comparison Experiment	
Initial pressure of oxygen			
5 atm.		30 atm.	
Sample			
1.98451 g. $Mn_2(CO)_{10}$		3.71482 g. $Mn(NO_3)_2 \cdot 10.309H_2O$	
(0.010178 g. atom Mn)		(0.010187 g. atom Mn)	
		0.88770 g. Benzoic Acid	
0.00115 g. Fuse (cotton thread)		0.00105 g. Fuse (cotton thread)	
Amounts in initial bomb solution, moles			
H_2O	2.497	H_2O	2.382
HNO_3	0.15743	HNO_3	0.13737
H_2O_2	0.006243	H_2O_2	0.003094
Amounts in final state, moles			
H_2O	2.511	H_2O	2.508
HNO_3	0.13708	HNO_3	0.13741
H_2O_2	0.002932	H_2O_2	0.003094
$Mn(NO_3)_2$	0.010178	$Mn(NO_3)_2$	0.010187
CO_2	0.05022	CO_2	0.05092
O_2	0.0276	O_2	0.2900
Energy of isothermal bomb process, $\Delta E_{I.B.P.}$, cal.			
−4047.9		−5661.4	

(11) In principle, the energy evolution could have been made the same in the comparison experiment by use of an auxiliary substance, such as succinic acid or oxalic acid, the combustion of which produces a large amount of carbon dioxide per unit evolution of energy. However, the extra complexity of such a procedure would cancel the advantage of having equal amounts of energy produced.

Experimental Procedures.—The calorimeter, laboratory designation BMR2, and bomb, laboratory designation B571, have been described.[8,9] The bomb was placed in the calorimeter in the inverted position, as shown in an earlier paper,[8] so that the valves and gaskets were protected from the combustion reaction by the aqueous solution. The calorimetric observations were made as described in reference 7, except that rotation of the bomb continued to the end of the calorimetric experiment,[8] and a longer reaction period was needed to allow solid combustion products to dissolve.

When the calorimetric observations were complete, the bomb was removed from the calorimeter, discharged and opened. In each case the bomb gas was checked for carbon monoxide, but none was detected. A sample of bomb solution was removed at once and the hydrogen peroxide content determined by titration with standard potassium permanganate solution. This determination was made as nearly as possible one hour after the midtime of the combustion experiment. The determination was repeated on another sample at the end of a second hour to establish the rate of the catalytic decomposition. Most of the "carbon residue" was deposited on the walls of the crucible, and smaller amounts were found suspended in the bomb solution. The crucible with its "carbon residue" was washed, dried and weighed to determine the mass of the deposit on the crucible by difference. The "carbon residue" in the bomb solution was determined by washing onto a previously washed, dried and weighed glass wool plug. The glass wool with the collected "carbon residue" was dried and reweighed. The mass of "carbon residue" on the crucible plus that collected on the glass wool was the total amount for which a thermochemical correction was required. Manganous ion was determined in the bomb solution by a bismuthate method much like that described by Kolthoff and Sandell.[12] Manganous ion was determined in the solutions from both the combustion experiments with manganese carbonyl and the comparison experiments; the analyses of the solutions from the comparison experiments served as a check on the method. Analyses of products from experiments with manganese carbonyl gave an average of 100.0 ± 0.2% of the manganese expected from the mass of the sample. Analyses of the solutions from the comparison experiments gave an average of 99.9 ± 0.3% of the manganese expected from the mass of manganous nitrate solution used.

Experiments for Determination of the Correction for "Carbon Residue."—The thermochemical correction for "carbon residue" was determined in separate experiments in which the crucible with its deposit of "carbon residue" was used for a calorimetric combustion experiment with benzoic acid. In these experiments, the residue was oxidized completely to leave only a minute trace of manganese-containing compounds on the crucible. The heat of combustion of the "carbon residue" was obtained as the small difference between the total energy from the combustion reaction and that from combustion of the benzoic acid and fuse. However, good precision was obtained, and values of $\Delta Ec°/1000\ M$ from −6.4 to −6.9 cal. mg.$^{-1}$ were obtained for the "carbon residue." The residue was evidently not pure carbon, for which $\Delta Ec°/1000M$(graphite) is −7.8 cal. mg.$^{-1}$. The value found for the deposit on the crucible was assumed to apply to all the "carbon residue" formed in the combustion experiment with manganese carbonyl and was used in calculating the thermochemical correction. The correction was in the range of 50 to 60 cal. per combustion experiment.

Correction for Formation of Nitric Acid.—Ordinarily, in combustion calorimetry, the amount of nitric acid formed in the combustion process from nitrogen impurity in the oxygen is determined, and the appropriate thermochemical correction is applied. However, in this investigation, it was impossible to determine a small amount of nitric acid formed in the combustion process in the presence of the large amount of nitric acid already present in the bomb. In calibration experiments in which nearly the same mass of benzoic acid reacted as in the comparison experiments, the nitric acid formed was equivalent to 0.4 to 0.7 cal. per combustion experiment. The average of the values obtained in the calibration experiments, 0.56 cal., was applied

(12) I. M. Kolthoff and E. B. Sandell, "Textbook of Quantitative Inorganic Analysis," Revised Edition, The Macmillan Co., New York, N. Y., p. 709.

as a thermochemical correction to the comparison experiments. The combustion of manganese carbonyl in 5 atm. of oxygen was shown by the time-temperature behavior of the calorimeter to be much slower than the combustion of benzoic acid in 30 atm. of oxygen. It is likely that only negligible amounts of nitric acid were formed in the less intense heat of the slower combustion. Therefore, no thermochemical corrections for nitric acid were applied to the combustion experiments with manganese carbonyl. It is unlikely that the approximations in the thermochemical corrections for nitric acid led to an error greater than 0.1 kcal. mole^{-1} in the final values of ΔEc° and $\Delta Hf^\circ_{298.16}$ for manganese carbonyl.

Reduction to Standard States. The calorimetric results were corrected to standard states by a procedure similar to that of Hubbard, Scott and Waddington[13] but modified to apply to manganese compounds instead of sulfur compounds. Certain physical constants needed for the corrections have not been determined accurately, and others must be estimated because experimental data are lacking. The use of comparison experiments ensures that errors from inaccurate values of physical constants used in the correction to standard states largely cancel in calculating the final value of ΔEc°.

Materials

Manganese Carbonyl. -Samples of manganese carbonyl were contributed by the Research Laboratories of the Ethyl Corporation. The sample used for the final calorimetric experiments had a reported purity, determined by a cryoscopic method, of 99.9$_2$ mole %. The exploratory experiments were done with a sample of lower purity. The material was pressed into pellets for combustion. Individual pellets weighed over extended periods decreased in weight less than 0.00001 g. per pellet per hour. Therefore, the volatility of manganese carbonyl is low enough for application of the pellet technique because the loss in weight of a pellet between weighing and combustion is almost at the borderline of detection with a microbalance.

Benzoic Acid.—The benzoic acid was National Bureau of Standards standard sample 39g with a certified heat of combustion of 26.4338 ± 0.0026 abs. kj. (6317.83 ± 0.62 cal.)/g. mass under certificate conditions. Conversion from certificate conditions to standard conditions by the method of reference[13] gives −6312.91 ± 0.62 cal./g. mass for $\Delta Ec^\circ/M$, the energy of the idealized combustion reaction.

Manganous Nitrate.—Fisher certified reagent grade manganous nitrate solution was used. Manganous ion determination by a volumetric bismuthate method showed the composition of the solution to be 49.07% manganous nitrate. A hypodermic syringe was used to introduce the viscous liquid into thin-walled Pyrex ampoules.

Results

Units of Measurement and Auxiliary Quantities. --The results of the combustion calorimetry are expressed in terms of the defined calorie equal to 4.1840 abs. joules and refer to the isothermal process at 25° and to true mass. The molecular weights were computed from the 1951 table of international atomic weights.[14] For use in reducing weights in air to weights *in vacuo*, in correcting the energy of the actual bomb process to the isothermal process and in correcting to standard states, the following values (for 25°) of density d, specific heat, c_p and $(\partial E/\partial P)_T$ for the various substances were used.

	d, g. ml.$^{-1}$	c_p, cal. deg.$^{-1}$ g.$^{-1}$	$(\partial E/\partial P)_T$, cal. atm.$^{-1}$ g.$^{-1}$
Manganese carbonyl	1.66	0.25	−0.003
Benzoic acid	1.32	0.289	−0.0028
$Mn(NO_3)_2 \cdot 10.309H_2O$	1.5	0.51	Negligible
Pyrex glass	2.6	0.17	Negligible

(13) W. N. Hubbard, D. W. Scott and G. Waddington, THIS JOURNAL, **58**, 152 (1954).

(14) E. Wichers, *J. Am. Chem. Soc.*, **74**, 2447 (1952).

For $\Delta Ec^\circ/M$ of the cotton thread fuse, the value −4050 cal. g.$^{-1}$ was used. The energy equivalent of the calorimetric system, as determined by six calibration experiments with benzoic acid, was 4057.5 ± 0.4 cal. deg.$^{-1}$.

Results with Manganese Carbonyl. Six satisfactory combustion experiments with high purity manganese carbonyl were obtained out of six attempts. A typical combustion experiment with manganese carbonyl and the corresponding comparison experiment are summarized in Table II. In this table, m(material) denotes the mass of the designated material that was used, and n^i(material) denotes the number of moles of the designated material initially present in the bomb. The

TABLE II

TYPICAL PAIR OF COMBUSTION AND COMPARISON EXPERIMENTS WITH MANGANESE CARBONYL

	Combustion expt.	Comparison expt.
m(manganese carbonyl), g.	1.98451	...
m(benzoic acid), g.	...	0.88770
$m[Mn(NO_3)_2 \cdot 10.309H_2O]$, g.	...	3.71482
$n^i(H_2O)$, moles	2.497	2.382
$n^i(HNO_3)$, moles	0.157430	0.137370
$n^i(H_2O_2)$, moles	0.006243	0.003094
Δt_c, deg.	0.98204	1.37957
ε(calor.)$(-\Delta t_c)$, cal.	−3984.63	−5597.61
ε(cont.)$(-\Delta t_c)$, cal.	−63.96	−65.49
$\Delta E_{ign.}$, cal.	0.69	1.70
ΔE, cor. to st. states, cal.	23.26	22.75
ΔE^f comb ("carbon residue"), cal.	−53.55	...
ΔE^f dec(HNO_3), cal.	...	0.56
ΔE^f dec(H_2O_2), cal.	75.95	...
$-m\Delta Ec^\circ/M$(fuse), cal.	4.65	4.25
$-m\Delta Ec^\circ/M$(benzoic acid), cal.	...	5603.97
$m\Delta Ec^\circ/M$(manganese carbonyl), cal.	−3997.59	...
$\Delta Ec^\circ/M$(manganese carbonyl), cal. g.$^{-1}$	−2014.4	...
ΔEc°(manganese carbonyl), kcal. mole^{-1}	−785.5	...
$m\Delta E^\circ/M[Mn(NO_3)_2 \cdot 10.309\ H_2O]$, cal.	...	−29.87
$\Delta E^\circ/M[Mn(NO_3)_2 \cdot 10.309H_2O]$, cal. g.$^{-1}$	...	−8.04
$\Delta E^\circ[Mn(NO_3)_2 \cdot 10.309H_2O]$, kcal. mole^{-1}	...	−2.93

quantity $\Delta t_c = t_f - t_i - \Delta t_{corr.}$ is the observed increase of the calorimeter temperature, corrected for Newtonian heat exchange, for the energy from stirring the calorimeter and from rotation of the bomb and for the energy from the slow catalytic decomposition of hydrogen peroxide. The symbols, ε(calor.) and ε(cont.), denote the energy equivalent of the calorimetric system and of the contents of the bomb, respectively. The term $\Delta E_{ign.}$ denotes the electrical energy used to ignite the fuse. The term ΔE, cor. to st. states, denotes the sum of all corrections to standard states. The terms ΔE^f_{comb} ("carbon residue"), $\Delta E^f_{dec}(HNO_3)$ and ΔE^f_{dec} (H_2O_2) are the thermochemical corrections for the "carbon residue," for formation of nitric

acid and for the hydrogen peroxide consumed. The symbol $\Delta Ec^\circ/M$(material) denotes the energy of the idealized combustion reaction for 1 gram of the designated material.

If the small concentrations of H_2O_2 in the bomb solutions are neglected, the values of ΔEc°(manganese carbonyl) and of $-2\Delta E^\circ[Mn(NO_3)_2 \cdot 10.309H_2O]$ in Table II refer to equations I and II below. Two dilution corrections are necessary. The first, equation III below, corrects for the difference in concentration of the initial bomb solutions, and the second, equation IV below, refers each experiment to the same initial concentration of nitric acid, HNO_3(in $16H_2O$).

$$Mn_2(CO)_{10} + 30.935HNO_3 \cdot 490.685H_2O + 0.658H_2O + 6O_2 = 2Mn(NO_3)_2 \cdot 26.935HNO_3 \cdot 493.342H_2O + 10CO_2 \quad \Delta E^\circ_{298.16} = -785.53 \quad (I)$$

$$2Mn(NO_3)_2 \cdot 26.935HNO_3 \cdot 493.342H_2O = 2Mn(NO_3)_2 \cdot 20.618H_2O + 26.935HNO_3 \cdot 468.436H_2O + 4.288H_2O \quad \Delta E^\circ_{298.16} = -5.86 \quad (II)$$

$$26.935HNO_3 \cdot 468.436H_2O = 26.935HNO_3 \cdot 427.238H_2O + 41.198H_2O \quad (III)$$
$$\Delta E^\circ_{298.16} = 0.54$$

$$4HNO_3 \cdot 64H_2O = 4HNO_3 \cdot 63.447H_2O + 0.553H_2O \quad (IV)$$
$$\Delta E^\circ_{298.16} = 0.01$$

The sum of equations 1 through IV is

$$Mn_2(CO)_{10} + 6O_2 + 4HNO_3(\text{in } 16H_2O) = 2Mn(NO_3)_2(\text{in } 10.309H_2O) + 10CO_2 + 2H_2O \quad (V)$$
$$\Delta E^\circ_{298.16} = -779.12$$

The results of the six pairs of combustion and comparison experiments are given in Table III. The value of $\Delta H^\circ_{298.16}$ (equation V) in Table III is the direct result of the calorimetric studies; aside from small thermochemical corrections, this value depends only on calorimetric experiments done in this Laboratory and the certificate value for the heat of combustion of benzoic acid used for calibration.

TABLE III

SUMMARY OF CALORIMETRIC EXPERIMENTS WITH MANGANESE CARBONYL

ΔE° (eq. I), kcal. mole^{-1}	$-\Delta E^\circ$ (eq. II), kcal. mole^{-1}	Dilution corn. (eq. III & IV), kcal. mole^{-1}	$\Delta E^\circ_{298.16}$ (eq. V), kcal. mole^{-1}
−785.53	5.86	0.55	−779.12
−785.64	5.96	.55	−779.13
−785.32	5.50	.55	−779.27
−784.45	5.84	.55	−778.06
−787.17	5.44	.55	−781.18
−785.70	5.64	.55	−779.51

$\Delta E^\circ_{298.16}$ (eq. V), mean	−779.38 kcal. mole^{-1}
$\Delta H^\circ_{298.16}$ (eq. V)	−777.01 kcal. mole^{-1}
Standard dev. of the mean	0.4 kcal. mole^{-1}
Uncertainty interval	0.8 kcal. mole^{-1}

Derived Results.—The values given in Circular 500,[10] or interpolated from values listed therein, for the standard heats of formation, in kcal. mole^{-1}, of HNO_3(in $16H_2O$), −49.18; $Mn(NO_3)_2$(in $10.309H_2O$), −148.75; H_2O(liq), −68.3174; and CO_2(g), −94.0518, were used to obtain a derived value for the heat of formation of manganese carbonyl.

$$10C(\text{graphite}) + 5O_2(g) + 2Mn(c, IV) = Mn_2(CO)_{10}(c)$$
$$\Delta Hf^\circ_{298.16} = -400.9 \text{ kcal. mole}^{-1}$$

Acknowledgment.—The Research Laboratories of the Ethyl Corporation have contributed financial support and a sample of purified manganese carbonyl to this investigation.

PROOF OF THE ACCURACY OF *p*H MEASUREMENTS WITH THE GLASS ELECTRODE IN THE SYSTEM METHANOL–WATER[1]

A. L. BACARELLA, E. GRUNWALD, H. P. MARSHALL AND E. LEE PURLEE

Contribution from the Chemistry Department of Florida State University, Tallahassee, Florida

Received April 9, 1958

Previous claims of discrepancies between pK_A values obtained potentiometrically with the glass electrode and conductometrically for acetic acid in methanol–water mixtures are shown to be incorrect. The two methods yield results that are identical with experimental error, thus establishing the accuracy of *p*H measurements with the glass electrode in solvent compositions up to 95% (wt.) methanol. Experimental conditions which must be satisfied in order to obtain accurate results with the glass electrode are reviewed.

Previous communications from this Laboratory[2–4] have emphasized that the glass electrode, when properly employed, correctly measures hydrogen ion activity in aqueous organic solvents. The glass electrode has been used in this Laboratory for the potentiometric determination of acid dissociation constants in methanol–water mixtures (including pK_A measurements for acetic acid) and water–dioxane mixtures.[3,5] In addition, we have employed the glass electrode in the potentiometric determination of ion-pair dissociation constants in the system dioxane–water.[4,5]

Direct evidence was reported by Purlee and Grunwald[4] that the glass electrode gives a constant e.m.f. *versus* the hydrogen electrode in 70% (wt.) dioxane–water over a wide range of hydrogen ion activity. Furthermore, comparison of e.m.f.'s measured with the glass electrode in 82% (wt.) dioxane–water[2] and in 70% (wt.) dioxane–water[4] with e.m.f.'s previously obtained with the hydrogen electrode in these solutions indicated that iden-

(1) This work was supported by a grant from the National Science Foundation.

(2) H. P. Marshall and E. Grunwald, *J. Chem. Phys.*, **21**, 2143 (1953).

(3) A. L. Bacarella, E. Grunwald, H. P. Marshall and E. L. Purlee, *J. Org. Chem.*, **20**, 747 (1955).

(4) E. L. Purlee and E. Grunwald, *J. Am. Chem. Soc.*, **79**, 1366 (1957).

(5) E. L. Purlee and E. Grunwald, *ibid.*, **79**, 1372 (1957).

tical measures of the hydrogen ion activity were obtained with both electrodes.

However, in the system methanol–water, values have been reported recently by Shedlovsky and Kay[6] for the acid dissociation constants of acetic acid which did not *appear* to agree with the results obtained in this Laboratory by potentiometric measurements with the glass electrode.[3] Since these data were obtained by precise conductometric methods, the *apparent* discrepancies between the two sets of values have cast some doubt on the validity of measurements obtained with glass electrodes in media rich in organic components.

In making comparisons with our results, Shedlovsky and Kay[6] interpolated between their measurements which were made at slightly different solvent compositions. Their interpolations indicated significant discrepancies with our results in the solvent composition range above 40% (vol.) methanol. On plotting both sets of data (pK_A *versus* wt. % methanol) on large-scale, precision graph paper, we find no such significant discrepancies. Both sets of data fall on a single smooth curve with a mean deviation of 0.009 pK_A unit. The best curve for our potentiometric data is identical, within experimental error, with the best curve constructed for their conductometric data. In Table I values obtained from the two best curves are compared with the actual experimental data. The mean value of the discrepancy, 0.017 pK_A unit, is slightly less than the standard error in the potentiometric pK_A values.[7]

To the best of our knowledge these results remove the last serious objection to the use of the glass electrode in slightly aqueous organic solvents and, along with previously reported results,[2,3] confirm that the glass electrode can correctly measure hydrogen ion activity in these solvents. We have previously called attention to the experimental conditions which yield accurate results with the glass electrode, which are:

(1) The glass electrode must be equilibrated with solvent of *exactly* the same composition as that in which measurements are to be made. (In 70% (wt.) dioxane–water we found equilibration to require *ca.* 24 hr.[4])

(2) When not in use the electrode must be stored in solvent of *exactly* the same composition as that in which measurements are being made.

(3) The glass electrode must be standardized in solvent of *exactly* the same composition as that in which it is to be used.

(4) If measurements are to be made with cells involving liquid junctions, small but significant corrections must be made for the variation of the liquid junction potentials with ionic strength (see ref. 3, p. 758). For the most accurate work, the standardizing buffer must be chosen to resemble the components of the test solution as nearly as possible with respect to structure, charge type and concentration.

TABLE I

COMPARISON OF POTENTIOMETRIC AND CONDUCTOMETRIC pK_A VALUES FOR ACETIC ACID IN METHANOL–WATER MIXTURES AT 25.00°

The values in parentheses were obtained by interpolation on large scale graphs.

Wt. % MeOH	pK_A Conductometric[5]	pK_A Potentiometric[3]	Difference
0.00	4.756	4.756	0.000
10.01	4.916	(4.910)	.006
16.47	(5.025)	5.011	.014
20.01	5.088	(5.071)	.017
34.47	(5.367)	5.334	.033
40.02	5.482	(5.458)	.024
54.20	(5.798)	5.808	.010
60.05	5.951	(5.954)	.003
75.94	(6.521)	6.500	.021
80.03	6.710	(6.703)	.007
90.02	7.395	(7.417)	.022
93.74	(7.881)	7.858	.023
95.02	8.092	(8.068)	.024
		Mean	0.017

(6) T. Shedlovsky and R. L. Kay, *J. Phys. Chem.*, **60**, 151 (1956).

(7) We believe that the apparent discrepancy between the two sets of data may have arisen from ambiguity in the definition of the term *volume per cent.* Shedlovsky and Kay[6] seem to have used *volume per cent.* in the manner described by Carr and Riddick[8a]

$$\text{Vol. \% MeOH at } t = (\text{wt. \% MeOH})[d_{H_2O-MeOH\ mixture}/d_{MeOH}]_t$$

where d is the density and t the temperature. In ref. 3 solvent compositions were reported in terms of both *weight per cent.* and *volume per cent.* The latter was computed according to the definition

$$\text{Vol. \% MeOH at } t = \left(\frac{v_{MeOH}}{v_{MeOH} + v_{H_2O}}\right)_t \times 100$$

where v denotes the volume of the respective pure component prior to mixing. In ref. 3, these density data were used at 25°: water, 0.99704, methanol, 0.78653.[8b] For any given methanol–water mixture, the two equations lead to quite different values of the *volume per cent.*

(8) (a) C. Carr and J. A. Riddick, *Ind. Eng. Chem.*, **43**, 692 (1951); (b) G. Scatchard and L. B. Ticknor, *J. Am. Chem. Soc.*, **74**, 3724 (1952).

PURIFICATION AND PROPERTIES OF PYRROLE, PYRROLIDINE, PYRIDINE AND 2-METHYLPYRIDINE[1]

BY R. VERNON HELM, W. J. LANUM, G. L. COOK AND J. S. BALL

Petroleum and Oil-Shale Experiment Station, U. S. Bureau of Mines, Department of the Interior, Laramie, Wyoming

Received April 17, 1958

Pyrrole, pyrrolidine, pyridine and 2-methylpyridine were purified to approximately 99.9 mole % purity. Precautions necessary in the purification of these nitrogen compounds are described, including protection from water and oxygen. Boiling points, freezing points, densities, viscosities, surface tensions and refractive indices were determined on each of the compounds. Derived functions, including refractivity intercept, specific dispersion, molecular refraction, parachor and molecular volume were calculated. Mass, infrared and ultraviolet spectra of the compounds were determined. The stability of the compounds under storage was investigated, so that they could be used as calibration standards.

Pyrrole, pyrrolidine, pyridine and 2-methylpyridine have been prepared in high purity for accurate determination of properties and for use as calibration standards. This is part of the fundamental research program of the American Petroleum Institute to study constituents of petroleum. A portion of this program, API Research Project 52,[2] is coöperatively sponsored by the Bureau of Mines and API, and is concerned with the purification and properties of nitrogen compounds as well as their occurrence in petroleum.

In order to meet the needs of the project, 1.0 to 1.5 liters of each nitrogen compound is purified to at least 99.9 mole %. Three groups of properties are determined on these compounds: (1) common physical properties including refractive index, density, viscosity, surface tension, melting point and boiling point; (2) thermodynamic properties (at the Bartlesville Laboratory of the Bureau of Mines); and (3) ultraviolet, infrared and mass spectral patterns. Samples of each of the compounds are made available for sale as calibration standards through the API Samples and Data Office at Carnegie Institute of Technology.

This paper reports on the purification of the four compounds, the determination of their common physical properties and their spectra. In addition, the stabilities of the compounds have been studied because of their use as calibration standards. The purities of the compounds are given in Table I.

TABLE I

COMPOUNDS PURIFIED FOR CALIBRATION STANDARDS

Compound	Sample no.	Impurity, mole %
Pyrrole	API-USBM 52-2-5S	0.006 ± 0.005
Pyrrolidine	API-USBM 52-3-5S	.15 ± .04
Pyridine	API-USBM 52-1-5S	.08 ± .02
2-Methyl-pyridine	API-USBM 52-4-5S	.09 ± .05

Purification

The four compounds purified were obtained from commercial sources. The purification procedures[3,4] were similar to those employed previously in this Laboratory on organic sulfur compounds. However, due to reactivity with oxygen and the hygroscopic nature of these nitrogen compounds, unusual precautions were necessary to achieve the high purities. Distillations were performed under an atmosphere of purified nitrogen[5] containing less than 2 parts per million of oxygen. Fractions from the distillations were collected and sealed in 150-ml. ampoules equipped with internal break-off tips. Selected fractions from the distillation were examined for purity by the freezing point-purity method.[6] Ampoules containing fractions of the highest purity were sealed to a glass manifold system, and the fractions were combined and degassed by vacuum distillation. The combined material was treated with calcium hydride to remove the last traces of water and finally vapor transferred and sealed in vacuum. Samples of the composites were examined for impurities by mass and infrared spectroscopy and freezing point measurements. The freezing point-purity method failed to give data that could be extrapolated to give the freezing point of the compound with zero impurity. However, freezing-point data obtained for samples under investigation did give reproducible values for the actual freezing points of the samples. Confirmations of purities were obtained by low-temperature calorimetric measurements by the Bureau of Mines at Bartlesville, Okla. Details of the purification of individual compounds are noted below.

Pyrrole.—Approximately 10 liters of pyrrole purchased from Eastman Kodak Company was distilled in an all-glass Oldershaw column, 1 inch in diameter and containing 80 perforated glass plates. The tested efficiency of this column was 65 theoretical plates. Six liters of the highest purity material from this distillation was redistilled in a 1-inch by 11-foot Helipac column (efficiency, 200 theoretical plates). The yield of highest purity material from this distillation was 1.1 liters of pyrrole having a purity of 99.994 mole %.

Pyrrolidine.—Approximately 6 liters of pyrrolidine, purchased from Eastman Kodak Company, was distilled in the 80-plate Oldershaw column. The major impurity, water, was removed as the pyrrolidine–water azeotrope in the first part of the distillation, but material of adequate purity could not be obtained by combining of later fractions. A second distillation in the same column of 4 liters of the highest purity material from the first distillation resulted in 1 liter of pyrrolidine with a purity of 99.85 mole %.

Pyridine.—Ten liters of Baker and Adamson ACS grade pyridine was distilled in the 1-inch by 11-foot Helipac column. Water was removed in the early part of the distillation as the pyridine–water azeotrope; the later fractions were of high purity. The composite sample of highest purity was 1.5 liters of pyridine, with a purity of 99.92 mole %.

2-Methylpyridine.—Six liters of 2-methylpyridine purchased from Koppers Company was distilled in a 1-inch by 6-foot Stedman column, having a tested efficiency of 65 theoretical plates. Water was separated as the 2-methylpyridine–water azeotrope, and later fractions of high purity (3.6 liters) were combined for redistillation in the same column. The yield of high purity material from the second

(1) This investigation was performed as part of the work of American Petroleum Institute Research Project 52 on "Nitrogen Constituents of Petroleum" which is conducted at the University of Kansas in Lawrence, Kans., and the Bureau of Mines Experiment Stations in Laramie, Wyo. and Bartlesville, Okla.

(2) J. S. Ball, C. A. VanderWerf, G. Waddington and G. R. Lake, *Proc. Amer. Pet. Inst.* **34**, [VI] 152 (1954).

(3) W. E. Haines, R. V. Helm, C. W. Bailey and J. S. Ball, THIS JOURNAL, **58**, 270 (1954).

(4) W. E. Haines, R. V. Helm, G. L. Cook and J. S. Ball, *ibid.*, **60**, 549 (1956).

(5) R. V. Helm, D. R. Latham, C. R. Ferrin and J. S. Ball, *Ind. Eng. Chem., Chem. Eng. Data Series*, **2**, 95 (1957).

(6) A. R. Glasgow, A. J. Streiff and F. D. Rossini, *J. Research Natl. Bur. Standards*, **35**, 355 (1945).

TABLE II

PROPERTIES OF FOUR ORGANIC NITROGEN COMPOUNDS

Compound	T.P., °C.	Cryoscopic constant, A, deg.$^{-1}$	B.p. at 760 mm., °C.	Temp. of measurement, °C.	Density at t, °C., g./ml.	Viscosity at t, °C., centipoises	Surface tension at t, °C., dynes/cm.
Pyrrole	−23.41	0.01525	129.8	20	0.96985	1.352	37.61
				25	.96565	1.233	37.06
				30	.96133	1.129	36.51
Pyrrolidine	−57.85	.0221	86.5	20	0.85859	0.756	29.65
				25	.85380	.702	29.23
				30	.84898	.655	28.80
Pyridine	−41.67	.01858	115.2	20	0.98319	0.952	36.88
				25	.97824	.884	36.33
				30	.97319	.815	35.78
2-Methylpyridine	−66.71	.0276	129.4	20	0.94440	0.805	33.18
				25	.93981	.753	32.78
				30	.93514	.703	32.33

TABLE III

REFRACTIVE INDICES FOR FOUR ORGANIC NITROGEN COMPOUNDS

Compound	Temp. of measurement, °C.	Helium r line, 6678.1 Å.	Hydrogen C line, 6562.8 Å.	Sodium D line, 5892.6 Å.	Mercury e line, 5460.7 Å.	Helium v line, 5015.7 Å.	Hydrogen F line, 4861.3 Å.	Mercury g line, 4358.3 Å.
Pyrrole	20	1.50503	1.50569	1.51015	1.51406	1.51923	1.52147	1.53075
	25	1.50272	1.50333	1.50779	1.51164	1.51683	1.51904	1.52830
	30	1.50038	1.50100	1.50543	1.50926	1.51440	1.51662	1.52588
Pyrrolidine	20	1.44009	1.44045	1.44283	1.44492	1.44763	1.44883	1.45363
	25	1.43740	1.43777	1.44020	1.44226	1.44498	1.44614	1.45090
	30	1.43477	1.43513	1.43753	1.43956	1.44224	1.44345	1.44816
Pyridine	20	1.50481	1.50551	1.51016	1.51426	1.51971	1.52207	1.53219
	25	1.50210	1.50278	1.50745	1.51147	1.51690	1.51927	1.52939
	30	1.49939	1.50000	1.50466	1.50873	1.51415	1.51650	1.52655
2-Methylpyridine	20	1.49590	1.49654	1.50102	1.50492	1.51008	1.51245	1.52211
	25	1.49329	1.49394	1.49839	1.50230	1.50747	1.50978	1.51939
	30	1.49072	1.49135	1.49582	1.49967	1.50486	1.50714	1.51669

distillation was approximately 1.6 liters of 2-methylpyridine having a purity of 99.91 mole %.

Stability

As one test on the suitability of these compounds as calibration standards, their stability in storage was tested in the following manner. One set of samples, sealed in Pyrex glass ampoules, was stored in the dark at room temperature as a control. A second set of samples, also in Pyrex ampoules, was exposed to direct sunlight on the laboratory roof for approximately 1 year. At the end of the test period, both the control samples and the ampoules exposed to the action of the sunlight were tested. First the liquid sample was frozen at Dry Ice temperatures and the ampoule opened directly into a mass spectrometer.[7] In this way, gaseous decomposition products formed were determined. The liquid samples were then analyzed for purity by the freezing-point method.

Analysis of the gaseous materials gave no evidence of decomposition in the samples of pyrrole and pyridine. For pyrrolidine, approximately the same amount of gaseous decomposition products was found in the control sample and in the sample exposed to sunlight. This was calculated as approximately 10 micromoles of decomposition products per mole of pyrrolidine. A comparable amount of impurity in the liquid sample would not be determined by the freezing-point purity method. Gaseous products identified from the decomposition of the pyrrolidine included methane, ethylene, hydrogen and ammonia. Stability tests are not yet complete on 2-methylpyridine, but its stability is expected to be similar to that of pyridine.

Freezing point-purity measurements on the liquid samples showed no decrease in purity either on the samples stored in the dark or those exposed to sunlight. A slight tan color was observed in the exposed sample of pyridine; however, the other samples remained colorless.

Some consideration was given to the susceptibility of pyrrole to oxidation through exposure to air. A sample of pyrrole in a loosely capped glass vial was exposed to air and light in the laboratory. The sample darkened with exposure, and a decrease in purity was found by the freezing-point purity method. Infrared spectra were determined on the sample at intervals during the test. The only change found in the infrared spectrum was an increased absorbance in the 5.87 μ (carbonyl) region. A plot of exposure time *vs.* relative absorbance at 5.87 μ (Fig. 1) shows increasing decomposition of pyrrole on exposure to air and light. When exposed pyrrole is refluxed with calcium hydride, a decrease in absorbance at 5.87 μ is obtained concurrent with an increase in the freezing-point purity of the exposed material. These data indicate that the initial decomposition of pyrrole when exposed to air may proceed by the formation of a ketone which is destroyed by treating with calcium hydride. Although the decomposition at 120 hours amounts to only a few hundredths of a mole per cent., another experiment conducted for 500 hours showed a loss in purity of approximately 1 mole per cent. as determined by the freezing-point method.

It has been reported[8] that pyrroles on exposure to air, light and water, form succinimides. However, the mass spectrum of pyrrole exposed to air and light for 70 hours had an 83 peak (pyrrole + 16) representing the only detectable impurity. No indication of succinimide (99 peak) was found. A mass spectrum of pyrrole stored in the laboratory for two years without protection did not show succinimide but indicated impurities with molecular weights greater than 100.

(7) W. E. Haines, G. L. Cook and J. S. Ball, *J. Am. Chem. Soc.*, **78**, 5213 (1956).

(8) A. A. Morton, "The Chemistry of Heterocyclic Compounds," McGraw-Hill Book Co., Inc., New York, N. Y., 1945, p. 68.

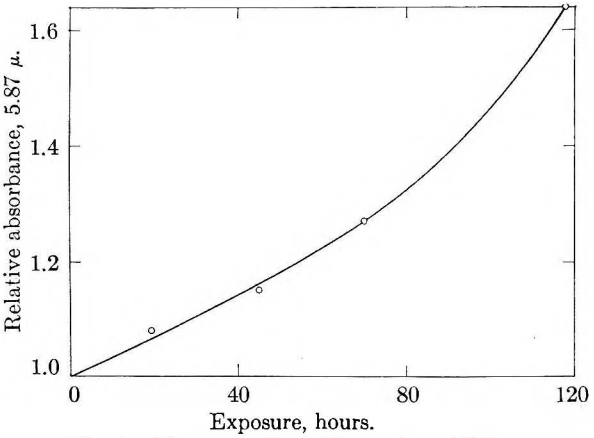

Fig. 1.—Exposure of pyrrole to air and light.

Physical Properties

Physical property data for the four organic nitrogen compounds are shown in Tables II and III. Except for surface tension, the apparatus and procedures used were similar to those described previously,[3] with the additional precaution that all measurements were made in an atmosphere of purified dry nitrogen gas. The triple point reported is for the pure compound with zero impurity and was determined by low-temperature calorimetric measurements at the Bartlesville Station of the Bureau of Mines. The cryoscopic constant also was determined from these measurements. The estimated accuracy of each of the physical property measurements is as shown: triple point, ±0.01°; boiling point, ±0.1°; density, ±0.00005 g./ml.; viscosity, ±0.001 centipoise; surface tension, ±0.08 dyne/cm.; and refractive index, ±0.00006.

Surface-tension measurements were made using the maximum bubble-pressure method, as described by Quayle.[9] Measurements were made on each sample in each of two units at 20, 25 and 30°. Each unit was calibrated using benzene and water as standards. The temperature of the xylene manometer was maintained at 25 ± 0.1°, and the temperature of each sample was maintained within ±0.005° of the temperature at which the values are reported. The measurements were made in an atmosphere of oxygen-free, dry nitrogen gas for maximum protection.

A compilation of physical properties of pyridine and 2-methylpyridine is included in Timmermans' book,[10] and later values have been given by Biddiscombe, *et al.*[11] A later compilation of the properties of pyrrole and 2-methylpyridine is given by Timmermans.[12] The values in the present report are consistent generally with these previous values, although the purity of the present samples appears to be greater than that of those previously studied. There is, however, a discrepancy of about 5° in the freezing point for pyrrole reported by Timmermans (−18.5°) and the value given in this report. No previous reports covering high-purity pyrrolidine were found.

Derived Functions

Two types of derived functions were calculated from the physical properties. Refractivity intercept and specific dispersion, which are non-additive functions, are used to analyze mixtures of hydrocarbons for the various classes. Molecular refraction, molecular volume and parachor are additive and constitutive functions and are used in structural characterization of compounds.

If nitrogen compounds are impurities in a hydrocarbon mixture being analyzed, they cause an error in the analysis. Values for refractivity intercept and specific dispersion at 20° are given in Table IV. Inasmuch as the refractivity intercepts of all four of the nitrogen compounds are low, they would cause the cycloparaffin content to appear high when analyses are made utilizing that function. The specific dispersions of three of the nitrogen compounds indicate them to be aromatic, whereas pyrrolidine is similar to the saturated hydrocarbons.

TABLE IV

VALUES FOR NON-ADDITIVE FUNCTIONS OF NITROGEN COMPOUNDS

Compound	Refractivity intercept, $n_D - \frac{d}{2}$	Specific dispersion, $(n_F - n_C) \times 10^4$
Pyrrole	1.02522	162.7
Pyrrolidine	1.01353	97.6
Pyridine	1.01856	168.4
2-Methylpyridine	1.02882	168.5

The molecular refractions, parachors and molecular volumes were calculated from data at 20° and are shown in Table V. Corresponding values for molecular refractions and parachors were calculated, using the increments of Auwers and Eisenlohr, and Mumford and Phillips.[13] These latter values agree very well with those from experimental data. Although much work has been done on molecular volume calculations, no values for a nitrogen increment were found. The four nitrogen compounds are compared to hydrocarbons in which nitrogen was replaced by carbon. For all four compounds it appears that the nitrogen occupies less volume than the carbon. However, a difference is noted between the compounds where NH is replaced and where N is replaced.

TABLE V

VALUES FOR CONSTITUTIVE PROPERTIES OF NITROGEN COMPOUNDS

	Pyrrole	Pyrrolidine	Pyridine	2-Methylpyridine
Molecular refraction				
From exptl. values	20.70	21.95	24.07	29.05
From increments	21.14	22.07	25.62	30.25
Difference	+0.44	+0.12	+1.55	+1.20
Parachor				
From exptl. values	171.3	193.3	198.3	236.7
From increments	169.4	193.0	198.3	238.3
Difference	−1.9	−0.3	0.0	+1.6
Molecular volume				
From exptl. values	69.18	82.84	80.46	98.61
Corresponding hydrocarbon	82.12	94.09	88.86	106.28
Difference	−12.94	−11.25	−8.40	−7.67

Spectra

Complete reproductions of the ultraviolet, infrared and mass spectra of the four nitrogen compounds will appear in the Catalogs of Spectral Data,[14] with descriptions of the instruments used and operating details. The high purity of the present compounds justifies examination of spectral patterns, despite previously published data. Special precautions were taken to assure that samples were not contaminated during determination of spectra. The liquids were transferred under a stream of purified nitrogen to protect them from contact with oxygen. The infrared and ultraviolet cells and all equipment used in transferring the samples were flushed and filled with purified nitrogen before use.

Ultraviolet Spectra.—The ultraviolet spectra of pyridine,

(9) O. R. Quayle, *Chem. Revs.*, **53**, 439 (1953).

(10) J. Timmermans, "Physico-Chemical Constants of Pure Organic Compounds," Elsevier Publishing Co., New York, N. Y., 1950, pp. 568–571.

(11) D. P. Biddiscombe, E. A. Coulson, R. Handley and E. F. G. Herington, *J. Chem. Soc.*, 1957 (1954).

(12) J. Timmermans and Hennaut-Roland, *J. chim. phys.*, **52**, 240 (1955).

(13) J. A. Leermakers and A. Weissberger, in Gilman, "Organic Chemistry," 2nd Ed., John Wiley and Sons, New York, N. Y., 1943, pp. 1746, 1751.

(14) American Petroleum Institute Research Project 44, Carnegie Institute of Technology, "Catalogs of Ultraviolet, Infrared and Mass Spectral Data."

pyrrole and 2-methylpyridine have been published[15] and the new data are in agreement. Because of the extreme reactivity of pyrrolidine with air, special equipment was used to obtain the ultraviolet spectrum of this compound.

A capillary tube, with a bulb on one end, was weighed and connected to a glass manifold. An appropriate quantity of sample was vacuum transferred into the bulb, the bulb sealed off and both pieces of the capillary reweighed. A correction for the weight of air removed under vacuum was necessary in calculating the weight of the sample. A quartz ultraviolet cell was connected by a graded seal to a side-arm on a large (150-ml. capacity) ampoule. The combined weight of the large ampoule, a gold-plated breaker, the filled sample bulb, and the quartz ultraviolet cell was obtained. The desired amount of solvent, in this instance, isoöctane, was introduced into the ampoule. The sample bulb was placed in the neck of the ampoule and was held in place by a constriction. The gold-plated breaker was placed on top of the sample bulb and the ampoule was attached to a glass manifold. The solvent was then degassed by freezing and thawing under vacuum and the ampoule sealed off from the manifold. The two parts of the ampoule were reweighed and the volume of solvent was calculated. The breaker was caused to crush the sample bulb. The bottom of the ampoule was cooled in liquid nitrogen creating a vacuum in the ampoule and causing any sample that remained in the sample bulb to be transferred into the solvent. The solvent-sample mixture was warmed, mixed thoroughly and again cooled to a temperature near its freezing point. The quartz cell was filled by pouring the mixture through the side arm of the ampoule. Both the quartz cell and the ampoule were immersed in liquid nitrogen to freeze the mixture of solvent and sample while the quartz cell was sealed off. The cell was then ready to be placed in the spectrophotometer to obtain a spectrum.

The spectrum of pyrrolidine obtained by this technique had no absorption maximum in the region 2100 Å. to 5300 Å. A weak absorption maximum was observed near 2800 Å. when the spectrum was obtained by the usual method. The use of the present method eliminated the 2800 Å. maximum from the spectrum.

Infrared Spectra. The locations of the principal absorption peaks for the infrared spectra are given in Table VI. Attention has been given in the literature to frequency assignments for pyrrole,[16] for pyridine[17-19] and for 2-methylpyridine.[20] The relationships of some of the vibrations of pyridine and 2-methylpyridine with higher members of the homologous series have been pointed out.[21]

Pyrrolidine has received less attention. However, Tschamler and Voetter[22] have made assignments in the 2.7- to 15-μ region. In comparing the spectrum of pyrrolidine with that of pyrrole, certain regularities are noted. Both have peaks in the 7.06- to 7.08-μ region. This suggests that the absorption is due to the C–N bond, which is a common structural feature of the two compounds. Peaks at 3.09, 8.37 and 17.32 μ in the spectrum of pyrrolidine probably arise from the vibrations of the NH group. These vibrations have been assigned[23] in pyrrole to peaks at 2.9, 8.7 and 17.7 μ. An unusual feature of the spectrum of pyrrolidine is the very broad absorption band extending from 11.3 to 12.5 μ.

Mass Spectra.—Table VII lists only those peaks that are 10% or a larger proportion of the base peak. The spectra of pyridine, 2-methylpyridine and pyrrole are typical of the spectra of aromatic systems. The base peak, which is underlined in the table for each of these compounds, occurs at the parent mass. The spectrum of pyrrolidine contrasts with the other three compounds in having the base peak at m/e 43. Although the base peak in the pyrrolidine spectrum may be formed by rearrangement of the molecule, the more probable formation is by direct splitting of a carbon–carbon bond and a carbon–nitrogen bond. This suggests that the ion at m/e 43 has the empirical formula C_2H_5N rather than C_3H_7. One can suggest the same type of reaction to arrive at the m/e 41 peak in pyrrole. The remaining features of the spectra of all four compounds are typical of what one would expect from small ring systems.

TABLE VI

PRINCIPAL ABSORPTION BANDS OF INFRARED SPECTRA, IN MICRONS

Pyrrole	Pyrrolidine	Pyridine	2-Methylpyridine
2.22	2.16	2.16	2.18
2.34	2.32	2.43	2.20
2.51	2.36	2.72	2.34
2.94 (broad)	2.43	3.25	2.46
3.23	3.09	3.30	3.28
3.40	3.48 (broad)	4.35	3.33
3.56	6.88	5.01	3.42
3.70	7.08	5.19	3.67
3.92	7.49	5.33	3.83
4.07	7.82	5.92	5.64
4.38	8.37	6.11	6.29
4.71	9.03	6.24	6.36
4.96	9.28	6.31	6.77
5.86	10.15 (broad)	6.73	6.88
6.37	11.30–12.50 region	6.95	6.97
6.53	17.32	8.22	7.26
6.81		8.73	7.73
7.06		9.35	8.09
7.79		9.71	8.71
8.78		13.45	9.09
9.31		14.29	9.53
9.55		16.63	10.03
9.87			12.51
11.54			13.35
13.83			13.70
15.24			15.88
17.88			18.25
19.71			21.20

TABLE VII

RELATIVE INTENSITIES OF PRINCIPAL IONS IN THE MASS SPECTRA

m/e	Pyrrole	m/e	Pyrrolidine	m/e	Pyridine	m/e	2-Methylpyridine
67	*100.0*	71	23.8	79	*100.0*	93	*100.0*
41	63.0	70	32.6	78	11.7	92	20.0
40	53.8	43	*100.0*	52	75.8	78	19.0
39	67.8	42	20.0	51	39.9	67	9.9
38	25.0	41	17.8	50	30.5	66	41.9
37	17.0	39	13.2	39	11.8	65	16.5
28	50.9	28	37.0	26	20.6	52	11.1
		27	13.4			51	19.2
						50	12.2
						40	10.7
						39	32.2
						38	12.6
						27	10.5
						26	10.0

(15) R. A. Friedel and M. Orchin, "Ultraviolet Spectra of Aromatic Compounds," John Wiley and Sons, New York, N. Y., 1951.

(16) R. C. Lord and F. A. Miller, *J. Chem. Phys.*, **10**, 328 (1942).

(17) C. H. Kline and J. Turkevich, *ibid.*, **12**, 300 (1944).

(18) L. Corrsin, B. J. Fax and R. C. Lord, *ibid.*, **21**, 1170 (1953).

(19) J. P. McCullough, D. R. Douslin, J. F. Messerly, I. A. Hossenlopp, T. C. Kincheloe and Guy Waddington, presented at 130th meeting of American Chemical Society.

(20) L. J. Bellamy, "The Infrared Spectra of Complex Molecules," John Wiley and Sons, New York, N. Y., 1954, pp. 232–236.

(21) G. L. Cook and F. M. Church, THIS JOURNAL, **61**, 458 (1957).

(22) H. Tschamler and H. Voetter, *Monatsh.*, **83**, 302 (1952).

(23) Mironi, Paolo and Drusiani, *Anna Maria. Atti. accad. nazl. Lincei Rend., Classe sci. fis. mat. e nat.*, **16**, 69 (1954).

Acknowledgments.—This work was done under a coöperative agreement between the Bureau of Mines, United States Department of the Interior, and the University of Wyoming. Assistance was rendered in various phases of the work by D. R. Latham, C. R. Ferrin, A. W. Decora, G. U. Dinneen, J. C. Morris, A. P. Marr and D. G. Earnshaw.

SOLUBILITY OF NOBLE GASES IN MOLTEN FLUORIDES. I. IN MIXTURES OF $NaF-ZrF_4$ (53–47 MOLE %) AND $NaF-ZrF_4-UF_4$ (50–46–4 MOLE %)

BY W. R. GRIMES, N. V. SMITH AND G. M. WATSON

Oak Ridge National Laboratory, P. O. Box Y, Oak Ridge, Tennessee

Received April 21, 1958

Solubilities of He, Ne, A and Xe have been determined at pressures from 0.5 to 2 atmospheres in $NaF-ZrF_4$ (53–47 mole %) at 600, 700 and 800°. The solubilities increase linearly with gas pressure, decrease with increasing atomic weight of the solute and increase with increasing temperature. Henry's law constants in moles of solute/(cm.^{3} solution)(atmosphere) at 600° are $21.6 \pm 1 \times 10^{-8}$, $11.3 \pm 0.3 \times 10^{-8}$, $5.06 \pm 0.15 \times 10^{-8}$ and $1.94 \pm 0.2 \times 10^{-8}$ while heats of solution are 6.2, 7.8, 8.2 and 11.1 kcal./mole for He, Ne, A and Xe, respectively. Solubilities and heats of solution for He and Xe in $NaF-ZrF_4-UF_4$ (50–46–4 mole %) are very similar to the values obtained with these gases in the $NaF-ZrF_4$ mixture.

Introduction

Solubilities of gases in liquids have been studied by many investigators; reviews covering much of the work in this field are available.[1–3] Recent studies of noble gases as solutes include measurements with He, Ne, A, Kr and Xe in organic liquids[4–6] and with radon in organic materials related to vegetable oils and animal fats.[7,8] However, no information regarding solubilities of noble gases in molten salt systems appears to have been published.

A molten fluoride mixture containing UF_4 has served as the fuel in a high temperature nuclear reactor.[9–12] Xe and Kr are produced in such a fuel as fission products; Xe is a serious nuclear poison. Ease of removal of these elements from the liquid fuel depends on their solubility in the molten fluoride. Since He (or A) is commonly used as a protective blanket and/or sparging gas during reactor operation the fluoride fuel is saturated with He at the contact temperature; bubble formation, which could lead to undesirable perturbations in nuclear reactivity, might be a consequence of the dependence of He solubility on temperature within the reactor fuel circuit. Accordingly, both absolute solubility and its temperature dependence for noble gases in molten fluorides are of importance in operation of such reactors.

Some preliminary measurements of the solubility of xenon in molten salt mixtures have been performed by R. F. Newton.[13] His technique consisted in saturation of the salt with xenon, transfer of the solution to an isolated section of the apparatus and recovery of the xenon by sparging with hydrogen in a closed system containing a trap cooled with liquid nitrogen. The hydrogen was subsequently removed and the recovered xenon was measured in a McLeod gage. Experiments with an all-glass apparatus showed that the solubility of Xe in the KNO_3-NaNO_3 eutectic[14] varied in the range 8×10^{-8} to 10^{-7} mole Xe/(cm.^{3} solvent) (atmosphere) between 260 and 450°; it appeared that the solubility increased slightly with increasing temperature. Experiments with the ternary eutectic[15] of LiF, NaF and KF in a metal–glass system were less successful since the recovered xenon was contaminated with considerable HF and SiF_4. It appeared that the solubility of Xe in this fluoride solvent at 500° was less than 5×10^{-8} mole Xe/(cm.^{3}) atmosphere.

Successful operation of the Aircraft Reactor Experiment[9,10] disclosed no detrimental effects due to behavior of the rare gases; it was observed that at least 95% of the Xe produced was evolved from the fuel.[12,16] The lack of quantitative information on this subject has prompted examination of the solubilities of noble gases in fluoride mixtures of interest to nuclear reactors. The solubilities of He, Ne, A and Xe in a mixture of NaF with 47 mole % ZrF_4 and of He and Xe in a mixture of NaF with 46 mole % ZrF_4 and 4 mole % UF_4 over the temperature interval from 600 to 800° are reported in this document.

Experimental

Materials. The noble gases were obtained in cylin-

(1) A. E. Markham and K. A. Kobe, *Chem. Revs.*, **28**, 519 (1941).

(2) J. H. Hildebrand and R. L. Scott, "The Solubility of Non-Electrolytes," Chapter XV, 3rd Ed., Reinhold Publ. Corp., New York, N. Y., 1950.

(3) M. W. Cook, U. S. Atomic Energy Commission, UCRL-2459, 1954.

(4) H. L. Clever, R. Battino, J. H. Saylor and P. M. Gross, THIS JOURNAL, **61**, 1078 (1957).

(5) H. L. Clever, J. H. Saylor and P. M. Gross, *ibid.*, **62**, 89 (1958).

(6) L. W. Reeves and J. H. Hildebrand, *J. Am. Chem. Soc.*, **79**, 1313 (1957).

(7) E. Nussbaum and J. B. Hursh, *Sci.*, **125**, 552 (1957).

(8) E. Nussbaum and J. B. Hursh, THIS JOURNAL, **62**, 81 (1958).

(9) A. M. Weinberg and R. C. Briant, *Nuclear Science and Engineering*, **2**, 797 804 (1957).

(10) E. S. Bettis, R. W. Schroeder, G. A. Cristy, H. W. Savage, R. G. Affel and L. F. Hemphill, *Nuclear Sci. Eng.*, **2**, 804 (1957).

(11) W. K. Ergen, A. D. Callihan, C. B. Mills and Dunlap Scott, *ibid.*, **2**, 826 (1957).

(12) E. S. Bettis, W. B. Cottrell, E. R. Mann, J. L. Meem and G. D. Whitman, *ibid.*, **2**, 841 (1957).

(13) R. F. Newton, Oak Ridge National Laboratory, unpublished work, 1954.

(14) P. I. Protsenko and A. G. Bergman, *J. Gen. Chem. SSSR*, **20**, 1365 (1950).

(15) A. G. Bergman and E. P. Dergunov, *Compt. rend., acad. sci. URSS.* **31**, 754 (1941).

(16) M. T. Robinson, W. A. Brookshank, Jr., S. A. Reynolds, H. W. Wright and T. H. Handley, "Some Aspects of the Behavior of Fission Products in Molten Fluoride Reactor Fuels," ORNL CF-58-1-36, Jan. 1958.

ders from commercial sources. The He was obtained from the Bureau of Mines at Amarillo, Texas; Ne, A and Xe were obtained from Linde Air Products Company. All gases used were delivered from the cylinder at purity exceeding 99.9% as shown by analysis with the mass spectrometer.

The molten fluorides were prepared from Reagent grade NaF, UF_4 obtained from the Mallinckrodt Chemical Company, St. Louis, Missouri and ZrF_4 which had been prepared by hydrofluorination of $ZrCl_4$ at 500° in equipment of Ni°. The fluorides were mixed in proper proportions and purified in a closed system of Ni at 800° by alternate sparging with anhydrous HF and H_2. The resulting liquid was transferred under pressure of He to the solubility apparatus without exposure to the atmosphere. Samples of the melt taken during this transfer operation showed no oxides or oxygen-bearing phases on examination with the petrographic microscope. Chemical analysis of such samples yielded these data

	$NaF-ZrF_4$ (53–47 mole %)		$NaF-ZrF_4-UF_4$ (50-46-4 mole %)	
	Theor. (% by wt.)	Obsd. (% by wt.)	Theor. (% by wt.)	Obsd. (% by wt.)
Zr	42.6	42.9	38.0	38.0
U	0	0	8.6	8.8
Ni	0	20[a]	...	25[a]
Fe	0	40[a]	...	45[a]

[a] Concentrations in parts per million.

Apparatus.—The apparatus, which consists of connected saturating and stripping sections, is shown schematically in Fig. 1. All sections of the apparatus in contact with the molten fluoride or at higher temperature were of nickel. Welded construction and Swage-lock fittings were used throughout this metal portion. Sections of the apparatus in contact only with the gases at low temperature were of glass; glass-metal connections were accomplished by use of Kovar seals.

The saturator consists of a cylindrical vessel 5 inches in diameter by 16 inches long containing a pair of thermocouple wells. The vessel is surrounded by a resistance furnace and is connected to a manifold so that the test gas (He, for example) at the desired pressure could be bubbled through the liquid or maintained as a covering atmosphere. Through a Teflon-packed seal in a riser through the top of the saturator protrudes a movable probe, which completes an electrical circuit on contact with the liquid surface, to permit measurement of the liquid level in the vessel. The saturator is connected to the stripping section of the apparatus by a length of $^3/_8$ inch diameter nickel tubing which is welded through the bottoms of both vessels and which can be heated by resistance heaters or cooled by a water coil as required. The stripper consists of a similar heated vessel which forms part of a simple manifold of known volume so that a second inert gas (argon, for example) at known pressure can be circulated through the melt to remove the dissolved test gas. A pump[17] in which a rubber tube is compressed by action of metallic fingers serves to circulate the stripping gas. The glass section of the stripping manifold includes a bank of evacuated 50-cc. glass sampling bulbs separated by a vacuum stopcock from the contents of the manifold. The saturator and stripper sections of the apparatus are isolated during the experiment by a frozen plug of the molten salt under study.

A chromel–alumel thermocouple in a well in the saturator activated a Brown-electronic recorder to provide temperature measurement. Once per day the temperature was checked with a standard platinum–platinum-rhodium thermocouple inserted in the second thermo-well in the saturator. Temperature control was accomplished by means of a Brown Pyrovane Controller activated by a chromel–alumel thermocouple in the furnace outside the vessel. Temperatures in the stripping vessel were measured from a similar couple in a central thermo-well.

Procedure.—The 10 kg. charge of molten salt was transferred completely to the saturator and was isolated from the stripper by establishment of the frozen seal. The melt was brought to temperature equilibrium in the saturator and was sparged with the test gas (He, for example) at the desired pressure. The sparging was discontinued after six hours and the He was maintained at pressure as a covering atmosphere. The liquid level in the saturator was measured

(17) Sigma Motor, Inc., Middleport, New York.

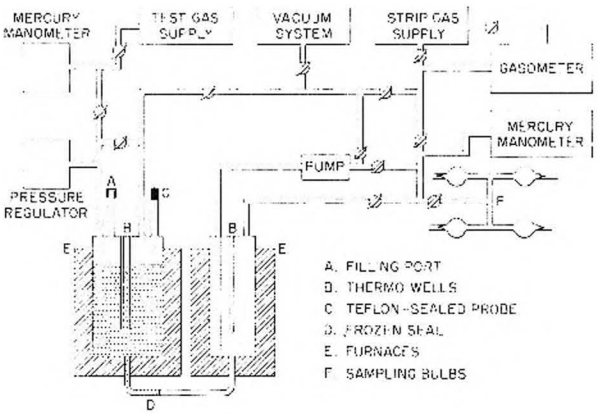

Fig. 1.—Gas solubility apparatus.

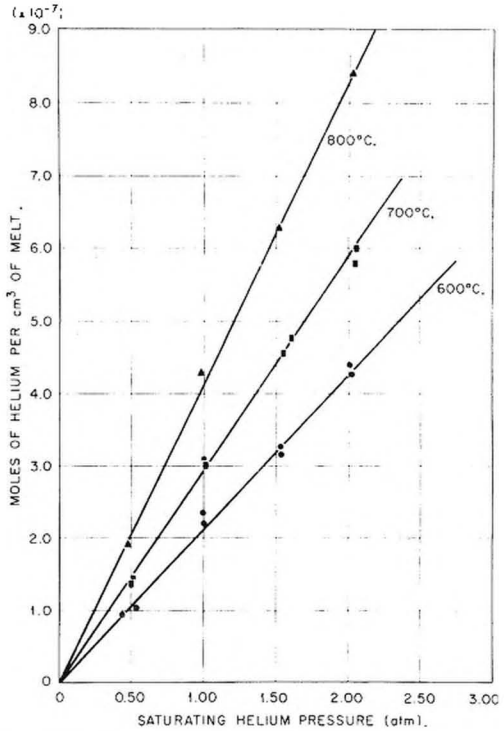

Fig. 2. Solubility of helium in $NaF-ZrF_4$ (53–47 mole %).

by use of the probe. Meanwhile, the stripping section of the apparatus was repeatedly flushed with the second inert gas (A, for example), evacuated, and ultimately filled from a gasometer with a known quantity[18] of A which had been shown by mass spectrometry to be free from He. The frozen seal was destroyed by application of heat and the molten salt was allowed to transfer to the stripping section till hydrostatic equilibrium was reached. The frozen seal was re-established immediately and the final liquid level in the saturator was determined. The dissolved helium was removed from the salt by circulation of argon for 12–15 passes (15 minutes) through the system. The resulting gas mixture was sampled by opening the stopcock to the bank of four evacuated sampling bulbs. The sampling bulbs were cut from the manifold by means of a glass blowing torch.

The helium concentration in the argon was determined by mass spectrometry. Each sample was analyzed in company with three or four samples of known composition prepared with gas burets and contained in sample bulbs of identical construction. These known samples were chosen to include concentrations more dilute and more concentrated than that anticipated for the unknown.

(18) The quantity was chosen so that 45–55% of the molten solution would transfer to the stripper under the saturating pressure of He when the frozen seal was melted.

The volume of transferred salt was established from the difference in levels in the saturator before and after transfer. The absolute amount of He dissolved was calculated from the analyzed concentration of He and the known quantity of argon used.

Solubility of He was determined as described using argon as the stripping gas. Solubility of A, Ne and Xe were determined in the same manner using He as the stripping gas.

Results

The solubilities of helium, neon, argon and xenon in molten $NaF-ZrF_4$ (53–47 mole %) have been examined at 600, 700 and 800° at pressures from 0.5 to 2 atmospheres. The experimental data are summarized in Tables I–IV; data obtained with helium in this solvent are shown in Fig. 2 which

TABLE I

SOLUBILITY OF He IN $NaF-ZrF_4$ (53–47 MOLE %)

Temp. (°C.)	Saturating pressure (atm.)	Solubility $\times 10^3$, moles He (cc. melt)	$K = c/p \times 10^3$, moles He (cc. melt)(atm.)
600	0.443	9.03	20.4
	.538	11.0	20.4
	.97	23.6	24.3
	.98	21.9	22.4
	1.52	31.6	20.8
	1.53	32.3	21.1
	2.00	43.9	22.0
	2.03	42.6	21.0
		Av.	21.6 ± 1.0
700	0.489	13.8	28.2
	0.504	14.1	28.0
	1.00	30.8	30.9
	1.02	30.4	29.9
	1.56	45.6	29.3
	1.60	47.8	29.9
	2.06	57.8	28.0
	2.07	60.2	29.1
		Av.	29.2 ± 0.7
800	0.447	19.1	42.7
	0.98	43.0	43.9
	1.53	61.4	40.1
	2.03	84.3	41.3
		Av.	42.0 ± 1.3

TABLE II

SOLUBILITY OF NEON IN $NaF-ZrF_4$ (53–47 MOLE %)

Temp. (°C.)	Saturating pressure (atm.)	Solubility $\times 10^6$, moles neon (cc. melt)	$K = c/p \times 10^3$, moles neon (cc. melt)(atm.)
600	1.04	11.5	11.1
	1.46	16.9	11.6
	1.82	20.6	11.3
		Av.	11.3 ± 0.3
700	1.03	18.2	17.7
	1.53	29.2	19.1
	2.00	36.9	18.5
		Av.	18.4 ± 0.5
800	1.02	25.8	25.4
	2.02	48.5	24.0
		Av.	24.7 ± 0.7

illustrates the linear dependence of solubility with pressure of the gas. The Henry's law constants

TABLE III

SOLUBILITY OF ARGON IN $NaF-ZrF_4$ (53–47 MOLE %)

Temp. (°C.)	Saturating pressure (atm.)	Solubility $\times 10^3$, moles argon (cc. melt)	K $c/p \times 10^3$, moles argon (cc. melt)(atm.)
600	0.530	2.63	4.96
	1.02	4.95	4.85
	1.50	7.92	5.28
	2.06	10.7	5.15
		Av.	5.06 ± 0.15
700	0.526	4.20	7.98
	1.05	8.60	8.21
	1.55	12.5	8.08
	2.09	16.8	8.01
		Av.	8.07 ± 0.08
800	0.432	5.55	12.8
	1.04	12.2	11.8
	1.53	16.8	11.0
	1.99	24.3	12.2
		Av.	12.0 ± 0.6

TABLE IV

SOLUBILITY OF XENON IN $NaF-ZrF_4$ (53–47 MOLE %)

Temp. (°C.)	Saturating pressure (atm.) Total	Net	Solubility $\times 10^6$, moles xenon (cc. melt)	$K = c/p \times 10^3$, moles xenon (cc. melt)/(atm.)
600	1.04	0.96[a]	1.77	1.85
	1.98	1.90[a]	3.84	2.03
			Av.	1.94
700	1.04	0.92[a]	3.25	3.56
	2.03	1.71[a]	6.08	3.56
			Av.	3.56
800	0.99	0.71	4.48	6.32

[a] Estimated on the assumption of a decrease of xenon purity of 4% per experiment.

(in moles of solute)/(cm.^{3} solvent)(atmosphere) for all these gases are plotted against the reciprocal of the absolute temperature in Fig. 3. Use of density values calculated from the equations[19] which are

$NaF-ZrF_4$ (53–47 mole %) ρ (g./cm.^{3}) =
$3.71 - 0.00089T$ (°C.)

$NaF-ZrF_4-UF_4$ (50–46–4 mole %) ρ (g./cm.^{3}) =
$3.93 - 0.00093T$ (°C.)

applicable over the temperature range of these experiments permits conversion of the data to concentrations in mole fractions or otherwise as desired.

TABLE V

HENRY'S LAW CONSTANTS FOR HELIUM AND XENON IN $NaF-ZrF_4-UF_4$ (50–46–4 MOLE %)

$K = c/p \times 10^3$ (moles gas)/(cc. melt)(atm.)

Temp. (°C.)	Henry's law constant $\times 10^3$ He	Xe
600	20	2.0
700	27	4.0
800	41	6.5

The solubilities of helium and of xenon have been determined over a similar pressure and temperature

(19) S. I. Cohen, W. D. Powers, N. D. Greene and H. F. Poppendiek, Oak Ridge National Laboratory, personal communication.

interval in $NaF-ZrF_4-UF_4$ (50–46–4 mole %); experimental data are shown in Table V. Since the solubilities of He and Xe in the two solvents are virtually identical, Fig. 3 represents to a good approximation the solubility behavior in the UF_4-bearing mixture.

Preliminary experiments indicated that sparging of the liquid with gas for periods less than 2 hours yielded values appreciably lower than the identical values obtained when periods of 3 to 24 hours were used; the procedure was standardized with 6 hours of sparging as ample and convenient. No evidence of entrainment of bubbles in the liquid was observed even when the transfer was made immediately after sparging was stopped; in general, 5–8 minutes was allowed after sparging was stopped before the liquid was transferred. Stripping of the dissolved gas appeared to be very rapid; the 15 minute removal period was shown to be ample for mixing of the gaseous solution. Temperature measurements should have been accurate to ± 5°, and the volume of salt transferred was known to ± 2%. Calibration of the mass spectrometer was possible at each determination from the results obtained from the standard samples. However, since the individual analyses agreed (to well within 10%) with the synthesized concentrations of the standards, the values obtained for the test samples were used directly. The mean values for quadruplicate samples from each experiment should, accordingly, be accurate to ±5%. The mole fraction of test gas in the binary gas mixture after stripping reached 0.03 in the tests with He at 800° and He pressures of 2 atmospheres. For all other gases the mole fractions were below, and usually much below, 0.015. The small corrections for quantities of test gas retained in the molten salt after stripping have not been applied.

Measurements with He, Ne and A could be duplicated in separate experiments to better than ±5%; the data may, accordingly, be claimed with confidence to be accurate to ±10%. The solubility of xenon is known with somewhat less certainty. Economic considerations made it expedient to recover and reuse the xenon. During the course of experiments with the $NaF-ZrF_4-UF_4$ mixture the xenon purity decreased to 95.6%; relatively small corrections in the data were made to reflect the real partial pressure of xenon. However, during experiments with the $NaF-ZrF_4$ mixture xenon purity decreased to 72%; substantial corrections were, accordingly, required. Nitrogen was the chief contaminant in each case; contamination by air, with the oxygen subsequently removed by the salt mixture, almost certainly occurred. While the precision of multiplicate determinations was again ±5%, the solubility data for xenon are probably accurate to within ±20%.

Discussion

Within the precision of the measured values the solubilities of the noble gases are identical in these two very similar salt mixtures. The solubility of each gas obeys Henry's law and increases with increasing temperature in both solvents. The solubility values decrease while the heat of solution increases with increasing atomic weight of the noble gas.

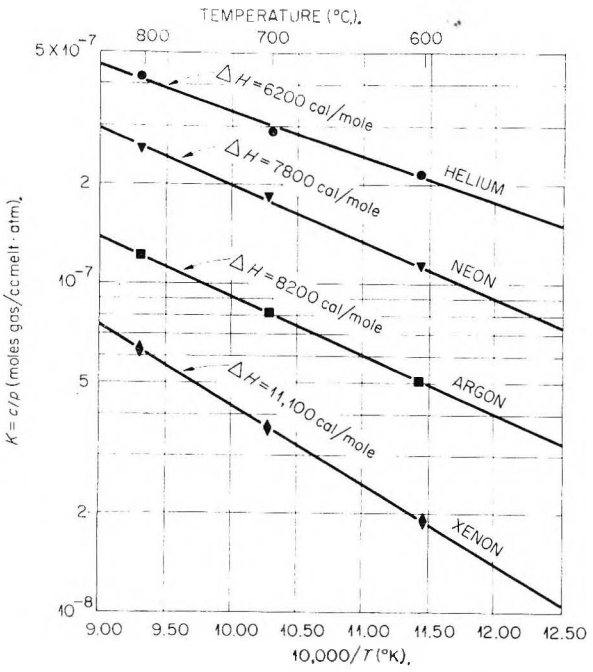

Fig. 3.—Temperature dependences of solubilities of noble gases in $NaF-ZrF_4$ (53–47 mole %).

Figure 3 shows the enthalpy changes obtained from the experimental data for the process

$$X_{(g,C_g)} \rightleftarrows X_{(d,C_d)} \qquad (1)$$

where X represents the noble gas, subscripts g and d indicate, respectively, that it is in the gaseous state or dissolved in the molten salt and C_d represents the concentration in moles/liter of dissolved gas in equilibrium with the noble gas at concentration C_g equivalent to a pressure of 1 atmosphere. For this equilibrium process the entropy change is given by $\Delta H/T$. Isothermal expansion of the gas through the same composition interval is represented by

$$X_{(g,C_g)} \rightleftarrows X_{(g,C_d)} \qquad (2)$$

If the noble gas is assumed to be ideal no enthalpy change occurs in (2) and the entropy change is given by

$$\Delta S_2 = R \ln \frac{C_g}{C_d}$$

Subtraction of (2) from (1) yields the process

$$X_{(g,C_d)} \rightleftarrows X_{(d,C_d)} \qquad (3)$$

of dissolving an ideal gas with equal concentrations in gaseous and liquid states. For (3) the enthalpy change is identical with that in (1) and the entropy of the ideal isothermal expansion is absent. Table VI presents the experimental enthalpy changes and the entropy changes for the four noble gases in each of these processes at 1000°K.

It will be noted, though the significance of the observation is not immediately obvious, that the heats of solution from Fig. 3 are approximated by $T\Delta S_2$. Thus the heat of solution can be estimated within 20% in the worst case by considering the gas to be ideal and calculating the entropy of isothermal

TABLE VI

ENTHALPY AND ENTROPY CHANGES ON SOLUTION OF NOBLE GASES IN MOLTEN NaF–ZrF_4 (53–47 MOLE %) AT 1000°K.

Gas	Equilibrium concn. (moles/l.) $C_g \times 10^3$	$C_d \times 10^5$	Enthalpy change (kcal./mole)	Entropy change (e.u.) ΔS_1	ΔS_2	ΔS_3
He	1.22	33.2	6.2	6.2	7.2	−1.0
Ne	1.22	20.0	7.8	7.8	8.2	−0.4
A	1.22	9.15	8.2	8.2	9.7	−1.5
Xe	1.22	4.30	11.1	11.1	11.2	−0.1

expansion over the concentration interval defined by a single solubility experiment.

In light of the precision of the experiments, no real significance can be attached to the absolute values of ΔS_3. It is possible that the fact that ΔS_3 is small compared with ΔS_2 is fortuitous and a consequence of effects inherent in these similar solvents. Solubilities of the noble gases are presently under examination in molten fluoride mixtures of considerably different chemical composition. Efforts to attach some fundamental significance to the results will be deferred until additional data are available.

Acknowledgments.—The authors are especially indebted to Mr. W. D. Harmon and his associates who were responsible for mass-spectrometric analysis of the many samples submitted. Many interesting and valuable discussions with Messrs. F. F. Blankenship, M. Blander and R. F. Newton are gratefully acknowledged.

NOTES

A REPLY TO LONG ON THE ACTIVATION ENERGY OF $CH_3 + H_2$

BY K. O. KUTSCHKE AND E. W. R. STEACIE

Division of Pure Chemistry, National Research Council, Ottawa, Canada

Received August 9, 1957

In a recent note[1] Long has argued that an incorrect interpretation has yielded erroneous values of the rate constants for some hydrogen abstraction reactions of methyl radicals. The methods by which these constants are obtained from the experimental data are now sufficiently well known to obviate the necessity of repeating them here.[2] The crux of Long's argument is that reaction (4) (Long's numbering throughout) is important both in the presence or absence of added reactants RH, where C_2H_6 is the product of methyl radical combination. Obviously (4) must be of importance if

$$CH_3 + C_2H_6 \longrightarrow CH_4 + C_2H_5 \qquad (4)$$

photolysis is allowed to proceed to a large fractional decomposition of the radical source and the question becomes one of the relative rate of reaction (2) and (4) under conditions normally encountered in this type of study. We propose to summarize here some

$$CH_3 + CH_3COCH_3 \longrightarrow CH_4 + CH_2COCH_3 \qquad (2)$$

of the evidence which indicates that (4) and the subsequent reactions discussed by Long are not important under normal conditions.

(1) The quantity $R_{CH_4}/R^{1/2}_{C_2H_6}[A]$ is independent of all variables other than temperature if acetone pressure is kept above about 50 mm. and temperature above about 120°. In particular it is "independent of intensity to a very good first approximation"[3]; actual figures show independence to within 15% over a one thousandfold change of I_a at constant acetone pressure. Moreover, the quantity is also independent of the fractional decomposition at least up to about 5% decomposition of acetone. This is shown by values obtained by independent investigations for the function $R_{CH_4}/R^{1/2}_{C_2H_6}[A]$ at 122°; the values are 3.3,[4] 3.7[3] and 3.5[5] $\times 10^{-13}$ (molecules cm.$^{-2}$)$^{-1/2}$ sec.$^{-1/2}$. The fractional decompositions are, respectively, 0.04%, 0.3% and 3%; the first fractional decomposition is quoted in reference (3) although it is not given explicitly in the original work (4). One further example taken from unpublished data[6] taken in connection with other work shows that the amounts of CD_4 and of C_2D_6 are linear in the amount of CO formed in the photolysis of acetone-d_6 in the range (CO formed)/(initial acetone) = 0.2 to 1.0%. We therefore conclude that in the absence of added reactants, (4) is unimportant.

(2) We might enquire as to the magnitude of the effect to be expected. Following Long we write

$(k_2[CH_3][A])^{-1}(d[CH_4]/dt) = 1 + (k_4/k_2)([C_2H_6]/[A])$

$[C_2H_6]/[A]$ can be taken as 2×10^{-2} as a most pessimistic estimate; this would imply that a steady value had been attained by $[C_2H_6]$ in a time which is short compared to the time of an experiment. The ratio k_4/k_2 may be approximated by $k_4/k_2 = (k_4'/k_2')(k_4/k_4')(k_2'/k_2)$ where the primed reactions are

$$CD_3 + CD_3COCD_3 \longrightarrow CD_4 + CD_2COCD_3 \qquad (2')$$

$$CD_3 + C_2H_6 \longrightarrow CD_3H + C_2H_5 \qquad (4')$$

In studying the system acetone-d_6–C_2H_6 Wijnen[7] and McNesby and Gordon[8] find that CD_3H/CD_4 is nearly unity when [acetone-d_6]/[C_2H_6] is unity; this is found to be independent of temperature to

(1) L. H. Long, THIS JOURNAL, **61**, 821 (1957).

(2) See, for example: (a) E. W. R. Steacie, "Atomic and Free Radical Reactions," Reinhold Publishing Corp., Inc., New York, N. Y., 2nd Edition, 1954; (b) A. F. Trotman-Dickenson, "Gas Kinetics," Academic Press, Inc., New York, N. Y., 1955.

(3) A. J. C. Nicholson, *J. Am. Chem. Soc.*, **73**, 398 (1951).

(4) L. M. Dorfman and W. A. Noyes, Jr., *J. Chem. Phys.*, **16**, 557 (1948).

(5) A. F. Trotman-Dickenson and E. W. R. Steacie, *ibid.*, **18**, 1097 (1950).

(6) M. Weston, unpublished data, N.R.C.

(7) M. H. J. Wijnen, *J. Chem. Phys.*, **23**, 1357 (1955).

(8) J. R. McNesby and A. S. Gordon, *J. Am. Chem. Soc.*, **77**, 4719 (1955).

about 500°. The most likely explanation of these data is that $k_4'/k_2' \simeq 1$. Similarly, work with mixtures of deuterated and normal methyl radicals[9,10] led to the conclusion that $k_4/k_4' \simeq 1$ and that $k_2'/k_2 \simeq \exp(-1600/RT)$. The correction term thus becomes about 0.003 in the middle of the temperature range at 400°K. Such an effect is negligible.

(3) A careful recalculation of the published and unpublished results of Whittle[10] on the acetone-d_2 system shows that, in the absence of D_2

$$13 + \log R_{CH_4}/R_{C_2H_6}^{1/2}[A] = 5.986 - (2119)/T$$

while in the presence of 5 or 20 cm. D_2 but with the same 10 cm. of acetone one finds

$$13 + \log R_{CH_4}/R_{C_2H_6}^{1/2}[A] = 5.829 - (2048)/T$$

This leads to an equation for the difference (Δ) between $R_{CH_4}/R_{C_2H_6}^{1/2}[A]$ in the presence and absence of deuterium of

$$\Delta = 0.16 - 71/T$$

indicating that all values in the presence of D_2 are too high below ~170° and too low above this temperature. In the temperature range usually studied this difference may be as high as 15%. It must be realized that over 40% of the methyl radicals which normally produce methane or ethane may produce CH_3D in the presence of D_2. With so large a perturbation in the system, the degree of agreement achieved (to within 0.4 kcal. mole^{-1}) is considered adequate. The residual uncertainty probably reflects the difficulty of analyses in the presence of large excesses of non-condensable gases. It is to be noted that these uncertainties are in the region of several tenths of a kcal. mole^{-1} rather than the several kcal. mole^{-1} required by Long's hypothesis. Similar results may be calculated from the data of other workers using other methyl radical sources. We conclude, therefore, that reaction (4) is of minor importance in the presence of D_2, and, by inference, in the presence of H_2 as well. This is also in agreement with the observations of Davison and Burton,[11] who noted that the ratio CH_3D/CH_4 was independent of decomposition provided $[CO]/[A] < 0.02$; this corresponded to $[CO]/[A] \simeq 0.04$.

In conclusion it might be pointed out that should Long's hypothesis be correct, the value of the activation energy for $CH_3 + H_2$ remains unsettled. Davison and Burton[11] determined only $E_2 - E_1$ and used $E_2 = 9.7$ kcal. mole^{-1}; the latter was measured by Trotman-Dickenson and Steacie[5] by the very method to which Long objects. We feel, however, that on the basis of the evidence as a whole, reaction (4) and subsequent steps may be ignored in the normal investigations, and that E_1 as given in reference 2(a) rests on as firm an experimental foundation as most values of activation energy.

(9) J. R. McNesby and A. S. Gordon, *ibid.*, **76**, 1416 (1954).

(10) E. Whittle and E. W. R. Steacie, *J. Chem. Phys.*, **21**, 993 (1953).

(11) S. Davison and M. Burton, *J. Am. Chem. Soc.*, **74**, 2307 (1952).

MECHANISM OF REACTION OF DIISOPROPYL FLUOROPHOSPHONATE WITH CUPRIC α,α'-DIPYRIDYL CHELATE[1]

BY F. M. FOWKES, G. S. RONAY AND L. B. RYLAND

Shell Development Company, Emeryville, California

Received December 23, 1957

T. Wagner-Jauregg and associates recently have published[2] rate measurements for the hydrolysis of DFP in solutions of cupric sulfate and α,α'-dipyridyl. As we have recently determined the type and distribution of species in solution of cupric nitrate and α,α'-dipyridyl,[3] these equilibrium data have been correlated with the rate data of Wagner-Jauregg and associates to determine the catalytic activity of the various species and to obtain a better understanding of the mechanism of the reaction.

Equilibria of Species.—In the above-mentioned publication[3] it was shown from potentiometric titration curves that in solutions of the 1:1 chelate of α,α'-dipyridyl and cupric salts the following species exist: the acidic ion, $DipyCu(H_2O)_2^{++}$, (species A); the soluble non-ionized base, $DipyCu(OH)_2$, (species B_2) and the weakly basic dimer,

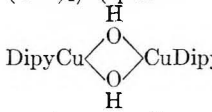

DipyCu CuDipy, (species $(B_1)_2$). Presumably an intermediate species B_1, $DipyCu(H_2O)OH^+$, also exists but was not detected in these studies. The distribution of species at various *p*H values and concentrations may be calculated from the equilibrium constants for 30°

$$A \rightleftharpoons B_2 + 2H^+ \quad K_A = 10^{-16.20} \qquad (1)$$

$$2A \rightleftharpoons (B_1)_2 + 2H^+ \quad K_{\alpha 2} = 10^{-10.67} \qquad (2)$$

Experimental Data and Discussion

The rate data shown in Table I for the hydrolysis of DFP in the presence of copper dipyridyl sulfate were obtained by Wagner-Jauregg and associates of the Army Chemical Center Medical Laboratory.[2] The solutions contained 1150 μmoles/liter of both α,α'-dipyridyl and cupric sulfate and 2300 μmoles/liter of DFP in 0.05 M KNO_3.

The data of Table I show how change of *p*H in solutions of 1:1 cupric dipyridyl salts alters the proportions of species A, B_2 and $(B_1)_2$ as calculated from K_A and $K_{\alpha 2}$. With increase of *p*H from 6 to 8, where only species A and $(B_1)_2$ are present in appreciable quantities, the rate is found to be proportional to the product of $[A] \times [OH^-]$ and is not affected by the concentration of $(B_1)_2$. It may be shown that at *p*H 9 to 11, the rate is also dependent on $[B_2]$ and on $[OH^-]$ as shown in the following equation, which shows the contribution of each catalytic species to the observed rate

$$k_1(\text{obs.}) = k_A[A][OH^-] + k_{B_2}[B_2] + k_{OH}[OH^-]$$

By using the calculated values of [A], and the observed first-order rate constants (k_1) at *p*H 6 to 8, the third-order rate constant k_A may be calculated from $k_1/[A][OH^-]$ to be 1.4, 1.05, 1.13, 1.16 or

(1) This paper reports work done under contract with the Chemical Corps, U. S. Army, Washington 25, D. C.

(2) T. Wagner-Jauregg, *et al.*, *J. Am. Chem. Soc.*, **77**, 922 (1955).

(3) L. B. Ryland, G. S. Ronay and F. M. Fowkes, THIS JOURNAL, **62**, 798 (1958).

TABLE I

HYDROLYSIS OF DFP IN SOLUTIONS OF COPPER DIPYRIDYL SULFATE

pH	[A], μmole/l.	$[B_1]$, μmole/l.	$(B_1)_2$, μmole/l.	$k_A[A][OH^-]$ per min.	$k_{B_2}[B_2]$ per min.	$k_{OH^-}[OH^-]$ per min.	k_1, per min. Calcd.	k_1, per min. Expti.	$t_{1/2}$, min. Calcd.	$t_{1/2}$, min. Expti.
6.0	1100	....	25	0.0121	....	....	0.0121	0.0154	57	45
6.0	1100	....	25	.0121	....	....	.0121	.0259	57	27
6.5	830	0.6	160	.0274	....	....	.0274	.0277	25	25
7.0	390	2.5	429	.0430	0.0001	....	.0431	.0443	16.0	15.7
8.0	47	30	536	.0517	.0011	0.0001	.0529	.0558	13.1	12.4
8.0	47	30	536	.0517	.0011	.0001	.0529	.0406	13.1	17
9.0	4.2	270	438	.0462	.0100	.0007	.0569	.0512	12.2	13.6
9.0	4.2	270	438	.0462	.0100	.0007	.0569	.0514	12.2	13.5
10.0	0.16	950	200	.0176	.0427	.0070	.0673	.0598	10.3	11.6
10.5	0.018	1130	20	.0060	.0509	.0210	.0779	.0895	8.9	7.8
10.9	0.0029	1150	<1	.0026	.0518	.0560	.1107	.1090	6.3	6.4

0.85×10^9 l.^{2}/mole^2/minute. The average value is 1.1×10^9. On the other hand, in the alkaline region, k_B can be evaluated only after subtracting $k_A[A][OH^-]$ and $k_{OH^-}[OH^-]$ from the observed k_1. A value of 70 is chosen for k_{OH^-} from the Kilpatricks' study of DFP.[4] At *p*H 10, 10.5, and 10.9 k_B is calculated from the equation

$$k_{B_2} = \frac{k_1 - k_A[A][OH^-] - k_{OH^-}[OH^-]}{[B_2]}$$

and values of 37, 55 and 44 l./mole/minute, respectively, were obtained. The average is 45 l./mole/minute. With these values for k_A, k_B and k_{OH^-}, the contributions of each to the rate of hydrolysis may be calculated and summed, and compared with actual experimental values as is shown in Table I. Except at *p*H 6 the agreement is excellent.

The data indicate that in the neutral region the principal catalytic species is the chelated metal ion $DipyCu(H_2O)_2^{++}$. It appears that these ions interact with DFP so as to increase the rate at which hydroxyl ions react with the molecule, with subsequent release of fluoride ion. It is suggested that the metal chelate ion forms a complex with DFP in which the cupric ion coördinates with the fluorine and the double-bonded oxygen of DFP

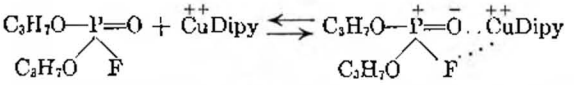

The effect of this coördination is to pull the electrons from the phosphorus atom and make it more electropositive. The effect on the hydrolysis of DFP is best pictured by resort to the generalized basic catalysis proposed by the Kilpatricks (ref. 4) in which a hydrated DFP molecule dissociates a hydrogen ion, and the resulting anion splits off fluoride ion. Since coördination of the metal ion causes the phosphorus to be more positive, the water of hydration is more easily dissociated (*i.e.*, coordination of the metal ion makes the hydrated DFP a stronger acid). The hydrolysis may be shown as

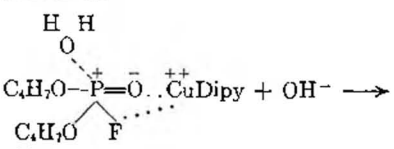

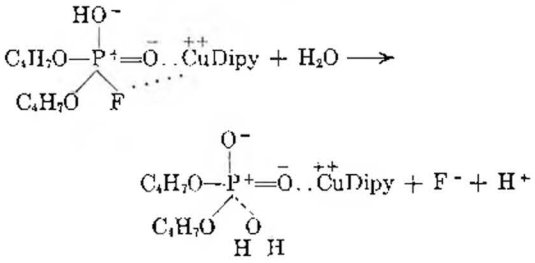

This reaction and the measured enhancement of rate of basic hydrolysis, $k_A[A][OH^-]$, are analogous to those published by Pedersen[5] where cupric ion accelerates the base-catalyzed bromination of ethyl acetoacetate by a rate $k_3[Cu^{++}][Ac]$, where the cupric ion and ethyl acetoacetate are assumed to form a complex which is more reactive with acetate ions, the basic catalyst. Here again the effect of coördination of the metal ion appears to make the ethyl acetoacetate become a stronger acid.

It is therefore suggested as a general rule that in base-catalyzed reactions (in which the rate determining step is the transfer of a proton from an acidic reactant to a basic catalytic species) coördination of a metal ion with the reactant increases its rate of reaction by increasing its acid strength. Metal ions and partially chelated metal ions are expected to act in this way; the advantage of chelation is to keep metal ions in solution at a neutral *p*H where hydroxides woud normally precipitate.[6]

The proportionality of the rate of hydrolysis to $[A][OH^-]$ has led some[7] to consider species B_1 as the catalyst, for $[B_1] = (K_w/K_{A1})[A][OH^-]$. This would lead to a very large second-order rate constant k_{B1}. Since K_{A1} is too small to measure, we can only estimate its upper limit[3] to be $10^{-8.7}$, giving a minimum value for k_{B1} of 2200 l./mole/min. (as compared with $k_{OH} = 70$ l./mole/min.). A cupric ion with three principal coördination sites occupied with bases (and one of these the very basic hydroxyl ion) is expected to have too weak a chelation tendency with DFP to show such phenomenal catalytic activity, unless the hydroxyl group is involved in the chelation (in a Cu–OH–P linkage). The latter is ruled out, however, with hydrolyses catalyzed by cations and bases such as acetate.[5]

(4) M. Kilpatrick and M. Kilpatrick, THIS JOURNAL, **53**, 1371 (1949).

(5) K. J. Pedersen, *Acta Chem. Scand.*, **2**, 253 (1948).

(6) R. C. Courtney, R. L. Gustafson, S. J. Westerback, H. Hyytiainen, S. C. Chaberek, Jr., and A. E. Martell, *J. Am. Chem. Soc.*, **79**, 3030 (1957).

(7) J. I. Hoppé and J. E. Pure, *J. Chem. Soc.*, 1775 (1957).

Therefore, we believe that species B_1 is not the main catalyst.

In the alkaline region the principal active catalyst is the uncharged chelated metal hydroxide $DipyCu(OH)_2$. Since the rate of hydrolysis of this species depends solely on its concentration, it is believed to act *via* a basic catalysis mechanism (as discussed by the Kilpatricks in the reference cited) by accepting a proton from a hydrated DFP molecule.

Acknowledgment.—The authors wish to acknowledge the helpful suggestions and criticisms of this study by members of the staff of the Army Chemical Center, especially Dr. T. Wagner-Jauregg and Mr. Joseph Epstein.

HETEROGENEOUS CHARACTER OF HYDROFORMYLATION CATALYSIS

By Clyde L. Aldridge, Egi V. Fasce and Hans B. Jonassen

Contribution from Esso Research Laboratories, Baton Rouge, La., and Dept. of Chemistry, Tulane University, New Orleans, La.

Received December 27, 1957

Although the first observers of the reaction of an olefin with hydrogen and carbon monoxide to form oxygenated compounds believed the reaction to be heterogeneous,[1] later the reaction was described as homogeneous.[2] Recent authors appear to have assumed homogeneity of this catalysis with dicobalt octacarbonyl and cobalt hydrocarbonyl as the active catalyst.[2-9] Various complexes have been proposed as the reaction intermediate.[6-8]

We have found that certain phenomena can be best explained by a heterogeneous mechanism, wherein cobalt in an insoluble form is essential. This insoluble cobalt may provide a fresh, highly active metal surface which is constantly being consumed and redeposited by carbonyl formation and breakdown. Data have been reported from which it can be deduced that the rate of hydroformylation of an olefin is not directly dependent upon the amounts of soluble cobalt present under reaction conditions.[10]

The effects of hydrogen and carbon monoxide partial pressures on the reaction rates of the hydroformylation reaction have been interpreted as resulting from a mass action competition with the olefin in the reactive complex.[6] Hypothesis of a heterogeneous mechanism allows an alternative interpretation; *i.e.*, at higher hydrogen and lower carbon monoxide partial pressures, the equilibrium proportion of the catalyst system which exists in an insoluble state is increased, thus increasing the catalytically active cobalt surface area. This effect is observable if the reaction is studied at various hydrogen and carbon monoxide ratios and various total cobalt concentrations. In the hydroformylation of a C_7 olefin (cut from the polymerization product of propylene and butene) in a small continuous unit with an oil soluble cobalt salt as the "catalyst," it was found that the proportion of cobalt insoluble in the reactor effluent increases with increasing hydrogen to carbon monoxide ratio (Fig. 1).

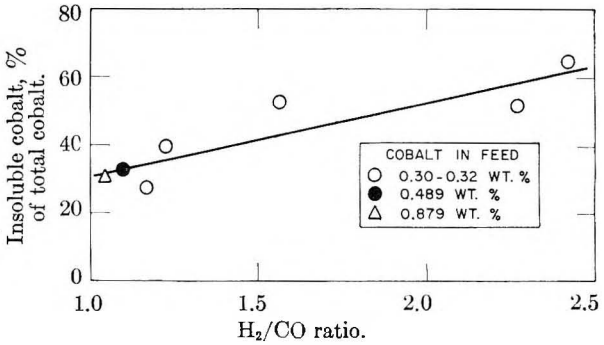

Fig. 1.—Insoluble cobalt, % of total cobalt in reactor effluent, as a function of H_2/CO ratio in exit gas: C_7 olefin (mixed isomers) feed; 2750–2900 p.s.i.g.; 177°; 0.7 hr. reaction time.

Scatter of the data may arise from two causes: (1) insoluble cobalt was obtained by difference and (2) slight decomposition of soluble cobalt compounds may have occurred. Product was accumulated 8 hours at 0° under an atmosphere of synthesis gas before a composite sample was preserved at Dry Ice temperature. At 0° and these low concentrations a half-life of cobalt hydrocarbonyl in the range of 40 hours should be expected.[11]

Mole % conversion (by distillation and chemical analysis) of olefin to oxygenated products increases with concentration of *insoluble* cobalt and is, within this limited range of conversions, a linear function thereof (Fig. 2a). At constant total cobalt concentration the conversion is inversely proportional to the concentration of soluble cobalt, while with varying total cobalt concentrations no correlation of soluble cobalt and conversion exists (Fig. 2b).

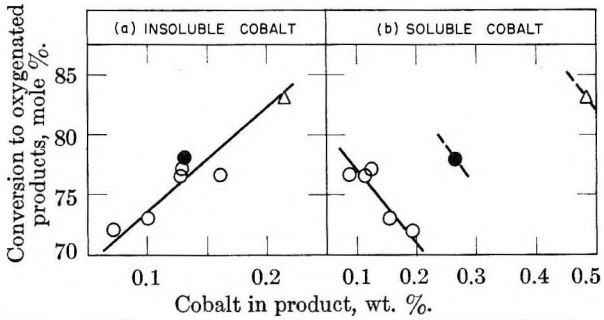

Fig. 2.—Conversion to oxygenated products as a function of cobalt concentration: C_7 olefin (mixed isomers) feed; 2750–2900 p.s.i.g.; 177°; 0.7 hr. reaction time; cobalt in feed, ○, 0.30–0.32 wt. %; ●, 0.489 wt. %; △, 0.879 wt. %.

It may be significant that the reported reaction

(1) D. F. Smith, C. O. Hawk and P. L. Golden, *J. Am. Chem. Soc.*, **52**, 3221 (1930).
(2) H. Adkins and G. Krsek, *ibid.*, **70**, 383 (1948).
(3) FIAT, Final Report 1000, "The Oxo Process," issued by the Office of Military Government for Germany through the Office of Technical Service of the U. S. Department of Commerce PB 81383, p. 29.
(4) I. Wender, H. Greenfield, S. Metlin and M. Orchin, *J. Am. Chem. Soc.*, **74**, 4079 (1952).
(5) I. Wender, H. W. Sternberg and M. Orchin, *ibid.*, **75**, 3041 (1953).
(6) G. Natta, R. Ercoli, S. Castellano and F. H. Barbieri, *ibid.*, **76**, 4049 (1954).
(7) A. R. Martin, *Chemistry & Industry*, 1536 (1954).
(8) I. Wender, S. Metlin, S. Ergun, H. W. Sternberg and H. Greenfield, *J. Am. Chem. Soc.*, **78**, 5401 (1956).
(9) M. Orchin, L. Kirch and I. Goldfarb, *ibid.*, **78**, 5450 (1956).
(10) C. L. Aldridge and E. V. Fasce, U. S. Patent 2,812,356 (1957).

of cobalt hydrocarbonyl with cyclohexene[5] apparently occurred only when the temperature of the mixture had risen to a point (15°) where cobalt hydrocarbonyl in the concentrations used is known to decompose rapidly.[11]

We believe these results are sufficient to warrant a re-examination of the fundamental postulate as to the nature of cobalt catalysis of the hydroformylation reaction. It appears likely that any direct role in hydroformylation catalysis that cobalt carbonyl or cobalt hydrocarbonyl may play must be carried out in conjunction with a solid cobalt surface.

(11) H. W. Sternberg, I. Wender, R. A. Friedel and M. Orchin, *J. Am. Chem. Soc.*, **75**, 2717 (1953).

COMPLEXES OF ETHERS WITH DIBORANE[1]

BY HENRY E. WIRTH, FRANKLIN E. MASSOTH AND DAVID X. GILBERT

Department of Chemistry, Syracuse University, Syracuse, N. Y.

Received January 11, 1958

In 1938, Schlesinger and Burg[2] showed that diborane and dimethyl ether formed the complex $(CH_3)_2O:BH_3$ at −80°. Elliot, Roth, Roedel and Boldebuck[3] found that the solubility of diborane in tetrahydrofuran depended on the square root of the diborane pressure, suggesting the formation of a tetrahydrofuran–borine complex in solution. No indication of a diethyl ether–borine complex was found. The existence of the complex $C_4H_8O:BH_3$ was established definitely by Rice, Livasy and Schaeffer[4] from the solid–liquid equilibrium in the diborane–tetrahydrofuran system. They suggest that the relative stability of the ether–borines is in the order

$$C_4H_8O:BH_3 > (CH_3)_2O:BH_3 >> (C_2H_5)_2O:BH_3$$

This order of stability was confirmed by Raman spectra.[5]

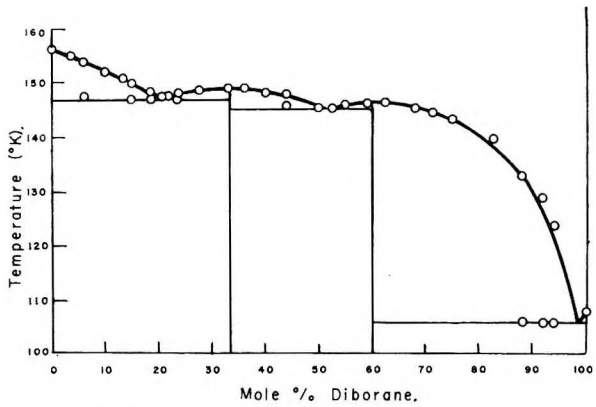

Fig. 1.—The diethyl ether–diborane system.

In this work phase diagrams are reported for systems with diborane and the following ethers: diethyl ether, methyl ethyl ether, dimethyl ether, ethylene oxide, tetrahydropyran, tetrahydrofuran, perfluoroether $[(C_2F_5)_2O]$ and cyclo-C_4F_8O.

Experimental

Materials.—Diethyl ether, tetrahydropyran and tetrahydrofuran were dried over lithium aluminum hydride and fractionally distilled before use. Methyl ethyl ether was prepared by the reaction of ethyl iodide and sodium methylate in absolute methanol and purified by fractional distillation from lithium aluminum hydride at 5°. The above ethers, as well as dimethyl ether, perfluoroether, cyclo-C_4F_8O,[6] ethylene oxide and diborane (supplied by the Olin Mathieson Chemical Corporation) was further purified if necessary by fractional distillation at low temperature until a purity of better than 98 mole % was attained, as determined by freezing point measurements.

Apparatus.—A freezing point cell of the type described by Davidson, Sisler and Stoenner[7] was attached to a vacuum gas-handling line which included manometers, calibrated flasks and traps for low temperature distillation. The composition of the liquid mixtures used was calculated from the pressure, volume and temperature of each of the gaseous components. From the volume of the freezing point cell and the observed pressure, the total moles of diborane added were corrected for the moles present in the gas phase at the freezing point of the mixture, assuming all gas present to be diborane.

A copper–constantan thermocouple was used to determine temperature. Cooling curves were recorded by a Brown Electronik recorder (full scale = 1 mv., variable range). Temperatures were reliable to ±0.5°, and mole fraction to ±2%.

Results and Discussion

Diethyl ether (Fig. 1) forms two complexes with diborane, the expected borine complex $(C_2H_5)_2O:BH_3$ and a second complex having the composition $(C_2H_5)_2O\cdot 3BH_3$. Methyl ethyl ether (Fig. 2) does not form a 1:1 borine complex, but does form a congruent melting compound $CH_3OC_2H_5\cdot 2BH_3$.

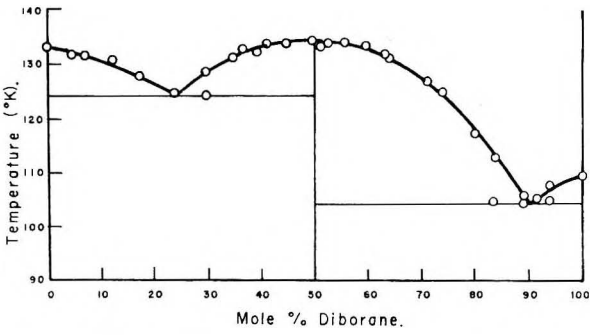

Fig. 2.—The methyl ethyl ether–diborane system.

Ethylene oxide (Fig. 3) forms no congruent melting compounds, but the freezing point diagram indicates the possibility of one and perhaps two incongruent melting compounds. The initial freezing points and the "flats" at 131 and 121°K. were definite and reproducible, but the secondary breaks between 70 and 95 mole % diborane were erratic. The formation of solid solutions in this range could explain these observations. While ethylene oxide is known to react vigorously with diborane at 190°K.,[8] there was no evidence of reaction at tem-

(1) This research was supported in part by the Department of the Navy, Bureau of Aeronautics, through subcontract with the Olin Mathieson Chemical Corporation.

(2) H. I. Schlesinger and A. B. Burg, *J. Am. Chem. Soc.*, **60**, 290 (1938).

(3) J. R. Elliot, W. L. Roth, G. F. Roedel and E. M. Boldebuck, *ibid.*, **74**, 5211 (1952).

(4) B. Rice, J. Livasy and G. W. Schaeffer, *ibid.*, **77**, 2750 (1955).

(5) B. Rice and H. S. Uchida, THIS JOURNAL, **59**, 650 (1955).

(6) The fluorinated ethers were supplied to us through the courtesy of the Minnesota Mining and Manufacturing Co.

(7) A. W. Davidson, H. H. Sisler and R. Stoenner, *J. Am. Chem. Soc.*, **66**, 779 (1944).

(8) F. G. A. Stone and H. J. Emeleus, *J. Chem. Soc.*, 2755 (1950).

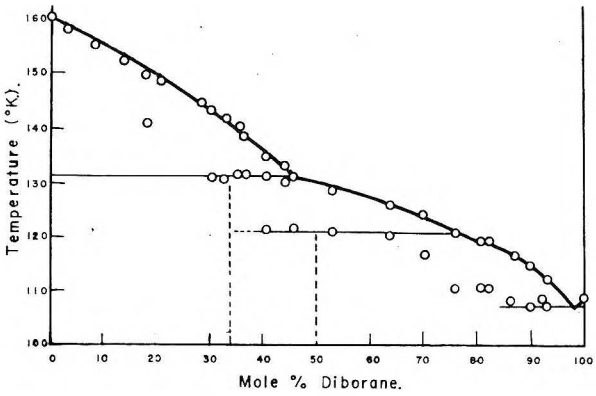

Fig. 3.—The ethylene oxide–diborane system.

peratures slightly above the melting points of the mixtures.

Dimethyl ether, tetrahydrofuran and tetrahydropyran (Figs. 4A, 4B and 4C, respectively) all form 1:1 borine complexes. The whole range of compositions could not be investigated, as the diborane pressure exceeded one atmosphere when the mole fractions of diborane were above 0.3–0.4.

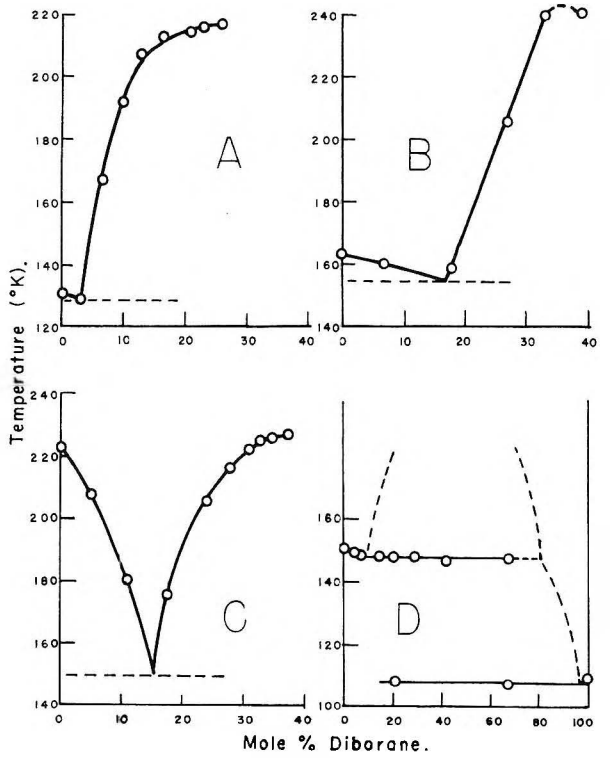

Fig. 4.—A, dimethyl ether–diborane; B, tetrahydrofuran–diborane; C ,tetrahydropyran–diborane; D, perfluoroether–diborane.

Perfluoroether and diborane (Fig. 4D) formed a partially miscible liquid system, with no indication of compound formation. Cyclo-C_4F_8O formed a similar system. Two liquid phases also were observed when perfluoroether and boron trifluoride were mixed at 155°K.

Brown and Adams[9] have shown that the relative stability of the etherates of boron trifluoride decreases in the order:

(9) H. C. Brown and M. Adams, *J. Am. Chem. Soc.*, **64**, 2557 (1942).

$C_4H_8O:BF_3$, $(CH_3)_2O:BF_3$, $(C_2H_5)_2O:BF_3$, $(iso\text{-}C_3H_7)_2:BF_3$

This order cannot be explained on the basis of the inductive effect of the alkyl groups, but is accounted for by the effect of steric strains.

The same order of relative stability was found, as expected, for the first three corresponding borine complexes by Rice and Uchida.[5]

It would be expected however that a borine complex of methyl ethyl ether would be intermediate in stability between those of methyl and ethyl ether, and that ethylene oxide would form a strong complex. That they do not show up on the phase diagrams may indicate that at low temperatures in these solvents the concentration of borine from the dissociation of diborane is too low to permit the formation of 1:1 complexes.

The inductive effect of the highly fluorinated substituents in perfluoroether and cyclo-C_4F_8O reduces the basic strength of these ethers so they cannot form complexes even with boron trifluoride.

The unexpected compounds found with methyl ethyl ether and diethyl ether could be regarded as molecular addition compounds of diborane to which the formulas $CH_3OC_2H_5 \cdot B_2H_6$ and $(C_2H_5)_2O:BH_3 \cdot B_2H_6$ could be applied. By analogy to the corresponding boron trifluoride complexes,[10] the formulations $CH_3OC_2H_5 \cdot 2BH_3$ and $(C_2H_5)_2O \cdot 3BH_3$ are preferred.

(10) H. E. Wirth, M. J. Jackson and H. W. Griffiths, THIS JOURNAL, **62**, 871 (1958).

COMPLEXES OF ETHERS WITH BORON TRIFLUORIDE

BY HENRY E. WIRTH, MIRIAM J. JACKSON AND HOWARD W. GRIFFITHS

Department of Chemistry, Syracuse University, Syracuse, N. Y.

Received January 11, 1958

Although 1:1 ether–boron trifluoride complexes are well known there are no reports in the literature of compounds containing more than one mole of boron trifluoride per mole of ether except for a single reference[1] to a second complex of diethyl ether containing 60–90 mole % BF_3. In their monograph Booth and Martin[2] refer to the compounds $2(CH_3)_2O \cdot BF_3$ and $2(C_2H_5)_2O \cdot BF_3$, but the reference cited[3] discusses compounds of the alcohols. Since recent work[4] in this Laboratory has demonstrated the existence of the borine complexes $(C_2H_5)_2O \cdot 3BH_3$ and $CH_3OC_2H_5 \cdot 2BH_3$, a survey of several ether–boron trifluoride systems was made to see whether similar compounds are formed with boron trifluoride.

Experimental

The apparatus described in the previous article[4] was used.

Methyl *n*-propyl ether and methyl isopropyl ether were prepared by the reaction of sodium methylate with 1-bromopropane and 2-bromopropane, respectively, in methyl alcohol solution. The mixtures were refluxed for 3 hours, and the material distilling below 60° collected. These products were washed with water, dried successively over

(1) A. F. O. Germann and M. Cleaveland, *Science*, **53**, 582 (1921).

(2) H. S. Booth and D. R. Martin, "Boron Trifluoride and Its Derivatives," John Wiley and Sons, Inc., New York, N. Y., 1949.

(3) H. Meerwein and W. Pannwitz, *J. prakt. Chem.*, **141**, 123 (1934).

(4) H. E. Wirth, F. E. Massoth and D. X. Gilbert, THIS JOURNAL, **62**, 870 (1958).

$CaCl_2$ and $LiAlH_4$, and fractionally distilled under reduced pressure before use. The other ethers were treated as described previously.[4]

Results

Diethyl Ether.—The phase diagram for the system diethyl ether–boron trifluoride is given in Fig. 1. In addition to the 1:1 complex melting at

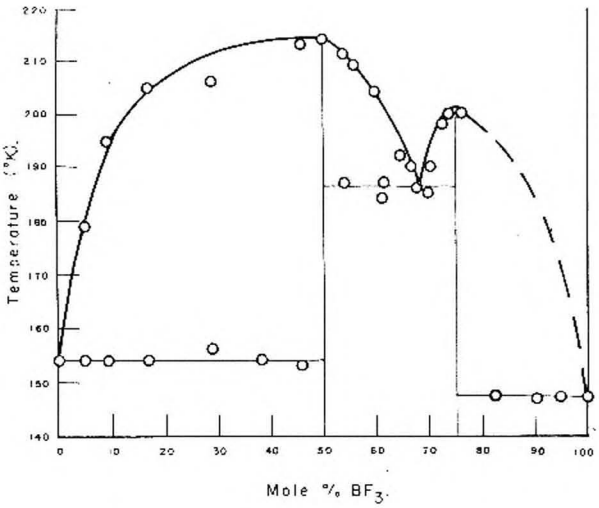

Fig. 1.—Diethyl ether–boron trifluoride system.

214°K. (literature values 215.5°,[5] 212.8°,[6] 222°K.[7]) a second complex $(C_2H_5)_2O{\cdot}3BF_3$ was found, m.p. 202°K. The eutectic between the two complexes melted at 186°K. (69 mole % BF_3). Within the accuracy of the temperature measurement (± 0.5°) the complexes formed do not lower the freezing point of either ether or boron trifluoride (monotectic behavior).

The system is complicated by the fact that in addition to the two known solid phases of diethyl ether (m.p. 156.9 and 149.9°K.) the 1:1 complex also appears to have two solid modifications. This probably accounts for the spread in freezing points reported. Between 0 and 50 mole % BF_3 the solutions supercooled so that freezing points were not well defined. Above 76 mole % BF_3 the pressure exceeded one atmosphere before the complex dissolved completely in the liquid.

Methyl Ethyl Ether.—Two compounds were formed, $CH_3OC_2H_5{\cdot}BF_3$, m.p. 210°K. (lit.[6] 175°K.) and $CH_3OC_2H_5{\cdot}2BF_3$, m.p. 198°K. The eutectic (62 mole % BF_3) melted at 189°K. It is probable that there are two solid modifications of the 1:1 complex. The pressure exceeded one atmosphere before the 1:2 complex dissolved for compositions containing more than 70 mole % BF_3. Monotectic behavior was exhibited at the ether and BF_3 extremes of the system.

Methyl *n*-Propyl Ether.—This ether (m.p. 139°K.) formed the two compounds $CH_3O(CH_2)_2CH_3{\cdot}BF_3$ (m.p. 222°K.) and $CH_3O(CH_2)_2CH_3{\cdot}2BF_3$ (m.p. 201°). The eutectic (60 mole % BF_3) melted at 198°K.

Methyl Isopropyl Ether.—Methyl isopropyl ether (m.p. 119°K.) also formed two compounds: $CH_3OCH(CH_3)_2{\cdot}BF_3$, m.p. 239°K., and $CH_3OCH(CH_3)_2{\cdot}2BF_3$, m.p. 206°K.; eutectic (63 mole % BF_3), m.p. 201°.

Ethylene Oxide.—Excess ethylene oxide reacts with BF_3 to give dioxane and a polymer.[8] With an excess of BF_3, a 1:1 complex is formed below −80°.[9] On warming to room temperature, the white complex decomposes. These results were qualitatively confirmed. In a quantitative experiment, a ten-fold excess of BF_3 was condensed on ethylene oxide at liquid nitrogen temperature. On warming the mixture, just at the melting point of BF_3 a vigorous reaction took place, and a white solid (presumably a complex) formed. This solid was insoluble in liquid BF_3. At a temperature just above the boiling point of BF_3, 1.1 moles of BF_3 per mole ethylene oxide were retained in the solid.

Other Ethers.—Tetrahydropyran and tetrahydrofuran gave 1:1 complexes melting at 283°K. (lit.[9] 255°K.) and 284°K. (lit.[7] 281–283°K.), respectively, but the phase equilibria could not be investigated beyond 52–55 mole % BF_3, as the pressure exceeded one atmosphere. When a ten-fold excess of BF_3 was condensed on these ethers, as in the experiment with ethylene oxide, 1.5 and 2.0 moles of BF_3 per mole of ether were retained by tetrahydropyran and tetrahydrofuran, respectively.

Diisopropyl ether absorbed two moles of BF_3 per mole of ether when treated with an excess of BF_3.

Dimethyl ether appears to form only the 1:1 complex.

Discussion

The compounds ether·$2BF_3$ formed with methyl ethyl, methyl *n*-propyl and methyl isopropyl ether, and the compound $(C_2H_5)_2O{\cdot}3BF_3$ are less stable than the 1:1 complexes, but do give congruent melting points at temperatures above the boiling point of BF_3 (172°K.). On being heated a few degrees above their melting points they dissociate into BF_3 and the 1:1 complex. It is also possible that tetrahydropyran, tetrahydrofuran and isopropyl ether give very unstable higher complexes.

The higher complexes of methyl ethyl and diethyl ether with boron trifluoride are analogous to the corresponding borine complexes.[4] The ether·$2BF_3$ complexes found with methyl ethyl and the methyl propyl ethers may also be analogous to the compounds $R_2O{\cdot}2BCl_2OR$ (R = methyl or ethyl) reported by Wiberg and Sütterlin[10] for which structures involving coördination of both boron atoms with the ether oxygen are assumed.[11] This attractive explanation does not account for the complex $(C_2H_5)_2O{\cdot}3BF_3$. Since dimethyl ether offers the least steric hindrance of the series of aliphatic ethers to the formation of the 1:1 complex, it would be expected to form a fairly stable higher complex if the boron fluorides are both coördinated with oxygen. Such a complex was not found.

(5) N. N. Greenwood, R. L. Martin and H. J. Emeléus, *J. Chem. Soc.*, 3030 (1950).
(6) A. W. Laubengayer and G. R. Finlay, *J. Am. Chem. Soc.*, **65**, 884 (1943).
(7) H. C. Brown and R. M. Adams, *ibid.*, **64**, 2557 (1942).
(8) F. G. A. Stone and H. J. Emeléus, *J. Chem. Soc.*, 2755 (1950).
(9) J. Grimley and A. K. Holliday, *ibid.*, 1215 (1954).
(10) E. Wiberg and W. Sütterlin, *Z. anorg. Chem.*, **202**, 1 (1931).
(11) E. Wiberg and W. Sütterlin, *ibid.*, **202**, 22 (1931).

THE ANION-EXCHANGE RESIN ADSORPTION OF ZINC(II) FROM AMINE-CHLORIDE SOLUTIONS[1]

BY R. A. HORNE[2]

Contribution of the Department of Chemistry and Laboratory for Nuclear Science of the Massachusetts Institute of Technology, Cambridge, Massachusetts

Received January 20, 1958

A theory of the dependence of the adsorption of metal complexes from aqueous solution onto anion-exchange resins on the nature of the cation of the supporting electrolyte has been described in previous papers.[3-5] This theory attributes the observed effect to ion-pair formation in the low dielectric constant medium of the resin phase or in both resin and external solution if the dielectric constants of these phases are comparable. The extent of ion-pairing between anionic metal complexes and the cation of the supporting electrolyte depends, among other factors, on the size of the latter. Unfortunately the degree of hydration of the simple, relatively small cations, *i.e.*, alkali and alkaline earth metal cations, results in ambiguities in their relative size assignments. This difficulty can be circumvented in part by the use of amine-chlorides as supporting electrolytes.

Experimental

The experimental procedures involved in batch anion-exchange resin studies of the present type, using tracer radiozinc, have been described previously.[3] The chloride concentrations were maintained by the addition of $CH_3NH_2 \cdot HCl$, $(CH_3)_2NH \cdot HCl$, $(CH_3)_3N \cdot HCl$, or $(CH_3)_4NCl$ as supporting electrolyte. Chloride was determined by rapid Volhard analyses.

Results and Discussion

Figure 1 shows the adsorption of tracer radiozinc(II) onto Dowex 1-X8 chloride at 25° from various amine-chloride media together with the adsorption from a tetramethylammonium chloride 50 vol. % ethanol-water solution. The retention at high chloride concentrations is greatest for the smallest cation, $CH_3NH_3^+$, and least for the largest, $(CH_3)_4N^+$. The similarity of the $CH_3NH_3^+$ curve with the NH_4^+ curve reported earlier[3] suggests some orientation preference in the ion-pair formation process. The results of lowering the dielectric constant of the external solution by ethanol-water media is comparable for $(CH_3)_4N^+$ with those reported earlier[5] for Li^+, H^+, K^+ and Cs^+. The present observations are compatible with the conclusion that ion-pair formation of the type described previously[3] and above is important in the resin phase only when the dielectric constant of the external solution is high. Presumably, by using a supporting electrolyte of sufficiently large cation, it should be possible to obtain an "ideal" adsorption curve for which the only important equilibrium at high chloride concentration is

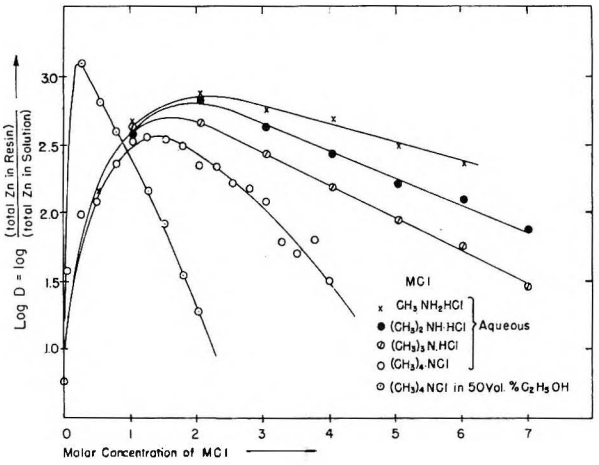

Fig. 1.—The adsorption of tracer radiozinc(II) on Dowex 1-X8 chloride from amine-chloride solutions at 25°.

$$2RCl + ZnCl_4^- \rightleftharpoons R_2ZnCl_4 + 2Cl^- \qquad (1)$$

and which lends itself immediately to analysis of the type proposed by Coryell and Marcus.[6]

(1) This work was supported in part by the U. S. Atomic Energy Commission.

(2) Radio Corporation of America, Needham Heights, Mass.

(3) R. A. Horne, THIS JOURNAL, **61**, 1651 (1957).

(4) R. A. Horne, R. H. Holm and M. D. Meyers, *ibid.*, **61**, 1655 (1957).

(5) R. A. Horne, R. H. Holm and M. D. Meyers, *ibid.*, **61**, 1661 (1957).

(6) C. D. Coryell and Y. Marcus, *Bull. Res. Council Israel*, **4**, 7 (1954); Y. Marcus and C. D. Coryell, *ibid.*, in press (1958).

INFRARED SPECTRUM AND BARRIER TO INTERNAL ROTATION IN ETHYL FLUORIDE[1]

BY EDWARD CATALANO AND KENNETH S. PITZER

Department of Chemistry, University of California, Berkeley, California

Received February 14, 1958

The infrared spectrum of ethyl fluoride has been measured in the 200–300 cm.$^{-1}$ region in a Perkin–Elmer 12-C spectrometer with CsI prism. The observed spectrum, Fig. 1, shows distinct bands at 243.5 and 227 cm.$^{-1}$ together with less distinct absorption in the region of the low frequency cut off the prism.

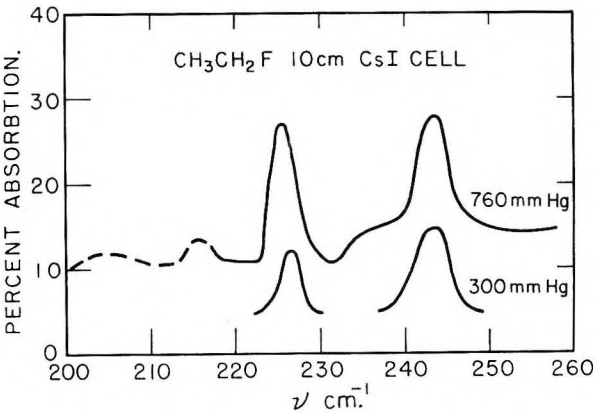

Fig. 1.—The absorption spectrum of ethyl fluoride.

Herschbach[2] obtained a value 3300 cal./mole for the torsional barrier in ethyl fluoride from the splitting of the first excited state lines in the microwave spectrum. He assumed the usual threefold cosine barrier function $V = {}^1/_2V_3(1 - \cos 3\phi)$.

(1) This research was a part of the program of Research Project 50 of the American Petroleum Institute.

(2) D. R. Herschbach, *J. Chem. Phys.*, **25**, 358 (1956).

Kraitchman and Dailey[3] give the reduced moment of inertia as 4.359×10^{-40} g. cm.^{2}. These data and assumptions yield 243 and 226 cm.$^{-1}$ for the 0-1 and 1-2 torsional level separations, respectively. The agreement is most satisfactory and confirms the values 3300 ± 30 cal./mole for the barrier and 243 cm.$^{-1}$ for the energy of the first excited torsional state. The value 278 cm.$^{-1}$ had been proposed for the latter quantity on the basis of a very weak line in the Raman spectrum[4] but the possibility that this line arose from an impurity also was mentioned. Kraitchman and Dailey[3] gave 300 ± 40 cm.$^{-1}$ for the energy of the first excited state from the temperature coefficient of intensity of satellite lines in the microwave spectrum, but it now appears to be necessary to increase somewhat their estimated uncertainty.

The calculated location of the 2-3 band is 207 cm.$^{-1}$. The observed spectrum is consistent with this but is not reliable because of heavy absorption by the prism at this frequency.

The thermodynamic properties were calculated by Smith, *et al.*,[4] and presented in itemized form so that it is easy to correct for the new barrier and the new moments of inertia. Table I gives the revised values.

TABLE I

CALCULATED THERMODYNAMIC PROPERTIES FOR ETHYL FLUORIDE (CAL./DEG. MOLE)

T, °K.	Cp^0	$\frac{H^0 - Hc^0}{T}$	$\frac{F^c - H_2^0}{T}$	S^0
235.5	12.16	9.52	50.73	60.25
298.15	14.10	10.26	53.04	63.30
400	17.60	11.70	56.26	67.96
600	23.45	14.67	61.57	76.24

(3) J. Kraitchman and B. P. Dailey, *ibid.*, **23**, 181 (1955).

(4) D. C. Smith, R. A. Saunders, J. R. Nielsen and E. E. Ferguson, *ibid.*, **20**, 847 (1952).

THE SPECTRA OF GLYOXAL SOLUTIONS[1]

BY CLARENCE L. CARPENTER, JR., AND LESLIE S. FORSTER

Department of Chemistry, University of Arizona, Tucson, Arizona

Received February 24, 1958

It has been found that solvents containing oxygen and nitrogen markedly diminish the intensity of portions of the visible absorption spectrum of biacetyl.[2] This study was initiated to determine whether analogous solvent effects exist in solutions of the simplest dicarbonyl, glyoxal. The gas phase spectrum is much more structured than that of biacetyl and much of this structure remains in hydrocarbon solvents.

Experimental

Glyoxal was prepared by the oxidation of ethylene with selenium dioxide[3] and was stored *in vacuo* at −78°. Samples were prepared by warming the storage bulb and freezing the glyoxal into an absorption cell containing degassed solvent cooled to −78°. This cell could be closed to prevent escape of glyoxal and the absorption of atmospheric moisture. All solvents were dried and purified by conventional methods. To minimize reaction of the glyoxal with the solvents and polymerization, spectra were recorded at 0° in a Beckman DU spectrophotometer. The spectra in mixed solvents were determined by first preparing a heptane solution and recording the extinctions at the maxima. The cell was opened, a measured volume of the second solvent added, and the cell closed again. This procedure was repeated for the successive dilutions. The recorded extinctions were then corrected for the volume changes. It was determined that the loss of glyoxal vapor during this procedure was negligible.

The spectrum of glyoxal vapor was determined in a 10 cm. cell.

Solutions of glyoxal in heptane, chloroform, dioxane and ethyl ether showed little change in spectral intensity in the time required for a determination (*ca.* 30 minutes). The change of intensity was appreciable for nitromethane, tetrahydrofuran and acetone solutions, but it was possible to determine the shape of the spectra by working rapidly. Solution of glyoxal in *n*-butyl alcohol, *n*-octyl alcohol, anisole, pyridine and acetonitrile resulted in an immediate reaction in which a white solid appeared (probably glyoxal polymer). Even in the stable solutions a slight turbidity often was observed. A correction for this turbidity was made by subtracting the extinction at 560 mμ where glyoxal absorption is negligible. Incorporation of the λ^4 dependence for this small scattering correction would only serve to exaggerate the effects and would leave the over-all conclusions unchanged.

Results.—Solvents containing oxygen atoms remove the structure in the glyoxal spectrum; Fig. 1 shows dioxane spectrum. This may be compared with the heptane spectrum (Fig. 2, curve 1). The spectra of nitromethane, tetrahydrofuran and ethyl ether solutions are very similar to that in dioxane. *Absorbance values are relative and no quantitative comparisons between the spectra are possible.* Chloroform does not remove the structure completely. These effects are similar to those observed in biacetyl solutions.[2] However, ether is much more effective in removing glyoxal structure than biacetyl structure. This is consistent with the interpretation that interaction between solvent oxygen and carbonyl oxygen atoms is responsible for the loss of structure. The steric interference to close oxygen-oxygen approach is less in glyoxal–ether than in biacetyl–ether systems.

In heptane the spectrum is shifted 300 cm.$^{-1}$ to the red compared to the gas phase spectrum. This is the same polarization red shift shown by biacetyl.[2a,4]

The mixed solvent spectra are shown in Fig. 2-4. For the mixed solvents heptane–dioxane and heptane–chloroform, the integrated intensity (21,000-27,000 cm.$^{-1}$) is reduced progressively as the mole fraction of heptane decreases. The dilution technique for these spectra makes quantitative comparison meaningful. No correlation between the integrated intensity and the refractive index exists.

Discussion.—Solvent effects in biacetyl and glyoxal solutions are closely parallel,[2a] making it unlikely that hyperconjugation enhanced by solvent interaction is the cause of the biacetyl spectral changes, since hyperconjugation is not possible in glyoxal. The small blue shift is comparable to that observed for pyrazine in propionitrile-hexane mixture.[5]

(1) (a) This research was supported by a grant from the National Science Foundation. Reported in part at the 33rd annual meeting of the Southwestern and Rocky Mountain Division of the A.A.A.S., Tucson, Arizona, May 1, 1957; (b) taken in part from the M.S. thesis of Clarence L. Carpenter, Jr., May, 1957.

(2) (a) L. S. Forster, *J. Am. Chem. Soc.*, **77**, 1417 (1955); (b) *J. Chem. Phys.*, **26**, 1761 (1957).

(3) J. C. Calvert and G. Lane, *J. Am. Chem. Soc.*, **75**, 856 (1953).

(4) N. S. Bayliss, *J. Chem. Phys.*, **18**, 292 (1950).

(5) G. Brealey and M. Kasha, *J. Am. Chem. Soc.*, **77**, 4462 (1955).

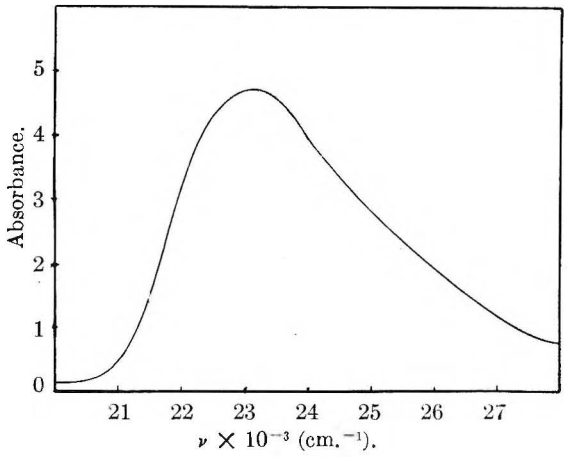

Fig. 1.—Glyoxal in dioxane.

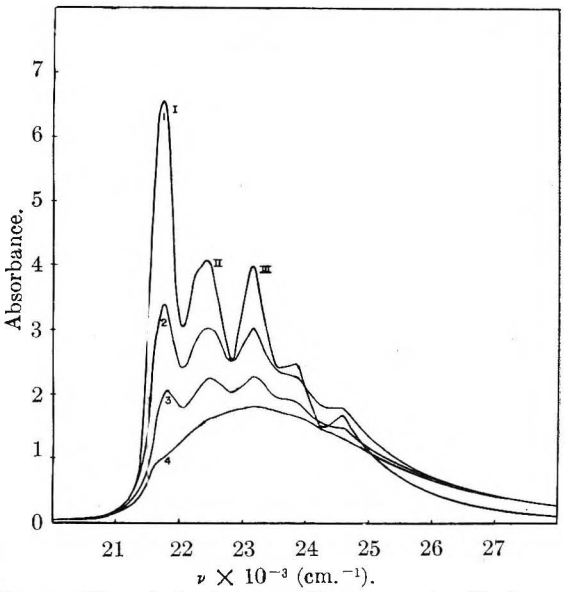

Fig. 2.—Glyoxal in heptane–dioxane, mole % dioxane: (1) 0%, (2) 8.3%, (3) 16.2%, (4) 42.5%.

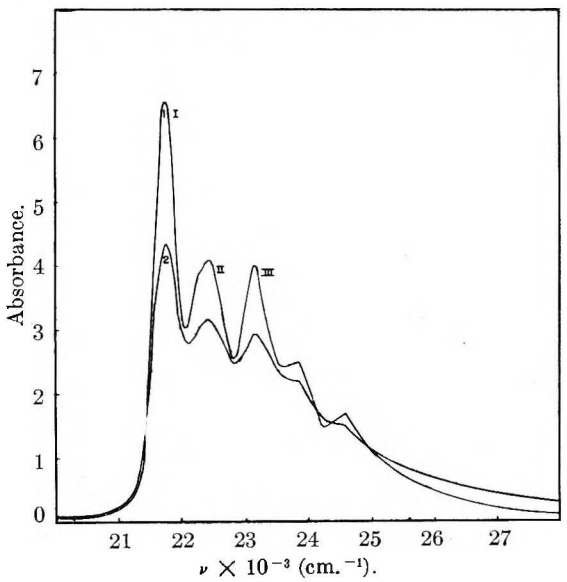

Fig. 3.—Glyoxal in heptane–chloroform, mole % chloroform: (1) 0%, (2) 55%.

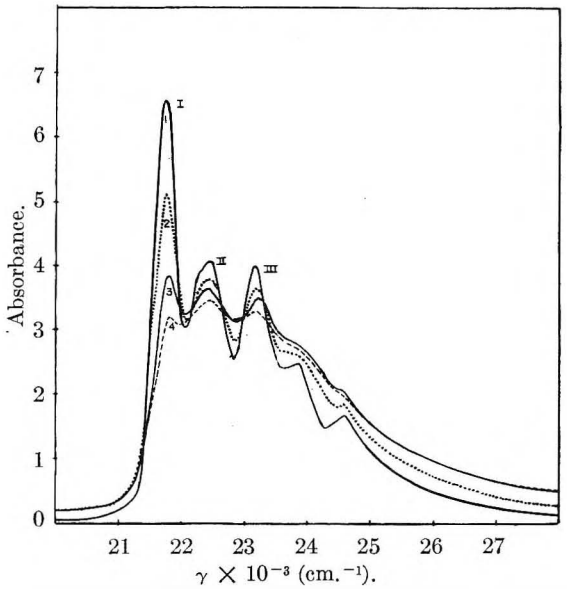

Fig. 4.—Glyoxal in heptane–ether, mole % ether: (1) 0%, (2) 13.6%, (3) 37.6%, (4) 58.4%.

It has been suggested[2b] that the biacetyl solvent effects might be related to an increase in the frequency of the acetyl torsional vibration.[6] The mixed solvent spectra for glyoxal do not support this speculation. A thorough vibrational analysis of the glyoxal vapor spectrum has been made.[7] It is possible to identify these transitions with the several largest peaks in the heptane solution spectrum as indicated: I (Fig. 2), 21977–22292 cm.$^{-1}$ (frequency range in gas spectrum corresponding to peak I in heptane spectrum); II, 22441-23015 cm.$^{-1}$; III, 23167–23876 cm.$^{-1}$. In all of these regions much of the intensity is due to transitions involving the torsional mode with a ground-state frequency of 127 cm.$^{-1}$. At 273°K. a substantial fraction of the molecules will populate the higher torsional vibrational levels. Any interaction that simply increases the vibrational separation will increase the fraction of molecules in the zero level. Transitions from the zero level are as intense as those from excited levels.[6] This doesn't imply a decrease in intensity in the bands I-III. No other vibration is involved in all three bands yet the intensity of all is reduced to about the same extent.

(6) J. Sidman and D. S. McClure, *ibid.*, **77**, 6461 (1955).
(7) J. C. D. Brand, *Trans. Faraday Soc.*, **50**, 431 (1954).

THE CRITICAL CONSTANTS AND VAPOR PRESSURE OF CYCLOPROPANE[1]

BY HAROLD S. BOOTH[2] AND WILLIAM C. MORRIS[3]

Received February 26, 1958

A study of the physical constants of cyclopropane, including the vapor pressure data above one atmosphere and the critical constants, was completed in 1935, shortly after cyclopropane was introduced to the market as an anesthetic. These

(1) This work was done in the Research Laboratories of the Western Reserve University and was supported by the Ohio Chemical & Manufacturing Co. (now the Ohio Chemical & Surgical Equipment Co.).
(2) Now deceased. Formerly Department of Chemistry, Western Reserve University, Cleveland, Ohio.
(3) Harshaw Chemical Co., Cleveland, Ohio.

data are of importance in connection with the handling and administration of this agent. Cyclopropane has become extremely important as an inhalation anesthetic and since a survey of the literature reveals that similar data have not been published, it seems worthwhile to make the data obtained in this study available at this time.

Experimental

The critical constants and vapor pressures of cyclopropane at high pressures were investigated utilizing a very accurate type of apparatus described by Booth and Swinehart.[4]

The procedure was to transfer fractionally distilled cyclopropane which exhibited a constant density at constant temperature and pressure to a manifold to which Cailletet tubes were sealed. The manifold and cells were rinsed 20 times with dry air and 15 times with cyclopropane, and the tubes finally were filled to a pressure of slightly less than one atmosphere. The cells were then broken under mercury and placed in the pressure well which was connected to the pump and dead weight gauge. The assembly was placed in the thermostat and a determination was made.

The critical temperature was determined by raising the temperature of the sample gradually, keeping the pressure high enough to maintain a liquid until the meniscus disappeared on stirring. The temperature was held constant at this point for 15 to 20 minutes to attain equilibrium. The temperature was then lowered and the pressure raised to liquefy the sample and the process was repeated. The highest temperature at which there were two phases visible and at which the meniscus did not reform after disappearing on stirring was taken as the critical temperature. The critical pressure was determined at this temperature as the pressure at which the mercury thread in the capillary did not move after standing for a long enough period to assure equilibrium.

Results.—The critical temperature and critical pressure of cyclopropane are given in Table I.

TABLE I

Sample No.	Critical temp., °C.	Critical pressure atm.
1	124.65	54.22
2	124.66	54.24
3	124.65	54.22
Av.	124.65	54.23

The vapor pressure of cyclopropane as a function of temperature was determined during the critical constant experiments on the same samples of cyclopropane. The results of these determinations are given in Table II.

TABLE II

VAPOR PRESSURE OF CYCLOPROPANE

Sample no.	Temp., °C.	Pressure, atm.	Sample no.	Temp., °C.	Pressure, atm.
C	115.34	45.26	C	61.32	16.66
B	110.02	40.98	B	52.42	15.25
A	105.30	39.20	C	43.28	12.15
B	101.31	34.14	B	36.25	9.60
A	91.10	30.13	A	32.42	7.82
B	88.29	27.18	B	16.78	5.30
A	81.19	25.79	A	11.02	4.01
C	76.38	23.48	B	7.56	3.62
B	71.42	22.32	A	3.00	2.38
A	64.92	18.08			

When the data in Table II are plotted as a function of temperature they yield the expression

$$\log P_{mm} = \frac{-1063.8}{T} + 7.261$$

This expression is in good agreement with the results of Ruehrwein and Powell[5] who determined the vapor pressure of cyclopropane at pressures below one atmosphere.

(4) H. S. Booth and C. F. Swinehart, *J. Am. Chem. Soc.*, **57**, 1337 (1935).

(5) R. A. Ruehrwein and T. Powell, *ibid.*, **68**, 1063 (1946).

HEAT OF FUSION AND HEAT CAPACITY OF INDIUM ANTIMONIDE

BY NORMAN H. NACHTRIEB AND NORIKO CLEMENT

Institute for the Study of Metals, University of Chicago, Chicago, Illinois

Received February 26, 1958

The latent heat of fusion of indium antimonide is sufficiently large that it could be determined with fairly high accuracy and precision by a simple drop calorimetric method. The heat capacity was also determined for several temperature intervals in the range 20-500°, although with lower accuracy. Analysis of the material for antimony gave 51.44 ± 0.16%, as compared with the theoretical value of 51.48%. Semi-quantitative spectrographic analysis revealed Fe (0.001%), Pb (0.001%), Sn (0.001%), Mg (0.001%), Si (0.0001%) and Cu (0.0001%). A weighed quantity of InSb, sealed in an evacuated Vycor bulb of known weight, was heated in a tube furnace; the temperature was controlled by a Leeds and Northrup Micromax with four chromel-alumel thermocouples in series to permit regulation to ±0.5°. For the latent heat of fusion, drops were made from temperatures just above and just below the melting point (525°).[1] (The melting point of the material was verified to lie within 1° of its reported value by trial inspections on withdrawing it quickly from the furnace at temperatures close to 525°.) The calorimeter was a 1-liter glass Dewar vessel equipped with a stirrer, Beckman thermometer, and a brass tube for guiding the specimen from the furnace. A copper gauze liner in the calorimeter gave protection against breakage even though the specimen fall was almost free. About 825 g. of water was used in the calorimeter, and weight losses by evaporation did not exceed 0.2 g. The water equivalent was determined by mixing weighed quantities of water of different temperature, and found to be 86.8 g. Two series of runs were made, with 0.2104 and 0.1620 mole of InSb. The average of six determinations was 11.2 ± 0.4 kcal.mole^{-1} and the entropy of fusion is accordingly 14.1 cal.mole^{-1}deg.$^{-1}$.

Measurements of the heat capacity were made in a similar manner for the temperature intervals 20-90°, 90-170°, 170-350° and 350-500°. Corrections for the heat capacity of Vycor were made from runs with an evacuated bulb filled with crushed Vycor. The measurements are of lower accuracy than the heat of fusion because the heat content of the Vycor was about equal to the heat content of the InSb. For the four temperature intervals above the heat capacity of InSb was found to be 0.052, 0.056, 0.062 and 0.062 cal.g.$^{-1}$-deg.$^{-1}$, respectively.

Acknowledgments.—The work described was in

(1) T. S. Liu and E. A. Peretti, *Trans. J. Metals*, **3**, 791 (1951).

part supported by the Air Force Office of Scientific Research under Contract No. AF-18(600)-1489 with the University of Chicago. The indium antimonide was provided by the Chicago Midway Laboratories.

TRANSPORT OF METALS BY GASEOUS CHLORIDES AT ELEVATED TEMPERATURES

By M. F. Lee

Contribution from Alcoa Research Laboratories, New Kensington, Pa.

Received February 28, 1958

The purpose of these experiments was to determine the transport of several metals by chlorides at elevated temperatures. The subhalides back react at lower temperatures to deposit the metal and to regenerate a normal halide. For example, when aluminum chloride is passed slowly over metallic aluminum at 800° and 0.001 atmosphere, 50% of the $AlCl_3$ reacts to form AlCl.[1] The AlCl vapor back reacts in a cooler zone of the reaction tube to deposit aluminum and regenerate $AlCl_3$. The effect of these reactions is to transport aluminum from a hot zone to a cold zone. The transported aluminum can be purified by this process.

In the work to be reported, reduced pressures were used to avoid the relatively high temperatures required at atmospheric pressure. Two types of reactions were investigated: (1) a metal with its anhydrous gaseous chloride, and (2) a metal with a dissimilar anhydrous gaseous chloride.

Most of the anhydrous chlorides (Table I) were prepared from the metal and chlorine immediately before use. Silicon tetrachloride was purchased from Fisher Scientific Co. The tantalum chloride listed in Table I was not used in the distillation experiments.

Table I

Preparation of Chlorides of M + Cl_2

Metal	Temp., °C.	Probable product	How identified
Cb	1000	$CbCl_5$	Orange salt
Cr	1000	$CrCl_3$	Light lavender salt
Fe	925–1050	$FeCl_2$	Purple salt
Ga	675	$GaCl_2$	M.p. 160–170°
Ge	800	$GeCl_4$	M.p. approx. −50°
Mn	900–1070	$MnCl_2$	Pink salt
Ni	1010	$NiCl_2$	Yellow salt
Ta	730	$TaCl_5$	Pale yellow salt
Ti	1250	$TiCl_4$	M.p. approx. −30°
W	950	WCl_6	Deep purple salt
Zr	1250	$ZrCl_4$	White salt

In the preparations chlorine gas was passed over an Alundum boat containing the metal surrounded by a quartz tube. Temperature was raised until a reaction took place. The salts condensed on the cold wall of the quartz tube and were removed in a dry air room.

When chlorine gas was passed over metallic tungsten in an Alundum boat at 950°, most of the Alundum boat was volatilized and the condensate was a pinkish-orange colored salt. This reaction may have taken place

$$3W + Al_2O_3 + 9Cl_2 \longrightarrow \underset{\text{Red}}{3WOCl_4} + \underset{\text{White}}{2AlCl_3}$$

The boiling points of the two salts are not too far separated: $WOCl_4$, b.p. 227.5° and $AlCl_3$ b.p. 178°. A mixture of the salts could give the pinkish orange color. A subhalide reaction may also have occurred to a small extent since 0.5% Al (as determined by hydrogen evolution) was condensed in one portion of the salt. Tungsten was contained in a graphite boat to produce the chloride.

The conditions for Type 1 reactions are given in Table II. The metal chlorides were passed slowly over a heated Alundum boat containing the metal. The transported metal and salts were condensed on an air-cooled silica tube and tube walls.

Table II

Reactions of M′ + M′Cl

Metal	Chloride	Temp., °C.	Pressure, mm.	Metal product
Cb	$CbCl_5$	1000	0.4	No reaction
Cr	$CrCl_3$	1250	0.2	Cr
Cr	$CrCl_2$	1250	0.2	Cr
Fe	$FeCl_2$	1300	2.3	Fe
Ga	$GaCl_2$	800	0.2	Ga
Ge	$GeCl_4$	1250	5.0	Ge
Mn	$MnCl_2$	1000	0.1	No reaction
Ni	$NiCl_2$	1010	0.05	No reaction
Si	$SiCl_4$	1000	3.0	Si
Ti	$TiCl_4$	1300	2.5	Ti
Ti	$TiCl_3$	1250	1.5	Ti
Zr	$ZrCl_4$	1225	0.2	Zr

In each of these reactions, the transported metal product was separated and identified by appearance and chemical analysis. Although Gross[2,3] reported subhalides of manganese (MnF) and nickel (NiBr, NiCl), there was no evidence of metal under the conditions of these experiments.

Appreciable amounts of metallic condensed products resulted when chlorides of iron, gallium, silicon and zirconium reacted with the corresponding metals. $CrCl_2$ produced a larger yield of chromium than $CrCl_3$, and $TiCl_3$ produced a larger yield of titanium than $TiCl_4$. The yield of germanium was very small at 1250°. $CrCl_3$, $GeCl_4$ and $TiCl_4$, on the basis of color and appearance, appeared to form the lower valence chlorides $CrCl_2$, $GeCl_2$ and $TiCl_3$, while in all other experiments the deposited chloride appeared to be the same as the starting material.

The conditions and products for Type 2 reactions are given in Table III.

X-Ray analysis of the deliquescent chlorides condensed on the cold region of the reactor tube were not conclusive. The elements in the chlorides were verified by analysis.

A Ga–Al alloy free from salt was produced in the heated boat when $GaCl_2$[4] vapor was passed over aluminum. The aluminum in the alloy increased from 35.3% at 800° to 68.3% at 1000°. Results

(1) A. S. Russell, K. E. Martin and C. N. Cochran, *J. Am. Chem. Soc.*, **73**, 1463 (1951).

(2) P. Gross, *Proc. Chem. Soc. Eng.*, **26**, (Feb., 1958).

(3) P. Gross, U. S. Patent 2,470,305–6 (to International Alloys Ltd.) May 17, 1949.

(4) A. W. Laubengayer and F. B. Shirmer, *J. Am. Chem. Soc.*, **62**, 1578 (1940).

TABLE III

REACTIONS OF M′ + M″Cl

Metal	Chloride	Temp., °C.	Pressure, mm.	Metal product	Deposited chlorides
Al	$GaCl_2$	800–1000	0.2	Ga–Al	Ga + Al
Ga	$AlCl_3$	800–1000	0.2	Ga–Al	Ga + Al
Al	$GeCl_4$	1000	2.0	Ge–Al	Al
Ge	$AlCl_3$	1000	0.5	Thin mirror	Al
Fe–Al	$FeCl_3$	1000	1.0	Fe–Al	Al
Fe	$AlCl_3$	1100	4.0	Al–Fe	Al + Fe
Si	$AlCl_3$	1000	0.7	Si	Al
Al	$SiCl_4$	1000	3.0	Si–Al	Al
Ti	$AlCl_3$	1250	0.4	Ti–Al	Al + Ti
Al	$TiCl_4$	1000	3.0	Al–Ti	Ti + Al
Fe + Al + Si + Ti	$TiCl_3$	1000	3.0	Al–Si	Al + Ti

were similar when $AlCl_3$ vapor was passed over gallium metal, except that in this case the Ga–Al alloy was in small globules mixed throughout the chlorides of gallium and aluminum. The metal deposit contained 66% germanium and 30% aluminum when $GeCl_4$ vapor was passed over aluminum. A very thin metallic mirror was produced when $AlCl_3$ vapor was passed over metallic germanium. Metallic iron and $AlCl_3$ were the chief products of passing $FeCl_3$ vapor over a ferro-aluminum alloy. An Fe–Al alloy and chlorides of both iron and aluminum were the result of passing $AlCl_3$ vapor over metallic iron. Elemental silicon was distilled when $AlCl_3$ vapor was passed over silicon. In contrast with this behavior, a 50-50% Si–Al alloy was distilled when $SiCl_4$ vapor was passed over aluminum. This reaction is similar to that for $AlCl_3$ vapor passed over germanium except that more silicon was condensed, possibly because of the difference in temperature. When $TiCl_4$ vapor was passed over aluminum, an alloy of 70% Al–30% Ti was transported. In this reaction the $TiCl_3$ must have been partially reduced to $TiCl_2$ evidenced by black crystals mixed with purple crystals. The percentage of aluminum and titanium was reversed when $AlCl_3$ vapor was passed over titanium. Aluminum and silicon were preferentially distilled when $TiCl_3$ vapor was passed over an alloy of 70.8% silicon, 10.1% iron, 9.0% titanium and 1.4% aluminum.[5–9]

(5) Sister Mary Martinette, *J. Chem. Ed.*, **26**, 101 (1949).
(6) V. Meyer and H. Züblin, *Ber.*, **13**, 811 (1880).
(7) C. B. Willmore, U. S. Patent 2,184,705 (Aluminum Company of America), December 26, 1939.
(8) R. Schwarz and C. Danders, *Chem. Ber.*, **80**, 444 (1947).
(9) G. Wehner, *Z. anorg. allgem. Chem.*, **276**, 72–76 (1954).

SURFACE TENSION AT ELEVATED TEMPERATURES. IV. SURFACE TENSION OF Fe–Se AND Fe–Te ALLOYS

BY W. D. KINGERY

Ceramics Division,[1] Department of Metallurgy, Massachusetts Institute of Technology, Cambridge, Mass.

Received March 1, 1958

Experimental data have previously been reported[2–4] giving the surface tension of pure iron and the effect of various surface active agents in solution. Among the most active surface active additives are oxygen and sulfur. In the present work, these studies have been extended to investigate the surface activity of selenium and tellurium in liquid iron.

Experimental

The sessile drop method which has been described in detail previously[2–4] was employed to determine surface tension of the liquids in contact with aluminum oxide. Maximum experimental deviations in measured values for a given composition vary between 1 and 3%.

High purity vacuum-melted iron (Vacuum Metals Corporation Ferrovac E ingot) was employed as the base material. This metal has the following impurities: 0.003 C, 0.007 O, 0.0005 N, 0.005 S, 0.01 Si, <0.003 Al, <0.006 Co, <0.001 Cu Mn, <0.01 Ni Pb, <0.0005 Sn, <0.003 Mo. Samples were prepared by melting this material with additions of high purity selenium and tellurium in purified helium after outgassing at red heat *in vacuo*, using pure aluminum oxide crucibles. The resulting ingots were cut up to provide samples which were used for experimental measurements.

After placing in the furnace and leveling, the system was heated to 1000° under vacuum (0.01 μ) and then heated to 1570° for measurements in 0.5 atm. of helium. Hospital grade helium was purified with a liquid nitrogen cold trap, Cu_2O at 400° to oxidize reduced gases, Mg chips at 400° and Ti at 1000° to remove oxidized gases, and activated charcoal at −200°.

Samples were analyzed for O, Se and Te after carrying out the surface tension determinations at 1570°. Results are given in Table I.

TABLE I

SURFACE TENSION MEASUREMENTS

Oxygen	Composition, % Selenium	Tellurium	Surface tension
0.020	0.03	..	1000
.010	0.10	..	740
.023	..	0.04	1325
.025	..	0.10	1300
.008	..	..	1632[3]
.020	..	..	1541[3]

Discussion

Surface tension is plotted as a function of log weight per cent. addition in Fig. 1. The oxygen content of the liquids makes for some difficulty in interpretation. In the case of tellurium, which is least surface active, it is reasonable to assume that the surface tension lowering due to the oxygen content is independent of the tellurium content. Experimental data have been adjusted in this way (open points) in Fig. 1 for the oxygen content. For the case of selenium, which is much more surface active, this assumption is not as satisfactory—the required correction being somewhat less due to selenium adsorption at the surface. We have indicated the maximum correction to be expected by open points on Fig. 1. Since selenium is strongly surface active, the general interpretation of the results is not affected by errors in this assumption.

Both selenium and tellurium additions decrease the surface tension of liquid iron, indicating a concentration at the surface. The excess surface

(1) With funds from the U. S. Atomic Energy Commission, under Contract No. AT (30-1)-1852.

(2) W. D. Kingery and M. Humenik, THIS JOURNAL, **57**, 359 (1953).
(3) F. A. Halden and W. D. Kingery, *ibid.*, **59**, 557 (1955).
(4) C. R. Kurkjian and W. D. Kingery, *ibid.*, **60**, 961 (1956).

concentrations can be calculated from the Gibbs isotherm

$$\Gamma = \frac{-d\gamma}{RT\, d \ln a} = \frac{-d\gamma}{RT\, d \ln c} \qquad (1)$$

These values have been calculated from the slopes of the corrected curves in Fig. 1. Selenium is found to have an excess surface concentration of 12.5×10^{-10} mole/cm.^{2} corresponding to an area of 13.3 Å.^{2}/atom. Using the Zachariasen[5] value of 1.96 Å. for $Se^=$ a close packed selenium monolayer would correspond to a surface concentration of 12.4×10^{-10} mole/cm.^{2}. That is, over the concentration range studied, a monolayer of selenium is adsorbed on the surface of liquid iron. As illustrated in Fig. 1, Se is similar to O and S.

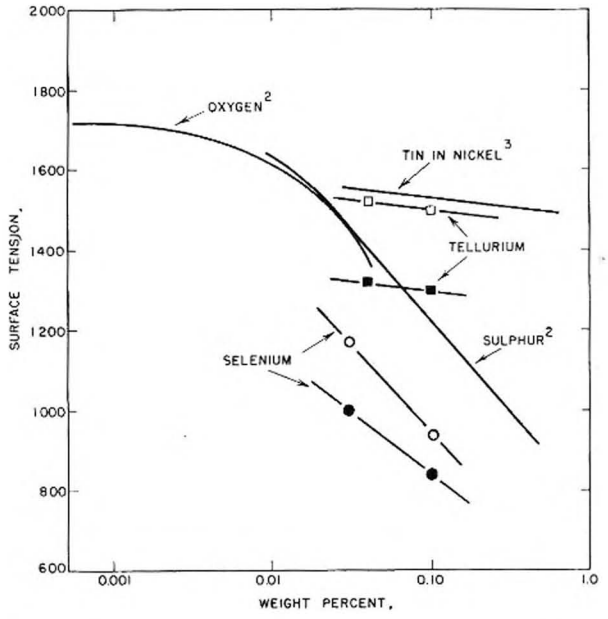

Fig. 1.—Surface tension data for additions to liquid iron.

While tellurium also decreases the surface tension of liquid iron, the effect is much less marked; additions of 0.1 weight % Te corresponding to a surface excess of about 1.4×10^{-10} mole/cm.^{2}—or about 12% of complete surface coverage. As indicated in Fig. 1, Te is similar to Sn.

As indicated by the concentration required to form a surface monolayer, the surface activity of group VI elements in liquid iron is O<S<Se>>Te. One would expect that the effectiveness of these materials in liquid iron in reducing the surface tension would be proportional to the polarizability, as is found to be the case for $O^=$, $S^=$ and $Se^=$ whose polarizabilities are 3.9, 10.2 and 10.5, respectively.[6] On this same basis, the polarizability of $Te^=$ is 14.0, but tellurium is found to have a much smaller effect on surface properties. The low surface activity of tellurium must be due to the low electronegativity of Te (2.1 e.v.) compared to O, S and Se (3.5, 2.5 and 2.4).[7] While oxygen, sulfur and selenium must be regarded as ionized in their marked effect on decreasing the surface tension tellurium forms essentially a metallic solution in liquid iron. Consequently its surface active behavior is much more similar to tin and indium than it is to the other group VI elements.

(5) W. H. Zachariasen, *Z. Krist.*, **80**, 137 (1931).
(6) L. Pauling, *Proc. Roy. Soc. (London)*, **A114**, 181 (1927).
(7) L. Pauling, "The Nature of the Chemical Bond," Cornell Univ. Press, Ithaca, N. Y., 1945.

THERMAL ANALYSIS OF SOME 12-HYDROXYSTEARATES

BY S. T. ABRAMS AND F. H. STROSS

Shell Development Company, Emeryville, California

Received March 11, 1958

During the last two decades thermograms characteristic of various types of alkali and alkaline earth soaps have been obtained by differential thermal analysis.[1-3] From these thermograms one can learn the number and temperatures of the transitions and the approximate latent heats involved.

This note records the thermal analysis of sodium 12-hydroxystearate, lithium 12-hydroxystearate and lithium hydrocastorate, which consists largely of lithium 12-hydroxystearate.

The two pure soaps differ principally in that the sodium soap changes appreciably on repeated analysis, while the lithium soap does not. Three successive analyses of the sodium 12-hydroxystearate are shown in Fig. 1. The initial transition

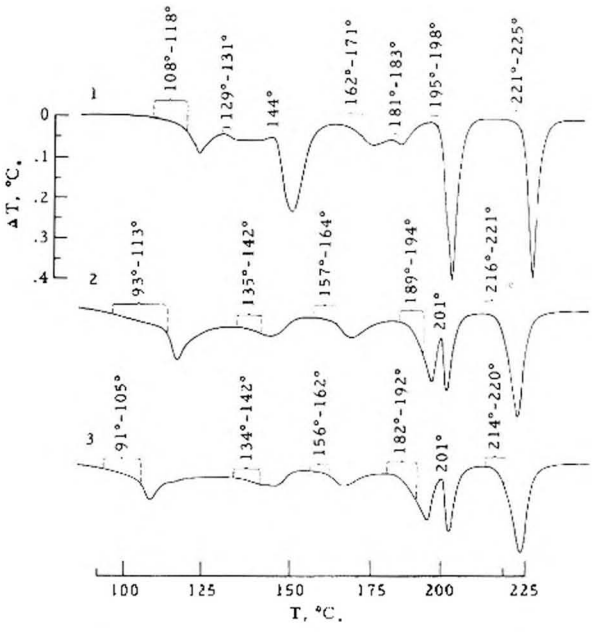

Fig. 1.—Thermogram of sodium 12-hydroxystearate: 1, original run; 2, re-run; 3, second re-run.

temperatures and the relations of the individual heats of transitions (represented by the peak areas) are changed on analysis; in addition, the summed latent heat drops from nearly 12 kcal. per mole in the first thermogram to less than 8 kcal. per mole. This change would be consistent

(1) R. D. Vold, *J. Am. Chem. Soc.*, **63**, 2915 (1941).
(2) C. J. Penther, S. T. Abrams, and F. H. Stross, *Anal. Chem.*, **23**, 1459 (1951).
(3) M. J. Vold, G. S. Hattiangdi and R. D. Vold, *Ind. Eng. Chem.*, **41**, 2539 (1949).

with the dehydration of the compound to form sodium oleate. The low total heat of fusion of sodium oleate as compared to the sodium soaps of saturated fatty acids has been discussed by Vold[1]; the third analysis of sodium 12-hydroxystearate (Fig. 1,3) also resembles the thermogram shown in Vold's paper more than the initial thermogram (Fig. 1,1).

The thermogram of lithium 12-hydroxystearate is shown in Fig. 2. The sharp peaks of the pure

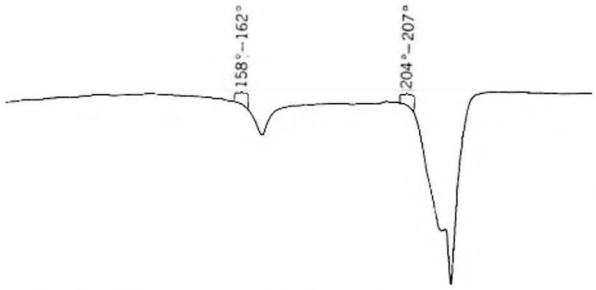

Fig. 2.—Thermogram of lithium 12-hydroxystearate.

lithium soap[4] condense into a single diffuse peak in the case of the lithium hydrocastorate (Fig. 3),

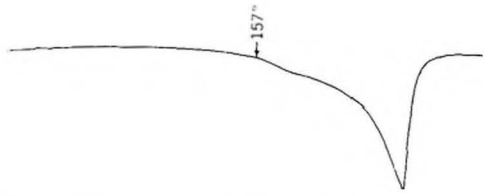

Fig. 3.—Thermogram of lithium hydrocastorate.

most probably because of the lower purity. Lithium 12-hydroxystearate has a total heat of fusion of about 10.5 kcal. per mole.

Lithium hydrocastorate is the lithium soap of hydrogenated castor oil acids, which consist of 12-hydroxystearic acid and stearic acid in the ratio of 5.7:1. The soap also contains 9% glycerol. The lack of distinctness of the initial part of the peak makes the evaluation of the latent heat difficult, but it was estimated to be 10 to 11 kcal. per mole of soap. As in the case of the pure soap, the hydrocastorate appears to have an initial transition temperature of about 157 to 160°.

(4) Prepared by E. R. White. This is the same preparation as that used in work reported by Bondi, *J. Coll. Sci.*, **5**, 458 (1950).

LIQUID–VAPOR EQUILIBRIA FOR THE SYSTEM NITROBENZENE–*t*-BUTYL ALCOHOL

BY F. F. MIKUS[1] AND C. W. LAWLER

Chemistry Department, Texas College of Arts and Industries, Kingsville, Texas

Received March 13, 1958

As part of an investigation of the behavior of some ternary systems it was necessary to determine the liquid–vapor equilibria for the system nitrobenzene–*t*-butyl alcohol.

Experimental

Materials.—Eastman Kodak No. 820 *t*-butyl alcohol was distilled from calcium oxide after refluxing for 12 hours. The middle portion boiling at 82.8° and having a refractive index 1.3877 at 20° was used. Eastman Kodak No. 387 nitrobenzene was distilled and the middle fraction boiling at 210.9° and having a refractive index of 1.5529 at 20° was used.

Procedure.—The determination of the liquid-vapor equilibrium data was carried out in a Colburn still.[2] The pressure was maintained at 760 mm. of mercury by means of a Cartesian manostat.[3] Temperature of the mixture in the equilibrium chamber was measured with a chromel *vs.* alumel thermocouple in conjunction with a Leeds and Northrup Type K potentiometer. It was assumed when samples taken at ten minute intervals had the same reading on an Abbe refractometer equilibrium had been attained. The compositions of the samples were determined from a refractive index-composition graph.

Experimental Data

The data obtained are presented in Table I and also graphically in Fig. 1.

TABLE I

VAPOR–LIQUID EQUILIBRIUM DATA FOR NITROBENZENE–*t*-BUTYL ALCOHOL

Temp., °C.	Liquid	Vapor
207.7	0.001	0.110
203.7	.002	.254
199.3	.003	.322
192.5	.006	.470
177.8	.014	.672
167.2	.015	.775
145.5	.049	.910
130.3	.075	.943
119.3	.114	.968
110.0	.160	.977
100.0	.219	.988
94.8	.307	.992
92.8	.372	.994
90.5	.464	.995
88.3	.549	.997
86.4	.659	.998
84.6	.736	.999
83.7	.884	.999

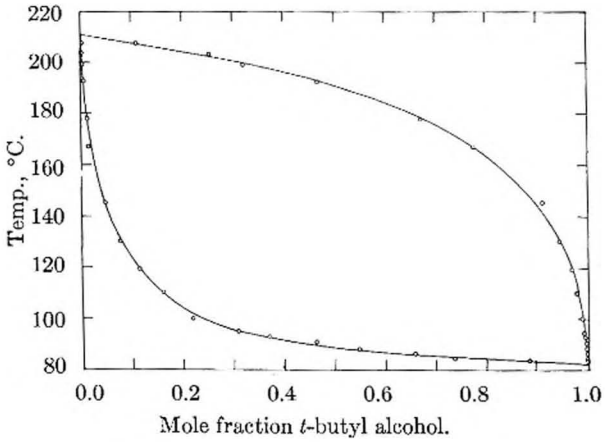

Fig. 1.—Liquid-vapor equilibria for the system nitrobenzene-*t*-butyl alcohol.

(1) General Electric Company, The Knolls Atomic Power Laboratory, Schenectady, N. Y.

(2) C. A. Jones, E. M. Shoenburn and A. P. Colburn, *Ind. Eng. Chem.*, **35**, 666 (1943).

(3) R. Gilmont, *Ind. Eng. Chem., Anal. Ed.*, **18**, 633 (1946).

SILVER HALIDE PRECIPITATION. III. CRYSTALLOGRAPHIC STUDY OF THE DOUBLE JET METHOD

BY C. R. BERRY AND S. J. MARINO

Communication No. 1932 from the Kodak Research Laboratories, Eastman Kodak Company, Rochester, N. Y.

Received March 18, 1958

Analysis of crystalline phases by X-ray diffraction is a powerful means of studying precipitation processes in which solid solutions are formed. Results of such studies in the AgBr–AgI system have been reported for the case where an $AgNO_3$ solution was added to a solution of halides (single-jet method).[1,2] The present investigation concerns the simultaneous addition of an $AgNO_3$ solution and an equimolar solution of halides to a gelatin solution in a precipitation vessel (double-jet method).

With single-jet precipitation, it was observed that more nearly homogeneous crystals were produced with an increased rate of precipitation, or with a greater KBr excess in the precipitation vessel. It will be seen that the same variables produce exactly reversed results in the double-jet scheme.

Although equilibrium conditions do not usually exist in these precipitations, it will be instructive to consider for a composition of 12 mole % iodide the equilibrium phases at different times during precipitation as given in Fig. 1. These curves are derived from the equilibrium diagram of AgBr–AgI in aqueous KBr,[1,3] and they are not very sensitive to the concentration of KBr.

A typical double-jet experiment was carried out under the conditions

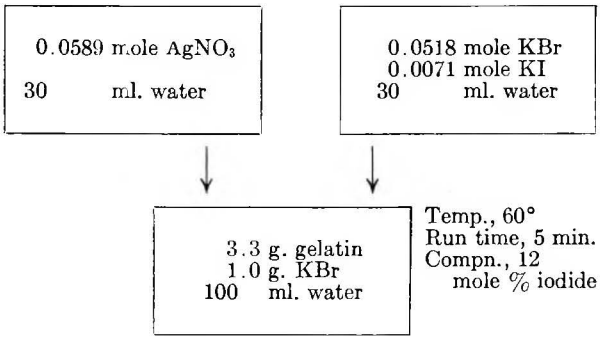

Variation in the concentration of excess KBr in the precipitation vessel has a profound effect on the double-jet precipitates, as shown in Fig. 2. It is seen that homogeneous crystals were produced only with small or zero concentrations of excess KBr. A reasonable explanation for the increasing departure from homogeneity with increasing KBr is that a high concentration of bromide ions everywhere in the precipitation vessel produces nuclei of silver bromide containing little or no iodide. These small crystals may grow rapidly in the solvent medium by Ostwald ripening so that rather large crystals are formed whose interiors are effectively isolated from the iodide ions. This point of view is consistent with earlier observations that crystals of AgBr, when put into a KI solution, progress through the stages of reaction indicated by reading the curves of Fig. 2

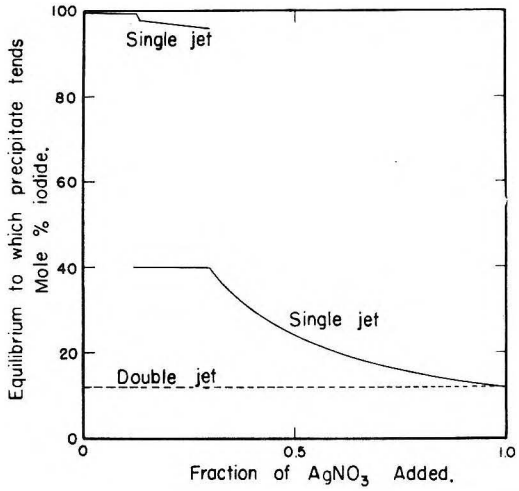

Fig. 1.—Equilibrium compositions at 50° which exist during the addition of $AgNO_3$ in precipitation of 12 mole % bromoiodides.

from high to low KBr concentration: the first reaction product being AgI, then a 45 mole % iodide, and finally the equilibrium composition. The

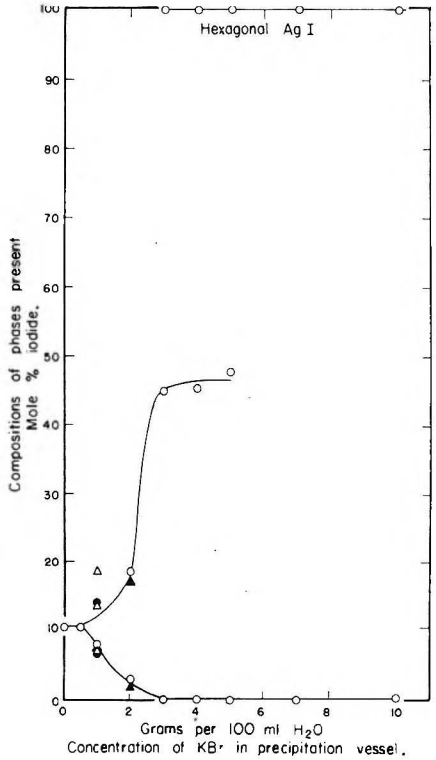

Fig. 2.—Phases present at the end of 5-minute double-jet precipitations of 12 mole % bromoiodide at 60°; concentration of KBr varied.

very different observation in the single-jet experiments, that homogeneity was encouraged with increasing KBr excess, was explained as the result of an increasing rate of solution of the AgI which pre-

(1) C. R. Berry and S. J. Marino, *Phot. Science and Technique*, [II] **2**, 149 (1955).
(2) C. R. Berry and S. J. Marino, *ibid.*, **4**, 22 (1957).
(3) H. Raynaud and J. Pouradier, *J. chim. phys.*, **52**, 133 (1955).

cipitated alone early in the run and then had to dissolve and recrystallize in solid solution with the silver bromide as the system attempted to follow the changing equilibrium curve of Fig. 1.

The results of changing both the precipitation rate and the KBr excess are summarized in Fig. 3. Clearly, an increase in the time of precipitation increased the homogeneity of the crystals in the double-jet method, just the reverse of the single-jet method. The curves of Fig. 1 give the clues to the reasons for this behavior. Slow precipitation by the double-jet method encourages the attainment of the equilibrium condition which is the same at every instant during the experiment. But, with the single-jet method, the equilibrium changes continually during the run so that a uniform iodide distribution can occur only when the crystals are in a highly reactive state (*i.e.*, more finely divided as in the faster precipitations) near the end of the runs.

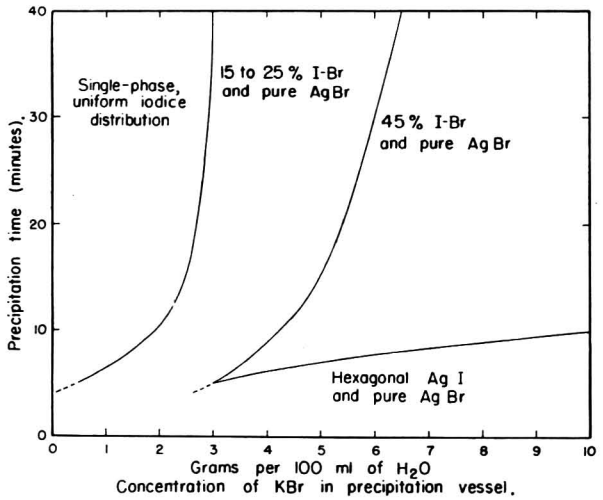

Fig. 3.—Phases present at the end of double-jet precipitations of 12 mole % bromoiodide at 60°; effects of varying the precipitation time and the KBr concentration.

Silver bromoiodide crystals are usually bounded by {111} faces. This most densely packed plane fulfills the Donnay–Harker[4] criterion for minimum surface energy. However, it was interesting to note that, in the double-jet experiments, regular cubes were produced when there was no excess KBr in the precipitation vessel.[5] With no halide ions in solution, the reduction in surface energy associated with electrically neutral {200} planes becomes important. It is also pertinent that no tabular crystals were observed among the cubes. This is reasonable in view of the explanation that tabular crystals of triangular and hexagonal outline are caused by twinning on {111} planes parallel with the platelets.[6] Since growth twins cannot occur on {200} planes in the NaCl type of structure, no tabular grains having {200} faces are to be expected.

(4) J. D. H. Donnay and D. Harker, *Compt. rend.*, **204**, 274 (1937).
(5) Also noted by V. N. Zharkov and E. P. Dobroserdova, *Zhur. Nauch. i Priklad. Fotografii i Kinematografii*, **1**, 250 (1956).
(6) R. W. Berriman and R. H. Herz, *Nature*, **180**, 293 (1957).

STUDIES ON SILICIC ACID GELS. XIX. THE EFFECT OF ELECTROLYTES UPON THE VISCOSITY OF THE SOL AND UPON THE TIME OF SET

By Charles B. Hurd, John W. Rhoades, William G. Gormley and Arthur C. Santora

Department of Chemistry, Union College, Schenectady, New York

Received March 24, 1958

The change in viscosity of hydrosols of silicic acid, during setting, is interesting because the curve of viscosity against age of sol resembles curves for other properties, such as the amount of light scattered. We have studied the effect of changing *p*H and of added salts upon these curves, also upon time of set.

In part 1, shown by Fig. 1, mixtures were made

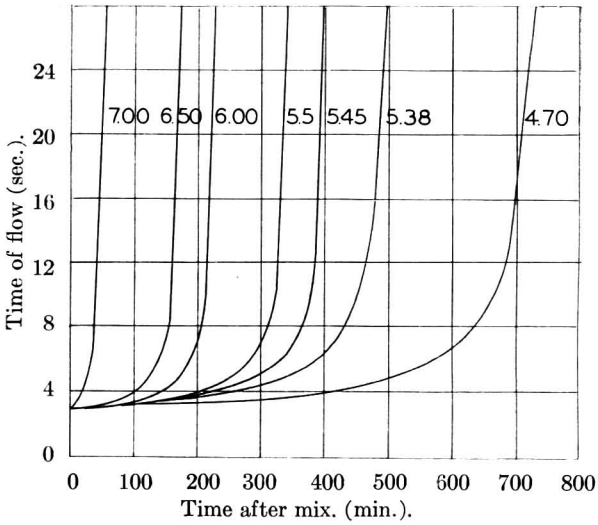

Fig. 1.—Time of flow of silicic acid gel mixtures as a function of age of sol and of *p*H.

by pouring solutions of E brand silicate (Philadelphia Quartz Company) into HCl solutions. Concentrations were SiO_2, 0.60, and NaCl from reaction, 0.36 mole per liter; excess HCl for *p*H 7.0, none, for *p*H 4.70, 0.0093 mole per liter. Curves shown in Fig. 1, composed of many points, are of the same shape and can be made to superimpose by plotting time of flow against relative age. Relative age is the ratio of actual time, since mixing, divided by time required for time of flow to reach an arbitrary value, 10 seconds here.

Time of flow was measured in an ordinary Ostwald viscometer pipet. No attempt was made to calculate actual viscosity, but the actual viscosity must be approximately proportional to time of flow. No kinetic energy corrections were made. All work was done at 25°.

To study effect of electrolytes added, upon time of flow and time of set, we used mixtures of sodium silicate and acetic acid solutions. If extra salt was added, it was in the acetic acid solution.

Each mixture contained Na^+ 0.42 mole per liter, SiO_2 0.70, CH_3COOH 0.68 and extra electrolyte, if added, 0.30. Silicate always was poured into the acid. Time of set was measured by the tilted rod method. Figure 2 shows the results with

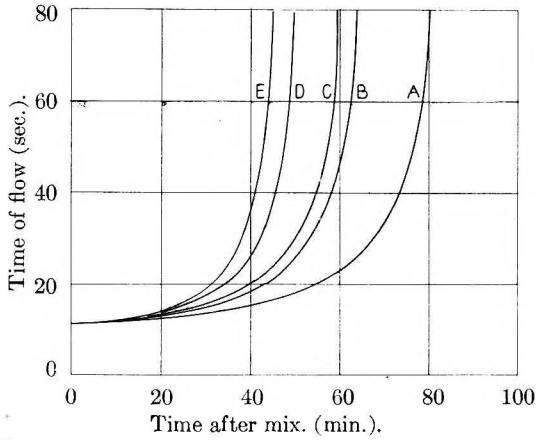

Fig. 2.—Time of flow of silicic acid gel mixtures as a function of age of sol as influenced by alkali chlorides: A, no salt; B, LiCl; C, NaCl; D, NH_4Cl; E, KCl.

alkali chlorides. Table I summarizes the results of many series of tests.

TABLE I

TIME OF SET AND THE *p*H OF SILICIC ACID GEL MIXTURES CONTAINING ADDED ELECTROLYTES AT 25°

	Time of set in min.					*p*H			
	Li	Na	K	NH_4		Li	Na	K	NH_4
Cl	85	74	58	66	Cl	4.8	4.8	4.7	4.8
Br	77	70	55	60	Br	4.9	4.9	4.9	4.8
I		66	51	55	I		4.7	4.8	4.6
NO_3		72	58	60	NO_3		4.7	4.7	4.7
CNS		63	52	56	CNS		4.8	4.9	4.9
	With no electrolyte added, 100					With no electrolyte added, 4.8			

Efficiency of ions used, for decreasing time of set or decreasing time required to produce a given increase in viscosity is shown as $K^+ > NH_4^+ > Na^+ > Li^+$ and $I^- > CNS^- > Br^- > NO_3^- > Cl^-$ for acid gels of *p*H 4.8 containing excess CH_3COOH and CH_3COONa produced in the reaction. This order of cation effectiveness agrees with the results of Pappada[1] on effectiveness of coagulation of SiO_2 hydrosols.

We believe the same process occurs in all of these gel mixtures because of the shape of the curves. Change of *p*H or presence of added salt merely accelerates the process. Further theoretical discussion is omitted because of space limitation.

(1) N. Pappada, *Gazz. chim. ital.*, **35**, I, 78 (1905).

THE VAPOR PRESSURE OF NICKEL FLUORIDE[1]

BY MILTON FARBER, RICHARD T. MEYER AND JOHN L. MARGRAVE

Jet Propulsion Laboratory, California Institute of Technology, Pasadena California
Department of Chemistry, University of Wisconsin, Madison, Wisconsin

Received March 25, 1958

One of the objections raised to values for the dissociation energy of fluorine as determined by pressure or effusion studies in metal systems,[2-4] concerns the possibility that metal fluorides like NiF_2 or CuF_2 might be sufficiently volatile at the high temperatures to complicate the interpretation of the data.[5] The vapor pressure of NiF_2 has been measured independently by two different methods at the Jet Propulsion Laboratory and at the University of Wisconsin to see whether this objection is valid for experiments in nickel containers. The only previous observation on NiF_2 was that of Poulenc[6] who stated that NiF_2 sublimes without melting under an HF atmosphere at about 1000°.

Samples of NiF_2 may be prepared conveniently by direct fluorination of $NiCl_2$ at 350–400°.[7] They then must be protected carefully from water vapor which could cause hydrolysis to NiO and HF on heating. The NiF_2 is contained without reaction in platinum vessels up to at least 1100°.

The Jet Propulsion Laboratory measurements were Knudsen effusion studies over the range 1026–1104°K. The University of Wisconsin work was by the flow method with N_2 as the flow gas, and yielded vapor pressures at 1233 and 1349°K. The results are shown graphically in Fig. 1. The solid

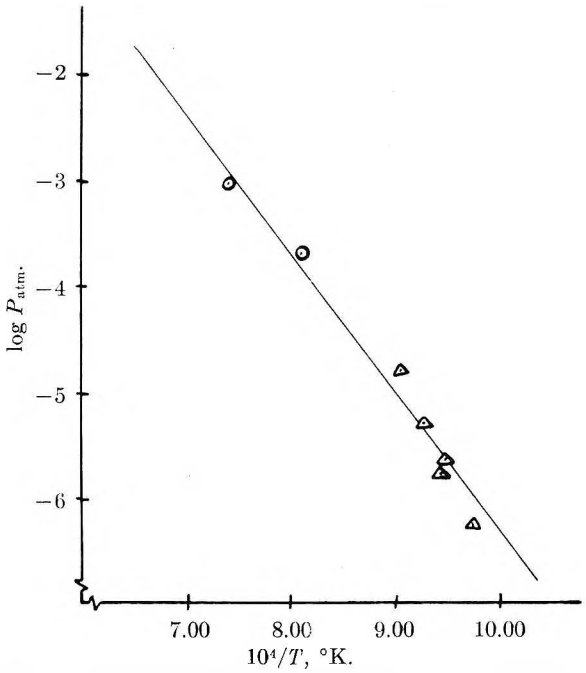

Fig. 1.—Vapor pressure of nickel fluoride: △, JPL Knudsen data; ⊙, UW flow data.

line drawn through the points indicates the vapor pressure equation to be

$$\log P_{NiF_2}(\text{atm}) = \frac{-13{,}100}{T} + 6.8 \quad (1026 < T < 1349°\text{K.})$$

with the assumption that $NiF_2(g)$ is the major vapor species. Simple thermodynamic arguments in combination with the observed weight losses show that decomposition to the elements or to NiF(g) and F(g) or $F_2(g)$ are not important in vaporization at these temperatures.

From these data, for the reaction $NiF_2(s) = NiF_2(g)$, one calculates the heat of sublimation

(1) Taken in part from the B.S. thesis of Richard T. Meyer, submitted to the University of Wisconsin, June, 1956.

(2) J. L. Margrave, Ph.D. Thesis, University of Kansas, 1950; P. W. Gilles and J. L. Margrave, *J. Chem. Phys.*, **21**, 381 (1953).

(3) R. N. Doescher, *ibid.*, **19**, 1070 (1951); **20**, 330 (1952).

(4) H. Wise, *ibid.*, **20**, 927 (1952).

(5) R. T. Sanderson, *J. Chem. Phys.*, **22**, 345 (1954).

(6) C. Poulenc, *Ann. chim. phys.*, **2**, 41 (1894).

(7) "Inorganic Syntheses," Vol. III, McGraw-Hill Book Co., New York, N. Y., 1950, p. 173.

$\Delta H_{sub} = 60 \pm 2$ kcal./mole, over the range 1026–1349°K. The normal boiling point is estimated to be slightly above 1950°K., and $\Delta S_{vap} \leq 31$ entropy units at the boiling point.

The vapor pressure of NiF_2 is, therefore, a negligible part of the fluorine pressure deviation observed by Doescher,[2] and $NiF_2(g)$ should not have been present in a high enough concentration to change the interpretation of the effusion data of Wise.[3]

In the course of these studies, NiF_2 was not observed to melt at temperatures up to 1365°K., which must, therefore, be specified as a lower limit for the melting point.

The authors wish to acknowledge the support of this work by the Office of Ordnance Research, the U. S. Army Ordnance Department and the Wisconsin Alumni Research Foundation.

THE PHOTO-IONIZATION OF SOME TRIPHENYLMETHANE-LEUCOCYANIDES CONTAINING CERTAIN GROUPS SUBSTITUTED IN THE *para*-POSITION DISSOLVED IN 1,2-DICHLOROETHANE

BY EDWARD O. HOLMES, JR.

Department of Chemistry, Boston University, Boston, Massachusetts

Received March 18, 1958

In a recent paper[1] the author investigated the effect of some solvent properties (dielectric constant and dipole moment) on the photo-ionization of malachite green leucocyanide. In this investigation, an attempt was made to relate structure to photo-ionization in one of the solvents previously used, namely, 1,2-dichloroethane.

The procedure was identical so far as possible with that described in the author's[1] previous publication. All solutions were 2.17×10^{-5} molar, the solvent the middle fraction of redistilled Eastman Kodak (#132) 1,2-dichloroethane, the solutions were enclosed in a 50-ml. Pyrex flask and irradiated by a Cooper–Hewitt low-pressure mercury lamp at a distance of one inch for 4 minutes. Following exposure all solutions were scanned immediately with a Beckman DU-K2 automatic spectrometer.

The results of this procedure are contained in Table I.

Discussion

The above results which show the absorbancies of the carbonium ions produced by photo-ionization of the various leucocyanides do not offer a good basis for comparing the effects of the various groups substituted in the *para*-position as one cannot be sure that there are no side-reactions involved. A better basis would be the degree of photo-ionization. In order to calculate this, it would be necessary to know the absorbancies of the various carbonium ions in the same solvent when pure compounds of the various dyes known to be 100% ionized were dissolved. No such information is now available nor are the compounds themselves obtainable in the proper degree of purity. Nevertheless the above results offer the first step forward toward this calculation.[2]

Points of special interest are that (a) the absorbancies of the ions of compounds II and IV are greater than those of the original leucocyanides themselves, (b) that the absorbancy of the ion of compound II is much larger than that of any of the others, and (c) that the ions of compounds III, IV and VI show no *z*-band.

(2) As circumstances will not permit the author to continue this investigation he sincerely hopes that the material herein presented will be of help to some other investigator who is interested in discovering the effect of group substitution in the *para*-position on the degree of photo-ionization.

TABLE I

Compound	Original soln. *z*-band Max. λ, mμ	Abs.[c]	After 4 min. irradiation *y*-band Max. λ, mμ	Abs.	*z*-band Max. λ, mμ	Abs.
I	275	1.65	586	1.186	350	0.12	306	0.52
II	275	0.86	625	1.530	433	.20	320	0.30
III	270	0.45	480	0.250	355	.10	x	x
IV	293	0.146	530	.473	350	.11	x	x
V	310	0.870	680	.235	470	.06	330	0.58
VI[a]	x	x	450	.050	293	.055	x	x

No.	Legend Compound	Corresponding dye
I	Tris-(*p*-N-dimethylaminophenyl)-methane leucocyanide	Crystal Violet
II	Bis-(*p*-N-dimethylaminophenyl)-phenylmethane leucocyanide	Malachite Green
III	*p*-N-Dimethylaminophenyl-diphenylmethane leucocyanide	Sunset Orange[b]
IV	Tris-(*p*-aminophenyl)-methane leucocyanide	*p*-Rosaniline
V	Bis-(*p*-N-diphenylaminophenyl)-phenylmethane methyl ether	x
VI	Tris-(*p*-*t*-butylphenyl)-methane leucocyanide	x

[a] On irradiation in quartz container with quartz lamp only. [b] Name assigned by author. [c] Abs. (absorbancy; formerly called optical density).

(1) E. O. Holmes, Jr., THIS JOURNAL, **61**, 434 (1957).

THE SOLUBILITY OF *cis*- AND *trans*-DINITROTETRAMMINE-COBALT(III) PICRATES IN ETHANOL–WATER MIXTURES

BY PHYLLIS M. BLOSSER AND FRANK H. VERHOEK

Contribution from the McPherson Chemical Laboratory of The Ohio State University, Columbus, Ohio

Received March 27, 1958

At present, it is not possible to predict the solubility of an electrolyte in one solvent from a knowl-

edge of its solubility in another. In order to provide additional data for the solution of this problem, an investigation of the solubility of slightly soluble electrolytes of the simplest valence type, 1-1, was undertaken. Since specific solvent effects might be expected to show up as a difference in the behavior of similar electrolytes of different structure, the *cis*- and *trans*-dinitrotetrammine-cobalt-(III) ions were chosen as cations. A search of the literature[1] showed that for the 1-1 salts of these ions which had been investigated, the *cis* cation was more soluble in water than the *trans*, except for the picrates. Several other slightly soluble 1-1 salts of these ions were prepared and their solubilities in water determined[2] at room temperature (24°); the periodate was the only one, in addition to the picrate, for which the solubility of the *cis* salt was less than that of the *trans*. It was further observed that the solubility of the picrates was the same in 44 weight % ethanol as in water, whereas those of other anions, including the periodates, showed a lesser solubility, as expected. The unusual behavior of *cis*- and *trans*-dinitrotetrammine picrates was therefore investigated further.

For the preparation of *cis*-dinitrotetrammine-cobalt(III) picrate (flavo picrate, $Co(NH_3)_4(NO_2)_2C_6H_2(NO_2)_3O$), carbonatotetrammine-cobalt(III) sulfate was first prepared[3] and changed to flavo nitrate,[4] using only well-formed deep red crystals of the carbonato compound.[5] Flavo picrate was prepared by mixing at 40° a 5% flavo nitrate solution with an equivalent quantity of 5% sodium picrate solution. A cream-colored gelatinous mass first formed which on stirring for 5–10 minutes settled out as fine yellow-orange crystals. Analysis gave 13.19 ± 0.07% Co, 15.32 ± 0.24% NH_3 (theoretical 13.18%, 15.23%).

trans-Dinitrotetrammine-cobalt(III) picrate (croceo picrate, $Co(NH_3)_4(NO_2)_2C_6H_2(NO_2)_3O\cdot H_2O$) was prepared from croceo chloride[4] by mixing at 40° a 3% solution of the latter with an equivalent quantity of 5% sodium picrate. The yellow gelatinous precipitate first formed changed to orange crystals when stirred vigorously for 10–15 minutes. The long yellow hair-like crystals reported by Ephraim[1b] as forming first in this preparation were only observed if the filtrate was allowed to stand for several hours; they were discarded. The salt first formed is a monohydrate, but loses water in a desiccator; analysis of the dried salt gave 13.13 ± 0.20% Co, 15.26 ± 0.12% NH_3 (theoretical 13.18%, 15.23%).

The purity of both salts was further tested by measuring the solubility, and then repeating the measurement with the undissolved residue. For both water and 44% ethanol, no leaching of impurities during the first determination was observed. To determine the stabilities of the salts, saturated solutions in water and in 44% ethanol were allowed to stand in contact with the solid in the artificial light of the laboratory for 126 hours. Analysis at intervals during this time showed no change in the concentration of the solutions. The time required to establish solubility equilibrium was measured by rotating glass sample tubes containing solvent and salt for varying lengths of time and measuring the concentration. Experiments with both salts using water and 44% ethanol, and with flavo picrate in 99.6% ethanol, showed that equilibrium was reached in a few hours and that no further change was observed for as long as 100 hours, for all five cases. Concentrations in the preliminary measurements described above were determined spectrophotometrically.

The solubilities reported below were determined by rotating solid and solvent for 35–40 hours at 25.0°, withdrawing solution through a filter stick, and analyzing by decomposing the cobalt ammine present with sodium hydroxide in a deaerated solution,[6] collecting the ammonia in sulfuric acid, and back-titrating with standard base. The recommended addition of arsenious oxide[7] to the sodium hydroxide gave erratic and high results.

Examination of the equilibrium solid phases was carried out by drying in air the residues from several of the saturation experiments and preserving weighed samples over phosphoric anhydride in a vacuum at room temperature until constant weight was obtained. No loss in weight was observed for the *cis* salt for any solvent mixture, and the data showed that the air-dried *trans* salt from 0, 60 and 99.6% ethanol was the monohydrate. Dehydrated samples of the *trans* salt from these and other solvent mixtures could be rehydrated at room temperature in an atmosphere of 30% relative humidity. Thus, if an alcohol solvate is formed, it decomposes or is displaced by water on standing in air.

The solubility data are shown in Fig. 1, in which the logarithms of the solubilities are given as a function of the weight per cent. ethanol in the solvent.[8] A minimum solubility occurs at 17.2 wt. % ethanol

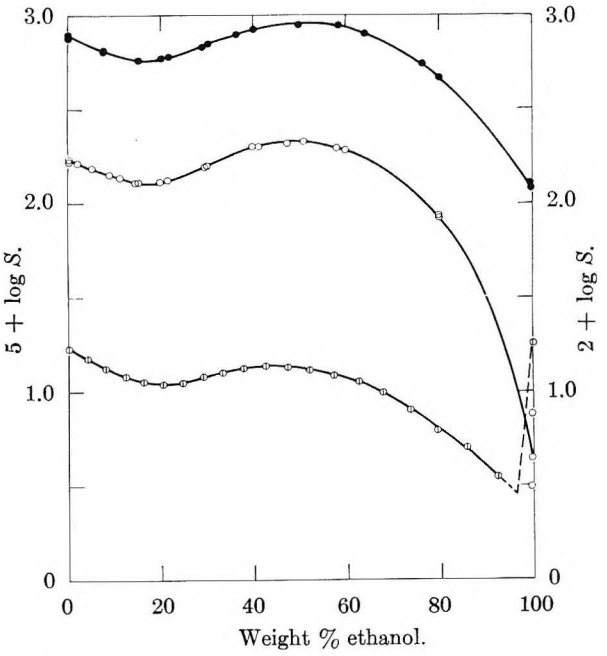

Fig. 1.—Solubility of picrates in ethanol–water mixtures. Scale at left for dinitrotetrammine-cobalt(III) picrates: solid circles, *trans;* open circles, *cis*. Lowest curve and scale at right for sodium picrate (ref. 11).

(1) Especially the tabulations of (a) J. N. Bronsted and A. Peterson, *J. Am. Chem. Soc.*, **43**, 2265 (1921); (b) F. Ephraim, *Ber.*, **56B**, 1530 (1923); (c) J. N. Bronsted, A. Delbanco and K. Volquartz, *Z. physik. Chem.*, **A162**, 128 (1932).

(2) *cis*-Acetate 0.15 mole/l. (*trans*-acetate 0.041 mole/l.[1c]); *cis*-benzene sulfonate 0.11 mole/l.; *cis*-iodate 0.059 mole/l. (*trans*-iodate 0.029 mole/l.[1c]); *cis*-periodate 0.0093 mole/l., *trans*-periodate 0.025 mole/l.; *cis*-permanganate 0.029 mole/l.; *cis*-dinitroöxalatodiammine cobaltate 0.0023 mole/l.; *trans*-dinitroöxalatodiammine cobaltate 0.00055 mole/l. The solubilities of the five other salts prepared (*cis*-bromide, perchlorate, iodide; *cis*- and *trans*-tetranitrodiammine cobaltate) agreed within the temperature limits with the literature data. Measured solubilities in 44% ethanol are: *cis*-periodate 0.0053 mole/l., *trans*-periodate 0.012 mole/l.; *cis*-tetranitrodiammine cobaltate 0.0021 mole/l.; *trans*-tetranitrodiammine cobaltate, 0.00021 mole/l.; *cis*-dinitroöxalatodiammine cobaltate 0.00026 mole/l.

(3) S. M. Jorgensen, *Z. anorg. Chem.*, **2**, 282 (1892).

(4) S. M. Jorgensen, *ibid.*, **17**, 455 (1898).

(5) S. A. Mayper H. L. Clever and F. H. Verhoek, THIS JOURNAL, **58**, 90 (1954).

(6) H. S. Miller, *Ind. Eng. Chem., Anal. Ed.*, **8**, 50 (1936).

(7) H. A. Horan and H. J. Eppig, *J. Am. Chem. Soc.*, **71**, 581 (1949).

(8) The original data have been deposited as Document No. 5542 with the ADI Auxiliary Publications Project, Photoduplication Service, Library of Congress, Washington, D. C., U. S. A. A copy may be secured by citing the document number and by remitting $1.25 for photo prints, or $1.25 for 35 mm. microfilm, payable in advance by check or money order to Chief, Photoduplication Service, Library of Congress.

for both salts, while a maximum occurs at 49.7 wt. % for the *cis* salt and 52.7 wt. % for *trans* salt.

Similar minima and maxima in ethanol–water mixtures were observed by Fischer[9] for the solubility not only of sodium, potassium and barium picrates, but also for sodium dinitro-, chloronitro-, and *p*-nitro-phenolates and barium dinitrosalicylate. Fischer's data for sodium picrate (a monohydrate), recalculated to a weight % and molar basis, are reproduced in Fig. 1; the curve for potassium picrate, an anhydrous substance, has a very similar shape. Sodium picrate is approximately 100 times, and potassium picrate 10 times, as soluble as the *cis*-cobaltammine picrate. We have confirmed, by spectrophotometric measurements, Fischer's observation that there is a second minimum for sodium picrate between 92 and 100% ethanol. Similar measurements have shown that this is not the case for the dinitrotetrammine cobalt picrates; for these salts, the solubility decreases steadily beyond the maximum.

In seeking an explanation of these results one notes that association into ion pairs is not likely to be appreciable in the low concentration range and relatively high dielectric constant range concerned in the present experiments. Solvolysis to picric acid may be shown to be insignificant, by calculations from the known dissociation constants.[10] The sulfates of the two cations in the same solvent pair[11] show no unexpected behavior, and one looks for a possible complex involving the picrate ion. Kortum[12] has observed shifts in absorption maxima of picrates in the intermediate range in alcohol–water mixtures, which he attributes to changes in solvation. Application of Walden's rule to ethanol–water mixtures shows a maximum in $\Lambda_0\eta$ for many electrolytes between 14 and 22 wt. % ethanol,[13–15] but this is attributed to the change in the mobility of the cation[14]; transference measurements[15] confirm this. There is, however, some increase in the product $l_0\eta$ for picrate ion in lithium picrate solution on addition of the first 12 wt. % ethanol, followed by a lesser increase and a very slight maximum at about 52 wt. %.[15] Comparison with the solubility data shows that the first rise corresponds to a decrease in solubility, yet the maximum appears near the maximum solubility.

It has been noted above that for the *cis*- and *trans*-dinitrotetrammine cobalt picrates the *trans* salt is more soluble than the *cis*. It is of interest that this holds throughout the solvent range and is such that a plot of the logarithm of the solubility of the *cis* salt against the logarithm of the solubility of the *trans* salt is a straight line. Relationships of this sort have been noted before[16] and hold also for the *cis*- and *trans*-sulfates,[5,11] but in the present case it holds in spite of the existence of minima and maxima as the solvent changes. Thus, it appears that addition of alcohol to the solvent affects the two salts proportionately, and again indicates that the presence of minima and maxima are concerned with effects on the picrate ion and not on the cations.

(9) W. M. Fischer, *Z. physik. Chem.*, **92**, 581 (1918).

(10) P. S. Danner, *J. Am. Chem. Soc.*, **44**, 2832 (1922); I. M. Kolthoff, J. J. Lingane and W. D. Larson, *ibid.*, **60**, 2512 (1938).

(11) H. L. Clever and F. H. Verhoek, THIS JOURNAL, **62**, 358 (1958).

(12) G. Kortum, *Z. physik. Chem.*, **B38**, 1 (1937).

(13) L. C. Connell, R. T. Hamilton and J. A. V. Butler, *Proc. Roy. Soc. (London)*, **A147**, 418 (1934).

(14) A. F. H. Ward, *J. Chem. Soc.*, 522 (1939).

(15) G. Kortum and A. Weller, *Z. Naturforsch.*, **5A**, 451, 590 (1950); G. Kortum and H. Wilski, *Z. physik. Chem. (Frankfurt)*, **2**, 258 (1954).

(16) J. N. Brønsted, "Chemistry at the Centenary Meeting of the British Association for the Advancement of Science," Cambridge, W. Heffer and Sons, Ltd., 1932, p. 39.

THE ALKALINE EARTH COMPLEXES OF THE ADENOSINE PHOSPHATES

BY GEROLD SCHWARZENBACH AND ARTHUR E. MARTELL

Eidgenossische Technische Hochschule, Zurich, Switzerland and Clark University, Worcester, Mass.

Received April 7, 1958

In his paper on the stabilities of the complexes of calcium and magnesium with AMP, ADP and ATP, Nanninga[1] compares his results with the constants obtained by Smith and Alberty[2] and with the data obtained by us.[3] Our measurements have been carried out at 20° in a solution of ionic strength $\mu = 0.1$ obtained by adding KCl. Smith and Alberty on the other hand had 25° and $\mu = 0.2$ obtained with a tetrapropylammonium salt, whereas Nanninga used mixtures of varying ionic strength (NaCl and tetraethylammonium bromide). In order to make a comparison of the data possible, Nanninga corrected his and our results for Na- and K-binding, assuming that both alkali ions would, according to Melchior,[4] form complexes of exactly the same stability. In applying these corrections, Nanninga increased twofold the association constants obtained by us for ATP and found that the "corrected" data are much larger than those obtained by other investigators. This was explained by Nanninga by making the statement that Martell and Schwarzenbach had implied the equality of K^{H}_{HZ} and K^{H}_{MHZ} in their derivation and that their equations were therefore incorrect.

In Table I, the data of the three groups of investigators are collected without making any corrections. The comparison shows very good agreement of the groups Smith–Alberty and Martell–Schwarzenbach. It seems that the potassium salt used by us has little influence on the apparent complex stabilities, a fact which is in harmony with the experience obtained with other complexing agents. Thus it was found[5] that potassium is only very weakly bound by the anion of uramildiacetic acid, which forms a sodium complex with a stability constant of 10^3. Van Wazer and Campanella[6] also found a considerable difference between K^+ and Na^+ when complexed with the polyphosphates. The somewhat smaller stability constants obtained by Smith and Alberty readily are explained by the higher ionic strength used by these authors. Binding of K^+ would on the other hand

(1) L. B. Nanninga, THIS JOURNAL, **61**, 1144 (1957).

(2) R. M. Smith and R. A. Alberty, *J. Am. Chem. Soc.*, **78**, 2376 (1956).

(3) A. E. Martell and G. Schwarzenbach, *Helv. Chim. Acta*, **39**, 653 (1956).

(4) N. Melchior, *J. Biol. Chem.*, **203**, 615 (1954).

(5) G. Schwarzenbach, E. Kampitsch and R. Steiner, *Helv. Chim. Acta*, **28**, 364 (1946).

(6) I. R. Van Wazer and D. A. Campanella, *J. Am. Chem. Soc.*, **72**, 655 (1950).

TABLE I

LOG OF EQUILIBRIUM CONSTANTS OF ADENOSINE MONO-, DI- AND TRIPHOSPHATE

(Represented by AMP^{2-}, ADP^{3-} and ATP^{4-}, respectively)

Reaction	Martell–Schwarzenbach[3] μ = 0, 1 (KCl); 20°	Smith–Alberty[3] μ = 0, 2 (n-$[C_3H_7]_4N^+$, Cl^-); 25°	Nanninga μ = 0, 1; 23°
$Ca^{2+} + AMP^{2-} \rightleftarrows Ca\text{–}AMP$	1.41 ± 0 03	1.43 ± 0.03	
$Ca^{2+} + ADP^{3-} \rightleftarrows Ca\text{–}ADP^-$	2.78 ± 0.03	2.81 ± 0.05	
$Ca^{2+} + ATP^{4-} \rightleftarrows Ca\text{–}ATP^{2-}$	3.60 ± 0.03	3.30 ± 0.06	3.14
$Ca^{2+} + HATP^{3-} \rightleftarrows Ca\text{–}HATP^-$	1.8 ± 0.1	1.61 ± 0.1	
$H^+ + Ca\text{–}ATP^{2-} \rightleftarrows Ca\text{–}HATP^-$	4 7 ± 0.1	(5.3)	
$H^+ + ATP^{4-} \rightleftarrows HATP^{3-}$	6.50 ± 0.01	(6.95)	
$Mg^{2+} + AMP^{2-} \rightleftarrows Mg\text{–}AMP$	1.69 ± 0.02	1.69 ± 0.02	2.0
$Mg^{2+} + ADP^{3-} \rightleftarrows Mg\text{–}ADP^-$	3.11 ± 0.05	3.00 ± 0.04	3.03
$Mg^{2+} + HADP^{2-} \rightleftarrows Mg\text{–}HADP$	4.7 ± 0.2	(5.1)	
$H^+ + ADP^{3-} \rightleftarrows HADP^{2-}$	6.35 ± 0.03	(6.68)	
$Mg^{2+} + ATP^{4-} \rightleftarrows Mg\text{–}ATP^{2-}$	4.00 ± 0.04	3.47 ± 0.03	3.61
$Mg^{2+} + HATP^{3-} \rightleftarrows Mg\text{–}HATP^-$	2.0 ± 0.1	1.49 ± 0 1	
$H^+ + Mg\text{–}ATP^{2-} \rightleftarrows Mg\text{–}HATP^-$	4.5 ± 0.1	(5.0)	
$H^+ + ATP^{4-} \rightleftarrows HATP^{3-}$	6.5 ± 0.01	(6.95)	

make the constants measured in KCl smaller than those measured in tetrapropylammonium chloride. If it is assumed that the differences of the numbers found by Martell-Schwarzenbach and Smith–Alberty are due mainly to differences in ionic strength, it also becomes clear that the differences increase from AMP to ADP and ATP because of the increase of charge of the anions. The large difference found for the stability of Mg–ATP seems to be the only unexplained result.

In our paper,[3] the individual constants K^{E}_{HZ} and K^{H}_{MHZ} (reactions $H^+ + Z \rightleftarrows HZ$ and $H^+ + MZ \rightleftarrows MHZ$, Z denoting the anion of ADP and ATP) were given to show that these constants are different and that we have by no means implied in our derivation that they must be equal. The criticism of Nanninga is due to a misunderstanding because he did not take into consideration the fact that the metal ion concentration which we employed was in considerable excess over that of the organic complexing agent. The experimental method which we used was described in detail as early as 1950,[7] and has been used with success also in other laboratories.[8,9]

The data for $\log K^{H}_{HZ}$ and $\log K^{H}_{MHZ}$ are the pK-values for the proton donators HZ and MHZ. The large difference in comparison to the data given by Smith–Alberty are due here to differences in the definitions of these pK's. Our data are "apparent" dissociation constants, $[H^-]$ being introduced as a concentration whereas Smith–Alberty used "mixed" constants in which $[H^+]$ is introduced as an activity. The following equations, in which C and a denote concentrations and activities respectively, make this difference clear

$$pK = -\log \frac{C_{Base}}{C_{Acid}} \times C_{H^+}$$

$$pK' = -\log \frac{C_{Base}}{C_{Acid}} \times a_{H^+}$$

(7) G. Schwarzenbach, *Helv. Chim. Acta*, **33**, 947 (1950).

(8) H. B. Jonassen and L. Westerman, *J. Am. Chem. Soc.*, **79**, 4275 (1957).

(9) S. M. Lambert and J. I. Watters, *ibid.*, **79**, 5606 (1957).

MICROWAVE ABSORPTION OF MIXTURES OF DIPOLAR LIQUIDS IN SOLUTION IN NON-POLAR SOLVENTS[1]

BY P. K. KADABA

Department of Electrical Engineering, Newark College of Engineering, Newark, New Jersey

Received April 11, 1958

The investigations of Schallamach[2] on the dielectric relaxation of binary mixtures of non-associated polar liquids at a frequency of 9 Mc./sec. in the temperature range −150 to −50° indicated a single absorption peak with the possibility of a single relaxation mechanism. By way of explanation, it was suggested that dielectric relaxation involved the disturbance of relatively large regions in the liquid. The use of a comparatively low frequency of 9 Mc./sec. required the use of liquids of a somewhat complex nature.

It was the purpose of this investigation to extend the measurements to much simpler liquids by the use of a suitable frequency in the microwave region. With a view to estimate the size of the regions involved in the relaxation process ternary mixtures containing two non-associated polar liquids in a suitable non-polar solvents were investigated. Based on Schallamach's observation it was reasonable to expect that at low concentrations two peaks in the loss factor (ϵ'') *vs.* temperature curves should be observed as the separation of the dipolar molecules of the two types is large. As the concentration is progressively increased the peaks might move closer and at sufficiently high concentrations when the molecules can interfere with each other one peak only should be found. The critical concentration corresponding to the single peak would then give an idea of the size of the region involved in the dielectric relaxation. Mixtures of nitriles, aliphatic nitro compounds and nitrobenzene were chosen because of their fairly good solubility. Also, their large dipole

(1) The principal work connected with the investigation was done at the Department of Electrical Engineering, University of Kentucky, Lexington, Ky.

(2) A. Schallamach, *Trans. Faraday Soc.*, **42A**, 180 (1946).

moments would enable the individual contributions to the dielectric loss of the two polar components to be traced even at low concentrations.

Experimental

All the measurements reported in this investigation were done at a frequency of 16,200 ± 1 megacycles as read on a high Q resonant cavity frequency meter. On account of the wide range of concentrations used in the measurements with the resulting range of dielectric loss, three different experimental arrangements were used. In the low concentration range extending from 0.04 to 0.1 mole fraction, two methods were used with equal success. One of them is based on the shift of the minimum point in the standing wave pattern and was first developed by Roberts and Von Hippel.[3] One disadvantage of this method is the difficulty in the measurement of high standing wave ratios which result when the dielectric loss is low. In view of this, in some of our low loss measurements we adopted a transmission method using a precision attenuator. This method is similar to the one used by Whiffen and Thompson.[4] The relative simplicity of this method and the ease of calculations as contrasted with the use of tables and charts in the former method should be noted.

In the high concentration range extending from 0.15 to 0.35 mole fraction, the experimental set-up was similar to

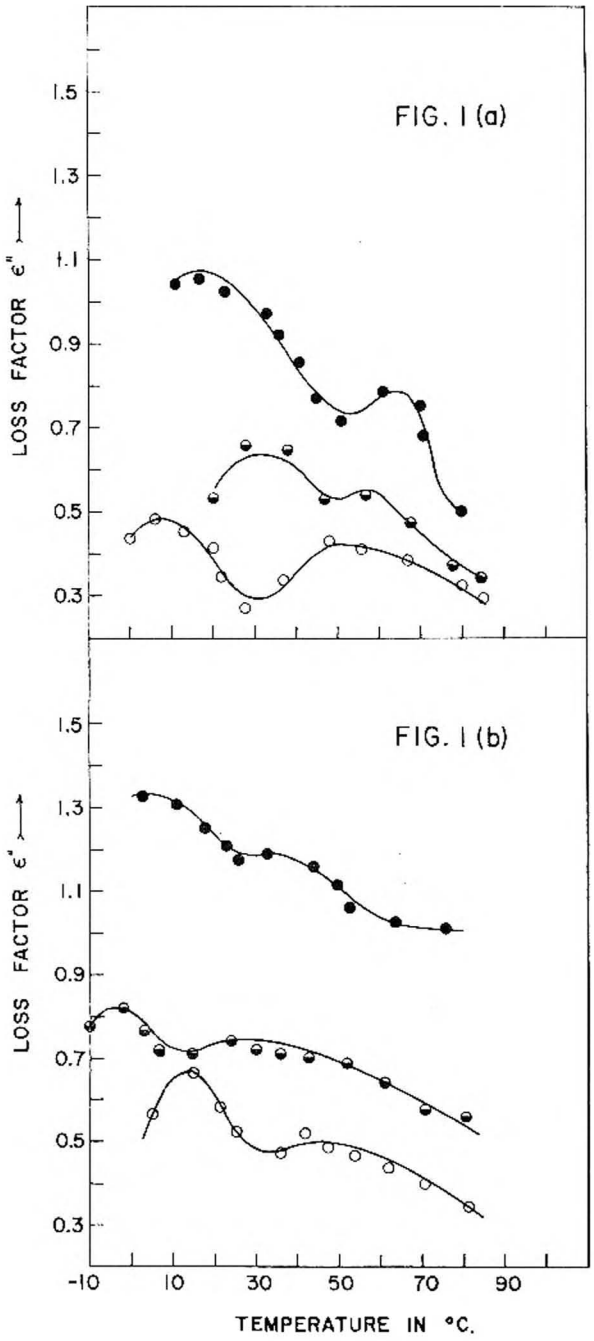

Fig. 1.—(a) Loss factor *vs.* temperature of solutions in *n*-heptane of nitrobenzene and nitroethane at: ○, mole fraction 0.046; ◒, mole fraction 0.064; ●, mole fraction 0.090. (b) Loss factor *vs.* temperature of solutions in *n*-heptane of nitroethane and *o*-nitrotoluene at: ○, mole fraction 0.041; ◒, mole fraction 0.059; ●, mole fraction 0.099. Frequency of measurement, 16,200 ± 1 Mc./sec.

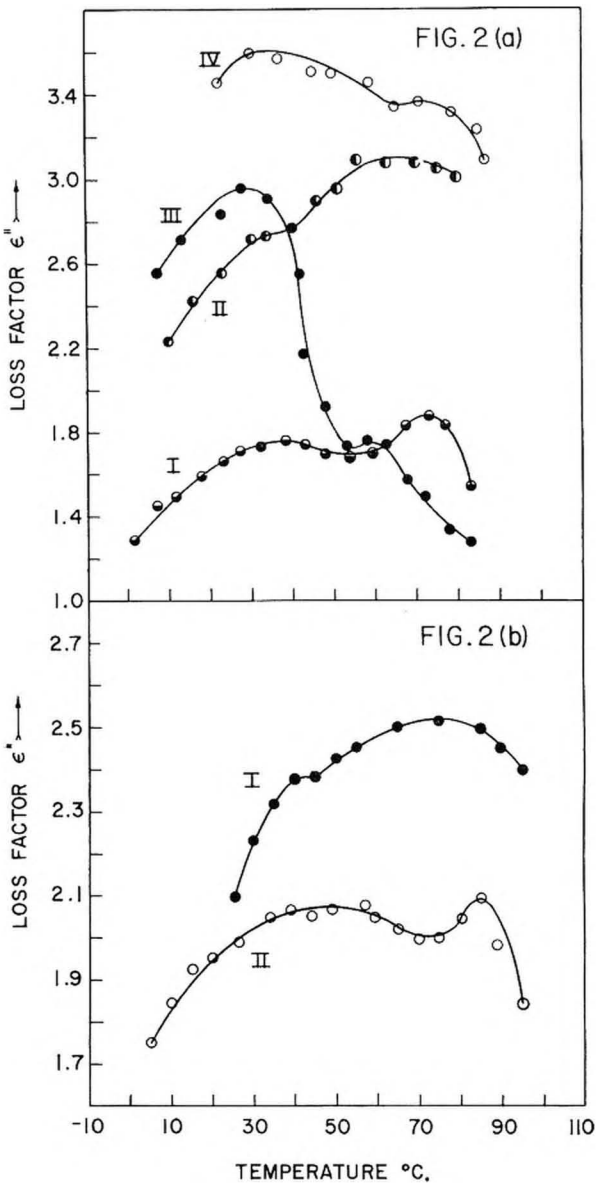

Fig. 2.—(a) Loss factor *vs.* temperature of solutions in cyclohexane of: I, nitrobenzene and *o*-nitrotoluene, mole fraction 0.15; II, nitrobenzene and *o*-nitrotoluene, mole fraction 0.23; III, nitroethane and *o*-nitrotoluene, mole fraction 0.23; IV, nitrobenzene and nitroethane, mole fraction 0.23. (b) Loss factor *vs.* temperature of solutions in *n*-dodecane of: I, nitrobenzene and *o*-nitrotoluene, mole fraction 0.286; II, benzonitrile and propionitrile mole fraction 0.32. Frequency of measurement, 16,200 ± 1 Mc./sec.

(3) S. Roberts and A. Von Hippel, *J. Appl. Phys.*, **17**, 610 (1946).

(4) D. H. Whiffen and H. W. Thompson, *Trans. Faraday Soc.*, **42A**, 114 (1946).

the one used by Smyth and others.[5] The X-12 Klystron[6] used by us as the source of microwave power had very little frequency drift over long time intervals (8 to 10 hours). The use of two slide screw tuners one to match the reflection from the dielectric window and the other to match the reflection from the crystal detector did insure a voltage standing wave ratio of 1.02 ± 0.01 with the liquid cell empty. It was found advisable to use a mechanically driven plunger in conjunction with a sensitive linear d.c. recorder as this meant a great saving in time while at the same time providing an accuracy in the wave length measurements comparable to the hand driven micrometer plunger. The position of the plunger could be read to 0.0005". The error in the determination of the loss factor (ϵ'') is about 2%. The temperature of the thermostatic liquid cell was controlled by suitable temperature regulators to within 0.5°, and the temperatures below room temperatures down to about −30° (the lowest used in our measurements) were obtained by circulating an appropriate mixture of antifreeze and water cooled by a hermetically sealed 1/3 h.p. compressor.

Results and Discussion

Loss Factor–Temperature Curves of Solutions in *n*-Heptane of i. Nitrobenzene and Nitroethane and ii.—Nitroethane and *o*-nitrotoluene are shown in Fig. 1. In each mixture the concentrations of the individual dipolar components were adjusted to be the same and are given in mole fraction. As the results at these comparatively low concentrations did not seem to indicate any clear trend as regards the separation of the peaks with change in concentration it was thought desirable to study the mixtures at substantially higher concentrations of the dipolar solutes.

As the solvent, *n*-heptane, would not retain the dipolar solutes at lower temperatures at these higher concentrations, solvents of higher viscosity were used so as to bring the loss factor peaks to higher temperatures. A high viscosity solvent like Nujol was found unsuitable because the solubility in it was rather poor. The solvents used in these measurements were cyclohexane and *n*-dodecane. Loss factor–temperature curves at higher concentrations using these solvents are shown in Fig. 2. As before in each mixture the concentrations of the individual dipolar constituents were adjusted to be the same and are given in mole fraction. The measurements in both the low concentration range as well as the high concentration range were carried down to as low a temperature as possible before there is any visual separation of the mixture.

It is rather surprising to note the distinctness of the two maxima in all the mixtures and particularly in the case of very similar nitrobenzene and *o*-nitrotoluene. The results thus seem to indicate that the mixtures chosen do not tend to one relaxation time, but that each polar liquid retains its own. From a comparison of the present curves with the corresponding curves for two component mixtures with only one polar component present it would be possible to determine how much the maximum is changed by the addition of the third component. The indication from the curves, however, is that such change as does occur is to be described as due to change of solvent, rather than coöperative motion of the dipoles. In conclusion it would perhaps be appropriate to mention that variable temperature curves are more difficult to interpret than variable frequency ones, especially if the change of relaxation time with temperature is small as in the case of the present investigation. Measurements with variable frequency have the advantage that the static permittivity of the polar constituents is not varied during a set of measurements at one concentration.

(5) See for example the paper by W. M. Heston, Jr., E. J. Hennelly and C. P. Smyth, *J. Am. Chem. Soc.*, **70**, 4093 (1948).

(6) Manufactured by the Varian Associates, Palo Alto, California.

Acknowledgments.—The author is grateful to the National Science Foundation for the award of a grant in support of the above investigation. The author also wishes to thank Dr. A. Schallamach for many helpful suggestions during the course of this investigation. Thanks are also due to Dr. D. H. Whiffen for valuable comments concerning the results. Part of the experimental work was done by Eugene A. Bradley.

SURFACE CONDUCTIVITY OF AN ANION-EXCHANGE RESIN

BY NORMAN STREET

University of Illinois, Urbana, Illinois

Received April 24, 1958

Recently several reports of investigations on surface conductance have been published, one by Watillon[1] on glass capillaries and another by van Olphen[2] on bentonite gels. Street[3] has reported measurements on the surface conductance of kaolinite suspensions, and O'Connor, Street and Buchanan[4] on some few measurements made on various minerals. These latter were carried out on plug packings concurrently with streaming potential measurements. One advantage of using packed plugs for the determinations is that the hydraulic radius (A/S) can be measured simultaneously. Thus knowing the flow rate of the electrolyte solution through the plug during the application of a known pressure drop, then, as shown by O'Connor, Street and Buchanan[4]

$$A/S = 0.00184(C\eta Q)^{1/2}$$

where

A/S = hydraulic radius (*i.e.*, ratio of, cross-sectional area available to flow, to wetted perimeter)
C = measured cell constant of the plug
η = viscosity of flowing fluid (poise)
Q = rate of flow (cc. min.$^{-1}$ cm.$^{-1}$ Hg)

Experimental

The resin was Amberlite IR-4, a weak base anion-exchange resin which was purified[5] by washing with water at 80° for eight weeks, regenerated with 0.1*N* ammonia solution for four weeks, then washed free from alkali and finally air dried.

The streaming potential and conductance measurements were made in a cell essentially similar to that described by Buchanan and Heyman[6] except that a U bend with sealed-in electrodes was fitted to the outlet tube so that conductivity measurements could be made more readily during the course of a run. Streaming potential and resistance measurements

(1) A. Watillon, *J. chim. phys.*, **54**, 130 (1957).

(2) H. van Olphen, THIS JOURNAL, **61**, 1276 (1957).

(3) N. Street, *Australian J. Chem.*, **9**, 333 (1956).

(4) D. J. O'Connor, N. Street and A. S. Buchanan, *ibid.*, **7**, 245 (1954).

(5) I. J. O'Donnell, M.Sc. Thesis, University of Melbourne, 1948.

(6) A. S. Buchanan and E. Heyman, *Proc. Roy. Soc.* (*London*), **A195**, 150 (1948).

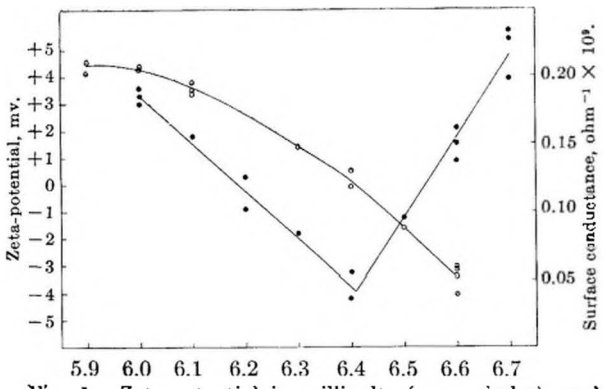

Fig. 1.—Zeta-potential in millivolts (open circles), and surface conductivity in ohm^{-1} (closed circles) *against* *p*H.

were made as described by Buchanan and Heyman. Electrolytes were HCl and KOH, and A/S was calculated for each plug packing following measurements of C and Q.

The surface conductivity (λ_s) was calculated by

$$\lambda_s = (A/S)K$$

where K is the difference between the conductivity of the electrolyte solution when filling the pores of the plug, and the bulk conductivity of the solution.

Results and Discussion

Figure 1 shows both surface conductance (λ_s) and zeta-potential (calculated by the Helmholtz–Smoluchowski equation) plotted against *p*H. Table I gives values of zeta and λ_s at higher *p*H's.

TABLE I

*p*H	Zeta-potential (mv.)	Surface conductivity (ohm^{-1}), × 10^9
8.7	−17.9	2.35
10.3	−22.8	2.74
10.7	−22.2	2.67

Generally, A/S was of the order of 5-6 × 10^{-4}. The surface conductivity calculated from the zeta-potentials is lower than the measured values, being of the order of 10^{-10} ohm^{-1} rather than 10^{-9} ohm^{-1}. On the other hand, the surface conductivity calculated from the exchange capacity (6.3 meq./g. of air-dried resin) is much greater than the measured value, being of the order of 10^{-6} ohm^{-1}.

One can conclude that the Stern layer ions at least, and probably also a swollen gel layer, contribute to the surface conductance of this resin. Nevertheless, there is correspondence between measured zeta and λ_s in that the surface conductance shows a minimum at approximately the isoelectric point. Rutgers and De Smet[7] also observed a minimum of surface conductance at the zero of zeta-potential when using thorium nitrate solutions on a glass surface.

(7) A. J. Rutgers and M. De Smet, Nat. Bur. Standards (U.S.) Circ. No. 524, 263, 1953.

THE LENNARD-JONES POTENTIAL FOR SPHERICAL MACROMOLECULES[1]

BY ANDREW G. DE ROCCO[2]

The Harrison M. Randall Laboratory of Physics, University of Michigan, Ann Arbor, Michigan

Received May 16, 1958

De Boer[3] and Hamaker[4] seem to have been responsible for the earliest calculations of the intermolecular potential between spheres of uniform composition. More recently Atoji and Lipscomb,[5] and Isihara and Koyama[6] have performed similar computations. The results of Atoji and Lipscomb depend on a series approximation valid for molecular distances fairly large in comparison to molecular radii, while those of Isihara and Koyama appear to be valid at all distances of approach. In this note we shall demonstrate that the original method of Hamaker may be employed to obtain results equivalent to those of Isihara and Koyama but having the feature of a notation more easily associated with recognizable molecular parameters.

In general the forces between macromolecules may be of several kinds, and for spherical macromolecules having static charge distributions, the interaction energy at values of *p*H well-removed from the isoionic points of the molecules may be described very nicely by a simple coulombic potential. Another related energy develops when a molecule has sites to which, for example, protons may be attached, and is determined by the excess of available sites over the average number of bound protons. Such a condition leads to a great many configurations which differ only slightly in free energy, and the consequent mobility of the protons over the sites results in an induced polarization leading at fairly long ranges to a potential decreasing as R^{-2}. This potential was described by Kirkwood and Shumaker[7] and shown by them to play an important role in the interaction of proteins at the isoionic points of the molecules, where, certainly, structure sensitive electrostatic forces play a serious role.

In addition to the energies mentioned above, a macromolecule also exhibits a considerably weaker kind of interaction, perhaps best described as a kind of Lennard-Jones potential. We mean by this, that part of the interaction energy for macromolecules which is analogous to the use of a Lennard-Jones (12:6) potential for, say, argon atoms. Clearly some kind of integration process is needed if we are to go from the 12:6 potential to its corresponding form for a macromolecule and one such procedure is described below, but before passing over to this consideration it should be emphasized that we are dealing with a strictly special case, *viz.*, a spherical macromolecule for which any static or fluctuating charge distributions are completely ignored. We are dealing with weakly interacting macrospheres or a small part of the interaction for the usual case.

Consider two macrospheres of radii R_1 and R_2, having atomic distribution functions ρ_1 and ρ_2 (taken as constants) and separated by an intermolecular distance R. We generalize the Hamaker formalism and write

(1) Aided by a grant from the American Cancer Society.

(2) Department of Chemistry, University of Michigan, Ann Arbor, Michigan.

(3) J. H. De Boer, *Trans. Faraday Soc.*, **32**, 10 (1936).

(4) H. C. Hamaker, *Physica*, **4**, 1058 (1947).

(5) M. Atoji and W. N. Lipscomb, *J. Chem. Phys.* **21**, 1480 (1953).

(6) A. Isihara and R. Koyama, *J. Phys. Soc. Japan*, **12**, 32 (1957).

(7) J. G. Kirkwood and J. B. Shumaker, *Proc. Natl. Acad. Sci.*, **38**, 863 (1952).

$$\phi(R) = \pi^2 \rho_1\rho_2 \frac{1}{R}\int_{R-R_2}^{R+R_2} f_2(z)dz \int_{z-R_1}^{z+R_1} f_1(s)\varphi(s)sds \quad (1)$$

where

$$f_1(s) = R_1^2 - (z-s)^2, f_2(z) = R_2^2 - (R-z)^2$$

The function $\varphi(s)$ represents the potential energy between atoms or small groupings of atoms (quasi-molecules) in the two macrospheres.

Equation 1 may be obtained in the following manner. Consider small volumes dV_1 in sphere 1 and dV_2 in sphere 2 separated by a distance s and interacting according to a potential $\varphi(s)$. If ρ_1 and ρ_2 represent the atomic density distribution functions, then $\rho_1 dV_1$ and $\rho_2 dV_2$ represent the total number of atoms in the two differential volumes. It is clear, then, that

$$\Phi(R) = \int_{V_2} \rho_2 dV_2 \int_{V_1} \rho_1 \varphi(s) dV_1 \quad (2)$$

Equation 1 results from eq. 2 when the indicated integrations are expressed in terms of the radii and the intermolecular separation of the macrospheres.

In order to compute $\Phi(R)$ for two spheres, we need only to specify a form for $\varphi(s)$ and, in keeping with the objectives of this note, we chose for $\varphi(s)$ the Lennard-Jones potential in the form

$$\varphi(s) = \varphi_0[(s_0/s)^{12} - 2(s_0/s)^6] \quad (3)$$

where s_0 is the equilibrium separation and φ_0 the concomitant energy.

If eq. 3 is inserted into eq. 1 two terms are obtained in $\Phi(R)$ which correspond to the repulsive and attractive terms in $\varphi(s)$. The attractive terms in $\varphi(s)$ go as s^{-6}, corresponding to the London dispersion forces and the indicated integrations were first performed (in a somewhat different style) by Hamaker to obtain

$$\Phi_{dis}(R) = -\frac{1}{3}\pi^2 \rho_1\rho_2\varphi_0 s_0^6 \left[\frac{2R_1R_2}{R^2 - r_1^2} + \frac{2R_1R_2}{R^2 - r_2^2} + \ln\frac{R^2 - r_1^2}{R^2 - r_2^2}\right] \quad (4)$$

where $r_1 = R_1 + R_2$ and $r_2 = R_1 - R_2$.

We shall find it instructive if at this point we introduce certain reduced variables and express $\Phi_{dis}(R)$ in terms of these variables. First we define the distance of closest separation by $d = R - r_1$; next the variables x and y are defined by

$$x = d/D_1, \qquad y = D_2/D_1 \quad (5)$$

If we arbitrarily call D_1 the diameter of the smaller sphere, then x measures d in terms of the smaller sphere. The ratio of the molecular sizes, y, is bounded by $1 \le y \le \infty$.

Introduction of eq. 5 into eq. 4 leads to the expression

$$\Phi_{dis} = -H\left[\frac{y}{x^2 + xy + x} + \frac{y}{x^2 + xy + x + y} + 2\ln\frac{x^2 + xy + x}{x^2 + xy + x + y}\right] \quad (6)$$

where we define H as the Hamaker constant and give it the value $H = (\pi^2\rho_1\rho_2\varphi_0 s_0^6/6)$. The quantity within the brackets represents a reduced potential whose limiting cases are of interest. We write

$$\Phi_{dis} = -H\Phi^*_{dis}(x,y) \quad (7)$$

Case 1 ($y = 1$).—This represents the interaction between spheres of identical radii. In general

$$\Phi^*_{dis}(x,1) = \left[\frac{1}{(x+1)^2} + \frac{1}{x(x+1)} + 2\ln\frac{x}{x+1}\right] \quad (8)$$

If the spheres now approach very closely, *i.e.*, $x << 1$, then

$$\Phi^*_{dis}(x,1) \simeq \frac{1}{2}\times\frac{1}{x} \quad (9)$$

a result which states that for identical macrospheres at close distances the dispersion potential is inversely proportional to R, the intermolecular separation.

Case 2 ($y \to \infty$).—For $y \to \infty$, $R_2 >> R_1$, and this is equivalent to saying that a sphere of radius R_1 "looks at" a flat surface. Certainly

$$\Phi^*_{dis}(x,\infty) = \left[\frac{1}{x} + \frac{1}{x+1} + 2\ln\frac{x}{x+1}\right] \quad (10)$$

and for close approach

$$\Phi^*_{dis}(x,\infty) \simeq \frac{1}{x} \quad (11)$$

From eq. 9 and 11 it is noted that a plane surface attracts a sphere twice as strongly as would an equivalent sphere.

All of the preceding remarks are valid for only the dispersion potential and were first noted by Hamaker.[2] We proceed now to discuss the terms representing the repulsive part of the potential, which terms are overshadowed until very close distances of approach. If we were to imagine these macromolecules as hard macrospheres, then the potential would become infinite at the cutoff value of $(D_1 + D_2)/2$. We treat here the case where the spheres are somewhat deformable.

The calculation of the potential energy of repulsion, $\Phi_{rep}(R)$, follows directly from eq. 1 upon insertion of the Lennard-Jones repulsive potential $\varphi(s) = \varphi_0 s_0^{12} s^{-12}$. Equation 1 may be evaluated by repeated integration-by-parts to yield

$$\Phi_{rep}(R) = \frac{1}{6}\pi^2\rho_1\rho_2\varphi_0 s_0^{12}\frac{1}{210R}\left[\left\{\frac{R_1R_2}{(R+r_1)^7} + \frac{R_1R_2}{(R-r_1)^7} + \frac{R_1R_2}{(R+r_2)^7} + \frac{R_1R_2}{(R-r_2)^7}\right\} + \frac{1}{6}\left\{\frac{r_1}{(R+r_1)^6} + \frac{r_2}{(R-r_2)^6} - \frac{r_2}{(R+r_2)^6} - \frac{r_1}{(R-r_1)^6}\right\} + \frac{1}{30}\left\{\frac{1}{(R+r_1)^5} + \frac{1}{(R-r_1)^5} - \frac{1}{(R+r_2)^5} - \frac{1}{(R-r_2)^5}\right\}\right] \quad (12)$$

Equation 12 may also be expressed in terms of the reduced variables introduced in eq. 6. To do so we require the quantities

$$(R+r_1)^n = (2R_1)^n(x+y+1)^n, (R-r_1)^n = (2R_1)^n x^n$$
$$(R+r_2)^n = (2R_1)^n(x+1)^n, (R-r_2)^n = (2R_1)^n(x+y)^n$$
$$R/R_1 = (2x+y+1), r_1 = R_1(y+1), r_2 = -R_1(y-1) \quad (13)$$

If the expressions of (13) are introduced into eq. 12 we obtain

$$\Phi_{rep} = H\frac{1}{210}\left(\frac{s_0}{D_1}\right)^6(2x+y+1)^{-1}\left[\frac{y}{2}\left\{\frac{1}{(x+y+1)^7} + \frac{1}{(x+y)^7} + \frac{1}{(x+1)^7} + \frac{1}{x^7}\right\} + \frac{1}{6}\left\{\frac{y+1}{(x+y+1)^6} - \frac{y-1}{(x+y)^6} + \frac{y-1}{(x+1)^6} - \frac{y+1}{x^6}\right\} + \frac{1}{15}\left\{\frac{1}{(x+y+1)^5} - \frac{1}{(x+y)^5} - \frac{1}{(x+1)^5} + \frac{1}{x^5}\right\}\right], \quad (14)$$

or

$$\Phi_{rep} = H\left(\frac{s_0}{D_1}\right)^6 \Phi^*_{rep}(x,y)$$

It is immediately clear from eq. 14 that if D_1 is at all large, then Φ_{rep} is very small until x (or d) becomes itself quite small.

Again two limiting cases become clear.

Case 1 ($y = 1$).—For identical spheres we have

$$\Phi^*_{rep}(x,1) = \frac{(x+1)^{-1}}{840}\left[\left\{\frac{1}{(x+2)^7} + \frac{2}{(x+1)^7} + \frac{1}{x^7}\right\} + \frac{2}{3}\left\{\frac{1}{(x+2)^6} - \frac{1}{x^6}\right\} + \frac{2}{15}\left\{\frac{1}{(x+2)^5} - \frac{2}{(x+1)^5} + \frac{1}{x^5}\right\}\right] \quad (15)$$

If now $x << 1$, then

$$\Phi^*_{rep}(x,1) \simeq \frac{1}{840}\left[\frac{1}{x^7} - \frac{2}{3}\frac{1}{x^6} + \frac{2}{15}\frac{1}{x^5}\right] \quad (16)$$

and finally

$$\Phi^*_{rep}(x,1) \simeq \frac{1}{840} \times \frac{1}{x^7} \quad (17)$$

This agrees with the previous result for the dispersion potential $\Phi^*_{dis}(x,1)$, where in the same limit $\Phi^*_{dis}(x,1)$ went to infinity five orders lower than the parent potential. This is clearly also true of eq. 17 and both results agree with the corresponding results of Isihara and Koyama.[4]

Case 2 ($y \longrightarrow \infty$).—We have now a somewhat more complicated case because for $y \longrightarrow \infty$ we obtain the quotient of terms which individually become infinite. L'Hopital's rule may, however, be applied to yield the result

$$\Phi^*_{rep}(x,\infty) = \frac{1}{420}\left[\frac{1}{(x+1)^7} + \frac{1}{x^7} - \frac{2}{3}\frac{1}{x^6}\right] \quad (18)$$

For very close approach $x << 1$, and we obtain, parallel to eq. 16 and 17

$$\Phi^*_{rep}(x,\infty) \simeq \frac{1}{420}\left[\frac{1}{x^7} - \frac{2}{3}\frac{1}{x^6}\right] \quad (19)$$

$$\Phi^*_{rep}(x,\infty) \simeq \frac{1}{420} \times \frac{1}{x^7} \quad (20)$$

We notice that for close approach, spheres of equal radii have, to the second order of approximation, an additional dependence on separation, $0(1/x^5)$, which is absent for the sphere-plane surface case. Finally, in the first approximation the ratio of the two repulsive energies for infinite and unit y has a value of two just as in the case of the dispersion potential and arising, clearly, from an equivalent functional dependence as expressed by eq. 3.

Equations 4 and 12 constitute together the complete Lennard-Jones potential. For the special case where both molecules are identical we obtain the result

$$\Phi(R) = 4H\left[\frac{1}{15}\left(\frac{s_0}{R_0}\right)^6\left\{\frac{1}{56} \times \frac{1}{R'}\left(\frac{1}{(R'+2)^7} + \frac{1}{(R'-2)^7} + \frac{2}{R'^7}\right) + \frac{1}{168\,R'}\left(\frac{1}{(R'+2)^6} - \frac{1}{(R'-2)^6}\right) + \frac{1}{1680\,R'}\left(\frac{1}{(R'+2)^5} + \frac{1}{(R'-2)^5} - \frac{2}{R'^5}\right)\right\} - \left\{\frac{1}{R'^2-4} + \frac{1}{R'^2} + \frac{1}{2}\ln\frac{R'^2-4}{R'^2}\right\}\right] \quad (21)$$

where both molecules have a radius R_0 and the reduced distance R' is defined by $R' = R/R_0$. Equation 21 corresponds to eq. 3.3 of Isihara and Koyama,[5] who have shown that the minimum value for the energy can be computed from eq. 21 and reads

$$\Phi_{min} = -\frac{1}{7}\,60^{1/6}\,\pi^2\,\varphi_0 s_0^5 R_0 \rho^2\left\{1 + \frac{7}{3}\,60^{-1/6}\left(\frac{s_0}{R_0}\right)\ln\left(\frac{s_0}{R_0}\right) - \ldots\right\} \quad (22)$$

from which we can see that the position of Φ_{min} appears to depend upon R_0 and the square of the distribution function ρ.

In order to avoid the explicit dependence of $\Phi(R)$ on R_0 it is convenient to remember that in terms of our reduced variables

$$\Phi = H\left[\left(\frac{s_0}{D_0}\right)^6 \Phi^*_{rep}(x,y) - \Phi^*_{dis}(x,y)\right] \quad (23)$$

and potential curves for eq. 23 are obtained easily in terms of the reduced potentials for selected values of y.

In conclusion we shall remark on an application of $\Phi(R)$ to the theory of polymer solutions.

One property of macromolecular solutions that is frequently discussed is the osmotic pressure, and for our purposes we shall use the form

$$\frac{\pi}{RTC} = \frac{1}{M} + A_2 c + A_3 c^2 + \ldots \quad (24)$$

where A_2 is the second virial coefficient, etc., and c is the concentration of the solution. According to present theory,[8] we can take A_2 to be given by

$$A_2 = -2\pi N_0 M^{-2}\int_0^\infty [g_2(R) - 1]\,R^2 dR \quad (25)$$

where N_0 is the Avogadro number and $g_2(R)$ the radial distribution function at infinite dilution for two polymer molecules. In the first approximation we follow Koyama[9] and take $g_2(R)$ to be represented by

$$g_2(R) = \exp[-\beta W(R)] \quad (26)$$

where $\beta = 1/kT$ and where $W(R)$ is understood to be the potential of the average force and is assumed for our spherical macromolecules to be represented by eq. 21. The integration of eq. 25 subject to eq. 21 and 26 may be shown to lead to

$$A_2 = \frac{16}{3}\,\pi N_0 R_0^3\,M^{-2}\left\{1 + \left(\frac{s_0}{R_0}\right) f(w)\right\} \quad (27)$$

where $w = -\Phi_{min}/kT$ and the object $f(w)$ for small values of w has been shown to have the form[6]

$$f(w) = \frac{1}{2}\left(\frac{\pi}{2}\right)^{1/2}\{6^{5/7}e^{-1}w^{1/7} - 7^{1/2}e^{-1/7}w\} \quad (28)$$

For w large $f(w)$ becomes approximately proportional to $w^{1/2}e^w$. We are presently studying this problem more carefully and will report our results at a later time.

(8) W. G. McMillan and J. E. Mayer, *J. Chem. Phys.*, **13**, 276 (1945); J. G. Kirkwood and F. P. Buff, *ibid.*, **19**, 774 (1951).

NON-EQUILIBRIUM PROPERTIES OF RARE GASES

BY M. P. MADAN

Department of Physics, University of Lucknow, India

Received February 3, 1958

The close relationship between the non-equilibrium properties of gases and intermolecular forces is well known. The observed temperature variation of thermal conductivity, viscosity, diffusion and thermal diffusion provides a very effective means of studying the nature of these forces. Various potential forms have been suggested for the study of the non-equilibrium properties and their correlation with intermolecular forces, the most important among them being the Lennard-Jones 12:6 form

$$E(r) = \epsilon[(r_m/r)^{12} - 2(r_m/r)^6] \qquad (1)$$

and the Exponential:6 form

$$E(r) = \frac{\epsilon}{1 - 6/\alpha}\left[\frac{6}{\alpha} e^{\alpha(1 - r/r_m)} (r_m/r)^6\right] \qquad (2)$$

where ϵ is the minimum potential energy taken as negative, r_m is the separation distance for which energy is minimum and α is the steepness of the repulsion energy, the later potential being more realistic and flexible. Usually the information about the values of the parameters of eq. 1 and 2 is obtained from compressibility and crystal data. Non-equilibrium properties such as diffusion and thermal diffusion are comparatively more sensitive to the intermolecular force law than any other property and are preferable for the evaluation of potential parameters to be used for predicting the non-equilibrium properties.

For rare gases, the experimental data on thermal diffusion, the property most sensitive to the force between molecules, are available only for argon, krypton and neon. For neon there is a considerable doubt about the reliability of the data. For argon and krypton results have already been reported by the author.[1-3] For other gases, under the circumstances, the next best course is to utilize the temperature variation of self-diffusion for this purpose. This has been done in the present report using the data for neon by Winn[4] and the most recent data for xenon by Amdur and Schatzki[5] for the potential form given by eq. 2. The necessary formulas for the transport coefficients have been given in references 1, 2, 3 and 6. The method used is analogous to that used by Srivastava and Madan.[7] An alternative method which can be theoretically more accurate, is to divide the expressions for self-diffusion (D_{11}) and thermal conductivity (λ), thereby eliminating the dependence of D_{11} and λ on the parameter r_m. This method is, however, not preferable over the first in practice, on account of the slow dependence of the collision integral ratio term occurring therein on the parameter ϵ and also for lack of extensive experimental measurements, but nevertheless can be used to check the self-consistency of both the methods. The values of α can be found using a method given in ref. 6. For xenon α was taken to be 13; for neon a comparison of various experimental properties with the theoretical family of curves for α suggested a value $13.5 < \alpha < 14.5$. We selected $\alpha = 14$ to provide a best fit with the experimental data. This is in good agreement with the value of $\alpha = 14.5$ obtained by Mason and Rice[6] and $\alpha = 13.6$ by Corner.[8] This gives for xenon, the average values of ϵ/k and r_m as $\epsilon/k = 168.5$°K. and $r_m = 4.883$ Å. and for neon as $\epsilon/k = 36.22$°K. and $r_m = 3.127$ Å. For the case of xenon these values can be compared with $\epsilon/k = 184.6$°K. and $r_m = 4.808$ Å. determined using the second method. The two set of values obtained from self-diffusion are consistent among themselves keeping in mind the comparative insensitiveness of the second method. The values used for calculating the

TABLE I

COMPARISON OF VALUES OF POTENTIAL PARAMETERS CALCULATED USING DIFFERENT METHODS

	Exp:Six Potential			12:6 Potential		Ref.
	α	ϵ/k (°K.)	r_m (Å.)	ϵ/k (°K.)	r_m (Å.)	
Xenon						
Self-diffusion	13	168.5	4.883			Present work first method
	13	184.6	4.808			Second method
Therma. conduct.				163 ± 24	4.84 ± 0.24	5
				216.3	4.511	10
Viscosity virial and crystal properties	13	231.2	4.450			6
Viscosity				229	4.552	11
Crystal				228	4.460	6
Neon						
Self-diffusion	14	36.22	3.127			Present work
Viscosity virial and crystal properties	14.5	38.0	3.147			6
Viscosity				35.7	3.132	11
Crystal				36.3	3.160	6
Crystal	13.6	37.1	3.160			6
Virial				35.7	3.076	11

(1) M. P. Madan, *J. Chem. Phys.*, **23**, 763 (1955).
(2) B. N. Srivastava and M. P. Madan, *ibid.*, **21**, 807 (1953).
(3) M. P. Madan, *ibid.*, **27**, 113 (1957).
(4) E. B. Winn, *Phys. Rev.*, **80**, 1024 (1950).
(5) I. Amdur and T. F. Schatzki, *J. Chem. Phys.*, **27**, 1049 (1957).
(6) E. A. Mason and W. E. Rice, *ibid.*, **22**, 843 (1954).
(7) B. N. Srivastava and M. P. Madan, *Phil. Mag.*, **43**, 968 (1952).
(8) J. Corner, *Trans. Faraday Soc.*, **44**, 914 (1948).

non-equilibrium properties are, for xenon: ϵ/k = 168.5°K., r_m = 4.883 Å., and for neon: ϵ/k = 36.22°K. and r_m = 3.127 Å. The values of the potential parameters are further compared with other determinations in Table I.

The computed values of self-diffusion, viscosity and thermal conductivity for xenon and neon at several temperatures are reported in Tables II and III. Mason and Rice,[6] Amdur,[9] Saxena[10] and others have also calculated these coefficients, using parameters obtained from different methods and with differently assumed potential forms, but the agreement has not been found to be satisfactory for these gases. Our values can be considered satisfactory, if the experimental errors in the measurement of self-diffusion are kept in mind, but cannot be taken to be in excellent agreement. The values of the self-diffusion coefficient calculated on the basis of the Lennard-Jones 12:6 form also show somewhat similar agreement.[5] This means that the assumed law of molecular interaction does not truly represent non-equilibrium properties of these gases, even though the discrepancies are sufficiently reduced by a proper evaluation of potential parameters. The present investigations and the previous work by the author and others indicates that both the potential forms, one hardly better than the other in predicting the transport properties, doubtless fit the experiment to a fair extent but are inadequate over a wide temperature range and for all the properties taken together. However, if two sets of potential parameters are taken, one for the low temperature range and the other for the high temperature range, good agreement between theory and experiment can be found.[5]

It is a pleasure to thank Prof. P. N. Sharma for his interest in this work.

TABLE IIA

COMPARISON OF OBSERVED SELF-DIFFUSION DATA FOR XENON WITH THOSE CALCULATED USING THE PARAMETERS α = 13; ϵ/k = 168.5°K.; r_m = 4.883 Å. D_{11} in cm.^{2} sec.$^{-1}$

Temp. (°K.)	Exptl.	Calcd.	Dev.
194.7	0.0257 ± 0.0003	0.0250	+0.0007
273.2	.0480 ± .0004	.0483	− .0003
329.9	.0684 ± .0013	.0695	− .0011
378.0	.0900 ± .0004	.0896	+ .0004

TABLE IIB

COMPARISON OF OBSERVED SELF-DIFFUSION DATA FOR NEON WITH THOSE CALCULATED USING PARAMETERS α = 14; ϵ/k = 36.22°K.; r_m = 3.127 Å. D_{11} in cm.^{2} sec.$^{-1}$

Temp. (°K.)	Exptl.	Calcd.	Dev.
77.7	0.0492 ± 0.0004	0.0498	−0.0006
194.7	.255 ± .004	.255	.0000
273.2	.452 ± .005	.455	− .003
298.2	.516 ± .005	.528	− .012
353.2	.703 ± .005	.704	− .001

(9) I. Amdur, *J. Chem. Phys.*, **16**, 190 (1948).
(10) S. C. Saxena, *Ind. J. Phys.*, **29**, 587 (1955).

TABLE III

COMPARISON OF OBSERVED THERMAL CONDUCTIVITY AND VISCOSITY DATA WITH THOSE CALCULATED THEORETICALLY

λ 10^6, cal. cm.$^{-1}$ sec.$^{-1}$-deg.$^{-1}$; η 10^6, g. cm.$^{-1}$ sec.$^{-1}$

I: Xenon—α = 13, ϵ/k = 168.5°K., r_m = 4.883 Å.

Temp. (°K.)	Thermal conductivity Exptl.[b]	Calcd.	Temp. (°K.)	Viscosity Exptl.[c]	Calcd.
194.7	0.91	0.88	289.7	22.35	22.60
273.2	1.21[c]	1.22	293	22.60	22.86
	1.21				
373.2	1.68	1.61	400	30.09	29.98
491.2	2.08	2.01	450	33.51	32.94
579.1	2.37	2.29	500	36.52	35.73
			550	39.54	38.52

II: Neon—α = 14, ϵ/k = 36.22°K., r_m = 3.127 Å.

90.2	4.89	5.02	100	14.35[d]	14.71
194.7	8.76	8.96	140	18.41[d]	19.10
273.2	11.10	11.32	200	23.76[d]	24.63
373.2	13.57	13.95	240	27.08[d]	27.95
491.2	15.95	16.75	300	31.73[d]	32.53

[a] F. G. Keyes, *Trans. Amer. Soc. Mech. Engrs.*, 1395 (Nov. 1955). [b] W. G. Kannuluik and E. H. Carman, *Proc. Phys. Soc. (London)*, B65, 701 (1952). [c] M. Trautz and R. Heberling, *Ann. Physik*, [5] **20**, 118 (1934). [d] H. L. Johnston and E. R. Grilly, *J. Chem. Phys.*, **46**, 938 (1942).

(11) Hirschfelder, Curtiss and Bird, "The Molecular Theory of Gases and Liquids," John Wiley and Sons, Inc., New York, N. Y., 1954.

COMMUNICATIONS TO THE EDITOR

DETERMINATION OF THE INTRINSIC VISCOSITY OF RIGID PARTICLES AT ZERO RATE OF SHEAR

Sir:

The interpretation of intrinsic viscosity, $[\eta]$, of highly asymmetric rigid particles often has been complicated by its rate of shear, D, dependence. Customarily, $[\eta]_{D=0}$ is determined through linear extrapolation ($[\eta]_D$ *versus* D), using a multigradient viscometer. This extrapolation is arbitrary and not consistent with theory,[1] and easily can lead to disastrous results,[2] especially when the $[\eta]_D$ *vs.* D plot curves rapidly upward (Fig. 2). We have found that the determination of $[\eta]_{D=0}$ can be realized with the aid of flow birefringence without the necessity of an extremely low rate of shear viscometer, which at present is unavailable to most workers.

Since both the intrinsic viscosity and extinction

(1) N. Saito, *J. Phys. Soc. Japan*, **6**, 297 (1951).
(2) E. Hisenberg, *J. Polymer Sci.*, **23**, 579 (1957).

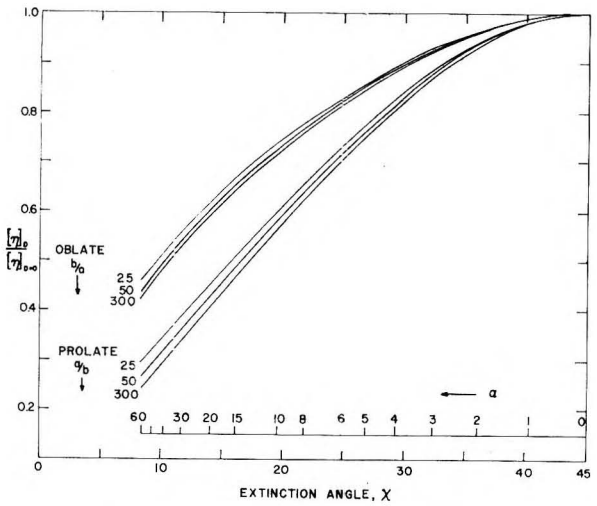

Fig. 1.—Correlation between $[\eta]_D/[\eta]_{D=0}$ and extinction angle, χ, of rigid particles with α ($= D/\theta$) and axial ratio as parameters.

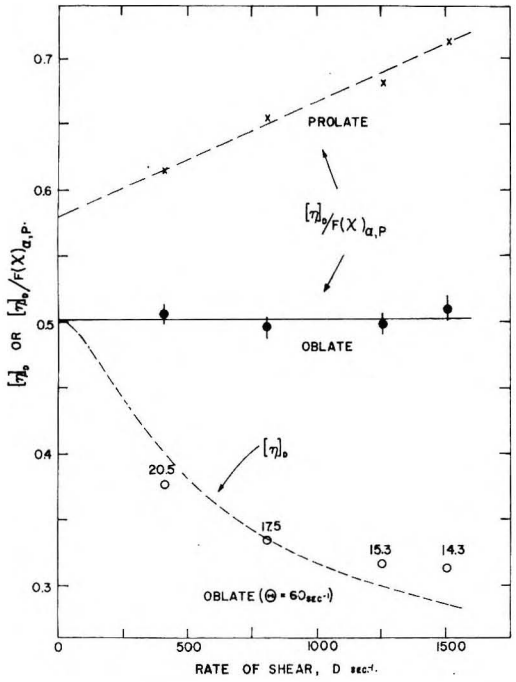

Fig. 2.—Graphic determination of intrinsic viscosity at zero rate of shear: open circle, experimental $[\eta]_D$; full circle and cross, calculated $[\eta]_D/F(\chi)_{\alpha,p}$ for oblate and prolate ellipsoids of revolution, respectively (assuming an axial ratio of 50); vertical bar representing a variation of ± 0.5 in χ; figure on top of open circle, experimental χ; lower broken curve, theoretical curve for a monodisperse oblate having $\theta = 60$ sec.$^{-1}$.

angle, χ (from flow birefringence), are a function of α ($= D/\chi$), where χ is the rotary diffusion constant of the solute, one can write

$$[\eta]_D/[\eta]_{D=0} = F(\chi)_{a,p} \qquad (1)$$

with α and p (axial ratio a/b or b/a) as parameters. The theoretical values for flow birefringence[3] and non-Newtonian viscosity[4] in Equation (1) of ellipsoids of revolution can be read off from a calibration curve (Fig. 1). It is noted that the effect of p on Equation (1) becomes insignificant for highly asymmetric particles. Thus by simultaneously measuring $[\eta]_D$ and χ one easily can evaluate the conversion factor $F(\chi)_{a,p}$ of a chosen model at constant D and thereby calculate $[\eta]_{D=0}$ from Equation (1). By plotting $[\eta]_D/F(\chi)_{a,p}$ against D a horizontal line results provided the chosen model is correct and the intercept is simply $[\eta]_{D=0}$. As an illustration we have treated the data on a colloidal dispersion of ramie crystallites.[5] The results in Fig. 2 are self-explanatory. It is noted that the cellulose crystallites fit with an oblate ellipsoid which resembles the brick-like structure as observed under electron microscope.[5] Thus Equation (1) provides in addition an independent method of distinguishing an oblate from a prolate ellipsoid. The applicability of this graphic method and its limitations will be discussed elsewhere.

The author wishes to thank Dr. R. H. Marchessault for providing the viscosity data and Dr. E. Passaglia for many helpful suggestions.

RESEARCH AND DEVELOPMENT DIVISION
AMERICAN VISCOSE CORPORATION JEN TSI YANG
MARCUS HOOK, PENNSYLVANIA

RECEIVED APRIL 24, 1958

(3) H. A. Scheraga, J. T. Edsall and J. O. Gadd, Jr., *J. Chem. Phys.*, **19**, 1101 (1951).

(4) H. A. Scheraga, *ibid.*, **23**, 1526 (1955); see also Tables I and II by J. T. Yang, *J. Am. Chem. Soc.*, **80**, 1783 (1958).

(5) R. H. Marchessault and F. F. Morehead, Abst. 132nd A. C. S. Meeting, New York, September, 1957, p. 7-E; S. M. Mukherjee and H. J. Woods, *Biochem. Biophys. Acta*, **10**, 499 (1953).

FRACTIONATION OF POISSON-DISTRIBUTED POLYMERS USING COUNTERCURRENT DISTRIBUTION

Sir:

Polyalkylene ether glycols have been fractionated by countercurrent equilibration between water and an organic solvent. Because of the rapid variation in distribution coefficient between suitable solvents with changing molecular weight, the separation was found to be very effective using only a few stages.

Polypropylene ether glycol, number average molecular weight 717, was fractionated in a 10-stage countercurrent distribution, using water and *n*-hexane as solvents. The results are given in Table I.

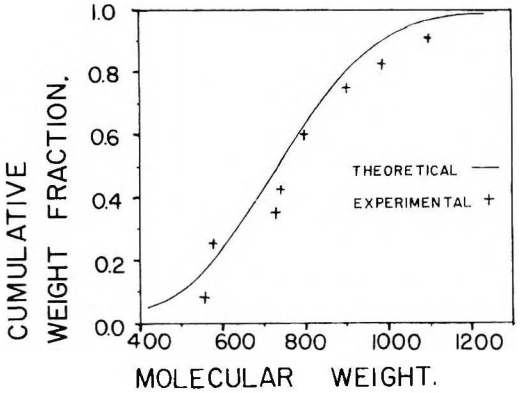

Fig. 1.—Cumulative distribution curve.

The ratio of distribution coefficients between adjacent polymeric species is about 1.4. The cumulative molecular distribution curve, Fig. 1, indicates a close agreement with the theoretical Poisson distribution, except that there is definite evidence of a high-molecular-weight "tail."

TABLE I

FRACTION DATA

Polypropylene glycol 750 (Dow Lot 07267-2, mol. wt. 717); each stage 500 ml. water, 400 ml. 2° hexane; 48.5 polymer originally added.

	Polymer, g.		Mol. wt.		
Stage	Water layer	Hexane layer	Water layer	Hexane layer	
1		2.1		1900	
	0.1				
2		1.1		1110	
	0.4				
3		1.2			
	0.7				
4		1.5		1170	
	1.3		990		
5		1.8		990	
	2.1		880		
6		1.6		920	
	3.1		810		
7		1.7		810	
	4.3		790		
8		1.6			
	5.8			740	
9		1.2			730
	7.6			580	
10		0.8			
	7.7			560	
	33.1	14.6			

A polyethylene ether glycol, molecular weight about 9000, also has been fractionated in a 10-stage countercurrent distribution, using water and a chloroform–benzene mixture as solvents. This solvent system has been used before,[1] in the fractionation of polyethylene ether glycol. The distribution coefficients vary in a similar manner, ranging from 0.033 to 12.

It would appear that this method is a powerful tool for the fractionation of certain polymers. The polyalkylene ether glycols are particularly suited to this method, due to the great difference in polarity of the chain and the end groups.

SCHOOL OF CHEMICAL AND
METALLURGICAL ENGINEERING
PURDUE UNIVERSITY
LAFAYETTE, INDIANA

L. C. CASE

RECEIVED MAY 5, 1958

(1) G. V. Shulz and E. Nordt, *J. prakt. Chem.*, **155**, 115–128 (1940).